Controls on microbial diversity and sediment biogeochemistry along a dynamic estuary

Andrea Vidal Durà

Submitted in accordance with the requirements for the degree of
Doctor of Philosophy

The University of Leeds
School of Earth and Environment

May 2017

Declaration

The candidate confirms that the work submitted is her own, except where work which has formed part of jointly-authored publications has been included. The contribution of the candidate and the other authors to this work has been explicitly indicated below. The candidate confirms that appropriate credit has been given within the thesis where reference has been made to the work of others.

The work in **Chapter 5** of the thesis reproduces a manuscript in preparation for submission to Estuarine and Coastal Shelf Science.

Vidal-Durà, A., Burke I.T., Stewart D.I., and Mortimer, R.J.G. (in prep) Reoxidation of estuarine sediments during simulated resuspension events: Effects on nutrient and trace metal mobilisation.

Field work was carried out by AVD, ITB, DIS and RJGM. AVD performed all the experimental work, data collection and analyses, and concept development. ICP-MS analyses were carried out by S. Reid at the University of Leeds. ITB and RJGM contributed to the initial concept, concept development and extensive manuscript review; DIS contributed to the initial concept, concept development and manuscript review.

For the work presented in **Chapter 6** "*Nitrate-dependent oxidation of undisturbed estuarine sediments and its effects on major and trace elements"*:

Field work was carried out by AVD, ITB, DIS and RJGM. AVD performed all the experimental work, data collection and analyses, and concept development. ICP-MS analyses were carried out by S. Reid at the University of Leeds. ITB and RJGM contributed to the initial concept, concept development and extensive manuscript review; DIS contributed to the initial concept, concept development and manuscript review.

The work in **Chapter 7** of the thesis reproduces a manuscript under review with Frontiers of Aquatic Microbiology.

Vidal-Durà, A., Burke I.T., Mortimer, R.J.G. and Stewart D.I. (in review) Diversity patterns of benthic bacterial communities along the salinity continuum of the Humber estuary (UK).

Field work was carried out by AVD, ITB, DIS and RJGM. Molecular biology work was carried out by AVD under supervision of DIS. The DNA sequencing was carried out at the Centre for Genomic Research at the University of Liverpool. All the analyses, data interpretation and production of figures and tables were completed by AVD. ITB and RJGM contribute to the initial concept, concept development and review of the manuscript. DIS contributed to the initial concept, concept development, data analysis and extensive manuscript review.

Acknowledgements

I am very grateful to Rob Mortimer, Ian Burke and Doug Stewart for being always supportive, optimistic and encouraging. They complement each other and form a balanced and easy-going team to work with. Thanks for taking in your team a Mediterranean touch this time.

I would like to thank the whole Cohen geochemistry group, especially to those who left too early (Steffi, Romain), Pilar and my lovely bonkers Burkos. Special thanks to all the technicians (including those from Civil Engineering and the Geography School) for their help and awesome work in the labs; and to Richard, from IT, who has saved me from hours and hours of Linux YouTube tutorials.

I am grateful to the University of Leeds for awarding me with the URS. Thanks to the SEE for helping to fund my PhD, and to the European Association of Geochemistry for additional financial support to attend science meetings, conferences and courses.

Finally I would like to special thank my Leeds family. Elisa for becoming my sister and best life-teacher; Montse for being 100% Starkmore, for keeping me smiling and for taking care of me always, but especially during the last sprint; Romain and Roger for being closer no matter what and where and for always believing in me (even if I don't follow the recipe). Massive thanks to all the people who have made me feel at home and gave me great moments of endless laughs, music (my beloved members of Conciertillos ID+), dancing floor (again…Elisa, Montse, Romain and… Goyo as special guest), lovely food (all of my four stars…again!), gardening, and sport (people from Republica, volleyball, climbing, squash, yoga, and insane gym!). To Edu, who always encourages me and is my best fan (just because I am his), thanks! And special thanks to my last find in Leeds for pushing me in and out of the pitch.

I would like also to thank the best two persons in the world, my grandparents, who love me, support me, and have asked me to go back every single time we have spoken on Skype since I started this PhD.

Abstract

Estuaries are the transition between freshwater and marine environments, and regulate the delivery of riverine fluxes to the oceans. The Humber estuary (UK) is considered a major source of nutrients to the North Sea. It is a highly turbid and dynamic macrotidal estuary that receives contaminated fluxes from agriculture, urbanisation, industry and historical mining activities. The chemistry of the river water and the sediments is modified within the estuarine continuum due to mixing. Sediments are subjected to resuspension periodically (on a tidal cycle timescale) and occasionally or seasonally (due to extreme rainfall or flooding episodes), which triggers a series of redox processes that control nutrient and pollutant cycling. During simulated sediment resuspension in aerated conditions, the release of accumulated reduced substrates (ammonium, manganese, iron, sulphur) and trace metals were reversed within relatively short timescales, which is important when assessing the environmental consequences of different resuspension episodes. However, the position in the salinity gradient was the dominant control on sediment geochemistry since a transition from the inner estuary (Mn/Fe-dominated redox chemistry) to the outer estuary (Fe/S-dominated redox chemistry) was observed. To better understand the role of the benthic biogeochemical denitrification processes in the nitrogen cycling, nitrate-dependent oxidation was also investigated in microcosm experiments. The same transition was observed in the nitrate reduction coupled with the oxidation of different inorganic species from the inner to the outer estuary. In this oxidation scenario there was also evidence of trace metal mobilisation. Due to the greater availability of electron donors in the mudflats of the outer estuary, they showed the greatest potential for denitrification and therefore are considered a relevant nitrogen sink in the Humber estuary. Furthermore, in this context of highly spatiotemporal variability, benthic microbial diversity showed a decreasing trend with increasing salinity, but sediment mixing and transport and the presence of strong redox transitions were also environmental parameters shaping the microbial communities in the Humber sediments.

Table of Contents

List of Figures

List of Tables

List of Abbreviations

AAS	Atomic Absorption Spectroscopy
AVS	Acid Volatile Sulphide
CCA	Canonical Correspondence Analysis
COD	Chemical Oxygen Demand
D_1^{α}	Alpha-diversity
D_1^{β}	Beta-diversity
D_1^{γ}	Gamma- or regional diversity
DET	Diffusion equilibrium in thin layer
DI	Deionised water
DIN	Dissolved Inorganic Nitrogen
DNA	Deoxyribonucleic Acid
DNRA	Dissimilatory Nitrate Reduction to Ammonia
DO	Dissolved Oxygen
DOC	Dissolved Organic Carbon
DOM	Dissolved Organic Matter
DON	Dissolved Organic Nitrogen
Dq	Hill numbers of order q
EDTA	Ethylenediaminetetraacetic acid
FeOB	Iron Oxidising Bacteria
HAB	Harmful Algal Blooms
IC	Ion Chroamtography
ICP-MS	Inductively Coupled Plasma Mass Spectrometry
IR	Infrared radiation
KED	Kinetic Energy Discrimination
LOD	Low Detection Limit
NMDS	Non-metric Multi Dimensional Scaling
OUT	Operational Taxonomic Unit
PCB	Polychlorinated Biphenyls
PHA	Polycyclic Aromatic Hydrocarbons
POM	Particulate Organic Matter
PON	Particulate Organic Nitrogen
qPCR	quantitative Polymerase Chain Reaction
rRNA	ribosomal Ribonucleic Acid
RSD	Relative Standard Deviation
SEP	Sequential Extraction Protocol
SOB	Sulphur Oxidising Bacteria
SPM	Suspended Particulate Matter
TBE	Tris-borate EDTA

TC	Total Carbon
TIC	Total Inorganic Carbon
TM	Trace metals
TMZ	Turbidity Maximum Zone
TOC	Total Organic Carbon
TON	Total Nitrogen Oxides
TS	Total Sulphur
UV	Ultraviolet irradiation
VIS	Visible light irradiation
XAS	X-ray Absorption Spectroscopy
XRD	X-ray Diffraction
XRF	X-Ray Fluorescence

Chapter 1
Introduction

1.1 Project context

Estuaries represent the transition between freshwater and marine environment. Nutrient inputs, mainly through river fluxes, to estuaries have been increased by anthropogenic activities due to the increasing populations, the more intensive agricultural practices, and industrialization (Howarth *et al.*, 1996). Nutrient enrichment is probably the most common problem in estuaries globally and it is linked to eutrophication in coastal waters (Nixon, 1995; Hobbie, 2000; Howarth *et al.*, 2000; Galloway *et al.*, 2004; Howarth & Marino, 2006).

The linkages between hydrological, physical and biogeochemical processes within estuaries show a great spatiotemporal variability. The mixing of river and seawater drives rapid changes in the physicochemical conditions that affect the speciation of the chemical components in solution, and therefore in their reactivity within the system (Statham, 2012).

Aquatic sediments are characterised by developing a redox profile in which different geochemical zonations associated with a dominant respiration process are organised following the availability of the preferred electron acceptor (the one that yields the highest amount of free energy in the microbial oxidation of organic matter). The original scheme of these redox zonations proposed by Froelich *et al.* (1979) constitutes a paradigm in biogeochemistry. However, such ideal zonation may not apply for sediments that are continuously being disturbed by physical forces or bioturbation; hence the complexity of studying benthic microbial processes in estuarine sediments.

Estuaries are typically very turbid due to the high concentrations of suspended particulate matter (SPM) derived from river and coastal inputs and resuspension of the benthic sediments. Estuaries act in fact as sediment traps and the particles have extended residence times due to the repeated cycles of sediment resuspension and

settling (Grabemann *et al.*, 1997). Particle-water interactions involve nutrients and other solutes such as organic matter and heavy metals (Millward & Turner, 1995; Gebhardt *et al.*, 2005). Moreover, during sediment resuspension high concentrations of SPM (especially at the estuarine turbidity maximum, Schubel (1968)) have been associated with intense microbial activity (Hollibaugh & Wong, 1999) and dissolved chemicals are released back to the water column (Corbett, 2010). In short, estuarine sediment dynamics plays an important role in the biogeochemical cycles controlling the fate and transport of nutrients and other chemicals therein.

The analysis of the role of biogeochemical processes in the chemistry and biology of estuaries, the composition of the fluxes, and the possible impacts on the coastal waters requires consideration of the physical processes as well (Hobbie, 2000). A comprehensive approach to estuarine ecosystems is fundamental for their modelling and management (Hobbie, 2000; Mitchell & Uncles, 2013). Furthermore, in a climate change scenario sea level rise and major changes in the precipitation patterns have been predicted, which will alter the inputs of nutrients to the estuaries and will require modification of flood defences (Jickells, 2005; Gao *et al.*, 2014). Therefore the likely effects of global warming on the estuarine processes, together with the trends in terms of agricultural practices and sediment supply, need to be taken into account in the management strategies of estuaries to ensure the coastal ecosystem sustainability.

The Humber estuary (UK) is representative of many major estuaries worldwide. It is a highly turbid and well-mixed estuary that has received important loads of nitrogen −mainly from its tributary rivers draining intensive agricultural catchments (Sanders *et al.*, 1997; Mortimer *et al.*, 1998)− and heavy metals –from legacy of contaminated sediments along the more industrial and mining catchments (Cave *et al.*, 2005). Additionally there has been a loss of intertidal-wetland environment over the last couple of hundred years, which has affected sediment and chemical fluxes (e.g. denitrification capacity and nitrogen retention and organic carbon storage have decreased) (Jickells *et al.*, 2000). The decrease of sites for sediment accumulation has impacted the cycles of particle resuspension since particles are continuously resuspended before they are exported eventually to the sea. During sediment mobilization, there is a potential source

of nutrients and metals that may be released back to the water column. So there is a scientific interest in studying the impacts of estuarine sediment biogeochemistry and dynamics on major and trace element cycling and transport to the coastal zone. This work also includes the first description of the benthic microbial populations of the Humber sediments by using high throughput DNA sequencing technologies, which has resulted in a deep coverage of individual samples. Improving the understanding of the benthic bacterial community distribution along the salinity continuum will help to better understand the relationship between microbiology and geochemistry and to constrain which are the environmental controls on the microbial communities.

1.2 Research aims and objectives

Previous work in the Humber Estuary has shown that gradients in porewater profiles, nutrient fluxes, and the redox and absorption state of sediment particles may be significantly affected by sediment mixing and resuspension on different timescales and by the activity of macrofauna. Those macrofaunal communities are largely influenced by sediment resuspension and salinity as well (Mortimer *et al*., 1999). However such conclusions were obtained from studies of nutrient diffusion fluxes in sediment cores and not from resuspension experiments. Anoxic nitrification processes and reoxidation of technicium in estuarine sediments from the Humber have been also studied. In this context, we found the need of a more comprehensive study of the multiprocesses occurring during sediment reoxidation (during resuspension and during anaerobic oxidation with nitrate as an oxidant), and therefore of the complex interlinks between nitrogen, iron, sulphur and trace metal cycling. To do so, we outlined a systematic study of four sites of different geochemical characteristics along the salinity continuum.

The overall aim of this research project was to improve the understanding of the biogeochemical processes of estuarine sediments along the salinity gradient of the Humber estuary. To achieve this, sediments and river water from the Humber estuary collected in the same tidal cycle have been used in different laboratory experiments in order to reproduce different natural scenarios and investigate nutrient and metal

behaviour in such circumstances, as well as to characterise the benthic microbial communities along the salinity gradient.

The first centimetres of the bed sediments from the Humber were simplified in two sedimentary units. The first unit corresponds to the upper first centimetre, this region of the sediment is re-suspended periodically (daily to weekly). Dissolved oxygen will penetrate a few millimetres into the sediment, so this surface layer tends to be in oxic/suboxic conditions. The second sedimentary unit we defined corresponds to the subsurface sediment, from 5-10 cm depth. This region of the sediment is rarely (seasonally to annually) disturbed, only when there is an extreme event such as a big storm or a flood event (Mortimer *et al.*, 1998). Oxygen does not penetrate down to this region of the sediment profile. In the absence of oxygen, other species will act as a terminal electron acceptor in the biotic and abiotic redox processes and reduced species of major and trace elements may be accumulated. The mobilisation of the subsurface sediment could become more frequent in the near future due to global warming since it has been predicted that extreme rainfall episodes will become increasingly common in temperate regions (Jones & Reid, 2001; Christensen *et al.*, 2007; Gao *et al.*, 2014). Therefore the more frequent mobilization of the subsurface sediment will impact the geochemistry of the system since buried chemicals will take part in the common reoxidation processes. Consequently, the composition of the nutrient fluxes coming into the coastal waters is likely to be modified which may lead to eutrophication problems if the nutrient load is being increased.

To achieve the aim, the objectives were:

- To characterise the porewater, overlying water and sediment composition along the estuarine continuum, with especial attention to the redox indicators.

- To monitor the behaviour of nitrogen species, iron, manganese, sulphate and trace metals (TMs) when sediments from different pools (surface and subsurface) are resuspended in oxic conditions

- To investigate the anaerobic oxidation processes coupled to nitrate reduction within the suboxic zone of the estuarine sediment profile and identify the dominant processes in the presence of sulphur or lack thereof along the estuarine continuum.

- To characterise the microbial communities living in the different geochemical environments of the Humber estuary and identify diversity trends along the salinity continuum.

1.3 Thesis outline

This thesis consists of eight chapters:

Chapter 1 contains the rationale of the project, the research aim and objectives and the thesis outline.

Chapter 2 contains a literature review about estuarine systems that addresses microbiology and sediment geochemistry in detail. Major elements and trace metal cycling are described as well as the geochemical gradients of interest (redox and salinity). This is followed by an overview of the Humber estuary which has been the study site for this work.

Chapter 3 contains the compilation of all the experimental and analytical methods used. Some of the laboratory techniques and instrument protocols were carried out according to the standard operational procedures available in the Cohen Geochemistry Labs (University of Leeds). The methodology for the molecular biology work is also included as well as the multivariate analysis tools used for the interpretation of the DNA sequencing data.

Chapter 4 provides characterisation data for all the sediments and waters used in the experiments.

Chapter 5 “Reoxidation of estuarine sediments during simulated resuspension events: Effects on nutrient and trace metal mobilisation”. This includes the results of sediment reoxidation experiments in which sediment resuspension in oxic conditions was simulated in the laboratory to analyse its effects on major and trace elements. Changes

over time were analysed according to natural timescales based on the duration of regular and a sporadic resuspension events.

Chapter 6 “Nitrate-dependent oxidation of undisturbed estuarine sediments and its effects on major and trace elements as a function of in situ geochemistry”. This chapter describes the microcosm experiments used to investigate nitrate-dependent oxidation processes in subsurface estuarine sediments during anaerobic incubations.

Chapter 7 “Diversity patterns of benthic bacterial communities along the salinity continuum of the Humber estuary (UK)”. We characterise the benthic microbial populations along the salinity continuum using amplicon sequencing of 16S rRNA gene. These data were used to measure the microbial diversity and in combination with geochemical data we investigate the environmental controls on the microbial community distribution along the estuary.

Finally, Chapter 8 contains a summary of the work presented in the thesis, conclusions and suggestions for future work.

1.4 References

[1] Cave, R. R., Andrews, J. E., Jickells, T., & Coombes, E. G. (2005). A review of sediment contamination by trace metals in the Humber catchment and estuary, and the implications for future estuary water quality. *Estuarine, Coastal and Shelf Science*, 62(3), pp.547-557. doi: 10.1016/j.ecss.2004.09.017

[2] Christensen, J. H., Hewitson, B., Busuioc, A., Chen, A., Gao, X., Held, I., Jones, R., Kolli, R. K., Kwon, W.-T., Laprise, R., Magaña Rueda, V., Mearns, L., Menéndez, C. G., Räisänen, J., Rinke, A., Sarr, A., & Whetton, P. (2007). Regional Climate Projections. *In* S. Solomon, D. Qin, M. Manning, Z. Chen, M. Marquis, K.B. Averyt, M. Tignor & H.L. Miller (Eds.), *Climate Change 2007: The Physical Science Basis. Contribution of Working Group I to the Fourth Assessment Report of the Intergovernmental Panel on Climate Change* Cambridge, United Kingdom and New York, NY, USA: Cambridge University Press, pp. 847-940.

[3] Corbett, D. R. (2010). Resuspension and estuarine nutrient cycling: insights from the Neuse River Estuary. *Biogeosciences*, 7(10), pp.3289-3300. doi: 10.5194/bg-7-3289-2010

[4] Froelich, P. N., Klinkhammer, G. P., Bender, M. L., Luedtke, N. A., Heath, G. R., Cullen, D., Dauphin, P., Hammond, D., Hartman, B., & Maynard, V. (1979). Early oxidation of organic-matter in pelagic sediments of the eastern equatorial atlantic - suboxic diagenesis. *Geochimica et Cosmochimica Acta*, 43(7), pp.1075-1090. doi: 10.1016/0016-7037(79)90095-4

[5] Galloway, J. N., Dentener, F. J., Capone, D. G., Boyer, E. W., Howarth, R. W., Seitzinger, S. P., Asner, G. P., Cleveland, C. C., Green, P. A., Holland, E. A., Karl, D. M., Michaels, A. F., Porter, J. H., Townsend, A. R., & Vorosmarty, C. J. (2004). Nitrogen cycles: past, present, and future. *Biogeochemistry*, 70(2), pp.153-226. doi: 10.1007/s10533-004-0370-0

[6] Gao, Y., Zhu, B., Yu, G., Chen, W., He, N., Wang, T., & Miao, C. (2014). Coupled effects of biogeochemical and hydrological processes on C, N, and P export during extreme rainfall events in a purple soil watershed in southwestern China. *Journal of Hydrology*, 511, pp.692-702. doi: 10.1016/j.jhydrol.2014.02.005

[7] Gebhardt, A. C., Schoster, F., Gaye-Haake, B., Beeskow, B., Rachold, V., Unger, D., & Ittekkot, V. (2005). The turbidity maximum zone of the Yenisei River (Siberia) and its impact on organic and inorganic proxies. *Estuarine Coastal and Shelf Science*, 65(1-2), pp.61-73. doi: 10.1016/j.ecss.2005.05.007

[8] Grabemann, I., Uncles, R. J., Krause, G., & Stephens, J. A. (1997). Behaviour of turbidity maxima in the Tamar (UK) and Weser (FRG) estuaries. *Estuarine Coastal and Shelf Science*, 45(2), pp.235-246. doi: 10.1006/ecss.1996.0178

[9] Hobbie, J. E. (2000). Estuarine Science: the key to progress in coastal ecological research. *In*: J. E. Hobbie, (Ed.), *Estuarine Science: A Synthetic Approach to Research and Practice*. Washington DC: Island Press, pp.1-11.

[10] Hollibaugh, J. T., & Wong, P. S. (1999). Microbial processes in the San Francisco Bay estuarine turbidity maximum. *Estuaries*, 22(4), pp.848-862. doi: 10.2307/1353066

[11] Howarth, R., Andreson, D., Cloern, J., Elfring, C., Hopkinson, C., Lapointe, B., Malone, T., Marcus, N., McGlathery, K., Sharpley, A., & Walker, D. (2000). Nutrient Pollution of Coastal Rivers, Bays and Seas. *Issues in Ecology: Ecological Society of America.*

[12] Howarth, R. W., Billen, G., Swaney, D., Townsend, A., Jaworsky, N., Lajtha, K., Downing, J. A., Elmgren, R., Caraco, N., Jordan, T., Berendse, F., Freney, J., Kudeyarov, V., Murdoch, P., & Zhao-Liang, Z. (1996). Regional Nitrogen budgets and riverine N & P fluxes for the drainages to the North Atlanthic Ocean: natural and human influences. *Biogeochemistry*, 35, pp.75-139. doi: 10.1007/BF02179825

[13] Howarth, R. W., & Marino, R. (2006). Nitrogen as the limiting nutrient for eutrophication in coastal marine ecosystems: Evolving views over three decades. *Limnology and Oceanography*, 51(1), pp.364-376. doi: 10.4319/lo.2006.51.1_part_2.0364

[14] Jickells, T., Andrews, J., G., S., Sanders, R., Malcolm, S., Sivyer, D., Parker, R., Nedwell, D., Trimmer, M., & Ridgway, J. (2000). Nutrient Fluxes through the Humber Estuary: Past, Present and Future. *Ambio; Royal Swedish Academy of Sciences*, 29(3), pp.130-135.

[15] Jickells, T. (2005). External inputs as a contributor to eutrophication problems. *Journal of Sea Research*, 54(1), pp.58-69. doi: 10.1016/j.seares.2005.02.006

[16] Jones, P. D., & Reid, P. A. (2001). Assessing future changes in extreme precipitation over Britain using regional climate model integrations. International *Journal of Climatology*, 21(11), pp.1337-1356. doi: 10.1002/joc.677

[17] Millward, G. E., & Turner, A. (1995). Trace metals in estuaries. *In* B. Salbu & E. Steinnes (Eds.), *Trace elements in natural waters*. CRC Press, Inc., Boca Raton, Florida, USA; CRC Press, London, England, UK, pp.223-245.

[18] Mitchell, S. B., & Uncles, R. J. (2013). Estuarine sediments in macrotidal estuaries: Future research requirements and management challenges. *Ocean & Coastal Management*, 79, pp.97-100. doi: 10.1016/j.ocecoaman.2012.05.007

[19] Mortimer, R. J. G., Krom, M. D., Watson, P. G., Frickers, P. E., Davey, J. T., & Clifton, R. J. (1998). Sediment-water exchange of nutrients in the intertidal zone of the Humber Estuary, UK. *Marine Pollution Bulletin*, 37(3-7), pp.261-279. doi: 10.1016/s0025-326x(99)00053-3

[20] Mortimer, R. J. G., Davey, J. T., Krom, M. D., Watson, P. G., Frickers, P. E., & Clifton, R. J. (1999). The effect of macrofauna on porewater profiles and nutrient fluxes in the intertidal zone of the Humber Estuary. *Estuarine Coastal and Shelf Science, 48*(6), pp.683-699. doi: 10.1006/ecss.1999.0479

[21] Nixon, S. W. (1995). Coastal marine eutrophication - a definition, social causes, and future concerns. *Ophelia*, 41, pp.199-219.

[22] Sanders, R. J., Jickells, T., Malcolm, S., Brown, J., Kirkwood, D., Reeve, A., Taylor, J., Horrobin, T., & Ashcroft, C. (1997). Nutrient fluxes through the Humber estuary. *Journal of Sea Research*, 37(1-2), pp.3-23. doi: 10.1016/S1385-1101(96)00002-0

[23] Schubel, J. R. (1968). Turbidity maximum of Northern Chesapeake Bay. *Science*, 161(3845), pp.1013-1015. doi: 10.1126/science.161.3845.1013

[24] Statham, P. J. (2012). Nutrients in estuaries--an overview and the potential impacts of climate change. *Science of The Total Environment*, 434, pp.213-227. doi: 10.1016/j.scitotenv.2011.09.088

Chapter 2
Literature Review

2.1 Introduction to estuaries

Estuaries and nearby wetlands are partially enclosed coastal bodies of water where rivers meet the sea. They host one of the most diverse and highly productive ecosystems in the word (Hobbie, 2000; Statham, 2012). Coastal zones in general and estuaries in particular have been a focus for human settlement and intense economic activity (industry, fishery, commercial ports). Estuaries provide valuable habitats (e.g. nurseries for many aquatic plants and animals) and ecosystem services such as coastal protection and nutrient cycling and storage (Jickells, 1998; NOAA, 2008). They receive particulate and dissolved materials mainly from river fluxes, but also from atmospheric deposition and groundwater (Nedwell *et al.*, 1999), and such inputs have been modified by anthropogenic activities. Estuaries are transitional environments showing strong chemical gradients and intense geochemical cycling, where organic matter and nutrients are transformed and retained (Garnier *et al.*, 2008). They act as buffers in the interface between land and ocean since they act as natural protective filters and traps for sediment, nutrients and contaminants (de Jonge *et al.*, 2002). There is a wide range of physical and biogeochemical processes operating over different time and spatial scales within the estuaries that regulate the chemistry and biology of the system and hence influence the composition of fluxes to coastal waters (Nedwell *et al.*, 1999; Hobbie, 2000).

It has been estimated that riverine N fluxes in many temperate regions have increased from pre-industrial times by 5 to10-fold in the last century due to population growth, urban and industrial expansion, the development of agricultural practices with a widespread use of fertilizers, and increased atmospheric deposition (Howarth *et al.*, 1996; Howarth *et al.*, 2000). This is important because nitrogen is normally the limiting nutrient for primary production in most estuaries and coastal waters in the temperate zone. Although nitrogen is not the only element of concern since phosphorous

(normally limiting in freshwaters, Nedwell *et al.*, 2002) can also be limiting in some coastal systems (Howarth & Marino, 2006). Excess nutrients in estuarine and adjacent coastal waters leads to eutrophication (Nixon, 1995; Howarth *et al.*, 2000). Eutrophication has been defined as the increase in the rate of organic matter supply to an aquatic ecosystem related to the enhancement of the primary production associated with the excess nutrient supply. As the algal bloom crashes and intensive heterotrophic bacterial activity develops, the oxygen concentration will drop. This can result in hypoxic (or even anoxic) water episodes, which have a negative impact on the ecosystem, for example the development of harmful algal blooms (HAB) and fish kills (Nixon, 1995; Hobbie, 2000; Howarth *et al.*, 2000; Galloway *et al.*, 2004; Howarth & Marino, 2006). Hypoxic episodes are unlikely in well-mixed estuaries since the oxygen is constantly supplied due to wave action and circulation patterns (NOAA, 2008), and besides, they are typically turbid environments and therefore primary production is limited due to the low light availability (Jickells, 1998). However, the environmental consequences of eutrophication may be intensified by other physicochemical processes associated with climate change: elevated temperatures, changes in wind patterns and hydrological cycle (frequency of extreme storm events, floods, droughts, stagnancy, etc.), and sea level rise (Statham, 2012).

2.1.1 Types of estuaries

Estuaries have their origin in the last Ice Age (Pleistocene), when the sea level started to rise due to the melting of the major continental glaciers (18,000 years ago). According to their origin, estuaries can be classified as coastal plain, fjord, tectonic and bar-built estuaries. However they can also been classified based on how river and sea waters mix in their confluence (Trujillo & Thurman, 2013).

In general, freshwater flows across the surface of the estuary towards the ocean, while the denser subsurface seawater moves landwards along the bottom of the estuary. The mixing occurs at the contact of the two water masses (Trujillo & Thurman, 2013). It is important to note that the Coriolis effect causes low-salinity surface-water in an estuary to curve to the right (in the Northern Hemisphere and in the opposite direction in the southern Hemisphere), so seawater coming in the estuary tends to flow in on the left

side (Gross, 1976). Additionally, estuarine mixing patterns vary with location, season and tidal conditions, but it is possible to simplify them in four models: vertically mixed, slightly stratified, highly stratified and salt wedge estuaries (Fig. 2.1).

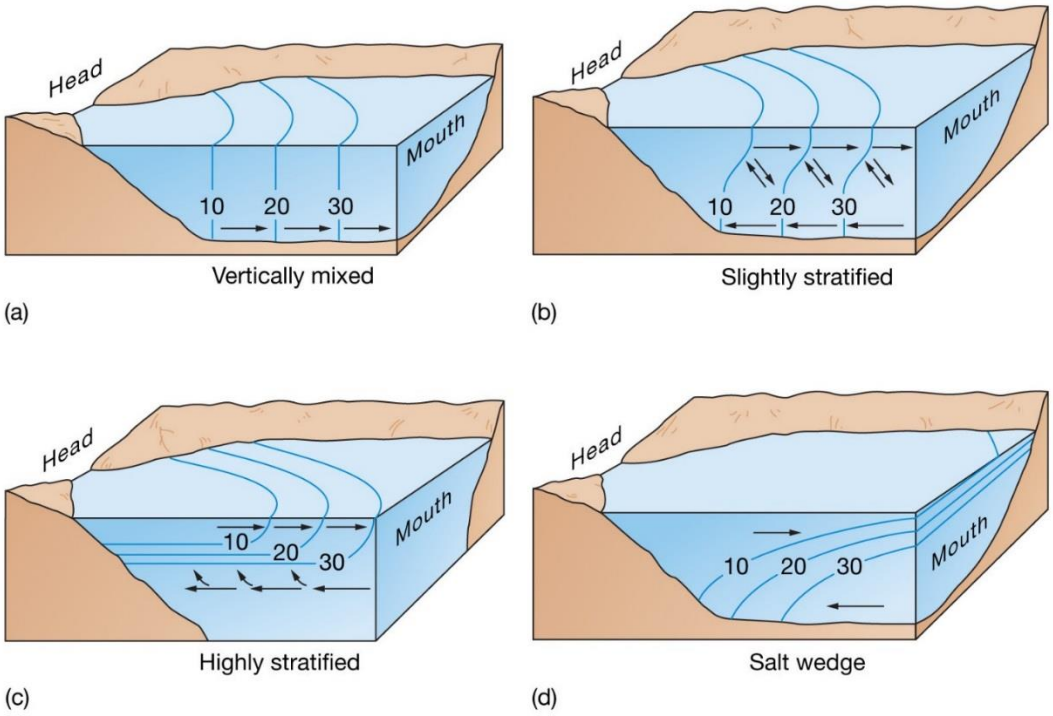

Figure 2.1: Classification of the estuaries by mixing. Diagrams of the four types of estuaries based on the type of mixing between fresh and sea water. Numbers represent salinity (psu) and arrows indicate flow directions. Source: Trujillo & Thurman (2013), page 363.

2.1.1.1 Vertically or well-mixed estuaries

A vertically mixed estuary is normally large and shallow estuary, and it occurs where river flow is low and tidal currents are moderate to strong (NOAA, 2008). There is a net flow going always from the head of the estuary towards the sea (Fig. 2.1a). The mixing between fresh and seawater is even at all depths and therefore salinity is uniform vertically at any point of the estuary. The strong influence of the tides annuls the vertical stratification, so salinity, influenced by the daily tidal range, increases from the head to the mouth. Salinity lines curve at the edge of the estuary due to the Coriolis effect (Trujillo & Thurman, 2013). The Humber or the Severn estuaries (both in the UK) or the Delaware Bay (US), or the Myall River (Australia) are well-mixed estuaries.

2.1.1.2 Slightly and highly stratified estuaries

These are deeper estuaries where tidal currents are strong and river discharges small; the mixing is vigorous and salinity increases seawards at any depth (Gross, 1976). However, two layers of water separated by a zone of mixing can be distinguished. The circulation pattern of slightly stratified estuaries is based on a net subsurface flow of the denser saline water towards the upper estuary and a net surface flow of low-salinity waters towards the mouth (Fig. 2.1b) (Trujillo & Thurman, 2013). A highly stratified estuary is also deep but only the upper-layer salinity increases seawards, whereas the bottom layer has a constant salinity (seawater salinity) along the estuary. Mixing occurs at the interface of the surface and subsurface water and it creates a net flow of deep water into the upper water (Fig. 2.1c). So the surface water mass simply moves forwards, increasing its salinity as it mixes with the deep layer. One of the most remarkable characteristics of these estuaries is the developing of strong haloclines at the boundary between the two layers (Trujillo & Thurman, 2013). The Chesapeake Bay, the San Francisco Bay (both in the US), or the Mersey estuary (UK) are examples of slightly stratified estuaries. The Vellar River (India) and the Doubtful Sound (New Zealand) are examples of highly stratified estuaries.

2.1.1.3 Salt wedge estuaries

Salt wedge estuaries are river-dominated and are the least mixed of all the estuaries (NOAA, 2008). The river flow is large and the salty water enters from the ocean beneath the upper freshwater layer (Fig. 2.1d). The weak tidal currents together with the force of the river flow determine the circulation pattern. There is no horizontal salinity gradient at the surface since it remains as freshwater throughout the length of the estuary (or even beyond in some cases). There is a wedge of saltwater on the bottom, which location varies with the weather and tidal conditions (NOAA, 2008). So there is a horizontal salinity gradient at depth and a distinct halocline at any point along the estuary. The halocline becomes shallower and more pronounced near the mouth of the estuary (Trujillo & Thurman, 2013). For example the Pearl River (China) or the Columbia and Mississippi Rivers (in the US) have a long salt wedge estuaries.

2.2 Microbiology of estuarine systems

Estuaries are very complex ecosystems which experience fluctuating conditions over both space and time to which estuarine microbial communities are exposed continuously (Attrill, 2002). The continuous mixing of waters, sediment resuspension, and, consequently, the high variability of the local physicochemical characteristics (pH, temperature, salinity, turbidity, oxygen, chemical composition of the fluxes.) can affect the stability and composition of microbial communities along the estuarine continuum (Crump *et al.*, 1999; O'Sullivan *et al.*, 2013; Liu *et al.*, 2014; Wei *et al.*, 2016).

Microbial populations play a key role in the estuarine biogeochemical processes (Federle *et al.*, 1983; Rink *et al.*, 2008). Estuaries are typically very turbid due to the high concentrations of SPM. Therefore heterotrophic activity will dominate over the primary production due to light limitation (Cole *et al.*, 1992; Jickells, 1998). In less turbid systems, such as some microtidal and oligotrophic estuaries, pelagic and benthic photosynthetic activity may be important in terms of nutrient input (Nedwell *et al.*, 1999).

Intense microbial activity is associated with areas of high SPM concentrations since microorganisms are attached to particle surfaces (Plummer *et al.*, 1987). However the microbial processes occurring in the water column will be still of lower magnitude than those in the sediments. High turbidity has been also associated in most estuaries with high sedimentation rates of organic matter rich materials (Nedwell *et al.*, 1999), which is highly relevant since the benthic aerobic and anaerobic heterotrophic microorganisms are responsible for the majority of the organic matter degradation in coastal and shallow estuaries (Canfield *et al.*, 2005b). Bacterial breakdown of organic matter drives a series of redox reactions that are involved in the different element cycles, but the vertical distribution of the different respiration processes is not as well stratified as in other aquatic sediments due to the continuous sediment remobilisation and bioturbation (Sørensen & Jørgensen, 1987; Aller, 1994).

2.2.1 Environmental variables influencing aquatic microorganisms in the estuarine environment

2.2.1.1 Temperature

Microbial metabolic and growth rates are affected by temperature. There are three cardinal temperatures that define the response of an individual organism to temperature: minimum, optimal and maximum growth temperature (Rheinheimer, 1985; Canfield *et al.*, 2005b). The optimum temperature is normally closer to the maximum than to the minimum (when enzymatic activity is too slow). When maximum growth temperatures are exceeded, proteins and membrane stability are damaged. Psychrophilic (maximum growth rates at <15°C) bacteria predominate in the marine environment (Rheinheimer, 1985; Canfield *et al.*, 2005b). In other inland water bodies of warmer zones and seawater near to the surface, mesophilic bacteria can predominate during some periods of the year (Rheinheimer, 1985).

2.2.1.2 Salinity

Salinity in estuarine systems ranges from near zero at the head of the estuary (freshwater) to seawater (or closer) salinity (35 psu). All microorganisms maintain cytoplasmic water activity lower than the external environment by keeping higher solute concentration within the cell and establishing the osmotic pressure needed for cell growth (Canfield *et al.*, 2005b). However, as salinity increases, there are more difficulties for the cells to maintain these physiological conditions. The majority of the microorganisms are adapted to a specific, and sometimes narrow, salinity range; and therefore they can be divided according to their tolerance to salinity in: mild (or halotolerant) (maximum growth 1-6% NaCl by weight), moderate (maximum growth 6-15% NaCl), and extreme halophile (maximum growth >15% NaCl) (Canfield *et al.*, 2005b). Most of the marine microorganisms are halophilic, whereas most of the freshwater microorganisms are halophobic and cannot grow at a salt concentration of more than 1% (Rheinheimer, 1985). There is a small percentage of organisms that can thrive in both fresh and seawater (Rheinheimer, 1985). In fact, in the estuarine environment, several studies have demonstrated that fresh and marine communities mix

along the salinity gradient, and there are few evidences of the existence of truly estuarine bacterial communities (Crump *et al.*, 2004).

2.2.1.3 Light and Turbidity

In coastal areas the depth of the photic zone depends on latitude, season and, especially, on the turbidity of the water. As mentioned before, light is the limiting factor for primary productivity in turbid estuaries. But in some shallow coastal areas and oligotrophic estuaries, benthic microalgae (cyanobacteria and unicellular eukaryotic algae) grow within the surface of illuminated sediments and the biomass of these mat-forming species can sometimes be larger than the biomass of the free-living species (i.e. phytoplankton in the water column) (Gray & Elliott, 2009). When there is benthic primary production, the nutrient exchange between sediment-water may be reduced due to the consumption of N and P (Nedwell *et al.*, 1999).

Estuaries typically have elevated concentrations of SPM that is very cohesive and readily flocculates. Turbidity can be extraordinarily high, especially in the turbidity maximum zone (TMZ) (see more in section 2.4.3). The number of free-living bacteria in these regions is very low, and conversely, the majority of the microbial population is attached to particle surfaces (Uncles *et al.*, 1998c; Herman & Heip, 1999). The SPM constitutes an optimal microenvironment since nutrients, normally present at low concentrations in the water column, are more accessible for the microbiota (Owens, 1986; Plummer *et al.*, 1987; Hollibaugh & Wong, 1999), and consequently organic matter mineralisation and nitrification (Owens, 1986; Barnes & Owens, 1998; Goosen *et al.*, 1999; Herman & Heip, 1999), and also denitrification if low oxygen concentrations (Abril *et al.*, 2000), are enhanced.

2.2.1.4 Inorganic and organic substrates

Inputs of dissolved and particulate organic matter (DOM and POM) and inorganic nutrients enter the estuaries mainly through the river or coastal waters, and support autotrophic and heterotrophic activity in different parts of the system (Bianchi, 2006). But in macrotidal and shallow estuaries, resuspension and diffusive fluxes from the bed

sediments also provide important amounts of substrates that support biogeochemical processes.

Inorganic nitrogen, phosphorous and silicon represent the most important nutrients for primary productivity in the aquatic environment since they are, together with light, the limiting factor for phytoplankton growth (Hessen, 1999; Howarth & Marino, 2006). They are also indicators of water quality. An excessive nutrient concentration can trigger excessive production of biomass (HAB/eutrophication), which may result in hypoxic or anoxic waters and its further impacts for the aquatic life (Nixon, 1995; Howarth *et al.*, 1996; Howarth *et al.*, 2000). Inorganic carbon enters living biomass through carbon fixation by autotrophic organisms. This biomass will be transformed back into inorganic carbon via hydrolysis, fermentation, and then mineralisation (respiration or oxidation of the organic carbon via various electron acceptors such as oxygen, manganese oxides, nitrate, iron oxides, and sulphate) (Canfield *et al.*, 2005b).

Organic matter buried into the sediments will be involved in early diagenesis through a combination of biological, chemical and physical processes. In fact, high rates of organic matter oxidation are expected in estuaries due to the high rates of sediment accumulation (Henrichs, 1992). Sediment organic matter is very poorly characterised because it is a mixture of labile and refractory compounds of different molecular weight (from small chemically-identifiable molecules, such as carbohydrates, amino acids or short chain fatty acids, to large macromolecules) (Henrichs, 1992; Seitzinger & Sanders, 1997). The periodic sediment reworking, the oxic-anoxic oscillations and bioturbation are some of the environmental processes that induce re-partitioning of organic substrates between particulate and dissolved phases which has further consequences in their degradability (Middelburg & Herman, 2007). Organic matter becomes more refractory with sediment depth and its fate will depend on the level of early diagenesis that occur in the upper sediments (Henrichs, 1992), which is controlled by the redox conditions and the degradability of the organic detrital input (Bianchi, 2006).

Trace metals are also important inorganic substrates as they are essential micronutrients for microbial metabolism as constituents of important enzymes (e.g. copper or cobalt).

However they can be toxic for microorganisms and inhibit their growth even in very small concentrations (Bruland *et al.*, 1991).

2.2.1.5 Dissolved oxygen

The level of dissolved oxygen (DO) in the estuarine water column determines the type and abundance of the organisms that can live therein. Dissolved oxygen can be produced in photosynthesis or it can come from the atmosphere by diffusion. It is the most favourable of the abundant electron acceptors and is consumed by aerobic heterotrophic bacteria, fungi and decomposer organisms during the breaking down of organic matter (Canfield *et al.*, 2005b). The temperature and salinity influence the solubility of oxygen (oxygen solubility decreases with increasing temperature and salinity). Thus, there are seasonal changes in the DO levels (NOAA, 2008).

Microorganisms can be classified according to their oxygen requirements: obligate aerobes (only grow when oxygen is present), facultative aerobes (oxygen not required but preferred), facultative anaerobes (can tolerate oxygen but grow better without), and obligate anaerobes (only grow in the absence of oxygen). There are also microaerophilic organisms which grow optimally at very low oxygen concentrations (Rheinheimer, 1985). The interfases between oxic and anoxic environments in sediments and also in water columns are sites of intense microbial activity (Canfield *et al.*, 2005b).

2.2.1.6 pH and redox potential

The growth and reproduction of microorganisms is affected by the pH of the medium in which they live. The optimum pH of most aquatic bacteria is between 6.5 and 8.5. In estuarine environments, the pH tends to be constant due to the buffering effect of the chemical composition of seawater; although the biological activity may induce significant pH changes (NOAA, 2008). For example, during photosynthesis, the consumption of CO_2 (which becomes carbonic acid when it dissolves in water) results in higher pH and more alkaline water.

The redox potential (Eh) of the water and sediments of estuaries is also of ecological importance. Redox reactions involve the transfer of electrons between an electron donor

(oxidation reaction) and electron acceptor (reduction reaction). Physiological groups of microorganism can grow only within a range of Eh, therefore the location of the microorganisms promoting different respiration processes in the environment depends on the availability of the electron acceptors and the thermodynamics of the reactions (Stumm & Morgan, 1970; Froelich *et al.*, 1979; Berner, 1981) (see Fig. 2.4 in section 2.3.3). The redox potential can be altered by the microbial activity to a varying extent (Rheinheimer, 1985).

There is evidence of an interesting processes in which one can see the fine relationship between pH, Eh and the microbial activity. Long filamentous bacteria (also known as "cable bacteria") are able to mediate long distance (>1cm) electron transport from sulphide to oxygen in different aquatic sediments (Nielsen *et al.*, 2010; Pfeffer *et al.*, 2012; Risgaard-Petersen *et al.*, 2012). Thus, electric currents directly connect oxygen reduction at the surface with sulphide oxidation in the subsurface through bacterial nanowires. One of the lines of evidence for this electric coupling of spatially separated electrochemical half reactions was distinct pH signatures in the oxic zone (sharp pH increase due to proton consumption during the oxygen reduction) and in the anaerobic zone (proton production consistent with sulphide oxidation) (Nielsen *et al.*, 2010; Risgaard-Petersen *et al.*, 2012). Being able to use spatially separated electron donors and acceptors, cable bacteria are able to monopolise major energy sources and thus have a competitive advantage (Pfeffer *et al.*, 2012).

2.3 Nutrients and geochemical gradients in estuaries

As mentioned in the introduction, estuaries are characterised by strong gradients in many different geochemical factors. These gradients determine which processes are dominant and how is the coupling between them. So biological and chemical processes influence physical and sedimentological processes and vice versa.

2.3.1 Nutrient and major elements cycles

Nutrient loads to estuaries have increased historically with the increase in human population, and agricultural and industrial activities within their catchments (Howarth *et al.*, 1996; Hessen, 1999; Boyer, 2002). The loads of soluble and particulate material

coming into estuaries reflect the nature of the catchment and the type of anthropogenic activities developing therein (Nedwell *et al.*, 1999). However, the transfer of riverine nutrient loads to coastal waters is not direct since an intense nutrient and other elements cycling can take place in the estuarine transition. Therefore estuaries play an important filtering role for DOM and POM, and are considered buffer systems or sinks for organic matter and nutrients (de Jonge *et al.*, 2002). Nutrient loads change spatiotemporally and they will reciprocally influence the biological and physicochemical processes operating in estuaries.

Nutrient cycling in estuaries not only changes the total nutrient loads, but also affects the ratios of nutrients which may have further implications in primary productivity (Hessen, 1999; Nedwell *et al.*, 1999). Although, as has been already discussed, primary productivity contribution to nutrient cycling in turbid estuaries does not appear to be a significant process due to the low light availability (Nedwell & Trimmer, 1996; Jickells, 1998). The bacterial breakdown of the organic matter associated with the sedimented material controls a series of redox reactions that will impact on the nutrient (N, P) and major elements (Fe, Mn, S) cycles.

Bottom sediments are more important than the water column in the budgets of biologically significant elements (Nedwell *et al.*, 1999). The microbial oxidation of organic matter needs of an electron acceptor supply and in the marine environment aerobic respiration and anaerobic sulphate reduction are the main metabolic processes for organic matter mineralisation (Sørensen *et al.*, 1979; Nedwell, 1984). However sulphate is not as abundant when we move towards the freshwater end of an estuary, thus, alternative electron acceptors such as nitrate become important. Consequently, geochemical gradients associated with the availability of electron acceptors happen along the estuarine continuum.

2.3.1.1 The nitrogen cycle

Nitrogen is a key constituent of many important biomolecules and it is an essential nutrient to all living organisms (Canfield *et al.*, 2005a). The N cycle (summarised in Fig. 2.2) is complex because N can be found in different redox states (from -3 to +5) and in a wide variety of forms (particulate, dissolved, organic, inorganic, gas)

(Galloway *et al.*, 2004; Statham, 2012). The redox reactions in which those N compounds are cycled are the base of microbial processes that simultaneously, control the availability of N in the environment (Canfield *et al.*, 2005b).

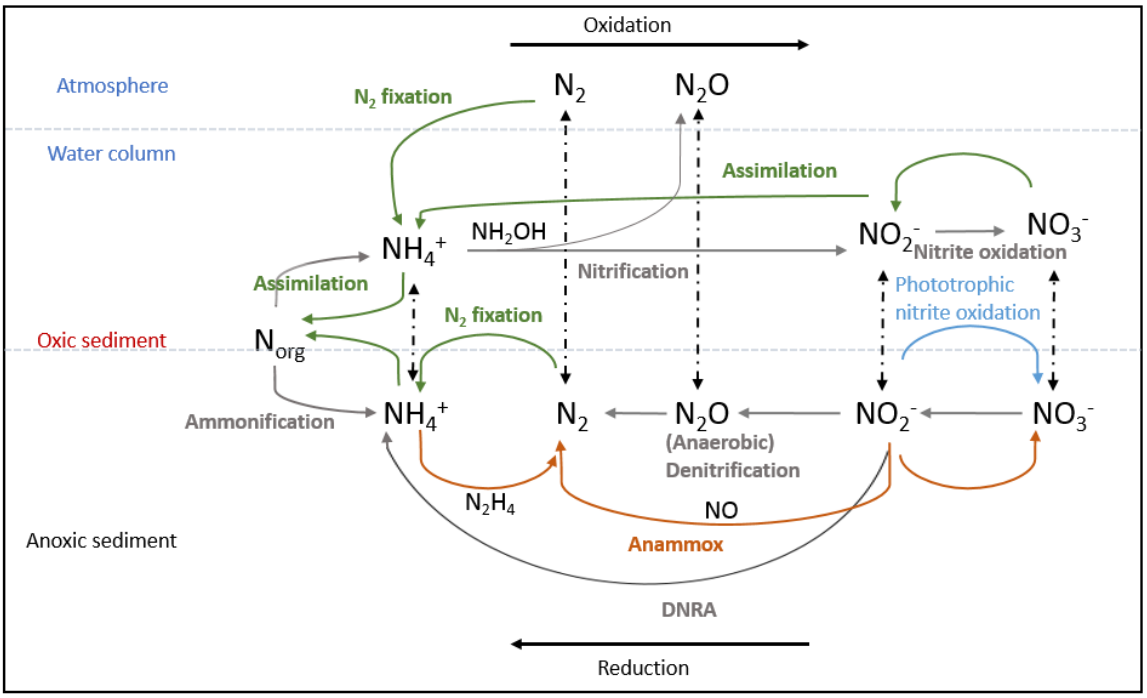

Figure 2.2: Diagram of the Nitrogen cycle. Arrows represent metabolic transformations: assimilation processes in green and dissimilation processes in grey. Dashed vertical arrows indicate exchange or transport between oxic and anoxic zones. After Thamdrup (2012).

River inputs are the main N sources to estuarine waters, although atmosphere and groundwater have been also recognised as important sources. From the total dissolved N inputs to an estuary, inorganic N (DIN) is generally the major portion, especially in hypernutrified estuaries; however organic N (dissolved (DON) or particulate (PON)) may be a significant input in some estuaries (20-90% of the total N load) (Seitzinger & Sanders, 1997). The speciation and distribution of N along the salinity continuum will be controlled by a complex group of dissimilatory and assimilatory transformations coexisting at a range of oxygen concentrations (Thamdrup, 2012); but denitrification is considered the major N-removal process to the atmosphere in shallow aquatic environments (Statham, 2012).

Despite their complexity, we can summarise the microbial N-transforming processes. To start with, atmospheric nitrogen (N_2) is fixed by microbes into ammonia (NH_3) which is biologically available; although N fixation contribution in the N cycling is probably small in estuaries (Nedwell & Trimmer, 1996). Ammonia may be also supplied by the breaking down of organic biomolecules containing N by microbes or animals (ammonification). Ammonium is only stable in reducing conditions. It can be assimilated by microbes and plants or oxidised 1) to nitrite (nitrification) (Owens, 1986) and ultimately to nitrate aerobically or anaerobically by a variety of chemolithoautotrophic prokaryotes (Canfield *et al.*, 2005a); and 2) to N_2 anaerobically in the anammox process (Mulder *et al.*, 1995; Thamdrup & Dalsgaard, 2002). From the resulting oxidised species, nitrate is the most stable in surface oxic waters. Nitrite is less stable, and it is considered an important intermediate product in nitrification, and denitrification. Both can be assimilated by microorganisms or denitrified to N_2 by a variety of heterotrophs (mostly facultative anaerobes) and chemolithoautotrophs (which use nitrate as electron acceptor in the oxidation of reduced inorganic compounds such as H_2, H_2S, Fe^{2+}, or Mn^{2+}). Dissimilatory nitrate reduction to ammonium (DNRA) is another nitrate reduction pathway that will retain N in the system in a bioavailable form (Tiedje *et al.*, 1982; Jørgensen, 1989) and it was found to be as important as denitrification in shallow estuaries and tidal flats (Koike & Hattori, 1978). The anammox process can account for up to 50% of the N_2 production in the marine environment (Thamdrup & Dalsgaard, 2002) and it has been also reported in estuarine systems and coastal sediments, although its importance increases with water depth as denitrification rates attenuate (Thamdrup, 2012). Anammox and DNRA may play a significant role in the N cycle, although their relative importance in different coastal environments is still in discussion (Song *et al.*, 2013; Roberts *et al.*, 2014). Organic N will be cycled during microbial metabolism and thus it also plays an important role in the estuarine geochemistry. However the organic N pool is difficult to characterise as it comprises a wide variety of compounds, the majority of which are complex high molecular weight compounds. These large molecules are more refractory and less bioavailable than low molecular weight compounds which are readily available for microbes and phytoplankton (Seitzinger & Sanders, 1997).

Nitrogen can be trapped in an estuary by primary productivity, organic matter burial and denitrification (Nedwell *et al.*, 1999). In some estuaries denitrification is a major sink for nitrate, although the large proportion of N inputs are removed via transmission to the coastal waters (Jickells *et al.*, 2000). Benthic bacterial denitrification is an important process of inorganic nitrate removal in muddy sediments, where there are high organic matter loads, low oxygen supply and high nitrate concentrations (Jickells, 1998; Teixeira *et al.*, 2010). The loss of intertidal areas due to human activity has supposed the detriment of denitrification capacity and sediment storage in temperate estuaries such as the Humber estuary (Jickells *et al.*, 2000). Among the final products of denitrification, N_2 is the predominant gas, however N_2O, always as a minor product though, seems to be favoured when nitrate concentrations are very high (Nedwell *et al.*, 1999), which is of relevance since N_2O is an important greenhouse gas.

2.3.1.2 Iron and manganese cycling

Iron and Mn are the most important redox-active metals in aquatic sediments and both elements show similarities in terms of geochemistry and microbiology. Iron and Mn cycles are interlinked with other major elements cycles (C, N, P and S) and furthermore they interact with other compounds and TMs of environmental significance (Canfield *et al.*, 2005b). In nature, under oxic conditions and at neutral pH, Mn (generally as Mn^{4+}) and Fe (as Fe^{3+}) are present as Mn and Fe oxides and oxyhydroxides (Stumm & Morgan, 1981), which are normally amorphous and poorly crystalline precipitates with high surface area, high adsorption capacity, and low solubility. They can also be in solution chelated with organic compounds (Canfield *et al.*, 2005b). Iron and Mn oxides will be transported, mixed and eventually buried into anoxic sediments where they will be reduced either abiotically (with sulphides, and also Fe^{2+} in the case of Mn oxides), or biotically by oxidation of organic matter (Postma, 1985; Lovley & Phillips, 1988a; Thamdrup *et al.*, 1994). Microbial Fe reduction can occur deeper in the sediment where it becomes the main C oxidation pathway and inhibits sulphate reduction and methanogenesis (Lovley & Phillips, 1987). There is an intensive redox-cycling of Fe and Mn as both (in their reduced and oxidised forms) react spontaneously with a range of compounds and are involved in a range of microbially mediated processes (Froelich *et al.*, 1979; Straub *et al.*, 1996; Luther *et al.*, 1997; Hulth *et al.*, 1999; Weber *et al.*,

2001; Straub *et al.*, 2004). Soluble Mn and Fe (Mn^{2+} and Fe^{2+}) can diffuse upwards and downwards the sediment profile but they will be trapped in the sediment due to oxidation and precipitation as they approach the oxic surface layer (Thamdrup *et al.*, 1994). Manganese is more mobile and less sensitive to oxygen than Fe^{2+}, so Mn^{2+} can migrate further up than Fe^{2+} in the sediment column towards a more oxidising zones (Postma, 1985). Due to differences in kinetics and thermodynamics, Fe^{2+} does not accumulate until Mn^{4+} is depleted (Froelich *et al.*, 1979; Lovley & Phillips, 1988b). Dissolved manganese could be also removed, mainly by carbonate precipitation, but also by adsorption to clay minerals, formation of metal oxides and precipitation with sulphides. Similarly, Fe^{2+} accumulation is regulated by precipitation in different mineral phases, including carbonates, silicates, phosphates and, preferably, stable iron sulphides (Middelburg *et al.*, 1987; Canfield *et al.*, 2005b; Hedrich *et al.*, 2011). The scavenging capacity of the Fe and Mn oxyhydroxides for TMs plays a key role in the distribution and transport of those in the aquatic sediments (Boyle *et al.*, 1977; Huerta-Diaz & Morse, 1990; Burdige, 1993).

2.3.1.3 The sulphur cycle

Sulphate is one of the major ions in seawater, with concentrations ranging from 24-28 mM, significantly higher than concentrations in freshwaters (0.1 mM). This difference sets an important gradient in estuarine biogeochemical cycling (Bianchi, 2006). Figure 2.3 shows the S cycle from a simplified microbiological perspective, so the reduction of sulphate to sulphide can be assimilatory or dissimilatory. The range of the oxidation states of the compounds involved in these processes goes from +6 (SO_4^{2-}) to -2 (H_2S). Sulphur is an important redox element due to its linkage with other major element and TM cycles, and it plays a key role in the early diagenesis of anoxic sediments (Jørgensen, 1977). Below the oxic and suboxic zones, bacterial sulphate reduction has a dominant role in organic matter mineralization at the sea bed (Jørgensen, 1982) and in most shallow aquatic environments (Canfield *et al.*, 2005b). However some coastal environments have shown metal oxide reduction as the dominant anaerobic C mineralization pathway (Aller, 1990; Canfield, 1993). Most of the sulphide produced will be trapped in the sediments as it precipitates with metal ions and eventually forms pyrite (Jørgensen, 1977). However some of the sulphide can stay in solution and

diffuses upwards to the oxic surface. In its way towards the surface most of the sulphide will be oxidised back to a variety of intermediate S compounds and eventually to sulphate chemically (with MnO_2) or microbially by chemoautotrophic or photoautotrophic sulphur bacteria (Jørgensen, 1977). The group of microorganisms involved in the S cycle is the most diverse of the microbial groups involved in an element cycling (Canfield *et al.*, 2005b). Stable sulphur isotopes have been used to determine the microbial pathways and the origin of the different S-pools (Jørgensen & Cohen, 1977; Peterson & Fry, 1987; Canfield & Raiswell, 1999). However there is still poor understanding of the quantitative importance of the many different intermediate processes of the cycle.

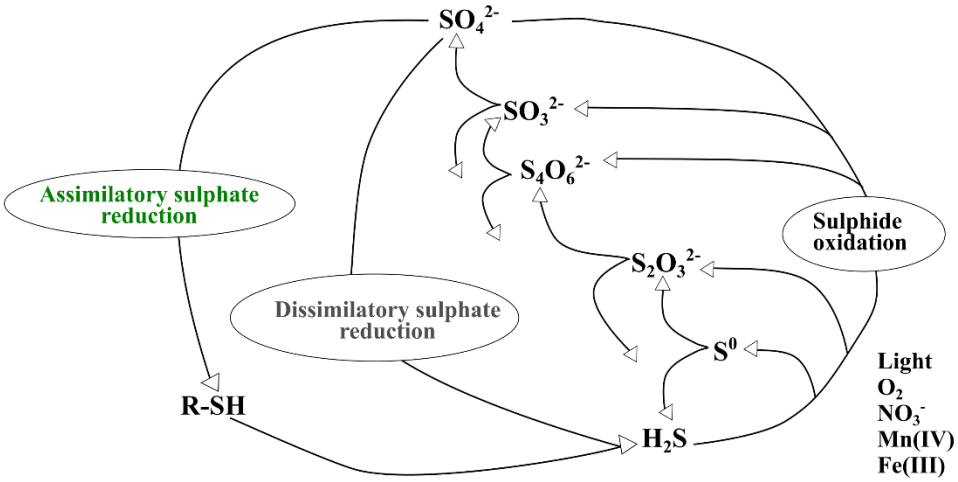

Figure 2.3: Diagram of the S cycle from a microbiological approach. After Canfield *et al.* (2005b).

2.3.2 Salinity gradient

The existence of a salinity gradient, due to fresh and saline waters mix, is the decisive characteristics of an estuary and distinguishes it from other aquatic or coastal environments. Salinity plays a critical role in in these transitional ecosystems since defines physical, chemical and biological features, and their interactions (Telesh & Khlebovich, 2010). In the river water, salinity, in the range of few hundreds of milligrams per litter, is more variable than in the seawater in which stable concentrations of salts are in the range of grams per litter. The salts in the river water

are mainly derived from the weathering of rocks within the catchment and human activities (Bianchi, 2006). The major components of the seawater are Cl^{-}>Na^{+}>SO_4^{2-} >Mg^{2+}>Ca^{2+} and K^{+} (Thurman & Trujillo, 2004). The relatively constant concentrations of these ions in the seawater indicate their non-reactive behaviour and their long residence times, but, in estuaries they can be altered significantly due to a range of processes (dissolution, oxidation, evaporation, etc.) (Bianchi, 2006).

Despite their limitations, "property salinity plots" (see an example in Fig. 6.4) are one of the most used methods to derive fluxes of dissolved constituents in estuaries (Nedwell *et al.*, 1999). This approach assumes that the estuary is well-mixed and is at steady state. So the parameter of interest (normally a dissolved component) is plotted against a conservative index of mixing (salinity or chlorinity) (Morris *et al.*, 1978). Therefore information about the interactive chemical processes involving removal or addition of that component in the estuarine continuum or about the variability of the riverine fluxes and their composition can be inferred. The region of salinities between 5–8 psu has been identify as a "critical salinity zone" and is where the most likely major biotic and abiotic processes show nonlinear dynamics of change (Telesh & Khlebovich, 2010).

2.3.3 Redox gradient

In aquatic sediments, there is a vertical progression of metabolic processes determined by the use of the available electron acceptors during organic matter mineralisation (Canfield & Thamdrup, 2009) (Fig. 2.4). The sequential utilization of the terminal electron acceptors is based on the thermodynamics of the process and the free energy yield (Stumm & Morgan, 1970; Froelich *et al.*, 1979; Berner, 1980) (Table 2.1).

Table 2.1: Principal pathways for organic matter (as acetate) mineralization in nature using different electron acceptors and standard Gibbs free energy associated with the reaction (source Canfield *et al*., 2005b).

	kJ per reaction ΔG (acetate)*
Oxic respiration	-402
$O_2 + 1/2\ C_2H_3O_2^- \rightarrow HCO_3^- + 1/2\ H^+$	
Denitrification	-359
$4/5\ NO_3^- + 3/5\ H^+ + 1/2\ C_2H_3O_2^- \rightarrow 2/5N_2 + HCO_3^- + 1/5\ H_2O$	
Mn reduction	-385
$7/2\ H^+ + 2\ MnO_2 + 1/2\ C_2H_3O_2^- \rightarrow 2\ Mn^{2+} + HCO_3^- + 2\ H_2O$	
Fe reduction (FeOOH)	-241
$15/2\ H^+ + 4\ FeOOH + 1/2\ C_2H_3O_2^- \rightarrow 4\ Fe^{2+} + HCO_3^- + 6\ H_2O$	
Sulphate reduction	-43.8
$1/2\ H^+ + 1/2\ 2SO_4^{2-} + 1/2\ C_2H_3O_2^- \rightarrow 1/2\ H_2S + HCO_3^-$	
Methanogenesis	-19.9
$1/2\ H_2O + 1/2\ C_2H_3O_2^- \rightarrow 1/2\ CH_4 + 1/2\ HCO_3^-$	

At the surface, dissolved oxygen can diffuse a few millimetres into the sediments (the *oxic* zone) where aerobic respiration is the dominant metabolic pathway. Beneath, there is often a suboxic zone, the *nitrogenous* zone, where nitrate (and nitrite as its reduction intermediate) accumulates and is actively reduced. Below or overlapping the *nitrogenous* zone, Mn^{2+} accumulates as a result of Mn reduction (the *manganous* zone). In the upper bound Mn^{2+} can react with oxygen, and maybe nitrite or nitrate (Canfield & Thamdrup, 2009), to Mn(IV) (mainly) and Mn(III). Sometimes, if the oxidation is not completed, Mn^{2+} diffuses upwards into the water column (Thamdrup *et al.*, 1994). Dissolved Fe^{2+} accumulates in the absence of oxygen and normally below nitrate- and Mn-reduction zones as a result of a combination of biotic and abiotic reduction of Fe oxides. This zone will be the *ferruginous* zone, and in its upper limit, Fe^{2+} can be oxidised by oxygen (biotically and abiotically), by nitrate and nitrite (biotically), and by Mn oxides (abiotically). Downward diffusion of Mn^{2+} and Fe^{2+} into anoxic zones may

result in their precipitation with different mineral fractions (carbonates, silicates phosphates and sulphides) (Berner, 1981; Middelburg *et al.*, 1987). In general, besides the effects of advection and bioturbation, Mn and Fe cycling in aquatic sediments implies upward and downward diffusion that depends on concentration gradients and it will be influenced by different environmental factors (pH, oxygen, hydrogen sulphide concentrations, organic matter, SPM, etc.) (Canfield *et al.*, 2005b). Finally, in anoxic conditions, sulphate reduction results in an accumulation of dissolved sulphide (the *sulphidic* zone). Sulphate is the second most abundant anion in seawater and its reduction is the major anaerobic mineralization process in coastal sediments (Jørgensen, 1977, 1982; Middelburg & Levin, 2009). Sulphide is very reactive and the upper bound of the *sulphidic* zone will be defined by its biotic and abiotic reaction with oxygen, nitrate and nitrite, and Mn/Fe oxides. Below, methane is accumulated at depth when sulphate is nearly depleted (Iversen & Jørgensen, 1985); this zone is known as *methanic* zone and methanogenesis will be the main metabolic process therein.

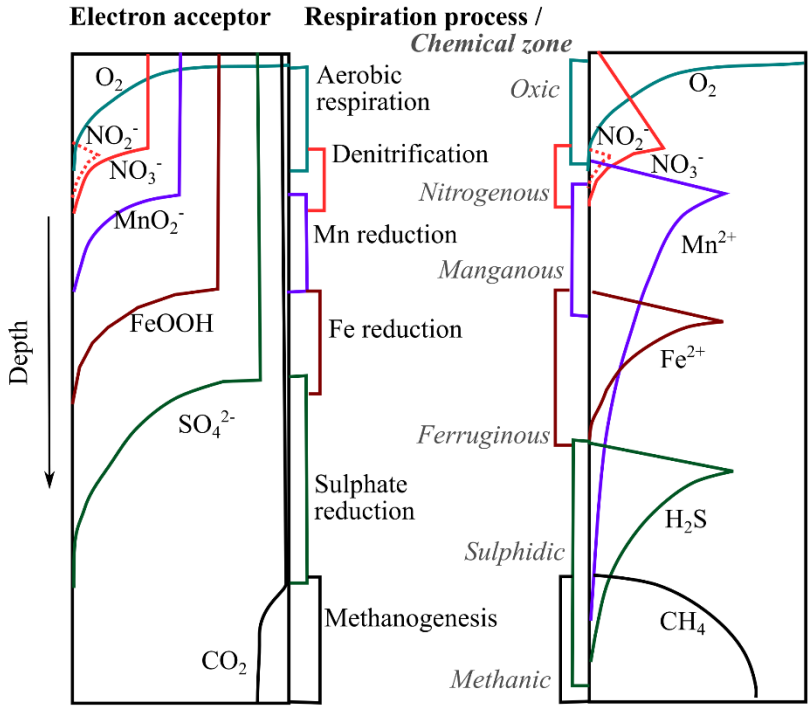

Figure 2.4: Idealised vertical distribution of electron acceptors within the sediment profile (left box) and the chemical zones (italic font) (right box) which typically accompany the respiration process (metabolic zonation). Note the overlap between zones and the not exact coincidence in some cases between chemical and metabolic zonations. After Canfield & Thamdrup (2009).

2.3.4 Contaminants

Among the many different types of pollution (from sewage, agricultural or industrial fluxes, runoff, atmosphere) and pollutants (metals, organic (PCBs and PHAs) and organometallic compounds, pathogens, oil, etc) that an estuary may receive, we will focus here on the trace metals (TMs).

The major inputs of TMs to estuaries are derived from riverine, atmospheric and anthropogenic sources (Millward & Moore, 1982; Du Laing *et al.*, 2009). Trace metal concentrations are typically low (in the order of ppb). Some TMs are micronutrients for many organisms, however they are also important because of their potential toxic effects (Di Toro *et al.*, 1990; Bruland *et al.*, 1991; Allen *et al.*, 1993). In general, metals in solution are more bioavailable and reactive, but the particle associated metals are very important because they may have a long-term impacts since the solid reservoir can

act as a buffer and a secondary source of dissolved metals (Turner & Millward, 2002). Trace metals have shown a non-conservative behaviour in many estuaries (Millward & Turner, 1995). Furthermore, all the metals do not behave in the same way and their behaviour may also vary among estuaries (Millward & Moore, 1982), and hence the difficulties in the study and modelling of TM cycling in the highly variable conditions of an estuary (Millward & Moore, 1982; Turner & Millward, 2002). The complex interactions between the aqueous and solid phases (sorption reactions, coagulation and flocculation, oxidation, precipitation) and the kinetics of such processes can explain some of these differences.

The environmental factors controlling the availability, recycling, transport and fate of TMs in the estuarine system are: redox, SPM, salinity, organic matter, pH, carbonates, and the presence of sulphides. Particularly in estuaries, SPM plays a very significant role in the chemical cycling due to the constant variations in SPM (composition, concentration and reactivity) related to the regular (tidal) and other sporadic resuspension events (Turner & Millward, 2002) (see also Fig. 2.5). Salinity is another important environmental parameter since seawater ions will compete for the sorption sites and there are important complexation reactions (Du Laing *et al.*, 2009). In general, TM mobility increases with increasing salinity. Organic matter influences on TM cycling due to the adsorption, complexation and chelation processes, however it has been associated with either an increase or decrease in TM mobility in different circumstances (Du Laing *et al.*, 2009). Iron, Mn and S cycling have direct links with the TM cycling. Iron and Mn oxides are the main carriers of TMs in oxic conditions, while in anoxic conditions, sulphides will decrease the mobility and availability of TMs via precipitation (Du Laing *et al.*, 2009).

2.4 Estuarine sediments

Estuaries are known as regions of sediment accretion (Schubel & Carter, 1984). Estuarine sediments are derived from a variety of sources such as atmospheric inputs, natural fluvial inputs, continental shelf, in situ chemical and biological processes, shoreline erosion, and anthropogenic activities. Their distribution is controlled by the

geomorphology, the hydrodynamics within the upper reaches of the estuary and tidal/sediment transport processes near the mouth (Bianchi, 2006). In general, sediments are transported mainly as suspended load (bed loads are minor), stored in the estuary, and eventually discharged into the coastal shelf (Mckee & Baskaran, 1999). The suspended load contains clays and silts and its distribution depends on the turbulence and water currents. Conversely, the coarse material (sands, gravel, etc.) is distributed by bed load transport, which includes saltation and is generally slower than the mean flow of water (Bianchi, 2006).

2.4.1 Sediment deposition and depositional features

In general, sediment deposition follows a pattern of sedimentation zones. The head of an estuary is dominated by fluvial deposition and biological inputs become more important in the higher salinity regions. The central region, typically a high productivity zone, is strongly influenced by biological processes such as bioturbation or faecal pellet deposition. At the mouth, sediment deposition is controlled by high energy marine processes (waves, littoral transport, tides). According to Nichols *et al.* (1991) model, the sediment is coarser in the upper estuary, becomes finer at the middle and coarser again at the mouth. The residence time of sediments is very variable (from days to years) since some of the particles entering the estuary with the river flows will remain in suspension and reach the sea fairly quickly, whereas a significant proportion will undergo many cycles of deposition on the bed and (re)suspension (Dyer, 1989).

The tidal classification comprises: microtidal (tidal range of <2 m), mesotidal (tidal range between 2-4 m), and macrotidal (tidal range >4 m) (Hayes, 1975). Tidal-dominated estuaries are characterised by macrotidal ranges and in general these estuaries have a funnel shape with strong tidal currents, enhanced by the large opening at the mouth, that control the transport of river-borne sediments (Wells, 1995). Some common features of many macrotidal estuaries are: subtidal sand ridges, sand wave migration, bordering intertidal mudflats and wetlands (marshes and mangroves). The intertidal area is usually one of the major sources and sinks for suspended sediment within an estuary (Dyer, 1989). Channel sands are the dominant sediment facies near the central and mouth regions, while finer sediments accumulate in the low-energy

margins and the narrow sinuous head of the estuary (Nichols *et al.*, 1991). Differences in physical forcing, carbon loading, remineralisation rates and burial will be reflected in the distinct sedimentary facies.

The four dominant processes controlling estuarine sediment dynamics are: erosion of the bed, transportation, deposition, and consolidation of the deposited sediments (Nichols & Biggs, 1985). Erosion will depend on how cohesive the sediments are, which is related to grain size and shear stress of the bed. The erodibility of the sediment varies spatially and temporally and it is also influenced by the microbial mats and biofilms formed on the sediment surfaces (Bianchi, 2006).

Furthermore neap-spring cycles have implications in the ratio of sedimentation to erosion in an estuary (Allen *et al.*, 1980). During periods of decreasing tidal amplitude, the peak current velocities decrease day by day while the duration of the slack increases; thus the ratio of sedimentation to erosion increases. On the contrary, when tidal range increases, there is net erosion due to the increasing current velocities at each succeeding tide. After the cycle is completed, a proportion of the sediment deposited during neap conditions gets compacted and resists erosion during the following spring tides, creating a thin layer of mud that accumulates in the estuary (Parker *et al.*, 1994) (see also section 2.4.3). Repeated neap-spring cycles have a role in the regulation of the residence time of suspended sediments in the estuary (Allen *et al.*, 1980). In macrotidal estuaries, seaward transport of sediments should be maximum during decreasing spring tides, when there is a residual tidal flow out of the estuary, while during the strongest spring-tides high levels of suspended material are maintained (Allen *et al.*, 1980).

2.4.2 Suspended particulate matter in estuaries

In aquatic environments, and particularly in estuaries due to their elevated concentrations, suspended particles are involved in controlling the reactivity, transport and biological impacts of substances, and provide a crucial link for chemical constituents between the water column, bed sediment and food chain (Turner & Millward, 2002) (see Fig. 2.5). SPM concentrations sometimes are high enough to limit light penetration and, consequently, productivity (Dyer, 1989). Although, SPM concentrations usually decline seawards allowing improved light conditions. Suspended

particles, which include sediments and seston, are suspended more or less temporarily in the water column, and are in continuous exchange with the bed sediment reservoir. The seston refers to biogenic material formed in situ (plankton, bacteria, invertebrate larvae and eggs, and assemblages thereof), and has a strong seasonal component. On the other hand, suspended sediments (mud, silt, sand and colloidal aggregates) include actually a complex assemblage of mineral, biotic and anthropogenic material (Turner & Millward, 2002).

Fine particles are cohesive and readily flocculate. Coagulation leads to the formation of: agglomerates (organic and inorganic matter weakly bound), aggregates (inorganic matter strongly bound) and floccules (non-living biogenic material bound by electrochemical forces) (Schubel, 1971). Moreover, coagulation is favoured as salinity increases because the repulsive forces between negatively charged particles, which prevent their flocculation, are destabilised by the increasing concentration of cations (positively charged) in solution (Stumm & Morgan, 1970). The salinity conditions and tidal gradients found in estuaries are ideal for coagulation processes, together with other factors, such as DOM, concentration and composition of SPM, particle size, etc. (Bianchi, 2006). Grain size is particularly important and sometimes is used to further classify SPM due to its implications in settling characteristics, residence time, and in the biogeochemical cycles (Dyer, 1989; Turner & Millward, 2002).

In estuaries, SPM concentrations show important spatiotemporal variations. Sediments are resuspended regularly in a normal tidal cycle, but also in occasional events related to weather conditions (winds, seasonal storms, rainfall, and floods) which will have further implications for the concentration and character of SPM. The role of suspended particles is also significant in estuarine systems because of the modification of chemical and particle reactivities by abrupt changes in salinity, pH, redox conditions and DOM (Turner & Millward, 2002). A wide variety of pollutants that have an affinity for fine particles can be trapped within the estuarine circulation system. For example, TMs can enter estuaries through river loads bound to particles and then, particle-water interactions during estuarine transport may enhance the particulate TM concentrations (Millward & Glegg, 1997). Thus the retention of contaminated sediments in estuaries

delays their transport to the ocean, and so, estuaries may become a long-term source of pollutants to the coastal waters as a result of internal cycling (Millward & Glegg, 1997; Mitchell, 1998).

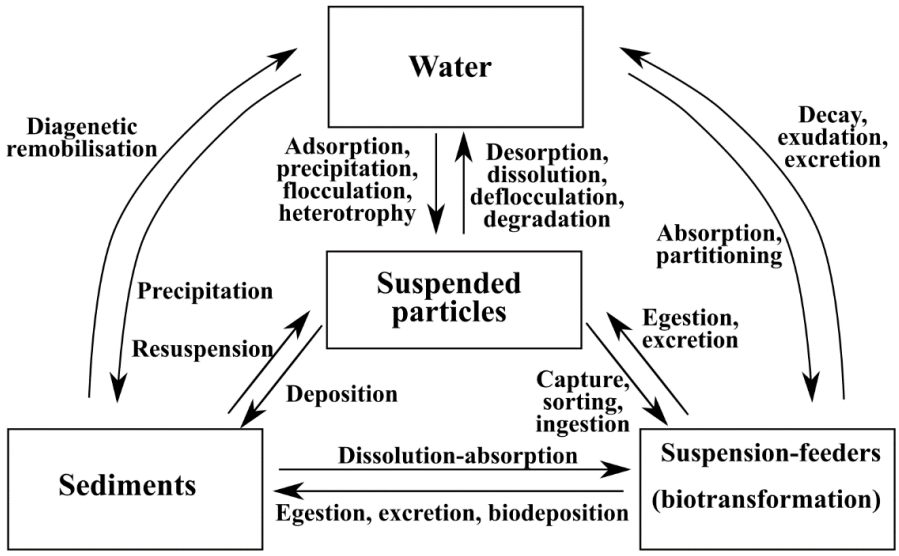

Figure 2.5: Summary diagram of the role of SPM in estuarine biogeochemical processes. The boxes represent the reservoirs of materials and chemicals, arrows represent physical and biogeochemical processes between compartments (after Turner & Millward, 2002).

2.4.3 Resuspension, estuarine turbidity maximum and fluid muds

Transport of water and suspended sediments in estuaries is a combination of density circulation (resulting from density gradients between fresh and sea water) and tidal processes; and the trapping of fine sediments in the upper and middle regions of an estuary is the main effect (Allen *et al.*, 1980). The mixing of fresh and saline water is a fundamental process because it controls the nature of longitudinal and vertical density gradients, and consequently the estuarine density circulation. Also turbulence, due to river and/or tidal currents, results in mixing and diffusion (Allen *et al.*, 1980).

In partly-mixed and well-mixed estuaries the freshwater-saltwater interface is associated with a region of high SPM concentration known as TMZ and it delimits the

intrusion of brackish waters into freshwaters within an estuary (Uncles *et al.*, 1998b). The TZM is a significant feature of an estuary and indicates the magnitude of sediment mobility (Dyer, 1989). By definition, the TZM is the region where SPM concentrations are significantly higher (10-100 times) than in adjacent fluvial or coastal waters (Schubel, 1968), often >10 g L^{-1} (Mitchell, 1998). The TMZ is located at the head of the estuary, but its position has a strong seasonal behaviour as it moves upstream and downstream the estuary depending on the freshwater inflow (Mitchell, 1998; Uncles *et al.*, 1998b). The turbidity maximum is often associated with an oxygen minimum and is generally considered an area of high microbial activity (nitrification-denitrification) as a result of bacterial association with the periodically resuspended particles (Owens, 1986; Plummer *et al.*, 1987; Barnes & Owens, 1998; Goosen *et al.*, 1999; Herman & Heip, 1999; Hollibaugh & Wong, 1999; Abril *et al.*, 2000).

The dynamics of the turbidity maximum is influenced by river flow, tidal amplitude variations, channel morphology, wind strength and direction, and sediment availability through a series of complex mechanisms involving turbulence, gravitational circulation, tidal asymmetry, tidal straining of particles on the ebb tide, solute transport, flocculation, sedimentation, erosion and consolidation processes (Allen *et al.*, 1980; Dyer, 1989; Mitchell, 1998). Particle trapping efficiency increases in the vicinity of the salt wedge front because density stratification supresses turbulent mixing (Geyer, 1993). Therefore, during ebb tide, the seaward flow in the lower layer favours the settling of materials in a highly stratified particle trapping zone. The cycles of resuspension and settling of this bulk of fine sediment material are intense (Grabemann *et al.*, 1997), and so, during flood tide, when erosion dominates, it will be redistributed landwards (Geyer, 1993).

Sedimentation rates are rapid and high in the TMZ, and so the trapping of particles in this benthic boundary layer can result in the formation of "fluid muds" (Allen *et al.*, 1980; Parker *et al.*, 1994). The fluid muds are described as a highly concentrated, high viscosity, benthic layer with SPM concentrations >10 g L^{-1} (may be >100); they are formed in many macrotidal estuaries at neap tides and show oxic/anoxic character with the tidal oscillations (Abril *et al.*, 2000). During spring tides, vertical stratification may

be disrupted and the fluid muds are more dispersed, so they will be called mixed or mobile muds instead (Bianchi, 2006).

2.5 The Humber Estuary

The Humber Estuary (Fig. 2.6) is a macrotidal and well-mixed estuary located on the east coast of Northern England, although it shows a weak vertical halocline in the outer part (Pethick, 1990). The tidal range, one of the largest in the word, varies between 2.5 and 7.2 m. It is the largest estuarine system in England in terms of catchment area (26,000 km^2, 20% of the area of England) and, it represents the largest freshwater contribution to the North Sea from all the British rivers (236 m^3 s^{-1} as an annual average) (Neale, 1988; Neal & Davies, 2003). It is considered a major source of nutrients to the North Sea, and these nutrient loads are affected by the agricultural, industrial and urban activities within the basin (Pethick, 1990; Uncles *et al.*, 1998a). The catchment area is very diverse in terms of natural environment and land use, including former coal and metal-mining areas, and so it is possible to distinguish between the more rural northern rivers (Derwent, Swale, Ure, Nidd and Wharfe, all tributaries of the River Ouse), and the more urban and industrial southern rivers (Aire and Calder which are tributaries of the Ouse, plus the Don and the Trent) (Jarvie *et al.*, 1997). The estuary has been heavily industrialised, hosts major ports, oil and gas refineries, receives several industrial and sewage discharges, and it is continuously dredged for maintenance of the shipping channels (Cave *et al.*, 2005). It has been estimated that the area surrounding the Humber reached its peak in pollution in the 50−70s (Lee & Cundy, 2001).

The Ouse and Trent Rivers are the main systems contributing to the freshwater flow to the Humber and they meet at the Trent Falls (62 km west of the Spurn Point). Upland, the tidal effect is limited by artificial locks and weirs and it reaches to the Naburn Weir (~60 km from the Humber) on the Ouse River and to the Cromwell Weir (~80 km to the Humber's confluence at Trent falls) on the Trent River.

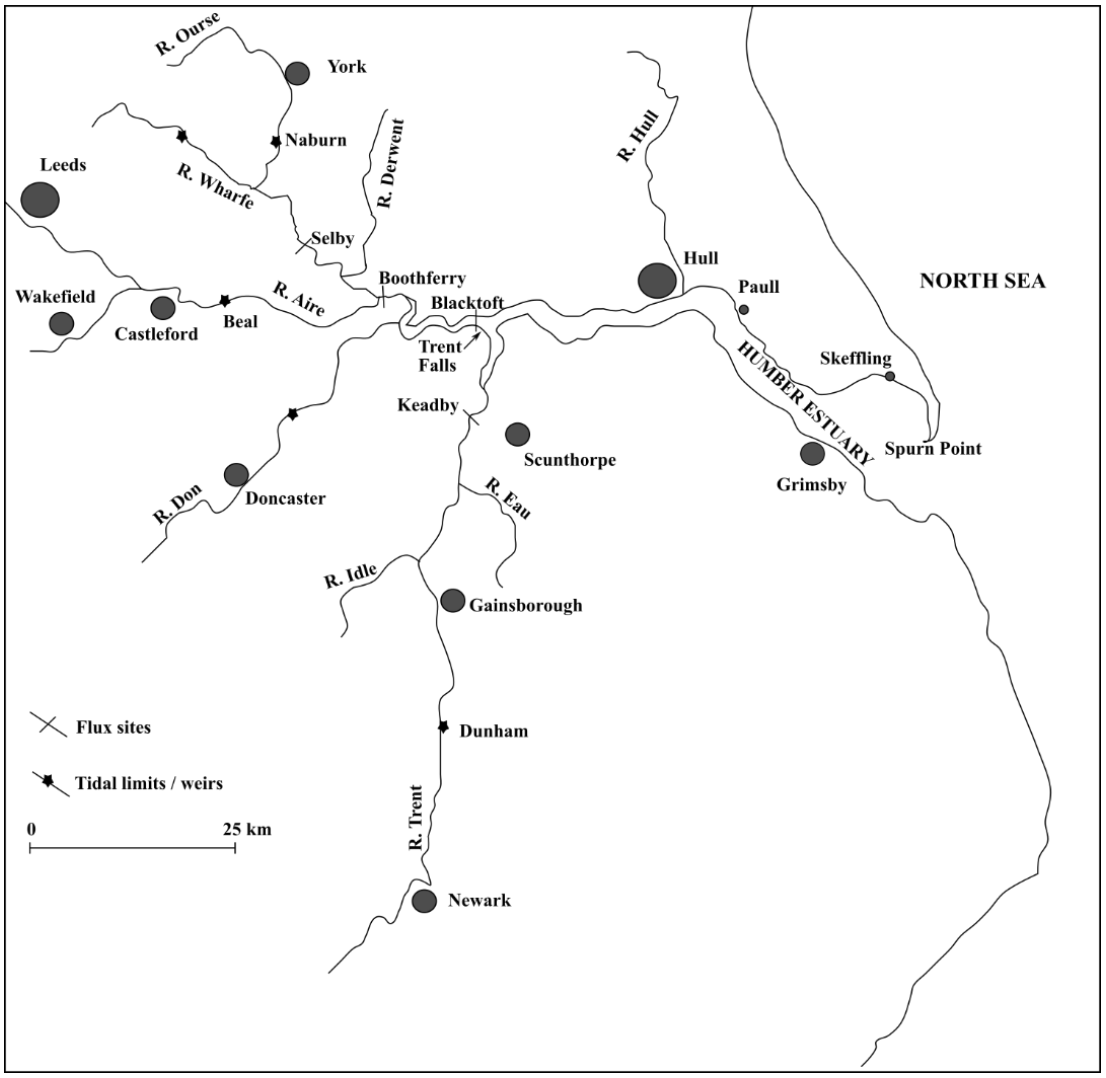

Figure 2.6: Map of the Humber catchment and its main tributaries.

2.5.1 Meteorology

The climate in the catchment area is characterised by an annual temperature of ~10°C approximately, with maximum temperatures in the range of 5-8 and 19-23°C in winter and summer respectively. In general the area receives an average annual rainfall of less than 700 mm (Met Office, 2012) which is associated with Atlantic depressions and convection, and it is well spread over the year. The area is considerable sunnier than most areas at this latitude in the British Islands and also drier due to the rain shadowing effect of the Pennines (Met Office, 2012).

2.5.2 Geology and geomorphology

The geology of the Humber catchment shows a variation from east to west (Jarvie *et al.*, 1997). In draining a fifth of England, the materials coming to the estuary reflect the different drainage surfaces they come from (Neale, 1988). The rivers of the western side of the Humber catchment (the Ouse catchment) flow eastwards across the Carboniferous rocks of the Pennines and the Triassic Sandstones of the Vale of York (Jarvie *et al.*, 1997). The Derwent drains an area of younger Jurassic Limestone and Clays of the North York Moors before joining the Ouse. On the other hand, the Trent drains a large part of the East Midlands, a more lowland system composed by several divisions of the Permian and Triassic (New Red Sandstone-aged sedimentary rocks), which are often overlain by superficial glacial deposits. The Trent also contains water from tributaries coming through Carboniferous rocks (from the Derbyshire Moors in the North Midlands) and Jurassic Limestone and Clays to the south east (Neale, 1988; Jarvie *et al.*, 1997).

The Quaternary period had a great influence on the Humber catchment. The majority of the deposits of this period have been attributed to the first part of the last glaciation (Devesian, 18,000-13,000 years BP) (Catt, 1990; Jarvie *et al.*, 1997). The drainages were blocked during the glaciation, and the resulting impounded lake accumulated several metres of laminated clays on its bed. When the Devesian ice melted away, the new coastline was positioned about 40 km eastwards of the pre-glaciation (Ipswichian period) coastline, and a network of streams draining towards the Humber developed across the exposed surface of the lake clays. These streams became the present-day rivers. During the early Holocene (12,000 years BP), sea level was low and rivers cut down deep valleys into the glacial deposits which, as the sea level rose, accumulated fine (silts and clays) alluvium (Jarvie *et al.*, 1997). The sea level reached the present level 6,000 years ago and, since then, the outline of the Humber has been developed.

The current geomorphology of the Humber reflects three centuries of urbanisation and land reclamation (Jickells *et al.*, 2000) and 405 km of coastal defences protect the Humberside from river and sea floodings (Andrews *et al*., 2006). Alteration of the river courses, draining low-lying lands, and reclamation processes, such as the practice

known as ‘warping’, are the principal human activities that have influenced fluvial processes. For example, during the warping water is retained by low walls or bunds at high tide and the suspended sediments are allowed to settle before the water is drained away (at low tide). This practice of sediment deposition, was carried out from the mid-eighteenth to the mid-twentieth century in the Humber area and has produced soils of great agricultural value in the banks of the estuary (Jarvie *et al.*, 1997).

2.5.3 Sediments, tidal processes and turbidity in the Humber Estuary

Tidal processes are the dominant processes controlling sediment transport in the Humber Estuary. It has been estimated that most of the sediment entering the Humber comes from the flooding marine tide, ca. 2.2×10^{6} m^{3} a^{-1}, compared to just 0.3×10^{6} m^{3} a^{-1} from rivers (Andrews *et al.*, 2008). Or in other words, the total annual SPM loads from the rivers is approximately equivalent to the sea-born sediment carried on a single storm tide into the estuary. Nearly 90% of the sediments carried up into the Humber by the currents and tidal flow are derived from the rapid erosion of the Holderness cliffs which are situated immediately north of the Spurn Point (Albakri, 1986; Jickells *et al.*, 2000; Cave *et al.*, 2005). However, only a small proportion (similar to the quantity brought in to the estuary by river flows) of these sediments is actually deposited (Cave *et al.*, 2005) because most is continuously resuspended and eventually re-exported to the North Sea (Jickells *et al.*, 2000). It has been estimated that the residence time for a standard particle in the Humber is ca. 18 years, whereas the residence time of estuarine water for the whole system is between 40-60 days (Millward & Glegg, 1997; Uncles *et al.*, 1998d). The continuous processes of erosion and deposition over each tidal cycle prevent the mobile sediment pool from settling and, hence to become part of a consolidated bed (Mitchell, 2005).

The estuarine channel is floored by sand and muds which alternate. They overlay glacial till (boulder clay). Mud deposits (medium silt class) dominate, although it changes into more sandy-silt deposits near the low water mark in the outer estuary and into silty-clay in the middle estuary (Freestone, 1987). The central channels, through where the strongest currents flow, contain instead coarser (sands) deposits (Freestone, 1987; Pethick, 1988).

The strong tidal asymmetry of the Humber results in high variations in the current velocities especially in the upper estuary. There is a short and fast flood tide (2-3 hrs, speed ca. 2 m s^{-1}), followed by a long slack period of slower ebb (~10 hrs) (Uncles & Stephens, 1999). This asymmetry is translated in an imbalanced transport of sediments into and out of the estuary. Thus, the weaker currents of the falling ebb do not evacuate the same amount of sediments carried into the estuary during the rising flood. It is the rapid narrowing inland which causes the reflection of the tidal wave in the Humber. As the reflected wave meets the oncoming wave, they cancel each other since the current flows are opposite, and so the water level is not the highest at this point. The fact that the fastest currents do not coincide at highest water level, explains the depositional processes along the banks of the estuary, on which so much of the human activity in the estuary depends (Pethick, 1988).

The Humber, as a macrotidal estuary, is typically very turbid. The concentrations of SPM exhibit important seasonal and longitudinal variability and are in the range of <10 mg L^{-1} in the tidal river to >10,000 mg L^{-1} in the TMZ (Uncles *et al.*, 2006). These concentrations are significantly greater compared to those found in other microtidal estuaries (400-700 mg L^{-1} (Weser estuary, Germany); 1000 mg L^{-1} (Seine estuary, France); 300-400 mg L^{-1} (Scheldt estuary, Belgium); Mitchell, 2013). The turbidity maximum is a strong feature of the Humber, however it is very variable and not static. It develops at salinities between 0-10 psu (Uncles *et al.*, 1998b) and normally, SPM within the TMZ has higher concentrations in the tidal Ouse (10-30 g L^{-1}, a peak of 35 g L^{-1} was observed in the summer of 1995) than in the tidal Trent (10-15 g L^{-1}) (Mitchell, 2005). The location of TMZ shows strong seasonal displacement (Uncles *et al.*, 1998b). During the summer and early autumn, the flood-ebb asymmetry moves the turbidity maximum up-estuary of the freshwater and seawater interface. During the winter and spring, when the river flows are greater, it is flushed down-estuary into more saline waters. However, in this period of the year, Uncles *et al.* (1998b) pointed that the level of SPM in this area of weaker tidal asymmetry can be maintained by the enhanced accumulation of fine sediments due to the stronger gravitational circulation in deeper high-saline waters. The TZM plays a major role in the nutrient, TM and organic matter cycling.

2.6 References

[1] Abril, G., Riou, S. A., Etcheber, H., Frankignoulle, M., de Wit, R., & Middelburg, J. J. (2000). Transient, tidal time-scale, nitrogen transformations in an estuarine turbidity maximum-fluid mud system (The Gironde, south-west France). *Estuarine Coastal and Shelf Science*, 50(5), pp.703-715. doi: 10.1006/ecss.1999.0598

[2] Albakri, D. (1986). Provenance of the sediments in the Humber estuary and the adjacent coasts, Eastern England. *Marine Geology*, 72(1-2), pp.171-186. doi: 10.1016/0025-3227(86)90105-2

[3] Allen, G. P., Salomon, J. C., Bassoullet, P., Dupenhoat, Y., & Degrandpre, C. (1980). Effects of tides on mixing and suspended sediment transport in macro-tidal estuaries. *Sedimentary Geology*, 26(1-3), pp.69-90. doi: 10.1016/0037-0738(80)90006-8

[4] Allen, H. E., Fu, G. M., & Deng, B. L. (1993). Analysis of acid-volatile sulfide (AVS) and simultaneously extracted metals (SEM) for the estimation of potential toxicity in aquatic sediments. *Environmental Toxicology and Chemistry*, 12(8), pp.1441-1453. doi: 10.1897/1552-8618(1993)12[1441:aoasaa]2.0.co;2

[5] Aller, R. C. (1990). Bioturbation and manganese cycling in hemipelagic sediments. *Philosophical Transactions of the Royal Society a-Mathematical Physical and Engineering Sciences*, 331(1616), pp.51-68. doi: 10.1098/rsta.1990.0056

[6] Aller, R. C. (1994). The sedimentary Mn cycle in Long-Island Sound - its role as intermediate oxidant and the influence of bioturbation, O_2, and C(org) flux on diagenetic reaction balances. *Journal of Marine Research*, 52(2), pp.259-295. doi: 10.1357/0022240943077091

[7] Andrews, J. E., Burgess, D., Cave, R. R., Coombes, E. G., Jickells, T. D., Parkes, D. J., & Turner, R. K. (2006). Biogeochemical value of managed realignment, Humber estuary, UK. *Science of The Total Environment*, 371(1-3), pp.19-30. doi: 10.1016/j.scitotenv.2006.08.021

[8] Andrews, J. E., Samways, G., & Shimmield, G. B. (2008). Historical storage budgets of organic carbon, nutrient and contaminant elements in saltmarsh sediments: Biogeochemical context for managed realignment, Humber Estuary, UK. *Science of The Total Environment*, 405(1-3), pp.1-13. doi: 10.1016/j.scitotenv.2008.07.044

[9] Attrill, M. J. (2002). A testable linear model for diversity trends in estuaries. *Journal of Animal Ecology*, 71(2), 262-269. doi: 10.1046/j.1365-2656.2002.00593.x

[10] Barnes, J., & Owens, N. J. P. (1998). Denitrification and nitrous oxide concentrations in the Humber estuary, UK, and adjacent coastal zones. *Marine Pollution Bulletin*, 37(3-7), pp.247-260.

[11] Berner, R. A. (1980). *Early diagenesis: A theoretical approach*. New York: Princeton University Press.

[12] Berner, R. A. (1981). A new geochemical classification of sedimentary environments. *Journal of Sedimentary Petrology*, 51(2), pp.359-365.

[13] Bianchi, T. S. (2006). *Biogeochemistry of Estuaries*. New York: Oxford University Press.

[14] Boyer, E. W., Goodale, Christine L., Jaworski, Norbert A., Howarth, R.W. . (2002). Anthropogenic nitrogen sources and relationships to riverine nitrogen export in the northeastern USA. *In:* Boyer E.W., and Howarth, R.W. (Eds.), *The Nitrogen Cycle at Regional to Global Scales*. Dordrecht, Netherlands: Kluwer Academic Publishers, pp. 137-169.

[15] Boyle, E. A., Edmond, J. M., & Sholkovitz, E. R. (1977). The mechanism of iron removal in estuaries. *Geochimica et Cosmochimica Acta*, 41, pp.1313-1324. doi: 10.1016/0016-7037(77)90075-8

[16] Bruland, K. W., Donat, J. R., & Hutchins, D. A. (1991). Interactive influences of bioactive trace-metals on biological production in oceanic waters. *Limnology and Oceanography*, 36(8), pp.1555-1577.

[17] Burdige, D. J. (1993). The biogeochemistry of manganese and iron reduction in marine-sediments. *Earth-Science Reviews*, 35(3), pp.249-284. doi: 10.1016/0012-8252(93)90040-e

[18] Canfield, D. E. (1993). Organic matter oxidation in marine sediments. *In:* Wollast, R., Mackenzie, F.T., Chou, L. (Eds.) *Interactions of C, N, P and S biogeochemical Cycles and Global Change*. Berlin: Springer, pp.333-363

[19] Canfield, D. E., & Raiswell, R. (1999). The evolution of the sulfur cycle. *American Journal of Science*, 299(7-9), pp.697-723. doi: 10.2475/ajs.299.7-9.697

[20] Canfield, D. E., Kristensen, E., & Thamdrup, B. (2005a). The Nitrogen Cycle. *In:* Southward, A.J., Tyler, P.A., Young, C.M. and Fuiman, L.A. (Eds), *Aquatic Geomicrobiology*. London: Elsevier Academic Press, pp. 205-267

[21] Canfield, D. E., Kristensen, E., & Thamdrup, B. (2005b). *Aquatic Geomicrobiology*. Advances in Marine Biology. London: Elsevier Academic Press.

[22] Canfield, D. E., & Thamdrup, B. (2009). Towards a consistent classification scheme for geochemical environments, or, why we wish the term 'suboxic' would go away. *Geobiology*, 7(4), pp.385-392. doi: 10.1111/j.1472-4669.2009.00214.x

[23] Catt, J. A. (1990). Geology and Relief. *In:* Ellis S. and Crowther, D.R. (Eds.), *Humber Perspectives, A region through the ages*. Hull: Hull University, pp. 13-28.

[24] Cave, R. R., Andrews, J. E., Jickells, T., & Coombes, E. G. (2005). A review of sediment contamination by trace metals in the Humber catchment and estuary, and the implications for future estuary water quality. *Estuarine, Coastal and Shelf Science*, 62(3), pp.547-557. doi: 10.1016/j.ecss.2004.09.017

[25] Cole, J. J., Caraco, N. F., & Peierls, B. L. (1992). Can phytoplankton maintain a positive carbon balance in a turbid, fresh-water, tidal estuary. *Limnology and Oceanography*, 37(8), pp.1608-1617.

[26] Crump, B. C., Armbrust, E. V., & Baross, J. A. (1999). Phylogenetic analysis of particle-attached and free-living bacterial communities in the Columbia river, its estuary, and the adjacent coastal ocean. *Applied and Environmental Microbiology*, 65(7), pp.3192-3204.

[27] Crump, B. C., Hopkinson, C. S., Sogin, M. L., & Hobbie, J. E. (2004). Microbial biogeography along an estuarine salinity gradient: Combined influences of bacterial growth and residence time. *Applied and Environmental Microbiology*, 70(3), pp.1494-1505. doi: 10.1128/aem.70.3.1494-1505.2004

[28] de Jonge, V. N., Elliott, M., & Orive, E. (2002). Causes, historical development, effects and future challenges of a common environmental problem: eutrophication. *Hydrobiologia*, 475(1), pp.1-19. doi: 10.1023/a:1020366418295

[29] Di Toro, D. M., Mahony, J. D., Hansen, D. J., Scott, K. J., Hicks, M. B., Mayr, S. M., & Redmond, M. S. (1990). Toxicity of cadmium in sediments the role of acid volatile sulfide. *Environmental Toxicology and Chemistry*, 9(12), pp.1487-1502. doi: 10.1002/etc.5620091208

[30] Du Laing, G., Rinklebe, J., Vandecasteele, B., Meers, E., & Tack, F. M. G. (2009). Trace metal behaviour in estuarine and riverine floodplain soils and sediments: A review. *Science of The Total Environment*, 407(13), pp.3972-3985. doi: 10.1016/j.scitotenv.2008.07.025

[31] Dyer, K. (1989). Sediment processes in estuaries: future research requirements. *Journal of Geophysical Research: Oceans*, 94(C10), pp.14327-14339.

[32] Federle, T. W., Hullar, M. A., Livingston, R. J., Meeter, D. A., & White, D. C. (1983). Spatial-distribution of biochemical parameters indicating biomass and community composition of microbial assemblies in estuarine mud flat sediments. *Applied and Environmental Microbiology*, 45(1), pp.58-63.

[33] Freestone, D., Jones, N., North, J.,Pethick, J., Symes, D., and Ward, R. (1987). The Humber Estuary, Environmental Background: Institute of Estuarine and Coastal Studies.

[34] Froelich, P. N., Klinkhammer, G. P., Bender, M. L., Luedtke, N. A., Heath, G. R., Cullen, D., Dauphin, P., Hammond, D., Hartman, B., & Maynard, V. (1979). Early oxidation of organic-matter in pelagic sediments of the eastern equatorial atlantic - suboxic diagenesis. *Geochimica et Cosmochimica Acta*, 43(7), pp.1075-1090. doi: 10.1016/0016-7037(79)90095-4

[35] Galloway, J. N., Dentener, F. J., Capone, D. G., Boyer, E. W., Howarth, R. W., Seitzinger, S. P., Asner, G. P., Cleveland, C. C., Green, P. A., Holland, E. A., Karl, D. M., Michaels, A. F., Porter, J. H., Townsend, A. R., & Vorosmarty, C. J. (2004). Nitrogen cycles: past, present, and future. *Biogeochemistry*, 70(2), pp.153-226. doi: 10.1007/s10533-004-0370-0

[36] Garnier, J., Billen, G., Even, S., Etcheber, H., & Servais, P. (2008). Organic matter dynamics and budgets in the turbidity maximum zone of the Seine Estuary (France). *Estuarine Coastal and Shelf Science*, 77(1), pp.150-162. doi: 10.1016/j.ecss.2007.09.019

[37] Geyer, W. R. (1993). The Importance of Suppression of Turbulence by Stratification on the Estuarine Turbidity Maximum. *Estuaries*, 16(1), pp.113-125.

[38] Goosen, N. K., Kromkamp, J., Peene, J., van Rijswik, P., & van Breugel, P. (1999). Bacterial and phytoplankton production in the maximum turbidity zone of three European estuaries: the Elbe, Westerschelde and Gironde. *Journal of Marine Systems*, 22(2-3), pp.151-171. doi: 10.1016/s0924-7963(99)00038-x

[39] Grabemann, I., Uncles, R. J., Krause, G., & Stephens, J. A. (1997). Behaviour of turbidity maxima in the Tamar (UK) and Weser (FRG) estuaries. *Estuarine Coastal and Shelf Science*, 45(2), pp.235-246. doi: 10.1006/ecss.1996.0178

[40] Gray, J. S., & Elliott, M. (2009). *Ecology of marine sediments: from science to management*. 2nd ed. New York: Oxford University Press.

[41] Gross, M. G. (1976). *Oceanography*. Columbus, Ohio: C. E. Merrill Publishing Company.

[42] Hayes, M. O. (1975). Morphology and sand accumulations in estuaries. *In*: Cronin L.E. (Ed.), *Estuarine Research*. New York: Academic Press, pp. 3-22.

[43] Hedrich, S., Schloemann, M., & Johnson, D. B. (2011). The iron-oxidizing proteobacteria. *Microbiology-Sgm*, 157, pp.1551-1564. doi: 10.1099/mic.0.045344-0

[44] Henrichs, S. M. (1992). Early diagenesis of organic matter in marine sediments: progress and perplexity. *Marine Chemistry*, 39(1), pp.119-149. doi: http://dx.doi.org/10.1016/0304-4203(92)90098-U

[45] Herman, P. M. J., & Heip, C. H. R. (1999). Biogeochemistry of the MAximum TURbidity Zone of Estuaries (MATURE): some conclusions. *Journal of Marine Systems*, 22(2-3), pp.89-104. doi: 10.1016/s0924-7963(99)00034-2

[46] Hessen, D. O. (1999). Catchment properties and the transport of major elements to estuaries. *In:* Nedwell D. B. & Raffaelli D. G. (Eds.), *Advances in Ecological Research, Estuaries*. San Diego: Academic Press, pp.1-41.

[47] Hobbie, J. E. (2000). Estuarine Science: the key to progress in coastal ecological research. *In*:. Hobbie J. E, (Ed.), *Estuarine Science: A Synthetic Approach to Research and Practice*. Washington DC: Island Press, pp.1-11.

[48] Hollibaugh, J. T., & Wong, P. S. (1999). Microbial processes in the San Francisco Bay estuarine turbidity maximum. *Estuaries*, 22(4), pp.848-862. doi: 10.2307/1353066

[49] Howarth, R., Andreson, D., Cloern, J., Elfring, C., Hopkinson, C., Lapointe, B., Malone, T., Marcus, N., McGlathery, K., Sharpley, A., & Walker, D. (2000). *Nutrient Pollution of Coastal Rivers, Bays and Seas*. Issues in Ecology: Ecological Society of America.

[50] Howarth, R. W., Billen, G., Swaney, D., Townsend, A., Jaworsky, N., Lajtha, K., Downing, J. A., Elmgren, R., Caraco, N., Jordan, T., Berendse, F., Freney, J., Kudeyarov, V., Murdoch, P., & Zhao-Liang, Z. (1996). Regional Nitrogen budgets and riverine N & P fluxes for the drainages to the North Atlanthic Ocean: natural and human influences. *Biogeochemistry*, 35, pp.75-139. doi: 10.1007/BF02179825

[51] Howarth, R. W., & Marino, R. (2006). Nitrogen as the limiting nutrient for eutrophication in coastal marine ecosystems: Evolving views over three decades. *Limnology and Oceanography*, 51(1), pp.364-376. doi: 10.4319/lo.2006.51.1_part_2.0364

[52] Huerta-Diaz, M. A., & Morse, J. W. (1990). A quantitative method for determination of trace metal concentrations in sedimentary pyrite. *Marine Chemistry*, 29(2-3), pp.119-144. doi: 10.1016/0304-4203(90)90009-2

[53] Hulth, S., Aller, R. C., & Gilbert, F. (1999). Coupled anoxic nitrification manganese reduction in marine sediments. *Geochimica et Cosmochimica Acta*, 63(1), pp.49-66. doi: 10.1016/s0016-7037(98)00285-3

[54] Iversen, N., & Jørgensen, B. B. (1985). Anaerobic methane oxidation rates at the sulfate methane transition in marine-sediments from Kattegat and Skagerrak (Denmark). *Limnology and Oceanography*, 30(5), pp.944-955.

[55] Jarvie, H. P., Neal, C., & Robson, A. J. (1997). The geography of the Humber catchment. *Science of The Total Environment*, 194, pp.87-99. doi: 10.1016/s0048-9697(96)05355-7

[56] Jickells, T., Andrews, J., G., S., Sanders, R., Malcolm, S., Sivyer, D., Parker, R., Nedwell, D., Trimmer, M., & Ridgway, J. (2000). Nutrient Fluxes through the Humber Estuary: Past, Present and Future. *Ambio; Royal Swedish Academy of Sciences*, 29(3), pp.130-135.

[57] Jickells, T. D. (1998). Nutrient biogeochemistry of the coastal zone. *Science*, 281(5374), pp.217-222. doi: 10.1126/science.281.5374.217

[58] Jørgensen, B. B. (1977). Sulfur cycle of a coastal marine sediment (Limfjorden, Denmark). *Limnology and Oceanography*, 22(5), pp.814-832. doi: 10.4319/lo.1977.22.5.0814

[59] Jørgensen, B. B., & Cohen, Y. (1977). Solar lake (Sinai) .5. Sulfur cycle of benthic cyanobacterial mats. *Limnology and Oceanography*, 22(4), pp.657-666.

[60] Jørgensen, B. B. (1982). Mineralization of organic-matter in the sea bed - the role of sulfate reduction. *Nature*, 296(5858), pp.643-645. doi: 10.1038/296643a0

[61] Jørgensen, K. S. (1989). Annual pattern of denitrification and nitrate ammonification in estuarine sediment. *Applied and Environmental Microbiology*, 55(7), pp.1841-1847.

[62] Koike, I., & Hattori, A. (1978). Denitrification and ammonia formation in anaerobic coastal sediments. *Applied and Environmental Microbiology*, 35(2), pp.278-282.

[63] Lee, S. V., & Cundy, A. B. (2001). Heavy metal contamination and mixing processes in sediments from the Humber estuary, Eastern England. *Estuarine, Coastal and Shelf Science*, 53(5), pp.619-636. doi: 10.1006/ecss.2000.0713

[64] Liu, J., Yang, H., Zhao, M., & Zhang, X.-H. (2014). Spatial distribution patterns of benthic microbial communities along the Pearl Estuary, China. *Systematic and Applied Microbiology*, 37(8), pp.578-589. doi: 10.1016/j.syapm.2014.10.005

[65] Lovley, D. R., & Phillips, E. J. P. (1987). Competitive mechanisms for inhibition of sulfate reduction and methane production in the zone of ferric iron reduction in sediments. *Applied and Environmental Microbiology*, 53(11), pp.2636-2641.

[66] Lovley, D. R., & Phillips, E. J. P. (1988a). Manganese inhibition of microbial iron reduction in anaerobic sediments. *Geomicrobiology Journal*, 6(3-4), pp.145-155.

[67] Lovley, D. R., & Phillips, E. J. P. (1988b). Novel mode of microbial energy-metabolism - organic-carbon oxidation coupled to dissimilatory reduction of iron or manganese. *Applied and Environmental Microbiology*, 54(6), pp.1472-1480.

[68] Luther, G. W., Sundby, B., Lewis, B. L., Brendel, P. J., & Silverberg, N. (1997). Interactions of manganese with the nitrogen cycle: Alternative pathways to dinitrogen. *Geochimica et Cosmochimica Acta*, 61(19), pp.4043-4052. doi: 10.1016/s0016-7037(97)00239-1

[69] Mckee, B. A., & Baskaran, M. (1999). Sedimentary processes of the Gulf of Mexico. *In* T. S. Bianchi, R. Pennock & R. R. Twilley (Eds.), *Biogeochemistry of Gulf of Mexico Estuaries*. New York: John Wiley, pp. 63-81.

[70] Met Office, U. s. N. W. S. (2012). *Regional Climate: Eastern England*. Retrieved 1 february 2014, 2014, from http://www.metoffice.gov.uk/climate/uk/ee/

[71] Middelburg, J. J., Delange, G. J., & Vanderweijden, C. H. (1987). Manganese solubility control in marine porewaters. *Geochimica et Cosmochimica Acta*, 51(3), pp.759-763. doi: 10.1016/0016-7037(87)90086-x

[72] Middelburg, J. J., & Herman, P. M. J. (2007). Organic matter processing in tidal estuaries. *Marine Chemistry*, 106(1–2), pp.127-147. doi: http://dx.doi.org/10.1016/j.marchem.2006.02.007

[73] Middelburg, J. J., & Levin, L. A. (2009). Coastal hypoxia and sediment biogeochemistry. *Biogeosciences*, 6(7), pp.1273-1293. doi: 10.5194/bg-6-1273-2009

[74] Millward, G. E., & Moore, R. M. (1982). The adsorption of Cu, Mn and Zn by iron oxyhydroxide in model estuarine solutions. *Water Res*, 16(6), pp.981-985. doi: 10.1016/0043-1354(82)90032-x

[75] Millward, G. E., & Turner, A. (1995). Trace metals in estuaries. *In:* Salbu B. & Steinnes E. (Eds.), *Trace elements in natural waters*. London, England, UK: CRC Press, pp. 223-245.

[76] Millward, G. E., & Glegg, G. A. (1997). Fluxes and Retention of Trace Metals in the Humber Estuary. *Estuarine, Coastal and Shelf Science*, 44, pp.97-105. doi: doi:10.1016/S0272-7714(97)80011-X

[77] Mitchell, S. B. (2005). Discussion on 'The effect of fresh water flow on siltation in the Humber estuary, Northeast UK' by Pontee NI, Whitehead PA and Hayes CM (ECSS vol. 60, 241–249). *Estuarine, Coastal and Shelf Science*, 62(4), pp.725-729. doi: 10.1016/j.ecss.2004.10.007

[78] Mitchell, S. B. (2013). Turbidity maxima in four macrotidal estuaries. *Ocean & Coastal Management*, 79, pp.62-69. doi: http://doi.org/10.1016/j.ocecoaman.2012.05.030

[79] Mitchell, S. B., West, R.J., Arundale, A.M.W., Guymer, I., Couperthwaite, J.S. (1998). Dynamic of the Turbidity Maxima in the Upper Humber Estuary System, UK. *Marine Pollution Bulletin*, 37, pp.190-205.

[80] Morris, A. W., Mantoura, R. F. C., Bale, A. J., & Howland, R. J. M. (1978). Very low salinity regions of estuaries - important sites for chemical and biological reactions. *Nature*, 274(5672), pp.678-680. doi: 10.1038/274678a0

[81] Mulder, A., Vandegraaf, A. A., Robertson, L. A., & Kuenen, J. G. (1995). Anaerobic ammonium oxidation discovered in a denitrifying fluidized-bed reactor. *FEMS Microbiology Ecology*, 16(3), pp.177-183. doi: 10.1111/j.1574-6941.1995.tb00281.x

[82] Neal, C., & Davies, H. (2003). Water quality fluxes for eastern UK rivers entering the North Sea: a summary of information from the Land Ocean Interaction Study (LOIS). *Science of The Total Environment*, 314, pp.821-882. doi: 10.1016/s0048-9697(03)00086-x

[83] Neale, J. W. (1988). The Geology of the Humber Area. *In:* Jones N.V. (Ed.), *A Dynamic Estuary: Man, Nature and the Humber*. Hull: Hull University, pp. 1-15.

[84] Nedwell, D. B. (1984). The input and mineralization of organic-carbon in anaerobic aquatic sediments. *Advances in Microbial Ecology*, 7, pp.93-131.

[85] Nedwell, D. B., & Trimmer, M. (1996). Nitrogen fluxes through the upper estuary of the Great Ouse, England: The role of the bottom sediments. *Marine Ecology Progress Series*, 142(1-3), pp.273-286. doi: 10.3354/meps142273

[86] Nedwell, D. B., Jickells, T. D., Trimmer, M., & Sanders, R. (1999). Nutrients in estuaries. *In:* Nedwell D. B. & Raffaelli D. G. (Eds.), *Advances in Ecological Research, Estuaries*. San Diego: Academic Press, pp.43-92.

[87] Nedwell, D. B., Dong, L. F., Sage, A., & Underwood, G. J. C. (2002). Variations of the Nutrients Loads to the Mainland U.K. Estuaries: Correlation with Catchment Areas, Urbanization and Coastal Eutrophication. *Estuarine, Coastal and Shelf Science*, 54(6), pp.951-970. doi: 10.1006/ecss.2001.0867

[88] Nichols, M. M., Johnson, G. H., & Peebles, P. C. (1991). Modern sediments and facies model for a microtidal coastal-plain estuary, the James estuary, Virginia. *Journal of Sedimentary Petrology*, 61(6), pp.883-899.

[89] Nichols, M. N., & Biggs, B. B. (1985). Estuaries. *In:* Davis R.A. (Ed.), *Coastal Sedimentary Environments*. New York: Springer-Verlag, pp.77-186.

[90] Nielsen, L. P., Risgaard-Petersen, N., Fossing, H., Christensen, P. B., & Sayama, M. (2010). Electric currents couple spatially separated biogeochemical processes in marine sediment. *Nature*, 463(7284), pp.1071-1074. doi: 10.1038/nature08790

[91] Nixon, S. W. (1995). Coastal marine eutrophication - a definition, social causes, and future concerns. *Ophelia*, 41, pp.199-219.

[92] NOAA. (2008, 25th March 2008). *NOAA Ocean Service Education, Estuaries, Classifying Estuaries by Water Circulation*. Retrieved 2-03-2017, 2017, from http://oceanservice.noaa.gov/education/kits/estuaries/estuaries05_circulation.html

[93] O'Sullivan, L. A., Sass, A. M., Webster, G., Fry, J. C., Parkes, R. J., & Weightman, A. J. (2013). Contrasting relationships between biogeochemistry and prokaryotic diversity depth profiles along an estuarine sediment gradient. *FEMS Microbiology Ecology*, 85(1), pp.143-157. doi: 10.1111/1574-6941.12106

[94] Owens, N. J. P. (1986). Estuarine nitrification - a naturally-occurring fluidized-bed reaction. *Estuarine Coastal and Shelf Science*, 22(1), pp.31-44. doi: 10.1016/0272-7714(86)90022-3

[95] Parker, W. R., Marshall, L. D., & Parfitt, A. J. (1994). Modulation of dissolved oxygen levels in a hypertidal estuary by sediment resuspension. *Netherlands Journal of Aquatic Ecology*, 28(3-4), pp.347-352. doi: 10.1007/bf02334203

[96] Peterson, B. J., & Fry, B. (1987). Stable isotopes in ecosystem studies. *Annual review of ecology and systematics*, 18(1), pp.293-320.

[97] Pethick, J. S. (1988). The physical characteristics of the Humber. *In:*. Jones N.V (Ed.), *A dynamic Estuary: Man, Nature and the Humber*. Hull: Hull University, pp.31-45.

[98] Pethick, J. S. (1990). The Humber Estuary. *In* Ellis S. and Crowther, D.R. (Eds.), *Humber Perspectives, A region through the ages*. Hull: Hull University, pp.54-67.

[99] Pfeffer, C., Larsen, S., Song, J., Dong, M. D., Besenbacher, F., Meyer, R. L., Kjeldsen, K. U., Schreiber, L., Gorby, Y. A., El-Naggar, M. Y., Leung, K. M., Schramm, A., Risgaard-Petersen, N., & Nielsen, L. P. (2012). Filamentous bacteria transport electrons over centimetre distances. *Nature*, 491(7423), pp.218-221. doi: 10.1038/nature11586

[100] Plummer, D. H., Owens, N. J. P., & Herbert, R. A. (1987). Bacteria particle interactions in turbid estuarine environments. *Continental Shelf Research*, 7(11-12), pp.1429-1433. doi: 10.1016/0278-4343(87)90050-1

[101] Postma, D. (1985). Concentration of Mn and separation from Fe in sediments .1. Kinetics and stoichiometry of the reaction between birnessite and dissolved Fe(II) at 10°C. *Geochimica et Cosmochimica Acta*, 49(4), pp.1023-1033. doi: 10.1016/0016-7037(85)90316-3

[102] Rheinheimer, G. (1985). *Aquatic microbiology* (Norman Walker, Trans. 3rd ed.). New York: John Wiley & Sons, Ltd.

[103] Rink, B., Martens, T., Fischer, D., Lemke, A., Grossart, H. P., Simon, M., & Brinkhoff, T. (2008). Short-term dynamics of bacterial communities in a tidally affected coastal ecosystem. *FEMS Microbiology Ecology*, 66(2), pp.306-319. doi: 10.1111/j.1574-6941.2008.00573.x

[104] Risgaard-Petersen, N., Revil, A., Meister, P., & Nielsen, L. P. (2012). Sulfur, iron-, and calcium cycling associated with natural electric currents running through marine sediment. *Geochimica et Cosmochimica Acta*, 92, pp.1-13. doi: 10.1016/j.gca.2012.05.036

[105] Roberts, K. L., Kessler, A. J., Grace, M. R., & Cook, P. M. L. (2014). Increased rates of dissimilatory nitrate reduction to ammonium (DNRA) under oxic conditions in a periodically hypoxic estuary. *Geochimica et Cosmochimica Acta*, 133, pp.313-324. doi: http://dx.doi.org/10.1016/j.gca.2014.02.042

[106] Schubel, J. R. (1968). Turbidity maximum of Northern Chesapeake Bay. *Science*, 161(3845), pp.1013-1015. doi: 10.1126/science.161.3845.1013

[107] Schubel, J. R. (1971). Tidal variation of the size distribution of suspended sediment at a station in the Chesapeake Bay turbidity maximum. Netherlands *Journal of Sea Research*, 5(2), pp.252-266. doi: http://dx.doi.org/10.1016/0077-7579(71)90012-3

[108] Schubel, J. R., & Carter, H. H. (1984). Estuary as a Filter for Fine-Grained Suspended Sediment The Estuary as a Filter. *In:* Kennedy V.S. (Ed.) *The estuary as a Filter*. Orlando FL.: Academic Press, pp.81-105.

[109] Seitzinger, S. P., & Sanders, R. W. (1997). Contribution of dissolved organic nitrogen from rivers to estuarine eutrophication. *Marine Ecology Progress Series*, 159, pp.1-12. doi: 10.3354/meps159001

[110] Song, G. D., Liu, S. M., Marchant, H., Kuypers, M. M. M., & Lavik, G. (2013). Anammox, denitrification and dissimilatory nitrate reduction to ammonium in the East China Sea sediment. *Biogeosciences*, 10(11), pp.6851-6864. doi: 10.5194/bg-10-6851-2013

[111] Sørensen, J., Jørgensen, B. B., & Revsbech, N. P. (1979). Comparison of oxygen, nitrate, and sulfate respiration in coastal marine-sediments. *Microbial Ecology*, 5(2), pp.105-115. doi: 10.1007/bf02010501

[112] Sørensen, J., & Jørgensen, B. B. (1987). Early diagenesis in sediments from danish coastal waters - microbial activity and Mn-Fe-S geochemistry. *Geochimica et Cosmochimica Acta*, 51(6), pp.1583-1590. doi: 10.1016/0016-7037(87)90339-5

[113] Statham, P. J. (2012). Nutrients in estuaries--an overview and the potential impacts of climate change. *Science of The Total Environment*, 434, pp.213-227. doi: 10.1016/j.scitotenv.2011.09.088

[114] Straub, K. L., Benz, M., Schink, B., & Widdel, F. (1996). Anaerobic, Nitrate-Dependent Microbial Oxidation of Ferrous Iron. *Applied and Environmental Microbiology*, 62(4), pp.1458–1460.

[115] Straub, K. L., Schonhuber, W. A., Buchholz-Cleven, B. E. E., & Schink, B. (2004). Diversity of ferrous iron-oxidizing, nitrate-reducing bacteria and their involvement in oxygen-independent iron cycling. *Geomicrobiology Journal*, 21(6), pp.371-378. doi: 10.1080/01490450490485854

[116] Stumm, W., & Morgan, J. J. (1970). *Aquatic chemistry: an introduction emphasizing chemical equilibria in natural waters*. New York: Wiley-Interscience.

[117] Stumm, W., & Morgan, J. J. (1981). *Aquatic chemistry* (2nd ed.). New York: Wiley-Interscience.

[118] Teixeira, C., Magalhaes, C., Boaventura, R. A. R., & Bordalo, A. A. (2010). Potential rates and environmental controls of denitrification and nitrous oxide production in a temperate urbanized estuary. *Marine Environmental Research*, 70(5), pp.336-342. doi: 10.1016/j.marenvres.2010.07.001

[119] Telesh, I. V., & Khlebovich, V. V. (2010). Principal processes within the estuarine salinity gradient: A review. *Marine Pollution Bulletin*, 61(4-6), pp.149-155. doi: 10.1016/j.marpolbul.2010.02.008

[120] Thamdrup, B., Fossing, H., & Jørgensen, B. B. (1994). Manganese, iron, and sulfur cycling in a coastal marine sediment, Aarhus Bay, Denmark. *Geochimica et Cosmochimica Acta*, 58(23), pp.5115-5129. doi: 10.1016/0016-7037(94)90298-4

[121] Thamdrup, B., & Dalsgaard, T. (2002). Production of N_2 through anaerobic ammonium oxidation coupled to nitrate reduction in marine sediments. *Applied and Environmental Microbiology*, 68(3), pp.1312-1318. doi: 10.1128/aem.68.3.1312-1318.2002

[122] Thamdrup, B. (2012). New Pathways and Processes in the Global Nitrogen Cycle. *Annual Review of Ecology, Evolution, and Systematics*, 43, pp.407-428. doi: 10.1146/annurev-ecolsys-102710-145048

[123] Thurman, H. V., & Trujillo, A. P. (2004). *Introductory Ocean*ography (10th ed.). New Jersey: Pearson Prentice Hall.

[124] Tiedje, J. M., Sexstone, A. J., Myrold, D. D., & Robinson, J. A. (1982). Denitrification - ecological niches, competition and survival. *Antonie Van Leeuwenhoek Journal of Microbiology*, 48(6), pp.569-583.

[125] Trujillo, A. P., & Thurman, H. V. (2013). *Essentials of Oceanography. (Pearson New International Edition)*. Harlow, Essex: Pearson Education.

[126] Turner, A., & Millward, G. E. (2002). Suspended Particles: Their Role in Estuarine Biogeochemical Cycles. *Estuarine, Coastal and Shelf Science*, 55(6), pp.857-883. doi: 10.1006/ecss.2002.1033

[127] Uncles, R., Howland, R., Easton, A., Griffiths, M., Harris, C., King, R., Morris, A., Plummer, D., & Woodward, E. (1998a). Concentrations of dissolved nutrients in the tidal Yorkshire Ouse River and Humber Estuary. *Science of The Total Environment*, 210-211, pp.377-388. doi: 10.1016/s0048-9697(98)00025-4

[128] Uncles, R. J., Easton, A. E., Griffiths, M. L., Harris, C., Howland, R. J. M., King, R. S., Morris, A. W., & Plummer, D. H. (1998b). Seasonality of the turbidity maximum in the Humber-Ouse estuary, UK. *Marine Pollution Bulletin*, 37(3-7), pp.206-215.

[129] Uncles, R. J., Joint, I., & Stephens, J. A. (1998c). Transport and retention of suspended particulate matter and bacteria in the Humber-Ouse Estuary, United Kingdom, and their relationship to hypoxia and anoxia. *Estuaries*, 21(4A), pp.597-612. doi: 10.2307/1353298

[130] Uncles, R. J., Wood, R. G., Stephens, J. A., & Howland, R. J. M. (1998d). Estuarine nutrient fluxes to the Humber coastal zone, UK, during June 1995. *Marine Pollution Bulletin*, 37(3-7), pp.225-233.

[131] Uncles, R. J., & Stephens, J. A. (1999). Suspended sediment fluxes in the tidal Ouse, UK. *Hydrological Processes*, 13(7), pp.1167-1179.

[132] Uncles, R. J., Stephens, J. A., & Law, D. J. (2006). Turbidity maximum in the macrotidal, highly turbid Humber Estuary, UK: Flocs, fluid mud, stationary suspensions and tidal bores. *Estuarine, Coastal and Shelf Science*, 67(1-2), pp.30-52. doi: 10.1016/j.ecss.2005.10.013

[133] Weber, K. A., Picardal, F. W., & Roden, E. E. (2001). Microbially catalyzed nitrate-dependent oxidation of biogenic solid-phase Fe(II) compounds. *Environmental Science & Technology*, 35(8), pp.1644-1650. doi: 10.1021/es0016598

[134] Wei, G., Li, M., Li, F., Li, H., & Gao, Z. (2016). Distinct distribution patterns of prokaryotes between sediment and water in the Yellow River estuary. *Applied Microbiology and Biotechnology*, 100(22), pp.9683-9697. doi: 10.1007/s00253-016-7802-3

[135] Wells, J. T. (1995). Tide-Dominated Estuaries and Tidal Rivers. *In*: Perillo G.M.E (Ed.), *Geomorphology and Sedimentology of Estuaries. Developments in Sedimentology*. New York: Elsevier Science. pp.179-205.

Chapter 3
Material and Methods

3.1 Sampling survey and locations

The sampling survey for this study was undertaken in the summer of 2014 (on the 15th July). All samples were collected during the low tide of a single tidal cycle. The survey started in the most seaward location, Skeffling, and continued inland following the direction of the flood tide until Boothferry. The aim was to find representative locations of estuarine environments (from fresh to saline water) within the salinity range.

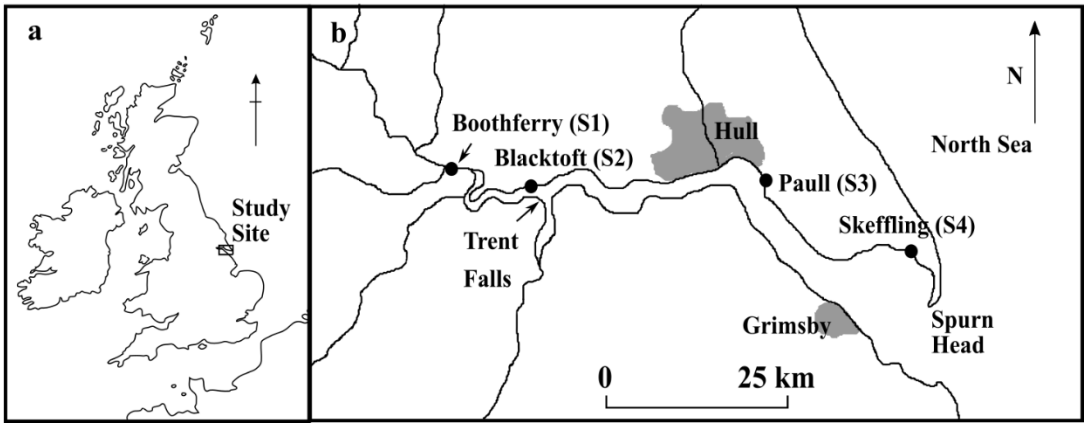

Figure 3.1: Map of the UK (a) and the Humber estuary with the locations of the sampling sites (b).

Table 3.1: Sampling location coordinates.

	Boothferry	Blacktoft	Paull	Skeffling
Longitude	0°53'25"(W)	0°43'57"(W)	0°14'01"(W)	0°04'13"(E)
Latitude (N)	53°43'38"	53°42'28"	53°43'04"	53°38'37"

The Boothferry site will be called Site 1 (S1). Boothferry is located after the river Ouse meets the river Aire. It was the most landward location in this survey. Sediments looked well stratified at first glance, with a clear colour change from brown to grey/black between surface and subsurface layers.

The Blacktoft site will be called Site 2 (S2). It is located in the inner estuary region, before the Trent Falls, the confluence between the Ouse and the Trent. The sediment contained a considerable amount of plant material and debris and looked fairly mixed without a clear stratification by colour.

The Paull site will be called Site 3 (S3). It is located in the north bank of the mid-estuary, after Hull. At first glance, sediment looked muddier and the colour stratification was abrupt (i.e. the very thin surface layer of sediments was brown compared to the bulk dark grey-black sediment underneath). A characteristic "rotten eggs" odour indicating the presence of hydrogen sulphide could be noticed when digging into the dark grey-black surface sediments.

The Skeffling site will be called Site 4 (S4). It is located in the north bank of the outer-estuary, after the Sunk Island. It was the most seaward location in this survey. There was a strong sediment colour stratification (i.e. the very thin surface layer of sediments was brown compared to the bulk dark grey-black sediment underneath) and the "rotten eggs" smell was also noticeable.

3.2 Sample collection, handling and storage

Surface (0-1 cm), subsurface sediments (5-10 cm) and river water adjacent to each site were collected into different brand-new and acid washed polythene containers (10% v/v HNO_3 and rinsed 5 times with DI water). Surface sediments were taken with care to collect only the top few millimetres of sediment using a spatula to scratch off the surface. Sediment from the subsurface (at the depth required) was dug with a spade rapidly to minimise oxidation. Care was taken to avoid mixing with surface sediments and macroorganisms (when seen) were avoided. No air space was allowed in the plastic containers in which sediment was collected to minimise oxidation of the sample before used in the laboratory experiments. River water pH, conductivity and temperature were determined in the field using a Myron Ultrameter PsiII handheld multimeter calibrated in-situ. The environmental temperature on the day of the sampling was in between 19-20°C at all sites.

Sediment and water samples were brought back to the laboratory within ~5 hours in a cold box and then stored in the fridge at 4°C (or freezer at -20°C in the case of sediment subsamples for microbiology analysis and AVS-pyrite extractions) until used. Subsamples of wet sediments were weighed and placed in the oven to dry (70°C) in order to determine water content and for further use (see below). Part of the river water was filtered (0.2 µm Minisart®), transferred to different Nalgene HDPE bottles, and subsamples were acidified with trace analysis grade acid (1% v/v HNO_3 conc.) for trace metal (TM) analysis. Porewaters were recovered from each sediment sample by centrifugation (30 min, 6000 *g*) within 6-8 hrs of sampling, filtered, acidified if needed , and stored in centrifuge tubes for further analysis. Acid extractable iron (II) (0.5 N HCl $Fe^{2+}_{(s)}$, see method below 3.3.1.3.3) was analysed directly the same day of sampling due to the redox sensitivity of reduced iron.

3.3 Geochemical analyses

3.3.1 Solid phase

3.3.1.1 Bulk mineral and chemical composition

Dry sediments were ground using pestle and mortar for X-Ray diffraction (XRD) and X-Ray fluorescence (XRF).

The bulk mineral composition was determined by XRD analysis, a technique to identify, quantify and characterise minerals in complex mineral assemblages. The identification of the minerals present is relatively easy to determine from the position and rough intensities of the diffraction peaks, however, the quantification of the individual mineral content is much more difficult because the modelling of the intensities of the peaks in the diffraction pattern has to be accurate (Stanjek and Hausler, 2004). Here, a beam of X-rays is directed at a sample which scatters the beam; the crystal planes of the mineral determine the scattering pattern. The distance the X-rays covered into the crystal before being reflected depends on the lattice planes distances (d) and the angle of the beam (θ). The interaction of waves with the crystal structures produces diffraction effects if the wavelength and the periodicity of the crystals are of similar magnitude, therefore diffraction redistributes the intensity of the

whole scattering sphere into distinct directions which results in a signal output called diffraction peaks (Stanjek & Hausler, 2004). The XRD analysis of the estuarine sediment samples was carried out on a Bruker D8 Advance diffractometer, using Cu Kalpha1 radiation from 2θ angles of 2-86°. The step size was 0.2° with counting of 2 seconds per step.

The concentration of major and trace elements were determined by XRF spectrometry. This technique is based on the excitation of atoms and subsequent relaxation. The sample is irradiated by a primary X-ray source that causes elements to emit (fluorescence) in their characteristic spectra with a certain intensity, which allows identification and quantification of the element and its concentration (Jenkins, 1988). When beam strikes the material, if the primary X-ray had sufficient energy, results in the ejection of electrons from the innermost shells of the atoms. These ejected electrons leave a vacancy, creating a brief period of atom instability; then the atomic electrons rearrange with electrons from a higher (outer) energy shell filling the vacancy left. By this relaxation process, an X-ray photon is emitted by the atom (fluorescence), the energy of which equals the difference between the binding energy of the corresponding shells (Jenkins, 1988). Energy disperse XRF analysis was carried out on an Olympus Innovex X-5000 spectrometer. The instrument was run in two separate modes using powdered samples. Major elements were determined using a calibration dependant method (using a range of certified natural sediment and shale rock standards). Minor and trace elements were determined using the manufacturers precalibration with Compton normalisation was also applied to reduce problems with matrix effects. Several relevant reference materials (standardized stream sediments) were run for quality check. Analytical uncertainty (measured values versus certified values) was < ±30% for Mg, < ±20% for S, Cl and K and, < ±10% for all other elements.

3.3.1.2 Carbon and sulphur analysis

Dry sediments were utilised to determine total sulphur (TS), total carbon (TC) and total organic carbon (TOC) in sediments on a LECO SC-144DR Dual Range Sulphur and Carbon Analyser by combustion with non-dispersive infrared detection. All sediments were ground and oven-dried (at 60°C). However, prior to the analysis on the LECO,

subsamples for TOC were acid-washed with 10% v/v HCl in order to remove inorganic carbon and other soluble elements such as Ca. Following the standard protocol, 5-10 blanks were run to calculate detection limit. Reference standards selected according to the range of C and S expected in the samples were used for calibration. Samples were run in triplicate and standards were re-run every 15 samples. During the analysis, the ceramic boats with the samples are introduced into the furnace (1350°C) under oxygen. The CO_2 and SO_2 gases produced are analysed by IR spectrometry, and the software gives the percentages of C and S in each sample.

3.3.1.3 Iron and manganese analyses

3.3.1.3.1 Total iron

Total Fe was extracted by a HNO_3–HF–$HClO_4$–H_3BO_3–HCl sediment digestion (Poulton & Canfield, 2005; Guilbaud *et al.*, 2015). Total iron will include the highly reactive phase and the continentally-derived background (silicates and ion oxides). Samples from the extraction were diluted in volumetric flasks with a 1 g L^{-1} of CsCl solution, and then further diluted (1:4) with the same CsCl solution directly on centrifuge tubes for analysis of the total iron concentration by Flame Atomic Absorption Spectroscopy (AAS) on a ContrAA 700 Analytik Jeta. The sample is aspirated and transformed into an aerosol which is atomised by the flame. The atoms absorb a specific wavelength light energy allowing the determination of the concentration of the element of interest, iron in this case. The instrument was calibrated with iron standards (with a range of standards from 0-10 ppm) made up with the same CsCl matrix than samples.

3.3.1.3.2 AVS and pyrite extraction

Sediment samples were freeze-dried for the Acid Volatile Sulphide (AVS) and pyrite extraction. Frozen sediment subsamples were then freeze-dried and frozen again prior to the extractions. The AVS extraction is a commonly used operational measurement of the amount of sulphide in sediments. The principle of this method is trapping H_2S as Ag_2S precipitates during the first step of the extraction (equations 3.1 and 3.2). Pyrite is calculated from the sulphide extracted as Ag_2S (equations 3.3 and 3.4) using hot

Chromium(II) Chloride ($CrCl_2$) distillation (Canfield *et al.*, 1986: Fossing & Jørgensen 1989).

The reactions involved in the AVS extraction are:

$$FeS + HCl \rightarrow H_2S + Fe^{2+} + Cl^- \qquad \text{Eq 3.1}$$

$$H_2S + 2Ag^+ \rightarrow Ag_2S + 2H^+ \qquad \text{Eq 3.2}$$

The reactions involved in the pyrite extraction are:

$$4H^+ + 2Cr^{2+} + FeS_2 \rightarrow 2H_2S + Cr^{3+} + Fe^{2+} \qquad \text{Eq 3.3}$$

$$H_2S + 2Ag^+ \rightarrow Ag_2S + 2H^+ \qquad \text{Eq 3.4}$$

All the reactants were prepared according to the protocol and 1 g of sample was used for the extraction. During this procedure, FeS or FeS_2 present in the sample react with the H^+ to release H_2S gas (see equations 3.1 and 3.3 above). The H_2S gas will travel up the condenser column and it is injected through the Pasteur pipette to the tube with the $AgNO_3$ solution. The H_2S reacts with the $AgNO_3$ (equations 3.2 and 3.4) to form $Ag_2S_{(s)}$ and HNO_3. The Ag_2S precipitated was filtered (using a vacuum pump), dried and weighed to work out the mass of iron as pyrite or iron sulphide contained in the sample.

3.3.1.3.3 Acid extractable Iron and Manganese

The amount of 0.5 N HCl extractable Fe^{2+} in sediments was determined following the method by Lovley and Phillips (1986). This type of extraction with HCl is used to analyse the production of biogenic Fe(II) from the microbial reduction of Fe(II) containing phases (Lovley & Phillips, 1986), and thus the bioavailable iron. This extraction targets the poorly crystalline iron oxides, FeS and $FeCO_3$ (Thamdrup *et al.*, 1994). A ratio (proportion of the total iron extractable that is in reduced state) is used due to the experimental set-up (i.e. difficulty to accurately determine the mass of sediment used in each individual extraction) and the redox sensitivity of the reduced iron. This technique has been widely used in different type of experiments as it provides a rapid indication of the redox status of the sediment sample (Lovley & Phillips, 1988; Lovley, 1991; Thamdrup *et al.*, 1994; Zachara *et al.*, 1998; Dong *et al.*, 2000; Islam *et*

al., 2004; Burke *et al.*, 2005; Roberts *et al.*, 2014). For the analysis, a soil pellet was added in a 10 mL test tube containing 5 mL of 0.5 N HCl very quickly in order to minimise oxidation of the sample. After exactly 60 minutes (on an orbital shaker) extraction time, the solution was filtered (0.2 µm) into a new test tube. The Fe extracted will be analysed by reaction with ferrozine (Viollier *et al*., 2000). Two 100 µL sub-aliquot of the filtrate were pipette into two 4 mL cuvettes (cuvette 1 and cuvette 2). In the first of the cuvettes, the filtrate was diluted with 2900 µL MilliQ, and then 300 µL ferrozine solution (5 g L^{-1} Ferrozine in 0.1 M ammonium acetate) was added. This cuvette will represent the amount of Fe(II) extractable by 0.5 N HCl in the sample. In the second cuvette, the filtrate was diluted with 2000 µL MilliQ, followed by the addition of 300 µL ferrozine solution, 600 µL of Hydroxylamine hydrochloride solution (1.4 M Hydroxylammonium hydrochloride solution in 2M HCl), and 300 µL of buffer solution (1M ammonium acetate, pH 9.5 adjusted with ammonium hydroxide) to reduce all Fe(III) in the sample. Both solutions were left for 10 minutes for colour to develop. The absorbance measured at 562 nm in both cuvettes (a reading of 0.500-1.000 in cuvette 2 is desirable for good statistics). The absorbance of the solution was corrected with respect to the absorbance of a reagent–only blank solution. The percentage of acid extractable Fe present as Fe(II) in the sediment is calculated as follows (equation 3.5):

$$(A_{562\ Cuvette\ 1}/A_{562\ Cuvette\ 2}) \times 100 = \%\ extractable\ Fe\ present\ as\ Fe(II) \quad \text{Eq. 3.5}$$

To actually quantify the hydroxylamine reducible Fe(III) in sediments and therefore have the amount of total extractable iron to which the percentage of acid extractable Fe(II) can be applied, the method by Lovley & Phillips (1987) followed by reaction with ferrozine were used. For the analysis, 10 mL test tubes containing 5 mL of 0.25 M $H_2NOH{\cdot}HCl$ were pre-weighted and afterwards, approximately 0.5 g of sediments were added. Operating very quickly was important to minimise oxidation of the sample. After an hour of extraction time (on an orbital shaker), the solution was filtered (0.2 µm) into a new test tube. A subsample of 100 mL was pipetted into a pre-weight 10 mL test tube (the weight was recorded). Subsequently, 3000 µL MilliQ water, 300 µL ferrozine solution (5 g L^{-1} ferrozine in 0.1 M ammonium acetate), 600 µL of 1.4 Hydroxylamine hydrochloride solution, and 300 µL of buffer solution (1 M ammonium acetate, pH 9.5

adjusted with ammonium hydroxide) were added and the weight of the tube was recorded. After ten minutes for colour to develop, the absorbance was measured at 562 nm. The amount of iron was calculated according to a calibration curve made with a range of standards from 0-4 mg L^{-1} Fe (treating as above excepting that 3000 µL of standard solution is used).

The same type of extraction was carried out to quantify extractable Mn in sediments. For the analysis, 10 mL test tubes containing 5 mL of 0.5 N HCl were pre-weighted and approximately 0.1 g of sediment were added. After an hour of extraction time (on an orbital shaker), the solution was filtered (0.2 µm) into a new test tube. The leachates from these extractions were acidified (1% v/v HNO_3 conc.) to be analysed on an ICP−MS (see below, section 3.3.2.2).

3.3.1.4 Trace metal partitioning

Sequential extractions procedures (SEP) are used to identify and quantify "the different, defined species, forms or phases in which an element occurs" (Tack & Verloo, 1995). Metal speciation is a function of the mineralogy and chemistry of the soil or sediment examined, and it is more of an interest to assess than the total metal content because it brings out information about metal bioavailability and mobility and therefore about their potential impact in the environment (Tessier *et al.*, 1979; Zimmerman & Weindorf, 2010). A series of reagents of different strengths and reactivities are applied to the solid sample in SEP to release metals bound to different fractions of the sediment, and the concentration of the metal of interest in each leachate is then measured. In SEP, the harshness of the reagents increases in each step, therefore the most mobile or weakly-bound metals are removed in the first steps and continue in order of decreasing mobility or increasing strength of the binding to the solid phase (Zimmerman & Weindorf, 2010).

Sequential extractions were performed following the commonly used scheme by Tessier *et al.* (1979). However, Step 3 (for the extraction of Fe/Mn oxides-bound metals) was modified due to the problems found when heating the samples at 96°C (see Table 3.2). The fifth step of this extraction protocol (for the extraction of metals bound to the residual fraction) was not performed, and modifications in the sediment:solution ratio

were applied based on Rauret *et al.* (1989) (see Table 3.2). When working with wet sediments an extra step to remove porewater was required. The extractions were carried out in batches of two samples (in triplicates) plus blank (7 tubes in total). Sediments were weighed (0.7 g dry weight) in 50 mL Teflon (FEP) tubes. All the reactants used for the preparation of the reagents were made up with high purity chemicals. When appropriate, samples were handled anaerobically and all reagents were deoxygenated until the oxidising stage (H_2O_2 leaching step). A summary of the reagents and procedure is given in Table 3.2. After each step, sample tubes were centrifuged (for 30 minutes, 15000 *g*) on a Sigma 4-16KS, then the leachate was filtered (0.2 µm) to a clean tube and further acidified with HNO_3 conc. (1% v/v). The fourth step was performed on a dry block heating plate (Grant, QBD2) inside a fume cupboard, and the oxidants (H_2O_2 and HNO_3) were added in few aliquots because the reaction can be quite aggressive and sample may be lost due to fizzing.

The leachates of each extraction step were analysed on an ICP-MS with the corresponding precautions to avoid polyatomic influences (see additional information in appendix A). The concentrations of the metals [M] in each fraction can be expressed in µg g^{-1} dry sediment, for which the data from the ICP-MS will need conversion (equation 3.6). The detection limits of the ICP-MS analysis can be found in the appendix A.

$$[M]_{leachate} x\, V_{leachate} / mass_{dry\ solids} = [M]_{dry\ solids} \qquad \text{Eq. 3.6}$$

Table 3.2: Summary of the sequential extraction protocol followed, based on Tessier *et al.* (1979) with modifications in the solid:solution ratios based on Rauret *et al.* (1989). *The Step 3 was modified: heating the samples at 96°C caused problems with the lids of the tubes, therefore, the extraction time was increased (from 6 to 12 hrs) and the agitation was performed at room temperature.

Step	Fraction	Leaching time	Temp. & agitation	V leachate (mL)	Leachate composition	Anaerobic chamber
1	Exchangeable	1 hr	Room temperature, continuous agitation (40 rpm)	5.6	1 M $MgCl_2$, pH 7	Yes
2	Bound to carbonates	5 hrs		35	1 M NaOAc, pH 5 (HOAc)	Yes
3*	Bound to Iron and Manganese oxides	Overnight (12 hrs)		35	0.04 M $NH_2OH{\cdot}HCl$ in 25% v/v HOAc	Yes
4	Bound to Organic matter	2 hrs (1st aliquot)	85±2°C with occasional agitation	2.1	0.02 M HNO_3	No
				3.5	30% H_2O_2 pH 2 (HNO_3)	
		3 hrs (2nd aliquot)	85±2°C with intermittent agitation	2.1	30% H_2O_2 pH 2 (HNO_3)	
		30 min (after cooling)	Continuous agitation	3.5 (diluted up to 14 mL, so add 2.8 mL of MilliQ water)	NH_4OAc in 20% v/v HNO_3	

3.3.2 Aqueous phase

For the analysis of the aqueous phase, all samples were filtered (0.2 μm Minisart®) and acidified when needed (for TM analysis). The aqueous solutions analysed consisted of: i) river water collected from the sampling sites; ii) porewater recovered from the original surface and subsurface sediments (recovered by centrifuging sediments (30 minutes, 6000 *g*)); and iii) aqueous phase of the sediment suspensions used in the different experiments (recovered by centrifugation of 1.5 mL Eppendorf tubes (6 minutes, 16000 *g*)). Due to the salinity range of the samples, the analyses in the

different instruments was split in two groups after different matrix-match tests were performed: low salinity (0-4 psu) and medium-high (>4 psu) salinity.

3.3.2.1 Dissolved nutrients

Inorganic nitrogen species (nitrate, nitrite and ammonium), sulphate and chloride were analysed using ion chromatography (IC) and colorimetry. Different methods were used due to sample volume constraints. The (i.e. large volumes of sample required by the multi-channel segmented flow analyser if simultaneous determination of the three nitrogen species). So, the simultaneous analysis of nitrate, nitrite and ammonium was not possible and the concentrations of the two nitrogen oxides were determined by ion chromatography (IC) with no need of large dilutions.

3.3.2.1.1 Colorimetric determination

Colorimetric analysis is a method of measure the concentration of a chemical species in aqueous solution based on relative absorption of light, being the absorbance of a solute at a particular wavelength function of its concentration in the solution according to the Beer's law. Therefore the absorbance measurement is used to determine concentration of the solute of interest. In continuous flow colorimetry instruments, different reagents continuously flowing through a closed system of tubing mix and colour develops due to the chemical reactions. The standard solutions for calibration and the samples are taken into the flowing system via an autosampler. The stream is segmented by air bubbling, and each liquid section is subjected to specific and controlled conditions (temperature, reaction time, injection of the reagents, etc.) for the chemical reaction developing the colour. Colorimetric determination of nitrogen species (NO_3^-, NO_2^-, and NH_3) was carried out on a multi-channel continuous flow segmented SEAL AutoAnalyser (AA3) HR following the manufacturer methodology (Table 3.3). Standards and the reagents needed were prepared according to the manufacturer's instructions with analytical grade chemicals and MilliQ water was used throughout (including all the cleaning steps) to avoid contamination. For the ammonia analysis the method is based on a modification of the Berthlot reaction (Krom, 1980), in which ammonia, salycilate and free chlorine form a blue-green coloured complex that is measured in the colorimeter at 660 nm. A complexing agent prevents the precipitation of calcium and manganese hydroxides and

sodium nitroprusside increases the sensitivity. The automated nitrite determination is an adaptation of the standard diazotization method (Kamphake *et al.*, 1967; APHA, 1980). Under acidic conditions, nitrite reacts with sulphanilamide to produce a diazo compound that couples with N−naphthylethylene diamine dihydrochloride to form a purple azo dye which is measured colorimetrically (550 nm). For the determination of total oxidized nitrogen (TON, nitrate plus nitrite) concentration in the TON-channel, nitrate is reduced to nitrite by a copper-cadmium reduction column (Armstrong *et al.*, 1967), then nitrite follows the same reaction described above and the coloured solution goes into the detector for the determination of nitrite concentration by the colorimeter (at 550 nm). The software directly calculates nitrate concentration by difference between the concentration in the TON and nitrite channel.

Table 3.3: SEAL AutoAnalyser (AA3) HR methodology references.

Analysis	Method number
Nitrite in water and seawater	G-062-92 Rev. 3
Nitrate and nitrite in water and seawater	G-172-96 Rev. 13
Ammonia in Seawater and Freshwater	G-320-05 Rev. 1

Calibration standards were prepared from standard stock matrix match solutions. The sensitivity was checked prior to analysis. Blank solutions were run every 3-4 samples and standard solutions were run during the analysis to check carry over and recovery. Typically the % RSD was ≤3% for ammonia, ≤5% for TON. The low detection limits (LOD) for the river water (0-4 psu) were 1.23 µM for TON, 0.07 µM for NO_2^- and 0.34 µM for NH_3. For the seawater (≥4 psu) LOD were 3.7 µM for TON, 0.01 µM for NO_2^- and 0.18 µM for NH_3.

3.3.2.1.2 Ion Chromatography

Ion Chromatography (IC) is an analytical method in which ions are separated by differences in the rate at which they pass through a column packed with either an anion or cation exchange resin (Fritz & Gjerde, 2009). Since different ions have different affinities for the exchange resin, they will move down the column at different times and when the eluent (containing the analytes) is run through a detector, the different ions

generate separated peaks at specific time points which can be quantified relative to standards. Anions (NO_3^-, NO_2^-, Cl^-, and SO_4^{2-}) concentrations in filtered samples were determined by IC on a DIONEX CD20. For detection of nitrate and nitrite concentrations an UV detector was also set (DIONEX AD20 UV absorbance detector (225 nm)) in parallel. Due to the high salinity of some samples, a column-switching method based on Bruno *et al.* (2003) was used. With this method, matrix chloride anions were pre-separated from the other analytes by a double in-line pre-column (AG9-HC 4mm). The four-way valve, placed after this double pre-column, allowed the elution of most of the chloride to waste before the rest of the nutrient ions were eluted to the analytical column (AS9-HC). Then, anions were detected by a conductimeter (DIONEX CD20, ED40 Electrochemical detector, %RSD <10%) and/or by spectrophotometry (UV absorbance at 225 nm). Samples were also run on a DIONEX 500 in order to measure Cl^- and SO_4^{2-} concentrations (%RSD ≤5%). The limits of detection were NO_3^- (19 and 41 µmol L^{-1} for river and seawater), SO_4^{2-} (73 and 885 µmol L^{-1} for river and seawater) and Cl^- (151 µmol L^{-1}). Nitrite was below detection limit. For the brackish-seawater (≥4 psu) samples, a 20 fold dilution was applied. During the IC analysis, standards made up with MilliQ water (with no chlorine in the matrix) were also run for quality control; two matrix-match standards were run every ten samples for calibration; reference material and a monitor sample were also introduced in every run in order to monitor the state (saturation) of the column.

3.3.2.2 Dissolved metals by Inductively-Coupled Plasma Mass spectrometry (ICP−MS)

The ICP-MS is an analytical technique used for elemental determination that combines a high temperature ICP source with a mass spectrometer. The instrument is capable to detect metals and several non-metals at very low concentrations (often at parts per trillion level). Samples are introduced, then atoms within the samples are ionized by the ICP source. These ions are then separated and detected by the mass spectrometer (Jarvis *et al.*, 1992). The analysis of dissolved metals was performed using a Thermo Scientific iCAPQc Inductively Coupled Plasma Mass Spectrometer (ICP-MS). The determination of trace elements in salt waters has been analytically challenging due to the potential interference of the matrix in the sensitivity and the formation of polyatomic ions (Reed *et al.*, 1994; Jerez Vegueria *et al.*, 2013), however precautions were taken in the

ICP−MS analysis of seawater and a validation method was developed (see Appendix A). Aluminium was analysed in standard mode and all other elements (V, Cr, Mn, Fe, Co, Cu, Zn, As, Cd and Pb) in Kinetic Energy Discrimination (KED) mode using helium as a collision gas to remove polyatomic interferences. A standard concentric ring nebuliser, spraychamber, injector and torch were used. All reagents used were trace analysis grade. All samples analysed were already acidified (1% v/v HNO_3 conc.). Medium-high salinity waters (≥4 psu) were diluted 50 fold in 1% v/v HNO_3 (0.2 mL sample plus 9.8 mL of eluent) before the analysis to reduce matrix effects. Calibrations were performed in the range of 1-100 µg L^{-1} using the standard additions technique with a 50 fold dilution of a seawater certified reference material (NASS-6 Seawater Certified Reference Material (CRM)) to ensure correct matrix matching. Blanks of 3% w/v NaCl solution were prepared and run every 20 samples. An internal standard of 1 ppb Rh was used for all samples and standards. Fresh-low salinity brackish waters (0-4 psu) were treated as above except they were analysed with no dilution. For the samples from sequential extraction procedures, samples were diluted 1:50 and four sets of standards were made up with different matrices matching the leachate solutions used in each step of the extraction protocol (see section 3.3.1.4). An internal standard of 1 ppb Rh was used for all samples and standards. The LOD were calculated from repeated measurements of 5 individual blank solutions. The LOD will equal three times the standard deviation of the blank values. The accuracy of the method was assessed by calculating the recovery of an analyte from 2 spiked samples (see Appendix A for more information). Finally, the precision of the method was assessed from the repeated measurement of a sample 6 times and reported as the 95% confidence interval of these results. More details about the precision, method validation, and LOD of the ICP-MS analyses in Appendix A.

3.4 Molecular biology methods

Immediately after coming back from the field, subsamples taken from bulk sediment samples were transferred into micro centrifuge tubes using a sterilised spatula. Care was taken to avoid any kind of contamination and samples were frozen at -20°C until used.

3.4.1 DNA extraction

Bacterial DNA was extracted from environmental samples (~0.5 g of wet sediment) using a FastDNA spin kit for soils (MP Biomedicals, USA). Unless explicitly stated, the manufacturer's protocols supplied with all kits employed were followed precisely. DNA fragment larger than 3 kb were isolated on a 1% agarose "1x" Tris-borate-EDTA (TBE) gel stained with ethidium bromide for flat electrophoresis and visualisation under UV light (10x TBE solution supplied by Invitrogen Ltd., UK). The DNA was extracted from the gel using a QIAquick gel extraction kit (QIAGEN Ltd, UK); final elution was by 1/10th strength elution buffer. DNA concentration was quantified fluorometrically using a Qubit dsDNA HS Assay (Thermo Fisher Scientific Inc., USA).

3.4.2 Sequencing of the V4 hyper−variable region of the 16S rRNA gene

DNA samples (1ng μL^{-1} in 20 μL aqueous solution) were sent for sequencing at the Centre for Genomic Research, University of Liverpool, where Illumina TruSeq adapters and indices were attached to DNA fragments in a two-step PCR amplification targeting the hyper-variable V4 region (with the forward target specific primer 5'-GTGCCAGCMGCCGCGGTAA-3' and the reverse target specific primer 5'-GGACTACHVGGGTATCTAAT-3') of the 16S rRNA gene (Caporaso *et al.*, 2011). Pooled amplicons were paired-end sequenced on the Illumina MiSeq platform (2x250 bp) generating ~12M clusters of data. Illumina adapter sequences were removed, and the trimmed reads were processed using the UPARSE pipeline (Edgar, 2013) within the USEARCH software package (version 8.1.1861) (Edgar, 2010) on a Linux platform. First of all, overlapping paired-end reads were assembled using the *fastq_mergepairs* command. Then the reads from single environmental samples were quality-filtered, relabelled, and de-replicated before they were randomly sub-sampled (500,000 reads with an average length of 296 bp) to produce a manageable sample size for combined analysis (~4M reads). After further de-replication of the combined pool of reads, clustering, chimera filtering and singletons removal were performed simultaneously within the pipeline by using the *cluster_otus* command. Operationally taxonomic units (OTUs) were defined based on a minimum sequence identity of 97% between the putative OTU members. The *utax* command was applied to assign to them a taxonomic

group using a confidence value of 0.7 to give a reasonable trade-off between sensitivity and error rate in the taxonomy prediction. The entire dataset (~6M reads) was then allocated to the defined OTUs using the *usearch_global* command and the results were reported in an OTU-table, which contained OTU-abundance data and the taxonomy classification for each OTU.

3.4.3 Diversity analysis and community composition

Traditional estimates of bacterial diversity can be distorted by rare taxa because these can be a small proportion of the bacteria population, but a large proportion of species present, so Hill numbers, D_q, were used to evaluate diversity (Hill, 1973; Jost, 2006).

Hill numbers (equation 3.7) define biodiversity as the reciprocal mean of proportional abundance, and compensate for the disproportionate impact of rare taxa by weighting taxa based on abundance (Hill, 1973; Jost, 2006, 2007; Kang *et al.*, 2016). The degree of weighting D_q is controlled by the index q (increasing q places progressively more weight on the high-abundance species within a population). Traditional diversity index can be converted to Hill numbers (Table 3.4). The unweighted Hill number, D_0, is exactly equivalent to the species richness. D_1 is a measure of the number of common species and is equivalent to the exponential of Shannon entropy; and D_2 is a measure of the number of dominant species and is equivalent to the inverse of Simpson concentration (Hill, 1973; Jost, 2006, 2007).

$$D_q = \left(\sum_{i=1}^{S} p_i^q\right)^{\frac{1}{1-q}} \quad \text{Eq. 3.7}$$

The bacterial diversity of each individual sample (alpha-diversity, D_q^{α}) was evaluated with different weightings on the high-abundance OTUs (D_0^{α}, D_1^{α}, D_2^{α}). The regional bacterial diversity (gamma-diversity, D_1^{γ}) was calculated from the combined dataset. The beta-diversity, D_1^{β} (which reflects the proportion of regional diversity contained in a single average community), was calculated from the gamma diversity and the statistically weighed alpha-diveristy ($^*D_1^{\alpha}$; Jost, 2007) using Whittaker multiplicative law (equation 3.8) (Whittaker, 1972). Additionally, beta-diversity has been analysed using compositional dissimilarities between two different samples (Bray-Curtis dissimilarity) in PAST software (https://folk.uio.no/ohammer/past/).

$*D_1^{\alpha} \times D_1^{\beta} = D_1^{\gamma}$ Eq 3.8

A heat map of OTUs abundance was generated in Rstudio v 0.99.486 (RStudio Team, 2015). For OTU taxonomic analysis, from the non-chimeric reads the OTUs classified as archaea and the OTUs which were not classified to the level of bacterial phylum with a confidence > 0.7 were excluded.

Table 3.4: Conversion of common indices to Hill numbers (D_q) for q=0 q=1 and q=2 (D_0, D_1, and D_2) (modified from Jost, 2007). D means diversity index; S represents the total number of species in the community; and p_i are species (OTUs) proportions.

Order of the diversity measurement (q)	**Traditional Diversity Index (D)**	**To convert diversity indices (D) to measurement of diversity (D_q)**	**Diversity in terms of p_i (D_q)**
0	Species Richness $D \equiv \sum_{i=1}^{S} p_i^0$	D	$D_0 = \sum_{i=1}^{S} p_i^0$=S
1	Shannon entropy $D \equiv -\sum_{i=1}^{S} p_i \ln p_i$	exp (D)	$D_1 = \exp\left(-\sum_{i=1}^{S} p_i \ln p_i\right)$
2	Simpson concentration $D \equiv \sum_{i=1}^{S} p_i^2$	1/D	$D_2 = {}^{1}/_{\sum_{i=1}^{S} p_1^2}$

3.4.4 Multivariate statistical analysis

The package ‘vegan’ was used for multivariate analyses (Oksanen *et al.*, 2013) in RStudio (v 0.99.486) (RStudioTeam, 2015).

Non-metric Multi-Dimensional Scaling (NMDS) is a method used to identify underlying gradients and to represent relationships based on various types of distance measures in an optimised low-dimensional (Ramette, 2007). The NMDS algorithm ranks distances between objects, and these ranks (and not the original distances) are used to distribute the objects nonlinearly in the ordination space. NMDS was carried out

by using Bray-Curtis dissimilarity matrix. The microbial community data were input as a matrix of the relative abundance of each OTU in each of the eight samples.

BIOENV ('biota-environment') analysis (Clarke and Ainsworth, 1993) was carried out also to further investigate the environmental variables that better correlate to sample similarities or dissimilarities (Bray Curtis dissimilarities) of the biological community using Spearman's rank correlation method. This test determines which combinations of environmental variables best explain patterns in the community composition. Finally, canonical correspondence analysis (CCA) is a constrained method based on unimodal species-environment relationships (Ramette, 2007). CCA tries to display only the part of the data that can be explained by the used constraints and not all the variation. It uses two matrices of data, the response matrix (i.e. the community composition like abundance data) and the explanatory matrix (i.e. environmental factors) in order to find a new mathematically simplified ordination that incorporates both data sets; the significance of these correlations is calculated by permutation. Axes are linear combinations of the environmental variables (Ramette, 2007). The environmental data used in these two tests included: salinity, major ion concentrations in the porewater, organic matter content, particle size and a range of redox indicators such as percentage of acid extractable $Fe^{2+}_{(s)}$, ammonium and dissolved Mn concentrations in porewater.

3.5 References

[1] APHA. (1980). *Standard Methods for the Examination of Water and Waste Water* (Mary Ann H. Franson Ed. 15 ed.). Washington D.C.: American Public Health Association.

[2] Armstrong, F. A., Stearns, C. R., & Strickland, J. D. (1967). Measurement of upwelling and subsequent biological processes by means of technicon autoanalyzer and associated equipment. *Deep-Sea Research*, 14(3), pp.381-389. doi: 10.1016/0011-7471(67)90082-4.

[3] Bruno, P., Caselli, M., de Gennaro, G., De Tommaso, B., Lastella, G., & Mastrolitti, S. (2003). Determination of nutrients in the presence of high chloride concentrations by column-switching ion chromatography. *Journal of Chromatography A*, 1003(1-2), pp.133-141. doi: 10.1016/s0021-9673(03)00785-4.

[4] Burke, I. T., Boothman, C., Lloyd, J. R., Mortimer, R. J., Livens, F. R., & Morris, K. (2005). Effects of progressive anoxia on the solubility of technetium in sediments. *Environ Sci Technol*, 39(11), pp.4109-4116. doi: 10.1021/es048124p.

[5] Canfield, D. E., Raiswell, R., Westrich, J. T., Reaves, C. M., & Berner, R. A. (1986). The use of chromium reduction in the analysis of reduced inorganic sulfur in sediments and shales. *Chemical Geology*, 54(1-2), pp.149-155. doi: 10.1016/0009-2541(86)90078-1.

[6] Caporaso, J. G., Lauber, C. L., Walters, W. A., Berg-Lyons, D., Lozupone, C. A., Turnbaugh, P. J., Fierer, N., & Knight, R. (2011). Global patterns of 16S rRNA diversity at a depth of millions of sequences per sample. *Proceedings of the National Academy of Sciences*, 108 (Supplement 1), pp.4516-4522. doi: 10.1073/pnas.1000080107.

[7] Clarke, K. R., & Ainsworth, M. (1993). A method of linking multivariate community structure to environmental variables. *Marine Ecology Progress Series*, 92(3), pp.205-219. doi: 10.3354/meps092205.

[8] Dong, H. L., Fredrickson, J. K., Kennedy, D. W., Zachara, J. M., Kukkadapu, R. K., & Onstott, T. C. (2000). Mineral transformation associated with the microbial reduction of magnetite. *Chemical Geology*, 169(3-4), pp.299-318. doi: 10.1016/s0009-2541(00)00210-2.

[9] Edgar, R. C. (2010). Search and clustering orders of magnitude faster than BLAST. *Bioinformatics*, 26(19), pp.2460-2461. doi: 10.1093/bioinformatics/btq461.

[10] Edgar, R. C. (2013). UPARSE: highly accurate OTU sequences from microbial amplicon reads. *Nature Methods*, 10(10), pp.996-1000. doi: 10.1038/nmeth.2604.

[11] Fossing, H., & Jørgensen, B. B. (1989). Measurement of bacterial sulfate reduction in sediments - evaluation of a single-step chromium reduction method. *Biogeochemistry*, 8(3), pp.205-222. doi: 10.1007/BF00002889.

[12] Fritz, J. S., & Gjerde, D. T. (2009). *Ion Chromatography*. Wenheim, Germany: Wiley-VCH.

[13] Guilbaud, R., Poulton, S. W., Butterfield, N. J., Zhu, M., & Shields-Zhou, G. A. (2015). A global transition to ferruginous conditions in the early Neoproterozoic oceans. *Nature Geoscience*, 8(6), pp.466-470. doi: 10.1038/ngeo2434 http://www.nature.com/ngeo/journal/v8/n6/abs/ngeo2434.html#supplementary-information.

[14] Hill, M. O. (1973). Diversity and evenness: a unifying notation and its consequences. *Ecology*, 54(2), pp.427-432. doi: 10.2307/1934352.

[15] Islam, F. S., Gault, A. G., Boothman, C., Polya, D. A., Charnock, J. M., Chatterjee, D., & Lloyd, J. R. (2004). Role of metal-reducing bacteria in arsenic release from Bengal delta sediments. *Nature*, 430(6995), pp.68-71. doi: 10.1038/nature02638.

[16] Jarvis, K. E., Gray, A. L., & Houk, R. S. (1992). *Handbook of Inductively Coupled Plasma Mass Spectrometry*. New York: Chapman and Hall.

[17] Jenkins, R. (1988). *X-ray Fluorescence Spectrometry*. New York: John Wiley & Sons.

[18] Jerez Vegueria, S. F., Godoy, J. M., de Campos, R. C., & Goncalves, R. A. (2013). Trace element determination in seawater by ICP-MS using online, offline and bath procedures of preconcentration and matrix elimination. Microchemical Journal, 106, 121-128. doi: 10.1016/j.microc.2012.05.032.

[19] Jost, L. (2006). Entropy and diversity. *Oikos*, 113(2), pp.363-375. doi: 10.1111/j.2006.0030-1299.14714.x.

[20] Jost, L. (2007). Partitioning diversity into independent alpha and beta components. *Ecology*, 88(10), pp.2427-2439. doi: 10.1890/06-1736.1.

[21] Kamphake, L. J., Hannah, S. A., & Cohen, J. M. (1967). Automated analysis for nitrate by hydrazine reduction. *Water Res*, 1(3), pp.205-216. doi: 10.1016/0043-1354(67)90011-5.

[22] Kang, S., Rodrigues, J. L. M., Ng, J. P., & Gentry, T. J. (2016). Hill number as a bacterial diversity measure framework with high-throughput sequence data. *Scientific Reports*, 6. doi: 10.1038/srep38263.

[23] Krom, M. D. (1980). Spectrophotometric determination of ammonia: a study of a modified Berthelot reaction using salicylate and dichloroisocyanurate. *Analyst*, 105(1249), pp.305-316. doi: 10.1039/AN9800500305.

[24] Lovley, D. R., & Phillips, E. J. P. (1986). Organic-matter mineralization with reduction of ferric iron in anaerobic sediments. *Applied and Environmental Microbiology*, 51(4), pp.683-689.

[25] Lovley, D. R., & Phillips, E. J. P. (1987). Rapid assay for microbially reducible ferric iron in aquatic sediments. *Applied and Environmental Microbiology*, 53(7), pp.1536-1540.

[26] Lovley, D. R., & Phillips, E. J. P. (1988). Manganese inhibition of microbial iron reduction in anaerobic sediments. *Geomicrobiology Journal*, 6(3-4), pp.145-155.

[27] Lovley, D. R. (1991). Dissimilatory Fe(III) and Mn(IV) reduction. *Microbiological Reviews*, 55(2), pp.259-287.

[28] MacArthur, R. H. (1965). Patterns of species diversity. *Biological reviews*, 40(4), pp.510-533.

[29] Oksanen, J., Blanchet, F. G., Kindt, R., Legendre, P., Minchin, P. R., O'Hara, R. B., Simpson, G. L., Solymos, P., Stevens, M. H. H., & Wagner, H. (2013). vegan: Community Ecology Package. R package version 2.0-10. Retrieved 22-08-2016, from http://CRAN.R-project.org/package=vegan.

[30] Poulton, S. W., & Canfield, D. E. (2005). Development of a sequential extraction procedure for iron: implications for iron partitioning in continentally derived particulates. *Chemical Geology*, 214(3-4), pp.209-221. doi: 10.1016/j.chemgeo.2004.09.003.

[31] Ramette, A. (2007). Multivariate analyses in microbial ecology. *FEMS Microbiology Ecology*, 62(2), pp.142-160. doi: 10.1111/j.1574-6941.2007.00375.x.

[32] Rauret, G., Rubio, R., & López-Sánchez, J. F. (1989). Optimization of Tessier Procedure for Metal Solid Speciation in River Sediments. *International Journal of Environmental Analytical Chemistry*, 36(2), pp.69-83. doi: 10.1080/03067318908026859.

[33] Reed, N. M., Cairns, R. O., Hutton, R. C., & Takaku, Y. (1994). Characterization of polyatomic ion interferences in inductively-coupled plasma-mass spectrometry using a high-resolution mass-spectrometer. Journal of Analytical Atomic Spectrometry, 9(8), 881-896. doi: 10.1039/ja9940900881.

[34] Roberts, K. L., Kessler, A. J., Grace, M. R., & Cook, P. M. L. (2014). Increased rates of dissimilatory nitrate reduction to ammonium (DNRA) under oxic conditions in a periodically hypoxic estuary. *Geochimica et Cosmochimica Acta*, 133, pp.313-324. doi: http://dx.doi.org/10.1016/j.gca.2014.02.042.

[35] Stanjek, H., & Hausler, W. (2004). Basics of X-ray diffraction. *Hyperfine Interactions*, 154(1-4), pp.107-119. doi: 10.1023/b:hype.0000032028.60546.38.

[36] Tack, F. M. G., & Verloo, M. G. (1995). Chemical Speciation and Fractionation in Soil and Sediment Heavy-Metal Analysis - A Review. *International Journal of Environmental Analytical Chemistry*, 59(2-4), pp.225-238. doi: 10.1080/03067319508041330.

[37] Team, R. (2015). RStudio: Integrated Development Environment for R (Version.0.99.486). Boston, MA: RStudio, Inc. Retrieved from http://www.rstudio.com/

[38] Tessier, A., Campbell, P. G. C., & Bisson, M. (1979). Sequential extraction procedure for the speciation of particulate trace-metals. *Analytical Chemistry*, 51(7), pp.844-851. doi: 10.1021/ac50043a017.

[39] Thamdrup, B., Fossing, H., & Jørgensen, B. B. (1994). Manganese, iron, and sulfur cycling in a coastal marine sediment, Aarhus Bay, Denmark. *Geochimica et Cosmochimica Acta*, 58(23), pp.5115-5129. doi: 10.1016/0016-7037(94)90298-4.

[40] Viollier, E., Inglett, P.W., Huntrer, K., Roychoudhury, A. N., and Van Cappellen, P. (2000). The ferrozine method revised: Fe(II)/Fe(III) determination in natural waters. *Applied Geochemistry*, 15, pp.785-790.

[41] Whittaker, R. H. (1972). Evolution and measurement of species diversity. *Taxon*, 21(2-3), pp.213-251. doi: 10.2307/1218190.

[42] Zachara, J. M., Fredrickson, J. K., Li, S. M., Kennedy, D. W., Smith, S. C., & Gassman, P. L. (1998). Bacterial reduction of crystalline Fe^{3+} oxides in single phase suspensions and subsurface materials. *American Mineralogist*, 83(11-12), pp.1426-1443.

[43] Zimmerman, A. J., & Weindorf, D. C. (2010). Heavy metal and trace metal analysis in soil by sequential extraction: a review of procedures. *International Journal of Analytical Chemistry*, 2010, pp.387803-387803. doi: 10.1155/2010/387803.

Chapter 4
Sediment and Water Characterisation

In this chapter data for sediment and water characterisation have been gathered into different tables, in order to better organise the full data set and to provide reference tables for the other chapters in the thesis.

4.1 Sediment characterisation

4.1.1 Elemental and bulk mineral composition

The elemental composition obtained from XRF analysis is summarised in Table 4.1. Al, Fe and Mn were the major elements. Ni and Cd were below the detection limit. For each metal, the concentration was relatively similar among samples. Zinc was the more abundant of the trace metals (TMs), but in general all were present in the same order of magnitude.

The XRD analysis was carried out only as a basic scan of the bulk mineralogy of each sample and no quantification method (TOPAS rietveld or RIR quantification) was applied. The images of the XRD scans can be found in the Appendix B.1. All sediments contained a mixture of quartz, carbonates (calcite and dolomite), and silicates (kaolinite, muscovite, clinochlore, albite, microcline). Halite was present at the samples from S3 and S4. Pyrite was only detected in the subsurface sediments from S4.

Table 4.1: Elemental composition of the estuarine sediments used throughout (in µg/g unless specified) by XRF analysis. Concentrations are averages and the quoted uncertainties are the range of duplicate analysis.

	S1		S2		S3		S4	
	Surface	**Subsurface**	**Surface**	**Subsurface**	**Surface**	**Subsurface**	**Surface**	**Subsurface**
Al (%)	3.1±1.0	3.9±0.1	3.6±0.2	3.9±0.2	5.1±0.3	5.0±0.4	5.6±0.4	5.5±0.4
Fe (%)	2.7±1.0	3.3±0.7	3.1±0.6	2.9±0.5	3.7±0.7	4.1±1.0	4.5±1.0	4.3±0.9
Mn	656±8	785±8	681±20	654±1	847±6	969±3	758±14	732±11
Zn	132±3	149±1	139±4	129±4	161±2	199±13	174±1	167±6
Cu	30±4	33±3	31±2	27±2	39±2	31±3	33±2	37±11
V	61±1	71±2	62±2	62±4	80±3	98±1	93±2	99±8
Ni	<4	<4	<4	<4	<4	<4	<4	<4
Cr	69±4	82±1	76±13	77±13	107±1	118±3	116±3	113±4
Pb	49±6	64±1	58±2	53±2	71±3	90±3	74±6	75±1
As	23±4	20±2	18±3	18±2	19±2	37±4	30±1	25±2
Cd	<2	<2	<2	<2	<2	<2	<2	<2

4.1.2 Grain size and porewater content

The percentage of water in the wet sediments (porewater) was determined by difference after subsamples of wet sediments were oven dried. Surface sediments were slightly more saturated than the correspondent subsurface sediment, and S3 and S4 sediments contained more water than S1 and S2 sediments (Table 4.2). This is in agreement with the grain size of the sediments. The particles of the samples S3 and S4 were finer than those for S1 and S2 samples. The particle size has been expressed as the upper bound diameter of the sample at 50% of cumulative percentage of particles by volume. The distribution curves for size-class, finer, and coarser material are included in Appendix B.2.

Table 4.2: Water content of the estuarine sediment (porewater, PW) (±σ of triplicates) and grain size. The size of the particle refers to the upper bound diameter of the sample when the cumulative percentage of the particles by volume is 50% (D_{50}) (based on six repeated measurements).

	S1		**S2**		**S3**		**S4**	
	Surface	**Subsurface**	**Surface**	**Subsurface**	**Surface**	**Subsurface**	**Surface**	**Subsurface**
% PW	42	35±1	42	39±1	55	41±5	54	37±2
Particle size (μm)	53	37	47	47	16	19	13	16

4.1.3 Carbon, sulphur and iron

The following table (Table 4.3) contains the data collected for carbon, sulphur and iron. The percentages of TIC, TOC and TS are averaged values and the error associated is the standard deviation of triplicates. The total Fe in this table was obtained from the total iron extraction. The reproducibility test for these measurements gave a standard deviation of 0.2% (σ of six reads for the same sample). Iron and sulphur associated with AVS and pyrite have been also reported although no AVS was extracted from S1 and S2 samples, whereas in S3 and S4 samples AVS concentrations were very low or under detection limit. The 0.5 N HCl extractable iron (total) was quantified and the values are averaged measurements with the standard deviation of triplicates. To finish, there is the

percentage of acid extractable reduced iron relative to the total acid extractable iron with the standard deviation of triplicates as well.

Table 4.3: Carbon, sulphur and iron content in the estuarine sediments. The percentages of TIC, TOC TS and iron and sulphur associated with AVS and pyrite represent percentages relative to the total dry weight of the sediment sample.

	S1		S2		S3		S4	
	Surface	**Subsurface**	**Surface**	**Subsurface**	**Surface**	**Subsurface**	**Surface**	**Subsurface**
%TIC	1.71±0.31	1.01±0.69	0.69±0.22	1.09±0.19	1.43±0.06	1.38±0.21	1.75±0.10	1.76±0.04
%TOC	1.28±0.29	2.34±0.68	2.48±0.21	1.75±0.15	2.06±0.04	2.58±0.17	2.17±0.04	2.69±0.03
%TS	0.16±0.01	0.18±0.01	0.18±0.00	0.14±0.01	0.22±0.00	0.35±0.00	0.31±0.00	0.52±0.01
Total Iron (%)	2.09	2.73	2.68	2.35	3.47	3.97	4.27	3.9
%Fe-AVS	nd	nd	nd	nd	<LDL	0.01	<LDL	0.09
%S-AVS	nd	nd	nd	nd	<LDL	0.01	<LDL	0.05
%Fe-Pyrite	0.08	0.10	0.09	0.10	0.10	0.12	0.12	0.18
%S-Pyrite	0.09	0.11	0.10	0.11	0.12	0.14	0.14	0.21
0.5 N HCl extractable Fe_{TOT} (µmols/g solids)	106±1	116±10	106±6	105±4	123±3	206±8	93±9	191±28
0.5 N HCl extractable Fe^{2+} (% Fe^{2+}/Fe_{TOT})	52±2	61±5	53±1	53±2	39±1	84±6	57±3	96±3

4.2 Water chemistry characterisation

The water chemistry has been analysed in detail. All the parameters with the exception of pH and conductivity, which are in situ measurements, have been determined for river water and porewater recovered from surface and subsurface wet sediments. Salinity has been calculated from chlorinity, and the other components (nutrients, major and TMs) are direct measurements.

Table 4.4: Water (river water, surface porewater and subsurface porewater) chemistry characterisation. Unless specified, all metal concentrations are in µM units.

	S1			S2			S3			S4		
	River	**Surface**	**Subsurface**	**River**	**Surface**	**Subsurface**	**River**	**Surface**	**Subsurface**	**River**	**Surface**	**Subsurface**
Salinity (psu)	0.4	0.3	0.2	3.5	3.1	1.8	21.6	17.0	17.7	26.1	28.0	32.1
pH	7.87	-	-	7.52	-	-	7.90	-	-	8.02	-	-
Conductivity (mS/cm)	0.7383	-	-	5.731	-	-	30.48	-	-	36.42	-	-
NO_3^- (µM)	266	36	37	250	17	26	248	66	17	24	78	7
NO_2^- (µM)	1.6	0.2	0.4	1.6	0.1	0.3	0.4	0.9	<DL	0.7	1.0	<DL
NH_4^+ (µM)	7	12	67	7	25	73	12	73	994	23	166	126
SO_4^{2-} (mM)	1	2±0	2±0	3	6±1	3±1	16	33±4	33±2	22	32±4	40±2
Cl^- (mM)	2	4	3	38	49	28	306	265	276	443	347	501
Al	0.26	0.53	0.29	0.32	0.43	0.37	47.44	47.81	47.44	49.30	41.88	48.93
Fe	0.1	0.4	4.9	0.1	0.1	0.3	1.2	1.6	3.6	1.8	0.9	3.3
Mn	1.4	3.4	82.3	1.0	5.1	49	0.6	60	0	23	15	62
Zn	0.15	0.12	0.01	0.16	0.06	0.04	8.49	3.87	3.52	8.03	3.53	3.53

Cu	0.05	0.08	0.10	0.05	0.06	0.05	3.70	8.26	8.32	3.76	8.94	8.06
As	0.06	0.10	0.19	0.07	0.08	0.08	0.07	0.20	0.99	0.07	0.01	0.25
Cr	3.96 nM	0.01	0.01	0.01	0.01	0.01	0.04	0.04	0.05	0.04	0.03	0.05
Cd	0.46 nM	0.08 nM	0.06 nM	0.84 nM	0.09 nM	0.09 nM	0.23	0.23	0.23	0.24	0.25	0.23
V	0.14	0.16	0.24	0.17	0.16	0.20	0.07	0.06	0.22	0.07	0.00	0.08
Co	0.08	0.13	0.24	0.09	0.10	0.10	0.08	0.25	1.25	0.08	0.01	0.32
Ni	0.07	0.12	0.27	0.07	0.09	0.13	4.92 nM	8.21 nM	4.63 nM	4.29 nM	2.68 nM	4.79 nM
Pb (nM)	1.21	1.53	1.60	2.34	1.71	1.13	-	-	-	-	-	-

4.3 Discussion

A broad interpretation of these data will be done in this chapter, because in the following chapters data will be further discussed in the context of the different experiments carried out with these materials.

The bulk elemental and mineral composition did not vary significantly among samples, although the TM concentrations were generally slightly higher in the sediments from the outer estuary (S3 and S4). The concentrations of TMs in the bulk sediment will be used to compare the present concentration with background levels and with the concentrations found in the period of greatest industrial activity within the Humber catchment (see Chapter 6). Furthermore, the analysis of metal partitioning will give us further information about the mobility and bioavailability of these elements in the estuarine environment (see Chapter 5 and 6).

The particle size was finer in the samples taken from the outer estuary mudflats. Very fine silt-clays were the predominant grain size classes in the outer estuary, whereas in the inner estuary (S1 and S2), sediments were sandier. But in general, all the samples had particles in the range from clays to very fine sands.

The content of TIC was ≤2% in all the samples with no significant differences between depths. TOC content was within the range described in the literature (1-4%, Freestone, 1987). The mudflats of the outer Humber estuary appeared to have a slightly higher organic content than the inner estuary sediments. Subsurface sediments showed some enrichment in organic matter with respect to their overlying material.

In terms of the iron, the total content in these sediments varied between 2-4% of iron (the results for total amount from the HNO_3–HF–$HClO_4$–H_3BO_3–HCl sediment digestion coincide with the XRF data) with no significant difference between sediment depths. Sediments from the outer estuary had more iron than those from the inner estuary sites and slightly more iron associated with pyrite. The content of sulphur was also higher in the outer mudflats. During the iron sulphide extractions no AVS was detected in any of the samples from S1 and S2, whereas all the samples from S3 and S4

showed Ag_2S precipitates at the end of the extraction. During the handling of the solids extracted for AVS analysis (filtering, drying, and weighting) errors were introduced and AVS quantification of the surface samples from S3 and S4 was not possible. The AVS concentrations measured (<0.02 μmoles AVS g^{-1}) in these estuarine sediments were low possibly due to the dynamic nature of the Humber, but other studies reported low AVS in estuarine and other aquatic environments (Di Toro *et al.*, 1990; Allen *et al.*, 1993; Fang *et al.*, 2005) (see Chapter 6). Although we expected to find more AVS, especially in the samples from the mudflats, these sediments could be characterised as reducing sulphidic sediments if we consider the combination of other redox indicators, field observations and previous studies in the area. Nevertheless, measurements of dissolved oxygen would have been desirable to complete the redox characterisation of the sediments. The 0.5 N HCl extractable iron showed also higher values in S3 and S4 samples, and at the subsurface, the concentrations were ~2 times the concentrations found in the inner estuary samples. Subsurface samples, especially in S3 and S4, accumulated reduced iron with respect to the surface sediment layer.

The water chemistry is discussed in depth in Chapter 5, 6 and 7 placing the emphasis on different aspects. In general, the nitrate concentrations in the river water were high until S3 and porewaters did not accumulate nitrate. Ammonium increased in solution seawards and it appeared to accumulate at depth. Dissolved Fe and Mn were low in the overlying water, and in general, concentrations increased in the porewaters. Dissolved manganese was greater than iron in the majority of the samples. Iron oxides react with free sulphides and, at the same time, the produced Fe^{2+} and H_2S reduce MnO_2 rapidly (Thamdrup *et al.*, 1994). This could be a reason for the low AVS detected and the accumulation of Mn^{2+} in porewaters. The reaction of MnO_2 with reduced iron produces more iron oxides that will reproduce this positive feedback mechanism. Furthermore, H_2S can also react with NO_3^- which would influence the distribution of free sulphides within the sediment (Sayama *et al.*, 2005). In terms of TMs, there were different patterns in the concentration changes with depth and with salinity. Zinc, Cd, Cu and Al showed significant differences in the concentrations between brackish-fresh waters and salt waters, in which the level of these TMs was two orders of magnitude higher than in the brackish-freshwaters. Nickel instead appeared in lower concentrations at the more

saline waters. The rest of the metals analysed (As, Cr, V and Co) were present in similar concentrations in all the samples. Porewaters showed broadly more dissolved TMs than their respective overlaying water, although there were exceptions (e.g. Zn showed opposite trend).

4.4 References

[1] Allen, H. E., Fu, G. M., & Deng, B. L. (1993). Analysis of acid-volatile sulfide (AVS) and simultaneously extracted metals (SEM) for the estimation of potential toxicity in aquatic sediments. *Environmental Toxicology and Chemistry*, 12(8), pp.1441-1453. doi: 10.1897/1552-8618(1993)12[1441:aoasaa]2.0.co;2

[2] Di Toro, D. M., Mahony, J. D., Hansen, D. J., Scott, K. J., Hicks, M. B., Mayr, S. M., & Redmond, M. S. (1990). Toxicity of cadmium in sediments the role of acid volatile sulfide. *Environmental Toxicology and Chemistry*, 9(12), pp.1487-1502. doi: 10.1002/etc.5620091208

[3] Fang, T., Li, X., & Zhang, G. (2005). Acid volatile sulfide and simultaneously extracted metals in the sediment cores of the Pearl River Estuary, South China. *Ecotoxicology and Environmental Safety*, 61(3), pp.420-431. doi: http://dx.doi.org/10.1016/j.ecoenv.2004.10.004

[4] Freestone, D., Jones, N., North, J.,Pethick, J., Symes, D., and Ward, R. (1987). The Humber Estuary, Environmental Background: Institute of Estuarine and Coastal Studies.

[5] Sayama, M., Risgaard-Petersen, N., Nielsen, L. P., Fossing, H., & Christensen, P. B. (2005). Impact of bacterial NO3- transport on sediment biogeochemistry. *Applied and Environmental Microbiology*, 71(11), pp.7575-7577. doi: 10.1128/aem.71.11.7575-7577.2005

[6] Thamdrup, B., Fossing, H., & Jørgensen, B. B. (1994). Manganese, iron, and sulfur cycling in a coastal marine sediment, Aarhus Bay, Denmark. *Geochimica et Cosmochimica Acta*, 58(23), pp.5115-5129. doi: 10.1016/0016-7037(94)90298-4

Chapter 5

Reoxidation of estuarine sediments during simulated resuspension events: effects on nutrient and trace metal cycling

Executive Summary

Estuarine environments are considered to be nutrient buffer systems as they regulate the delivery of nutrients from rivers to the ocean. In the Humber Estuary (UK) seawater and freshwater mixing during tidal cycles leads to the mobilisation of oxic surface sediments (0-1 cm). However, less frequent seasonal events can also mobilise anoxic subsurface (5-10 cm) sediments, which may have further implications for the estuarine geochemistry. A series of batch experiments were carried out on surface and subsurface sediments taken from along the salinity range of the Humber Estuary. The aim was to investigate the geochemical processes driving major element (N, Fe, S and Mn) redox cycling and trace metal behaviour during simulated resuspension events. The magnitude of major nutrient and metal release was significantly greater during the resuspension of sulphidic (outer estuary) rather than from non sulphidic (inner estuary) sediments. When comparing surface versus subsurface sediment reoxidation, only the outer estuary experiments showed significant differences in major nutrient behaviour with sediment depth. In general, any ammonium, manganese and trace metals (Cd, Cu and Zn) released during the reoxidation experiments were rapidly removed from solution as new adsorption sites (i.e. Fe/Mn oxyhydroxides) formed. Therefore Humber estuary sediments showed a scavenging capacity for these dissolved species and hence may act as an ultimate sink for these elements. Due to the larger aerial extent of the outer estuary intertidal mudflats in comparison with the inner estuary area, the mobilisation of anoxic iron sulphide rich sediments would have a greater impact on the transport and cycling of nutrients and trace metals. Climate change scenarios predict an increasing frequency of major storm events in temperate regions which are more likely to mobilise deeper sediment regions, altering nutrient and metal inputs to the coastal waters, and therefore enhancing the likelihood of eutrophication in this environment.

5.1 Introduction

Estuaries are highly dynamic coastal environments regulating delivery of nutrients and trace metals (TMs) to the ocean (Sanders *et al.*, 1997; Statham, 2012). In most coastal ecosystems in the temperate zone, nitrogen controls primary productivity as it is usually the limiting nutrient; therefore an increased load flowing into such oligotrophic waters could lead to eutrophication, and the subsequent environmental impacts due to hypoxia, shifts in biological community structures and HAB (Howarth *et al.*, 1996; Abril *et al.*, 2000; Boyer & Howarth, 2002; Roberts *et al.*, 2012; Statham, 2012). This has been focus of attention because human activities over the last century have increased nitrogen fluxes to the coast in some regions of the world due to intensive agricultural practices, and wastewater and industrial discharges (Howarth *et al.*, 1996; Canfield *et al.*, 2010).

River inputs are the main nitrogen sources to estuarine waters, although atmosphere and groundwater have been also recognised as important nitrogen sources. From the total dissolved nitrogen inputs to an estuary, inorganic nitrogen (DIN) is generally the major portion, especially in hypernutrified estuaries; however organic nitrogen (DON or PON) may be a significant input in some estuaries (20-90% of the total N load) (Seitzinger & Sanders, 1997; Nedwell *et al.*, 1999). The speciation and distribution of nitrogen along the salinity continuum will be controlled by a complex group of dissimilatory and assimilatory transformations coexisting at a range of oxygen concentrations (Thamdrup, 2012); but denitrification is considered the major removal process of nitrogen to the atmosphere in shallow aquatic environments (Statham, 2012). Nitrate is the most stable nitrogen species in surface oxic waters. Nitrite is less stable, and it is considered an intermediate product in nitrification, and denitrification. Ammonium, in contrast, is only stable in reducing conditions. It can be stored within the sediments, from which can be readily released back to solution through porewater dilution and desorption from particles (Morin & Morse, 1999). Anammox and dissimilatory nitrate reduction to ammonium (DNRA) can also play a role in the nitrogen cycle, although the relative importance and magnitude of such processes in different coastal environments is still in discussion (Song *et al.*, 2013; Roberts *et al.*, 2014). The organic nitrogen pool will be cycled during microbial metabolism and thus it also plays an important role in the

estuarine geochemistry. However this organic nitrogen pool is difficult to characterise as it comprises a wide variety of compounds, the majority of which are complex high molecular weight compounds. These large molecules are more refractory and less bioavailable than low molecular weight compounds which are readily available for microbes and phytoplankton (Seitzinger & Sanders, 1997). Organic matter buried into the sediments will be involved in the early diagenesis through a combination of biological, chemical and physical processes. In fact, high rates of organic matter oxidation are expected in estuaries due to the high rates of sediment accumulation, organic matter flux into the sediment and organic matter burial (Henrichs, 1992).

Estuarine sediments may also have accumulated contaminants such as TMs carried by river loads. Sediment geochemistry and dynamics will control the mobility and bioavailability of TMs, and therefore estuarine sediments subjected to reoxidation processes may be potential sources of TMs (Salomons *et al.*, 1987; Di Toro *et al.*, 1990; Allen *et al.*, 1993; Calmano *et al.*, 1993; Simpson *et al.*, 1998; Saulnier & Mucci, 2000; Caetano *et al.*, 2003). Trace metals can be in solution, adsorbed (or co-precipitated) to different mineral surfaces and organic matter, but in anoxic sediments, iron sulphides are thought to be the main solid phases controlling TM mobility and bioavailability due its high affinity for a wide variety of TMs (Salomons *et al.*, 1987; Huerta-Diaz & Morse, 1990; Allen *et al.*, 1993). When sediments are exposed to oxic conditions, dissolved Fe and Mn will precipitate rapidly as amorphous and poorly crystalline Fe/Mn oxyhydroxides, incorporating the released TMs by co-precipitation and/or adsorption (Burdige, 1993; Calmano *et al.*, 1993; Simpson *et al.*, 1998; Saulnier & Mucci, 2000; Gunnars *et al.*, 2002; Caetano *et al.*, 2003). These newly formed minerals will be transported, mixed, and maybe, eventually buried into the underlying anoxic sediment again.

In aquatic sediments, there is a vertical progression of metabolic processes determined by the use of the available electron acceptors during organic matter mineralisation (Canfield & Thamdrup, 2009). The sequential utilization of the terminal electron acceptors is based on the thermodynamics of the process and the free energy yield (Stumm & Morgan, 1970; Froelich *et al.*, 1979; Berner, 1980). At the surface, dissolved

oxygen can diffuse a few millimetres into the sediments (the *oxic* zone). Beneath, there is often a zone where nitrate (and nitrite as its reduction intermediate) accumulates and is reduced under anoxic conditions (the *nitrogenous* zone). Below, zones dominated by metal reduction (the *manganous* and *ferruginous* zones), sulphate reduction (the *sulphidic* zone), and methanogenesis (the *methanic* zone) occur in sequence (Canfield & Thamdrup, 2009) (see more details about the geochemical zonations in the section 2.3.3 of this thesis).

However, in coastal and estuarine sediments, these geochemical zones and the correspondent metabolic zones are not normally well delineated and they tend to overlap because sediment profiles are often disturbed by mixing and/or bioturbation (Sørensen & Jørgensen, 1987; Aller, 1994; Postma & Jakobsen, 1996; Mortimer *et al.*, 1998; Canfield & Thamdrup, 2009). Rapid redox changes at the estuarine sediment-water interface due to successive cycles of suspension and settling of surface sediments will control the speciation and cycling of nutrients and trace elements on a tidal-cycle timescale (Morris *et al.*, 1986). Yet, less frequently, seasonal or annual resuspension events (for example, due to very intense storms) can affect sediment to depths that are not disturbed normally, intersecting different pools of sediments and therefore altering the biogeochemistry of the system (Eggleton & Thomas, 2004).

In this study sediments from four different sites along the salinity range of the Humber Estuary (UK) were used in order to investigate the impact of sediment resuspension on the redox cycling and transport of the major elements and TM to the coastal waters. The authors have worked in the Humber since 1994 (Mortimer *et al.*, 1998; Burke *et al.*, 2005) and have observed the frequency and magnitude of resuspension events. Small scale resuspension of the upper 1-2 mm occurs on a tidal cycle; medium scale resuspension of the order of centimetres occurs during large flooding or moderate storm events which occur approximately twice a year. Very significant resuspension events that strip off the mud from intertidal areas occur on a timescale of several decades (a removal of about 10 cm deep intertidal mudflat was observed following a storm in early 1996) (Mortimer *et al.*, 1998). Accordingly, for this experiment, two sediment depths (the mobile oxic surface layer, 0-1 cm, and the suboxic/anoxic subsurface layer, 5-10

cm) were selected to simulate different timescales of resuspension and analyse their effects on nutrient and TM behaviour. The aim of this work is to better understand the environmental impact of remobilisation events within the estuary since climate change scenarios suggest extreme rainfall episodes will become increasingly common in temperate regions (Jones & Reid, 2001; Christensen *et al.*, 2007). The more frequent disruption of subsurface sediments will affect the geochemistry of estuarine sediments, porewater profiles may not reach steady state between resuspension episodes, and there may be impacts on the nutrient and TM fluxes to the sea.

5.2 Material and Methods

5.2.1 Field sampling

The Humber Estuary is a macrotidal estuary on the east coast of northern England (see Fig. 2.6). It is 60 km in length, contains ~115 km^2 of mudflats, and is highly turbid (Pethick, 1990). The Humber is also considered a major source of nutrients for the North Sea (Pethick, 1990; Mortimer *et al.*, 1998; Uncles *et al.*, 1998b).

Samples of intertidal mudflat sediments and river water were collected at low tide during the same tidal cycle on the 15th July 2014 along the north bank of the Humber Estuary (Fig. 3.1). The four sites were Boothferry (S1) and Blacktoft (S2) on the inner estuary, and Paull (S3) and Skeffling (S4) on the outer estuary. These sites were selected to cover the salinity range within the estuary (Mortimer *et al.*, 1998; Burke *et al.*, 2005; Uncles *et al.*, 2006). A sample of surface sediment (0-1 cm), subsurface sediment (5-10 cm) and river water were recovered from each sampling location. Sediments and river water samples were transferred into acid washed polythene containers, and stored at 4°C until used in resuspension experiments (started within 48 hrs). In order to minimise sediment air oxidation, no air space was left in the containers, although during the sampling, redox sensitive elements from porewater could have undergone partial oxidation. River water pH, conductivity and temperature were determined in the field using a Myron Ultrameter PsiII handheld multimeter. Subsamples of sediments and river waters were stored for further analysis. Porewaters

were recovered from each sediment sample by centrifugation (30 min, 6000 *g*) within 6-8 hrs of sampling, and stored for further analysis.

5.2.2 Sample characterisation and analytical methods

The sediments were oven dried at 70°C for 24 hrs prior to XRD analysis on a Bruker D8 Advance diffractometer and XRF analysis on an Olympus Innovex X-5000 spectrometer. From the dried sediments, two subsamples were analysed by XRF in two different runs. The percentage of AVS and pyrite present were determined on freeze dried sediments using the methods described in Canfield *et al.* (1986) and Fossing & Jørgensen (1989) respectively, and the extractions were carried out in triplicates. Total extractable Fe and extractable $Fe^{2+}_{(s)}$ contents of the sediments were determined after 60 min extraction in 0.25 M hydroxylamine HCl (Lovley & Phillips, 1987) and 0.5 N HCl respectively (Lovley & Phillips, 1986), followed by ferrozine assay (Viollier *et al.*, 2000). Each of the extractions was also carried out in triplicates. TS and TOC in sediments (before and after HCl (10% v/v) treatment were determined in triplicate on a LECO SC-144DR Sulphur and Carbon Analyser by combustion with non-dispersive infrared detection. TIC was determined by difference.

All water samples were filtered (<0.2µm Minisart®) prior to analysis. A continuous segmented flow analyser (SEAL AutoAnalyser 3 HR) was used to measure ammonium (%RSD was 3% and 1% for fresh and brackish-saline waters respectively). Ion chromatography (IC) was carried out to determine inorganic anions (NO_3^-, NO_2^-, SO_4^{2-} and Cl^-). Chromatographic analysis of high chloride samples required the use of a column-switching method (Bruno *et al.*, 2003) where matrix chloride anions were pre-separated from the other analytes by a double in-line pre-column (AG9-HC 4 mm). The four-way valve, placed after the last pre-column, allowed the elution of most of the chloride to waste before the remaining analytes were eluted to the analytical column (AS9-HC). Then, ions were detected by conductivity (DIONEX CD20, ED40 Electrochemical detector, %RSD <10%) and spectrophotometry for differentiation of nitrite and nitrate (DIONEX AD20 UV absorbance detector (225 nm)). For high salinity samples a second run with a DIONEX 500 (using a 20-fold dilution samples) was needed in order to measure chloride concentrations (%RSD ≤ 2%).

5.2.3 Resuspension experiments

Sediment samples (30 g wet weight) from each location were used to prepare sediment slurries. The natural river waters were directly used to make up the suspensions without any pre-treatment (no deoxygenation or filtration applied). To prepare each specimen, 120 mL of the corresponding river water were added to the weighed solids in an open 500 mL Erlenmeyer flask, which was covered with a foam bung that allowed gas exchange with the atmosphere, but excluded dust. Each experiment (for each of the eigth sediment types) was run in triplicate (24 flasks in total), which will be the basis of the precision estimates on the figures presented. Thereafter, the slurries were maintained in suspension using an orbital shaker (120 rpm) at laboratory temperature (21±1°C). A series of 5 mL subsamples of sediment suspension were withdrawn from all flasks at different intervals from 0.02 hrs (1 min) to 336 hrs (two weeks). The sampling frequency was progressively decreased with time in order to more intensively monitor changes occurring at the start of the experiment relative to those occurring over longer time periods. During our experimental time (two weeks), the sampling schedule was planned to cover not only short-term, but also medium-term (2-3 days) changes, which would represent the duration of a very significant resuspension event like that suggested in Kalnejais *et al.* (2010).

After sampling, the aqueous phase was separated from solids by centrifugation (5 min; 16,000 *g*). Eh and pH were determined in the aqueous phase using a Hamilton PolyPlast ORP BNC and an Orion Dual Star meter (with the electrode calibrated at pH 4, 7 and 10) respectively. Aqueous samples were filtered and retained for analysis. Subsamples of each replicate were acidified with 1% v/v AnalR HNO_3 (VWR) for TM analysis by ICP-MS on a Thermo Scientific iCAPQc ICP-MS. Precautions were taken due to the high salinity of some of the samples and to avoid polyatomic interferences (see Appendix A for more details). Nutrients in the aqueous phase were measured as described above; and acid extractable $Fe^{2+}_{(s)}$ was determined immediately on solid residues from centrifugation following the method described above.

5.2.4 Sequential extractions

To support the understanding of the changes in TM speciation due to reoxidation, sequential extractions were performed concurrently. The partitioning of selected metals (Zn, Cu and Cd) between different operationally-defined geochemical fractions was determined using the Tessier *et al.* (1979) procedure as optimised for riverine sediments by Rauret *et al.* (1989). The extractions were carried out in triplicate with the original wet sediment samples and with the dried solid residues recovered from each specimen, and therefore in triplicates as well, at the end of the resuspension experiments. Four extractants were used: 1 M magnesium chloride ($MgCl_2$) at pH 7 (to determine the "exchangeable" fraction), 1 M sodium acetate (NaOAc) at pH 5 (for the bound-to-carbonates, "weak acid extractable"), 0.04 M hydroxylamine hydrochloride ($NH_2OH{\cdot}HCl$) in 25% v/v acetic acid (HAc) (bound to Fe/Mn oxides), and 0.02 M HNO_3, plus 30% H_2O_2 at pH 2 followed by ammonium acetate (NH_4Ac) (bound to organic matter and sulphides). The third step of the extraction protocol was modified by reducing the extraction temperature (from 96°C to room temperature), and increasing the extraction time (from 6 to 12-14 hrs (overnight)). With the original wet sediments, the first three steps of the extraction protocol were carried out in an anaerobic chamber and the reactants needed were deoxygenated prior to use inside the chamber. Metal concentrations associated with the residual phase were not determined. The concentrations of the metals in the extractants were analysed by ICP-MS.

5.3 Results

5.3.1 Sample characterisation

5.3.1.1 Site characterisation

The basic physicochemical parameters at the four sampling sites are reported in Table 5.1. During sampling the light brown oxic surface sediments contrasted visually with the underlying dark grey materials, except at S2 (Blacktoft), where there was no colour change but abundant plant material throughout. The full chemical characterisation of the river waters and porewaters from both sediment depths are given in Chapter 4.

Table 5.1: Characterisation of the river waters at the four study sites. Conductivity, temperature and pH were measured in situ. Eh was measured prior to resuspension in the laboratory.

	S1	S2	S3	S4
Conductivity (mS/cm)	0.7383	5.731	30.48	36.42
Salinity (psu)	0.4	3.5	21.6	26.1
Temperature (°C)	20.0	19.7	19.2	19.5
pH	7.87	7.52	7.90	8.02
Eh (mV)	+151±24	+109±23	+75±8	+75±4
NO_3^- (µM)	266	250	248	24
NH_4^+ (µM)	7	7	12	23
Mn^{2+} (µM)	1.4	1.0	0.6	23
SO_4^{2-} (mM)	0.8	3.4	16	22
Fe^{2+} (µM)	0.1	0.1	1.2	1.8

5.3.1.2 Solid phase

The bulk mineralogy of the dried sediments was characterised for all sample locations. All sediments contained a mixture of quartz, carbonates (calcite and dolomite), and silicates (kaolinite, muscovite, clinochlore, albite, microcline). Pyrite was only detected in the subsurface sediments from S4. The concentrations for Zn, Cu and Cd are included in Table 5.2 (for the rest of metals see Chapter 4).

The average TIC, TOC and TS contents of inner estuary sediments (S1 and S2) were 1.1%, 2.0%, and 0.17% respectively, with little systematic variation with depth. The average TIC, TOC and TS contents of outer estuary sediments (S3 and S4) were 1.6%, 2.4%, and 0.35%, respectively, with both TOC and TS increasing with sample depth. The average amount of iron in the inner and outer estuary sediments were 3% and 4% by weight, respectively, with 0.09% and 0.13% associated with pyrite. AVS were only detected in the samples from the outer estuary but not in all the replicates. The iron associated with AVS in S3 and S4 subsurface sediments was 0.01 and 0.09% respectively, however it was not possible to quantify the very little amount extracted from surface samples. The average amount of 0.5 N HCl extractable $Fe^{2+}_{(s)}$ was 108 and

153 µmols g^{-1} in the inner and outer estuary sediments, respectively, with no depth trend in the inner estuary, but a trend of increase with depth in the outer estuary (see Table 5.2).

Table 5.2: Carbon, sulphur and iron characterisation in estuarine sediment and the bulk content of trace metals (Zn, Cu and Cd). The errors associated are the standard deviation (1σ) of three (or two replicates in the case of XRF measurements of Mn, Zn, Cu and Cd).

	S1		S2		S3		S4	
	Surface	**Subsurface**	**Surface**	**Subsurface**	**Surface**	**Subsurface**	**Surface**	**Subsurface**
%TIC	1.71±0.31	1.01±0.69	0.69±0.22	1.09±0.19	1.43±0.06	1.38±0.21	1.75±0.10	1.76±0.04
%TOC	1.28±0.29	2.34±0.68	2.48±0.21	1.75±0.15	2.06±0.04	2.58±0.17	2.17±0.04	2.69±0.03
%TS	0.16±0.01	0.18±0.01	0.18±0.00	0.14±0.01	0.22±0.00	0.35±0.00	0.31±0.00	0.52±0.01
Total Iron (%)	2.77±0.76	3.30±0.74	3.05±0.63	2.89±0.52	3.75±0.74	4.07±0.85	4.48±0.99	4.28±0.89
%Fe-AVS	nd	nd	nd	nd	<LDL	0.01	<LDL	0.09
%Fe-Pyrite	0.08	0.10	0.09	0.10	0.10	0.12	0.12	0.18
Total 0.5 N HCl extractable Fe (µmols/g solids)	106±1	116±10	106±6	105±4	123±3	206±8	93±9	191±28
0.5 N HCl extractable Fe^{2+} (% Fe^{2+}/Fe_{TOT})	52±2	61±5	53±1	53±2	39±1	84±6	57±3	96±3
Mn (µg/g)	656±8	785±8	681±20	654±1	847±6	969±3	758±14	732±11
Zn (µg/g)	132±3	149±1	139±4	129±4	161±2	199±13	174±1	167±6
Cu (µg/g)	30±4	33±4	31±2	27±2	39±2	31±3	33±2	37±11
Cd (µg/g)	<2	<2	<2	<2	<2	<2	<2	<2

5.3.2 Major element behaviour during sediment resuspension

Changes in the concentration of the major elements (NO_3^-, NH_4^+, Mn^{2+} and SO_4^{2-}) in solution, and 0.5 N HCl extractable $Fe^{2+}_{(s)}$ during the oxic resuspension of estuarine sediments are shown in Figure 5.1 (inner estuary) and Figure 5.2 (outer estuary). The initial concentration of each major species in the river waters (and solids in the case of reduced Fe) has been plotted with an open symbol on the y-axis (i.e. zero time). Nitrite was below the detection limit and therefore it has not been included.

5.3.2.1 Inner estuary

In the experiments using surface sediments from the inner estuary sites (S1 and S2) nitrate seemed to be released immediately on resuspension, particularly in S2 experiments (~400 μM) (Fig. 5.1a). Nitrate concentrations then remained relatively constant in these tests until 72 hrs, after which time concentrations steadily decreased towards the end of the test at 2 weeks. In the experiments using inner estuary subsurface sediments, nitrate concentrations followed similar trends to those exhibited by the surface sediment experiments (Fig. 5.1b), however there was significantly more data scatter observed in these tests (especially at the later time points).

Ammonium concentrations in the experiments carried out with surface sediments decreased immediately after resuspension started (Fig. 5.1c) and remained close to detection levels until 48 hrs when concentrations transiently increased to around 20-30 μM before decreasing to low concentrations by the end of the test. On the other hand, ammonium concentrations in experiments using subsurface sediments (Fig. 5.1d) increased modestly and slightly in S1 and S2 experiments respectively when resuspension started. Levels of ammonium in the subsurface sediment experiments remained relatively constant after the first day of reoxidation.

In the experiments using inner estuary surface sediments, $Mn^{2+}_{(aq)}$ concentrations were initially very low (≤5 μM), yet higher than the initial concentration in the water column (Fig. 5.1e), and decreased to detection limit levels after the first day of the reoxidation experiment, coinciding with the peak observed in ammonium. In the experiments using subsurface sediments, $Mn^{2+}_{(aq)}$ concentrations showed an immediate increase to ~10-20

µM, followed by a very rapid decrease (within hours) to close to detection levels (Fig. 5.1f).

The sulphate concentrations were low in the inner estuary sediments, although slightly higher at S2 due to its position along the salinity gradient, and increased only marginally during the experiments (Fig. 5.1g and 5.1h).

The initial 0.5 N HCl extractable $Fe^{2+}_{(s)}$ represented between 12-18% of the total iron in these sediments, being slightly lower in the surface sediments (Fig. 5.1i) than in the subsurface sediments (Fig. 5.1j). The percentage of extractable $Fe^{2+}_{(s)}$ decreased over the duration of the experiments to a similar extent in all inner estuary sediments (between 20-40 µmol Fe^{2+} g^{-1} were removed in each experiment which represented 4-7% of the total iron in the sediments).

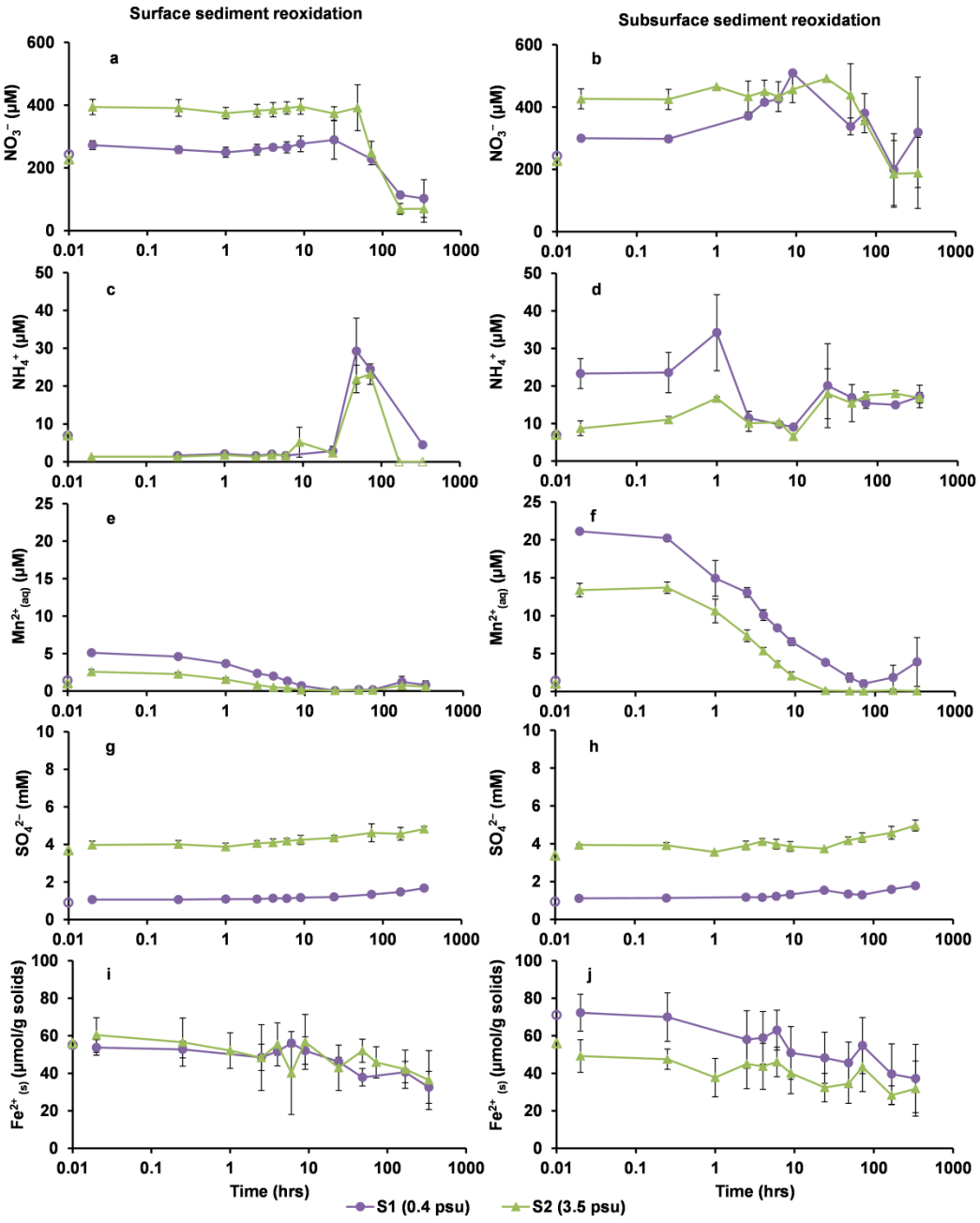

Figure 5.1: Major element behaviour during resuspension of inner estuary sediments. The purple line with circles represents S1 (Boothferry) and the green line with triangles represents S2 (Blacktoft). Open symbols on the y-axis indicate the initial concentrations of the major elements in the river water (a-h) and the initial 0.5 N HCl extractable $Fe^{2+}_{(s)}$ in the sediments (i and j). The vertical error bars in all the figures represent one standard deviation (1σ) of triplicates.

5.3.2.2 Outer estuary

The experiments using surface sediments from the outer estuary (S3 and S4) showed differences in the nitrate behaviour between both sites (Fig. 5.2a and 5.2b). The initial nitrate concentrations in experiments using S3 surface experiments were higher than at S4 and similar to those found in the inner estuary sites; they remained relatively constant over the tests. In contrast, in the experiments using surface sediments from S4, nitrate concentration were initially very low, but it increased by six-fold within the first 48 hrs (190±30 µM) and nearly by 30-fold (~900±300 µM) by the end of the experiment. In the tests using subsurface sediments from S3, initially nitrate concentration behaved similarly than in the tests using surface sediments; however, after a week, the nitrate concentration dropped below detectable levels. The experiments using subsurface sediments from S4, showed very low nitrate concentrations (close to or below detection levels) throughout.

Ammonium concentrations in experiments using outer estuary surface sediments were initially low (<20 µM), similar to the concentrations in the original river water, and remained so until the end of the test (Fig. 5.2c). There was a very different trend in ammonium concentrations in the experiments using subsurface sediments (Fig. 5.2d), which increased significantly (by ~2.5 times) within the first few hours of resuspension. Ammonium concentration peaks in the experiments were 260±20 (S3) and 130±40 (S4) µM. Following this initial release, ammonium levels in solution decreased to ~20 µM by the end of the first week to remain stable until the end of the tests.

In experiments using outer estuary surface sediments, Mn^{2+} concentrations increased immediately on resuspension to three times (~30-70 µM) the concentration of the river water (Fig. 5.2e). This rapid release of Mn^{2+} to solution was followed by a very rapid decrease to close to detection levels after about 4 hrs. In the experiments using subsurface sediments from S4, $Mn^{2+}_{(aq)}$ concentrations sharply decreased from ~20 µM to detection limits after the first 10 hrs of resuspension, whereas for subsurface S3 experiments there was no clear release-uptake trend in $Mn^{2+}_{(aq)}$ concentrations (Fig. 5.2f).

Sulphate is a more important species in solution in the outer estuary samples because the proximity to the coastal waters. In experiments using surface sediments the sulphate concentrations remained fairly constant throughout (Fig. 5.2g). However, in the experiments using subsurface sediments (Fig. 5.2h) the sulphate concentration increased with time, particularly in the S4 experiment (from 21±1 to 34±2 mM).

Iron oxidation trends differed between the surface and subsurface sediments. The initial amounts of 0.5 N HCl extractable $Fe^{2+}_{(s)}$ in the outer estuary surface sediments (Fig. 5.2i) were 54±3 (S3) and 40±6 (S4) µmols Fe^{2+} g^{-1}, which represented around 40% of the total 0.5 N HCl extractable Fe and the <9% of the total iron. By the end of the 2-weeks reoxidation experiment, the percentage of $Fe^{2+}_{(s)}$ decreased to around the 20% and 10% in the S3 and S4 surface sediment slurries respectively. The initial amounts of extractable $Fe^{2+}_{(s)}$ in the subsurface sediments (193±8 (S3) and 179±27 (S4) µmols Fe^{2+} g^{-1} respectively) represented more than 90% of the total 0.5 N HCl extractable Fe pool of the subsurface sediments and ~30% of the total iron. By the end of the tests, the percentage of $Fe^{2+}_{(s)}$ decreased to ~21% of the total iron (45±3 (S3) and 36±6 (S4) µmols Fe^{2+} g^{-1}) (Fig. 5.2j). These outer estuary subsurface sediments experienced a rapid colour change (from black to brown) during the first hours of the experiment.

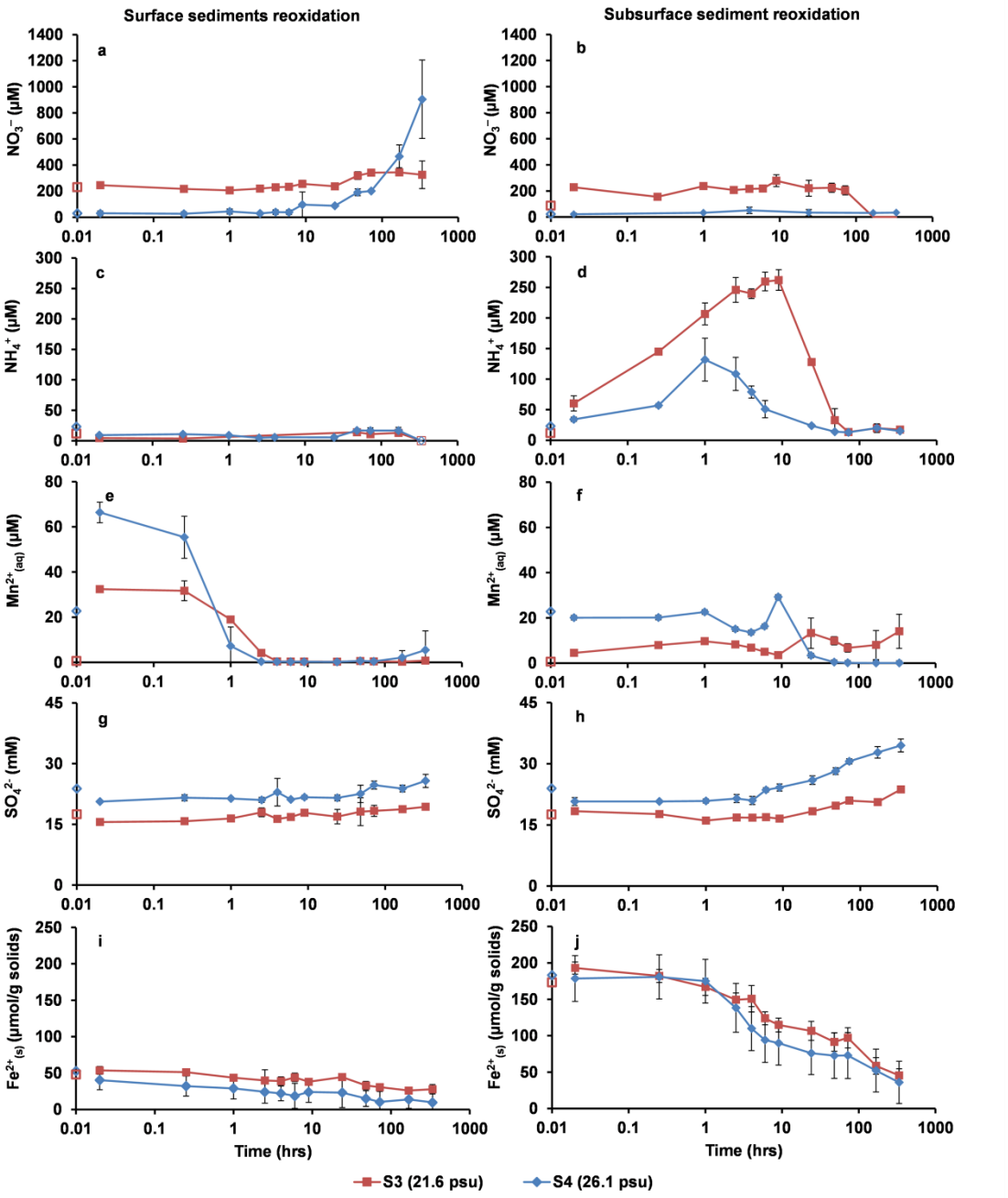

Figure 5.2: Major element behaviour during resuspension of outer estuary sediments. The red line with squares represents S3 (Paull) and the blue line with diamonds represents S4 (Skeffling). Open symbols on the y-axis indicate the initial concentrations of the major elements in the river water (a-h) and the initial 0.5 N HCl extractable $Fe^{2+}_{(s)}$ in the sediments (i and j). The vertical error bars in all the figures represent one standard deviation (1σ) of triplicates.

5.3.3 Trace metal mobility during sediment resuspension

The release of Zn, Cu and Cd during sediment resuspension experiments is shown in Figure 5.3 (inner estuary) and Figure 5.4 (outer estuary). Data of TMs in solution have been normalised to show µg of metal released per kg (dry weight) of sediment used.

5.3.3.1 Inner Estuary

In the experiments carried out with inner estuary sediments, the pattern of Zn behaviour depended on the sample depth. In the surface sediment experiments (Fig. 5.3a), Zn concentration increased immediately upon resuspension to values 2-3 times the initial concentration in the experiment (154±89 (S1) and 120±35 (S2) µg Zn kg^{-1}), but decreased with time to below the detection limit by the end of the experiment. In contrast, in the experiments using subsurface sediments (Fig. 5.3b), the initial Zn concentration did not show an important increase, and decreased gradually to a final level close to the detection limit. Initially, Cu concentrations remained stable (at about the in the river water) in the four sets of experiments, but increased after ~10 hrs of resuspension, reaching concentrations around 3-4 times its initial values (about 120±17 (S1) and 100±35 (S2) µg Cu kg^{-1}) (Fig. 5.3c and 5.3d). Cadmium was below detection limit (with one single exception) throughout these experiments (Fig. 5.3e and 5.3f).

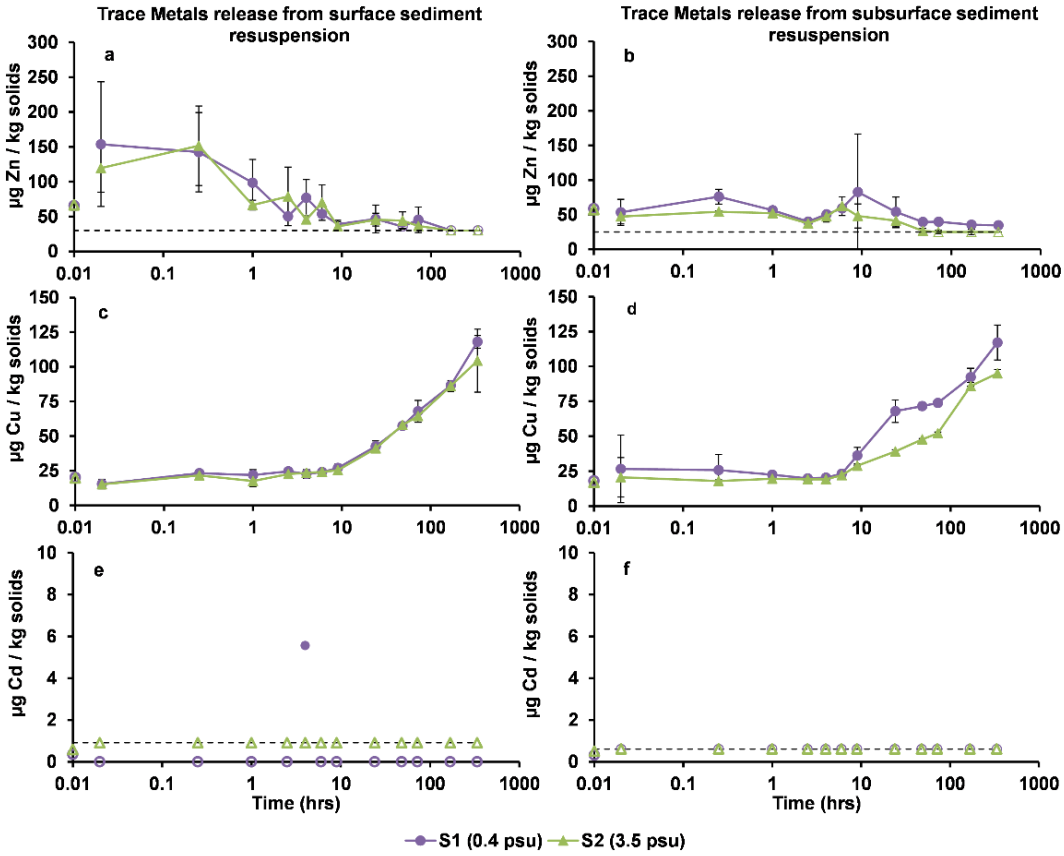

Figure 5.3: Selected trace metals (Zn, Cu, and Cd) released to solution from solids during resuspension experiments using S1 and S2 sediments. Zinc released from surface (a) and subsurface (b) sediments; Cu released from surface (c) and subsurface (d) sediments; Cd released from surface (e) and subsurface (f) sediments. Open symbols on the y-axis indicate the initial concentrations of the selected TMs in the experiment. The vertical error bars in all the figures represent one standard deviation (1σ) of triplicates. Dashed lines indicate the LOD of the ICP-MS analysis.

5.3.3.2 Outer estuary

The resuspension experiments using outer estuary sediments showed a clear release-uptake trend for Zn, Cu and Cd. Zinc was immediately released to solution, reaching concentrations 3-6 times higher than the initial concentrations in the experiment, and then concentrations rapidly decreased to concentrations before mixing (~4500 µg kg^{-1}) (see Fig. 5.4a and 5.4b). The greatest Zn concentrations were observed in experiments with S4 sediments. Similarly, there was an immediate release of Cu to solution,

followed by rapid decrease (within hours) to concentrations below 1000 µg Cu kg^{-1}. The maximum concentrations were ~5000-13000 µg Cu kg^{-1} (Fig. 5.4c and 5.4d), which were 2 to 6 times Cu concentration prior to the mixing. Cadmium showed the same behaviour (Fig. 5.4e and 5.4f), reaching maximum concentrations of ~2000-3000 µg Cd kg^{-1} after about 1 hr of sediment resuspension.

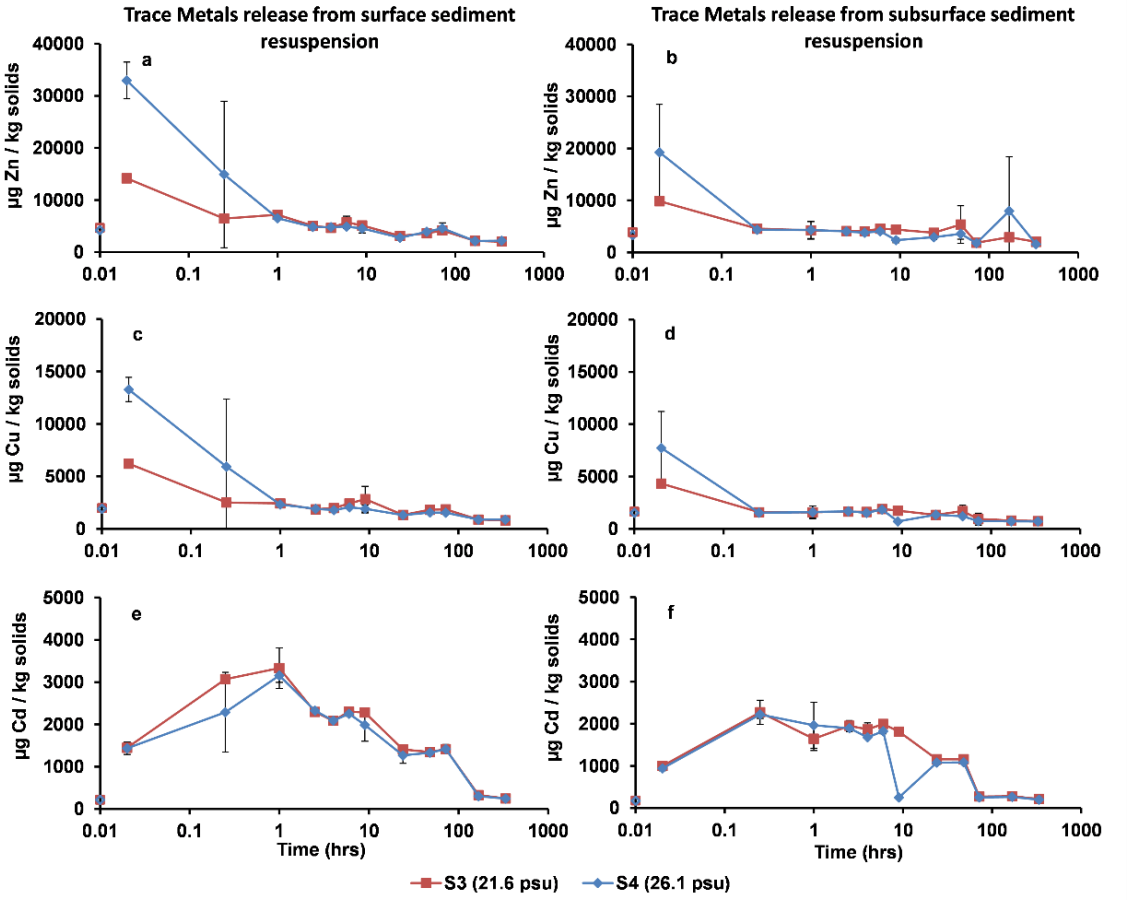

Figure 5.4: Selected trace metals (Zn Cu, and Cd) released to solution from solids during resuspension experiments using S3 and S4 sediments. Zinc released from surface (a) and subsurface (b) sediments; Cu released from surface (c) and subsurface (d) sediments; Cd released from surface (e) and subsurface (f) sediments. Open symbols on the y-axis indicate the initial concentrations of the selected TMs in the experiment. The vertical error bars in all the figures represent one standard deviation (1σ) of triplicates.

5.3.4 Changes in trace metal partitioning during resuspension

Partitioning of Zn, Cu and Cd in the sediments before and after the reoxidation experiment, as determined by sequential extraction, are reported in Figure 5.5. In all the original sediments, Zn was predominantly associated with carbonates (and other weak-acid extractable phases) and Fe/Mn oxyhydroxides, and the trends for Zn partitioning changes were similar in, both, surface and subsurface sediments (Fig. 5.5a and 5.5b). After two weeks of resuspension, Zn concentration slightly decreased in the Fe/Mn oxyhydroxides fraction and increased in the more weakly-bound (exchangeable and bound-to-carbonates) fractions. In the organic matter-sulphide fraction, Zn was only detected at the end point samples (concentrations in the leachate were equivalent to ~10-15 μg Zn g^{-1}).

Copper partitioning (Fig. 5.5c and 5.5d) showed similar changes in all the samples. In the original sediments, almost all the Cu extracted was associated with the Fe/Mn oxyhydroxides fraction, although almost no Cu was extracted from S3 and S4 subsurface sediments. Upon resuspension, there was a general shift from the Fe/Mn oxyhydroxides fraction to the weak acid extractable, and the organic matter-sulphide fraction. Copper concentrations for each leachate were similar between samples.

Although Cd partitioning was more variable between sites than that of Zn and Cu, the concentrations in the extractants were equivalent to less than 0.5 μg Cd g^{-1}. There was a general shift in Cd partitioning to more easily to extract fractions after 2-weeks of experiment (Fig. 5.5e and 5.5f). The most evident change was observed in the experiments using sediments from the outer estuary sites, in which Cd moved from high-energy bound fractions (organic matter-sulphides and Fe/Mn oxyhydroxides) to bound-to-carbonates and exchangeable fractions.

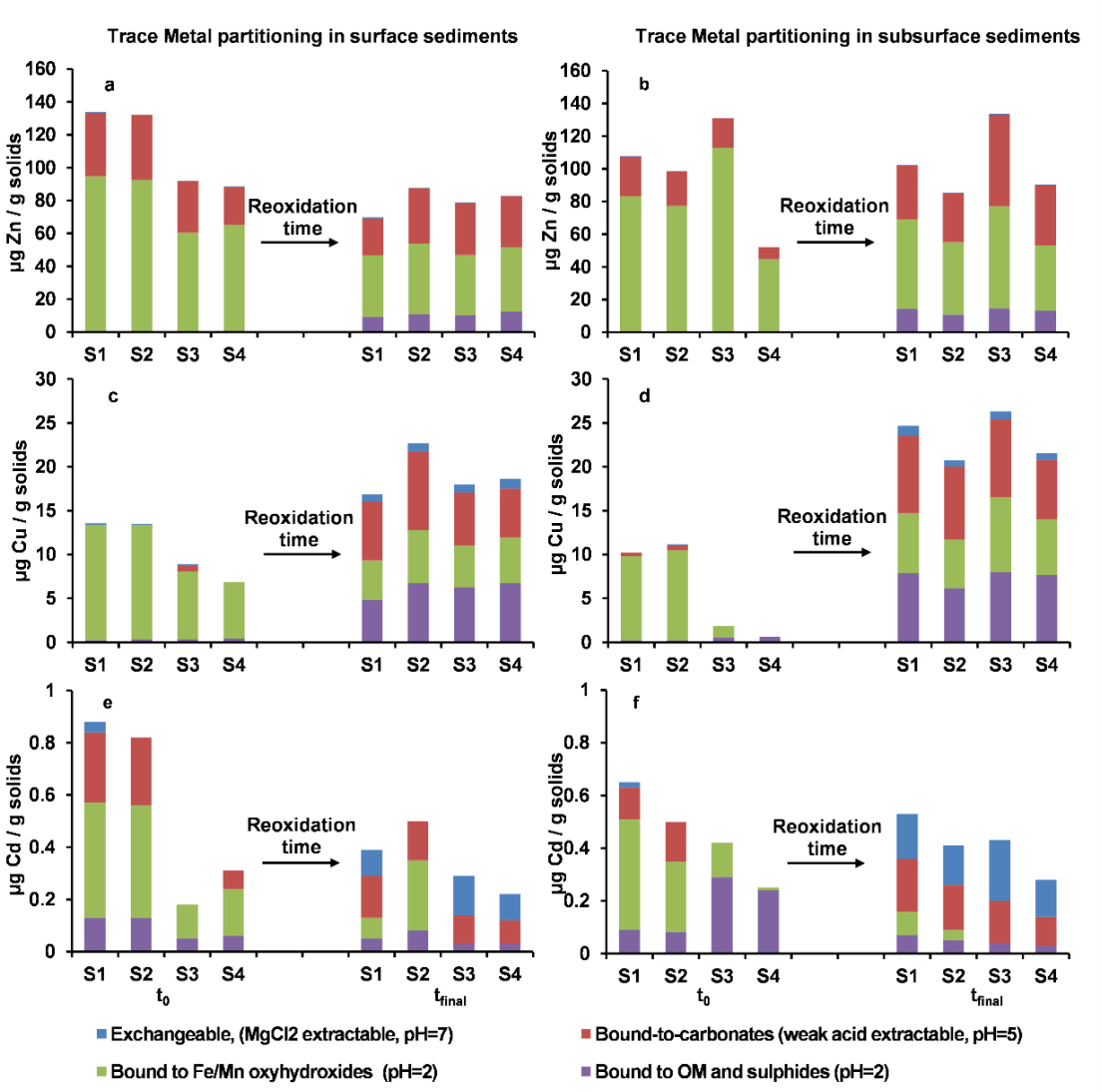

Figure 5.5: Trace metal partitioning changes after estuarine sediment reoxidation determined by sequential extractions using Tessier *et al.* (1979) protocol with modifications. The concentration (averaged from triplicates) is expressed in µg of the trace metal found in the extractant solution by the mass of solids used in the extraction. Zinc partitioning in surface (a) and subsurface (b) sediments; Cu partitioning in surface (c) and subsurface (d) sediments; and Cd partitioning in surface (e) and subsurface (f) sediments. Sites are ordered according to their location within the salinity gradient and the arrows represent the time of the reoxidation experiment (2-weeks).

5.4 Discussion

5.4.1 Geochemical characterisation of river water and sediment along estuarine continuum

The four sites along the Humber estuary represented the gradual change from a typical freshwater environment to an intertidal mudflat with brackish waters. This salinity profile was similar to that measured in other surveys (NRA, 1995, 1996; Sanders *et al.*, 1997; Mortimer *et al.*, 1998). Along the salinity gradient, nitrate concentrations in the overlying waters were inversely correlated with the ammonium concentrations. The nitrate concentration in the river water samples generally decreased with increasing salinity. Previously nitrate has been described to show a conservative behaviour along the mixing line, although there may be specific locations that show net nitrate production or removal during the year (Sanders *et al.*, 1997; Barnes & Owens, 1998). Generally ammonium concentrations measured were of the same order of magnitude, if not slightly higher, than the typical Humber waters. We observed increasing ammonium concentrations with increasing salinity, but the 90s surveys showed that ammonium trends varied throughout the year. All porewaters recovered were enriched in ammonium but not in nitrate. Ammonium enrichment was enhanced in the outermost estuary sites, which was most likely a reflection of in situ production from organic matter degradation during sulphate reduction. Sulphate concentrations increased seawards.

All surface sediments used in the resuspension experiments were in contact with air at the time of sampling. The subsurface sediments collected in the inner estuary sites appeared to be moderately reducing compared to the subsurface sediments from the outer estuary which appeared to become more reducing in depth (with ~90% of the acid extractable Fe as Fe (II), presence of AVS, and high ammonium concentrations in porewater) (Table 5.2). The better defined redox stratification between the two sediment depths sampled at the outer estuary sites was supported by in situ observations (colour change and odour of the sediments). Moreover, the total acid extractable Fe in the subsurface outer estuary sediments was ~2 times the content of the equivalent sediments

from the inner estuary. Thus, it seems that the outer estuary mudflats hold the largest Fe-pool within the Humber estuarine continuum.

Furthermore, the mudflats of the outer Humber estuary accumulated finer materials and they appeared to have a slightly higher organic content than the inner estuary sediments (see Table 5.2). Organic matter often accumulates with finer grained sediments, and its concentrations in coastal sediments are often lower at the sediment-water interface (Mayer, 1994). The organic matter depletion in the surface layer relative to the immediate subsurface, suggests that frequent mobilisation of surface sediments leads to greater organic matter degradation, which will be specially important in the areas of maximum sediment mobilization (i.e. TMZ) (Abril *et al*., 2002, Middelburg & Herman, 2007) situated in the inner estuary. There is an excess of, DOC concentrations in the TMZ of the Humber that is progressively removed and controlled by conservative mixing (Alvarez-Salgado & Miller, 1998; Middelburg & Herman, 2007). Therefore metabolizable organic matter is progressively depleted along the estuaries, and despite the high rates of sediment accumulation in the outer estuary, which allows high organic matter burial, this organic matter will be likely more refractory and may be further degraded during early diagenesis (Henrichs, 1992; Tyson 1995).

5.4.2 Geochemical responses of major elements to sediment resuspension

The oxic resuspension experiments showed that geochemical behaviour of the major elements varied on different timescales. So the discussion about those changes upon sediment resuspension and their impacts on estuarine geochemistry will be framed by two time-windows (Fig. 5.6). Firstly, the immediate changes upon sediment resuspension in river water, which are important as they will occur naturally at any type of resuspension event (from regular tidal cycles to less frequent extreme events). Secondly, longer timescale changes expected during major storms, which typically last 2-3 days in the Humber region (Lamb & Frydendahl, 1991; EASAC, 2013), and potentially mobilise deeper sediments that are not normally disturbed. For the immediate changes (left column), differences between the average concentration after the first hour of resuspension (as a final concentration datum) and the original concentrations of the river water (RW) (baseline) have been calculated. Changes during

a major storm timescale (right column) are represented by the difference between the average concentration over the first hour (baseline) and the concentration at 48 hrs of resuspension.

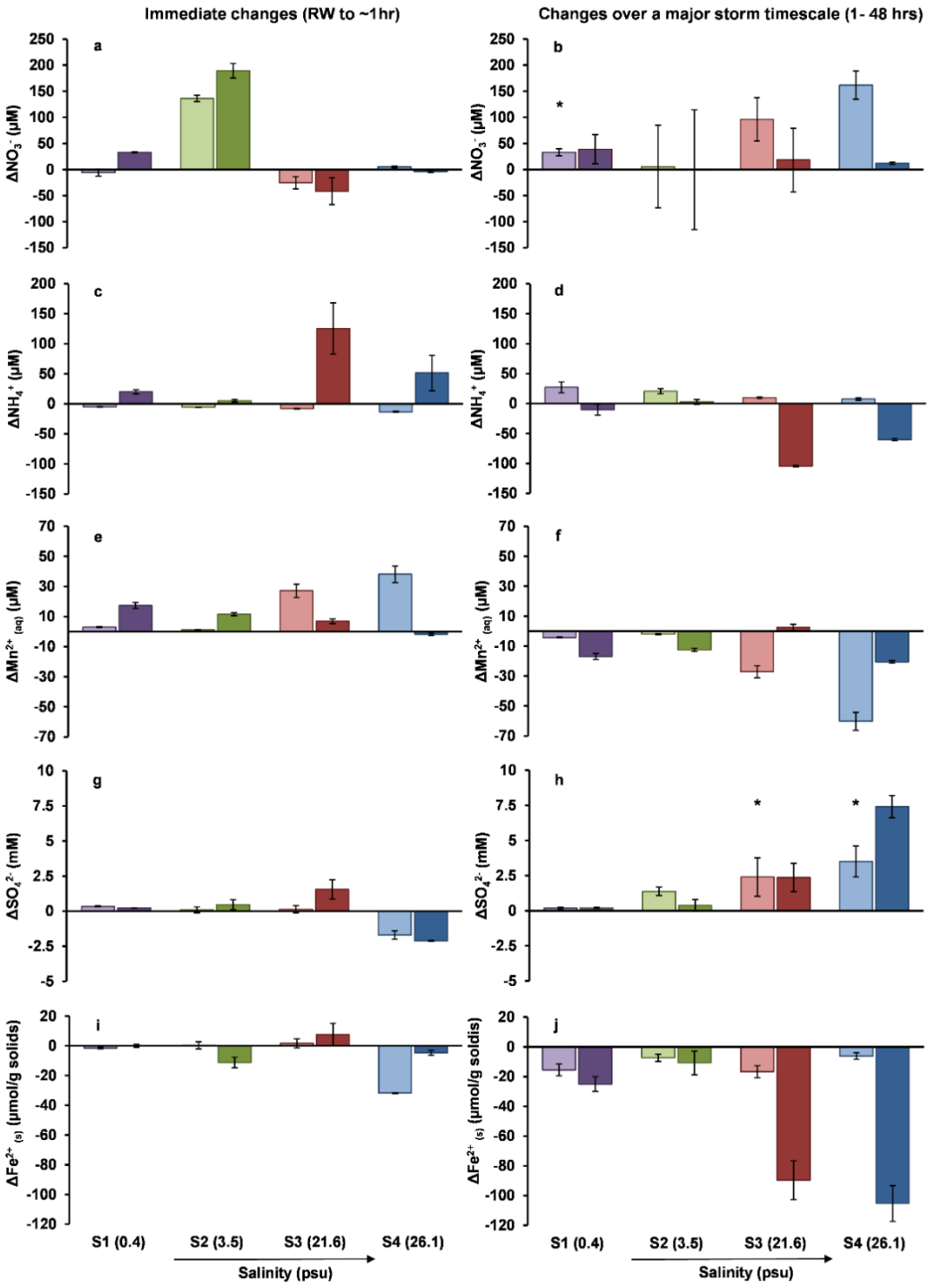

Figure 5.6: Major elements changes over time during sediment resuspension experiments at different time windows. Immediate changes (left) and changes over a major storm timescale (48 hrs) (right) for nitrate (a and b), ammonium (c and d), dissolved Mn (e and f), sulphate (g and h), and 0.5 N HCl extractable $Fe^{2+}_{(s)}$ from solids (i and j). Light coloured bars represent surface sediments and dark coloured bars represent subsurface sediments. *Delta calculated for 72 hrs when datum for 48 hrs was not available.

Nitrate showed no big releases in the short term (Fig. 5.6a), with the exception of S2 which may be explained by oxidation of reduced nitrogen species as porewater from the sediments did not accumulate nitrate. A combination of oxidation processes may also explain the nitrate increases in the longer timescale (Fig. 5.6b). For example the later significant increase in nitrate concentration in the experiments using S4 surface sediments may in part be associated with nitrification processes, as observed by Couceiro *et al.* (2013). Although a proportional ammonium consumption coupled to the production of nitrate was not observed in this experiment, coupled nitrification-denitrification can occur very fast, especially if other oxidants such as Mn oxides are competing with the oxygen for the oxidation of ammonia (to N_2) and organic-N (Luther *et al.*, 1997; Anschutz *et al.*, 2000). Therefore in this mosaic of redox reactions, a combination of aerobic oxidation of organic matter and nitrification may be the major nitrate sources. The nitrate produced can be subsequently used in other reactions. In fact under longer time intervals (1-2 weeks), the concentrations of nitrate decreased progressively in the experiments possibly due to the development of suboxic conditions in the experiments (i.e. conditions developed perhaps in isolated micro-niches in the bottom of the flasks (Triska *et al.*, 1993; Lansdown *et al.*, 2014; Lansdown *et al.*, 2015), such that denitrification could be supported despite the constant influx of air to the experiments). As such, the longer term removal of nitrate observed in these experiments may be an artefact of the experimental set-up (i.e. the higher sediment to water ratios used) and may not be representative of nitrate dispersion following a large resuspension event.

Ammonium showed significant releases (70-140 μM) in the first hour of resuspension in the experiments carried out with subsurface sediments from S3 and S4 (Fig. 5.6c), likely due to the accumulation of ammonium in porewaters of outer estuary mudflats like suggested by Morgan *et al.* (2012). However, other processes, such as reversible desorption from sediments and/or ion-exchange reactions likely have also contributed to the ammonium increase (Morin & Morse, 1999; Kalnejais *et al.*, 2010; Morgan *et al.*, 2012; Percuoco *et al.*, 2015) since porewater contribution to the mixture by simple diffusion cannot explain the concentrations reached. The ammonium released in those experiments was completely removed after 48 hrs (Fig. 5.6d). Transitory ammonium

release also occurred in S1 and S2 surface sediment experiments and these peaks coincided with the depletion of Mn^{2+} in solution. Nitrification and ammonium oxidation to N_2 by Mn oxides could have been the ammonium removal processes. Any $Mn^{2+}_{(aq)}$ product of these reaction pathways would readily react with the oxygen present to regenerate reactive oxides which will act as a catalysts to continue the oxidation of ammonium and organic-N (Luther *et al.*, 1997) or, if suboxic conditions, it may react with nitrate (Sørensen & Jørgensen, 1987; Murray *et al.*, 1995; Luther *et al.*, 1997; Hulth *et al.*, 1999). In the natural environment, the occurrence and magnitude of nitrification depends on the availability of oxygen and ammonium (Canfield *et al.*, 2005), and it will play a major role in the nutrient exchange processes within the sediment-water interface as the nitrate produced will, in turn, sustain denitrification (Barnes & Owens, 1998; Mortimer *et al.*, 1998). In the Humber, an intense zone for nitrification-denitrification has been associated with the TMZ due to the enhanced chemical and microbial activity as suspended particles provide a large additional surface area (Barnes & Owens, 1998; Mortimer *et al.*, 1998; Uncles *et al.*, 1998a). On the other hand, nitrifiers can be inhibited by sulphide concentration, light, temperature, salinity and extreme pH (Canfield *et al.*, 2005). The inhibition of nitrification by sulphide could favour the preservation of ammonium in porewaters (Joye & Hollibaugh, 1995; Morgan *et al.*, 2012), which may be a possible reason for the limited evidence of nitrate production in these experiments and may help to explain spatial differences in coupled nitrification-denitrification within this estuary. Alternatively, re-adsorption of ammonium onto particles, is likely to be an important removal process (especially as Fe/Mn oxides were likely to be forming in experiments as a result of metal oxidation; see below) which, in the natural estuary systems may be key in terms of the nutrient buffering capacity of the sediments (Morin & Morse, 1999; Song *et al.*, 2013).

Dissolved Mn behaviour varied significantly between the short and the long remobilisation timescales examined. There was a general immediate release of $Mn^{2+}_{(aq)}$ from the porewater to solution (Fig. 5.6e) that was completely reversed within a major storm time interval (Fig. 5.6f). The release (and later uptake) appeared to be more important in the experiments carried out with surface sediments. For the inner estuary experiment the released-uptaked $Mn^{2+}_{(aq)}$ closed numerically. However, from the outer

estuary, only the S3 surface sediment experiments, showed an equivalent release and uptake of $Mn^{2+}_{(aq)}$. This and the initial concentration of $Mn^{2+}_{(aq)}$ in surface porewater (see Table 4.4 in Chapter 4) may indicate that these sediments were poised at Mn-reduction at the time of sampling. Site 4 surface experiments showed slightly more Mn−uptake because $Mn^{2+}_{(aq)}$ decreased to levels below the initial $Mn^{2+}_{(aq)}$ concentrations in the river water. As mentioned above, coupled ammonium and/or organic-N oxidation with Mn oxides reduction, may also have been a short-term source of $Mn^{2+}_{(aq)}$.

Sulphate and Fe did not show significant changes in the resuspension experiments during the first hour (Fig. 5.6g and 5.6i), but after, important changes in these species occurred during the oxidation. After 48-72 hrs, there was a net production of sulphate in the experiments with an increasing trend from S1 to S4, which evidences again the more reducing conditions of the outer estuary sediments which probably contained reduced S species (e.g. sulphide, thiosulphate) that were oxidised to form sulphate during the experiments (Fig. 5.6h). The differences in the concentration of acid extractable $Fe^{2+}_{(s)}$ over 48 hrs of resuspension (Fig. 5.6j) became more important in the experiments using outer most estuary sediments due to their more reducing nature and their higher rective Fe content.

The net removal of reduced Mn and Fe in all the experiments is attributed to a series of oxidation reactions occurring during sediment resuspension in aerated conditions, and the consequent precipitation of insoluble Mn/Fe oxyhydroxides (e.g. birnessite and ferrihydrite). During oxic resuspension, abiotic oxidation processes are expected to be the dominant mechanism operating. However, microbially mediated Mn- and Fe-oxidation are the dominant mechanism operating in micro-aerophilic and suboxic environments (Froelich *et al.*, 1979; Thamdrup *et al.*, 1994; Canfield *et al.*, 2005). In natural conditions, Mn/Fe oxides may accumulate at or above the oxygen penetration depth in much higher concentrations than oxygen, and they can be transported deeper into the anoxic zone by bioturbation, where they can couple the oxidation of reduced sediment components (for example oxidation of sulphite to sulphate and ammonia to nitrate, Luther *et al.*, 1997; Hulth *et al.*, 1999; Anschutz *et al.*, 2000). Upward diffusing

Mn^{2+} and Fe^{2+} will also participate in chemo denitrification processes (Sørensen & Jørgensen, 1987).

To summarise, the initial geochemical state of the sediments and their position along the estuarine continuum are the biggest influence on the geochemical progression during their resuspension. The availability of seawater sulphate, which likely promotes the development sulphidic sediments, and $Fe^{2+}_{(s)}$ accumulation in the outer estuary mudflats may be the major control on the reoxidation processes, and hence Fe- and S-oxidation processes will dominate in this part of the Humber. However, the interlinks of N, Mn, Fe and S cycles and the spatiotemporal variability of the estuarine environments make it extremely difficult to constrain which are the principal reaction pathways occurring during resuspension events in natural conditions.

5.4.3 Trace metal behaviour and changes during resuspension

Zn and Cu were selected for analysis because they are known to be significantly enriched in the Humber sediments due to industrial contamination (Middleton & Grant, 1990; Cave *et al.*, 2005; Andrews *et al.*, 2008). Cadmium, which is normally found in very low concentrations (<5 nM) in the Humber estuary waters (Balls, 1985; Comber *et al.*, 1995), has been included because its behaviour during resuspension experiments using outer estuary sediments was noticeable due to the significant immediate release upon resuspension. Although the total concentrations in the solid phase were not significantly different between samples, during the resuspension experiments the release of Zn, Cu and Cd was significantly lower in the experiments carried out with sediments from the inner estuary than when using the outer estuary sediments. Despite all the precautions taken in the ICP−MS analysis, the determination of trace elements in salt waters has been analytically challenging due to the potential interference of the matrix in the sensitivity and the formation of polyatomic ions (Reed *et al.*, 1994; Jerez Vegueria *et al.*, 2013). However, the difference between the concentrations measured immediately upon resuspension and the concentrations after 48 hrs indicated that, even if there were polyatomic interferences on the baseline, the trend was not an analytical artefact. Despite the differences in magnitude, these TMs showed a general release-uptake trend in the resuspension experiments. The very rapid increase of TM

concentrations in solution upon resuspension (Fig. 5.7a, 5.7c and 5.7e) occurred due to a combination of mixing and desorption from different mineral phases (Calmano *et al.*, 1993; Cantwell *et al.*, 2002). Salinity has been shown to promote metal desorption because metals can be mobilised as soluble chloride complexes (Gerringa *et al.*, 2001; Millward & Liu, 2003; Du Laing *et al.*, 2008), which may help to explain the higher concentrations of metals in the experiments carried out with the outer estuarine sediments. Furthermore, very early Fe/Mn oxides-colloids formed (before they aggregate to larger particles) may have passed the filters used and therefore any metal associated would have been deemed as solutes. Nevertheless, the release of TMs was reversed to a considerable extend by the time of a major storm (Fig. 5.7b, 5.7d and 5.7f) as a result, most probably, of co-precipitation and adsorption processes to newly formed Mn and Fe oxyhydroxides (Burdige, 1993; Calmano *et al.*, 1993; Simpson *et al.*, 1998; Saulnier & Mucci, 2000; Gunnars *et al.*, 2002; Caetano *et al.*, 2003). This is evidence of the importance of Fe/Mn transformations in the transport and fate of TMs in the estuarine sediment-water interface (Du Laing *et al.*, 2009). Further, the presence of soluble organic compounds can affect positively or negatively the mobility of TMs (Du Laing *et al.*, 2009) which may have had some effects in the trends observed in these experiments as well.

The mobilisation of TMs upon resuspension is also supported by the general shift in metal partitioning towards ‘easier to extract’ fractions (exchangeable and bound-to-carbonates fractions). Although metal release was reversed in a relative short term, changes in metal partitioning may have implications in metal bioavailability. The Zn released in the inner estuary experiments was <0.1% of the total Zn in the experiment, which was within the range of the Zn associated with the exchangeable fraction. This release was reversed. Zinc showed no significant changes in partitioning, but the decreases in the “weak acid extractable” and Fe/Mn oxides-associated fractions did not match quantitatively with any Zn increase in other fractions in the final sediments, which may be probably explained by protocol limitations (see below). However in the outer estuary experiments the average peak of Zn released was 11% of the total Zn in the experiments, and such release was also reversed with time. This released Zn to solution was higher than the Zn associated with the exchangeable fraction of these

sediments, which suggests that Zn was likely mobilised from other fractions. Probably Zn experienced a transient release (i.e. Zn likely sourced from absorption complexes and returned to new absorption complexes). This transient release may be what was measured in solution at the beginning of the resuspension (Zn concentration peak) (Fig 5.7). Zinc speciation varied among the outer estuary sediments, and only two of them showed changes that quantitatively matched (loss in the Fe/Mn oxides-bound fraction was equivalent to the increase in carbonates and organic matter-sulphide fraction). On the other hand, the Cu released to solution in the inner estuary experiments represented about 0.1% of the total Cu in the solids, which coincided with the Cu found in the exchangeable fraction, and, contrary to what was observed in other experiments, Cu remained in solution. In the outer estuary experiments, the average peak of Cu released to solution was 22% of the total Cu in solids, which suggests that not only the Cu associated with the exchangeable fraction was mobilised. For all the speciations carried out with end point sediments, Cu was found in all the fractions, whereas in the initial samples Cu was found generally only associated with the Fe/Mn oxides-bound fraction. Thus, Cu may have been mobilised from high-energy binding sites to weaker binding sites. However, errors introduced during the extractions or errors associated with protocol limitations cannot be discarded. The total amount of Cd extracted was <1 µg/g which was consistent with XRF results (Cd was below detection limit, <2 µg/g). In the experiments carried out with inner estuary sediments, Cd was not released to solution and its partitioning did not show important changes. Contrarily, in the experiments carried out with the outer estuarine sediments, Cd was released to solution and showed a release-uptake trend likewise the other metals. However, we suspect the concentrations measured have been overestimated because they were >2 µg/g. Therefore, even if the trend was real, the concentrations reported may have been influenced by polyatomic influences and we cannot discard other contamination errors. Cadmium speciation did not show important changes between the initial and the reoxidised sediments.

Numerous limitations have been reported about this extraction protocol (Gleyzes *et al.*, 2002). The concentrations in the exchangeable phase were generally very low or below detection limit, probably because the adsorption-desorption processes are normally pH-

dependent, and therefore desorption of the specifically adsorbed metals may not be complete at neutral pH (Tessier *et al.*, 1979; Du Laing *et al.*, 2009). Furthermore, none of the Zn or Cu bound to organic matter-sulphides were extracted from the original sediments, which seems contrary to what was expected for initially sulphate reducing sediments, as TMs are normally associated with sulphide minerals (Di Toro *et al.*, 1990; Allen *et al.*, 1993). However the absence of Zn and Cu in this fraction may be explained by protocol limitations since in this step sulphides may be partially dissolved and organic matter not completely destroyed (Anju & Banerjee, 2010; Gleyces *et al*., 2002). There may be matrix effects and also readsoptions (by complexation, precipitation, coprecipitation, adsorption and loss on the vial walls) during the extraction (Martin *et al*., 1987). In particular, for example, "weak acid-extractable" fraction could not only include metals bound to carbonates, but also specifically sorbed to exchangeable sites of clay, organic matter or oxides surfaces (Gleyzes *et al.*, 2002). The modification of the third step, which was performed at ambient temperature and in which the extraction time was increased, may not have been sufficient to complete the extraction of the Fe/Mn oxides-associated metals (Gleyzes *et al*., 2002).

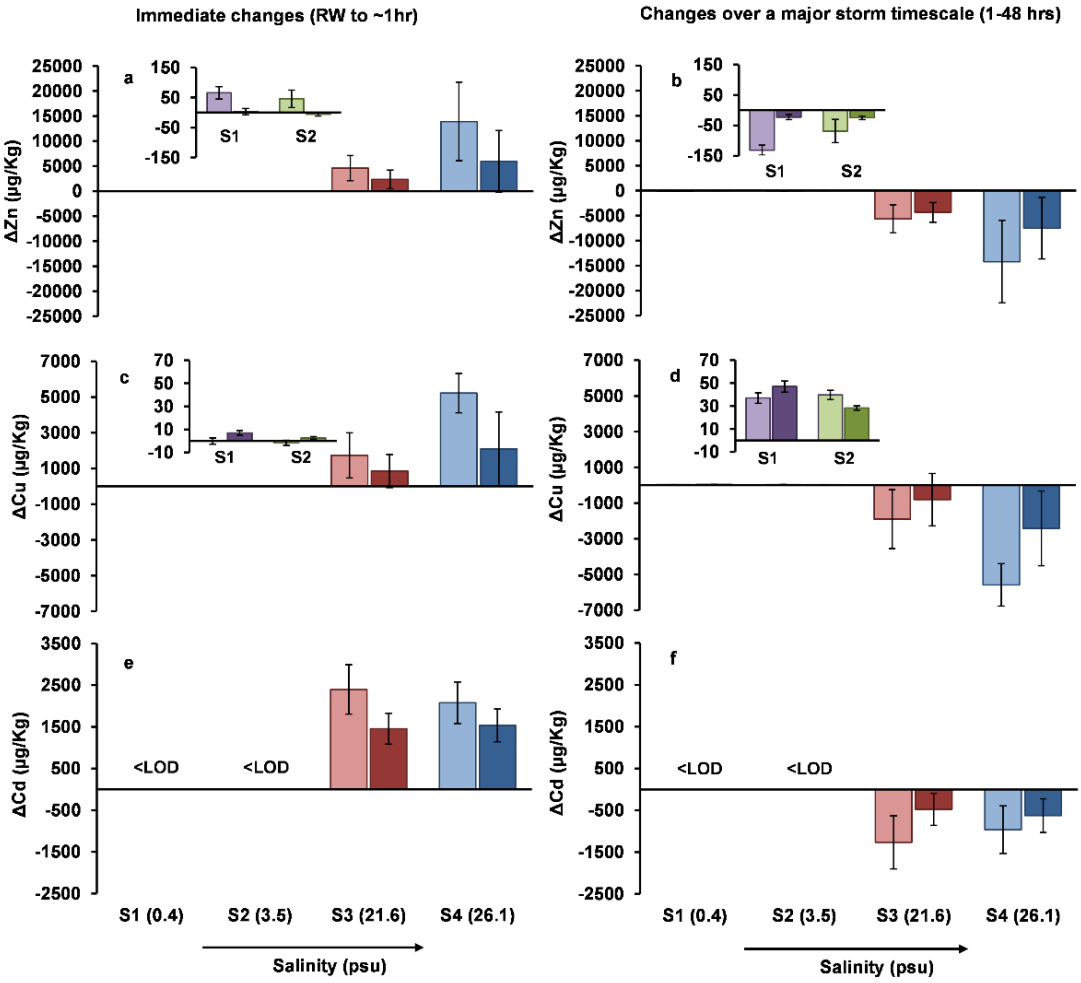

Figure 5.7: Trace metals changes over time during sediment resuspension experiments at different time windows. Immediate changes (left) and changes over a major storm timescale (48 hrs) (right) for Zn (a and b), Cu (c and d) and Cd (e and f). Light coloured bars represent surface sediments and dark coloured bars represent subsurface sediments. Due to the differences in the order of magnitude of the changes between the inner and the outer estuary sediments, zoom-plots have been included for Zn and Cu in S1 and S2 (Cd was below detection limit in samples from S1 and S2).

5.4.4 General implications of sediment resuspension for nutrient and trace metal transport and mobility in estuaries

The reoxidation of estuarine sediments due to remobilisation events enhanced the release of both nutrients and metals. The major element geochemical progression was conditioned by the depth of the sediment being mobilised, whereas the release-uptake

trend in TMs behaviour was observed in all sediment types. Humber sediments may act as an ultimate sink for major (Fe and Mn) and trace metals; while for nutrients, they may act as a major source in some occasions, as argued by Millward and Glegg (1997).

Nitrate (autochthonous or as product of nitrification processes) was the only major nutrient that seems to remain in solution for few days in both resuspension scenarios simulated. Hence, although nitrate concentrations were low in the outer estuary, during a major storm, important nitrate inputs from the estuary to the coastal waters may occur. During sediment reoxidation, any ferrous iron (in solution or associated with particles) will be rapidly oxidised, and hence iron will be transported mainly as ferric iron (as particles, colloids, or organic-matter complexed). Fe supplied from resuspended sediments is likely to be an important source of Fe to the coastal environment as suggested by Kalnejais *et al.* (2010).

The area of the outer estuary intertidal mudflats, is the largest in terms of aerial extent (see Mortimer *et al.*, 1998), and therefore the potential amount of sediments, and consequently nutrients and metals, mobilised will be significantly larger during an extraordinary resuspension event than during normal circumstances, which may have further implications in the coastal ecosystem. In these mudflats, the larger amount of Fe and the continuous availability of sulphate seem to promote the development of sulphidic conditions at depth which are not observed at the depth sampled in the inner estuary sites. The total oxidation of the inorganic species released during the resuspension of estuary sediments would equate to oxygen consumption of 20±10 mmols O_2 $kg^{-1}$of sediment, and to 70±40 mmols O_2 $kg^{-1}$of sediment for the inner and outer estuary sediments respectively. This amount of oxygen removal could result in full deoxygenation of surface waters at relatively low solid-solution ratios (15 g L^{-1} for the inner estuary; 4 g L^{-1} for the outer estuary). However, well-mixed estuaries rarely exhibit water column hypoxia (Paerl, 2006). The kinetics of the reoxidation processes (especially those of Fe and S) are such that resupply of oxygen (by diffusion from atmosphere or mixing with adjacent oxygenated waters) is likely to prevent anoxic conditions from developing in all but the very largest of remobilisation events.

During estuarine resuspension events changes in TM speciation due to redox changes and desorption from resuspendable sediments are likely to be the main source of TMs to the water column; although direct diffusion of porewaters from undisturbed sediments can be also an important source of dissolved species (Martino *et al.*, 2002; Kalnejais *et al.*, 2010). In these experiments, TM release was followed by an uptake in a relatively short time-window (<48 hrs, mostly in 10 hrs). Hirst and Aston (1983) suggested, that the metal concentration in the fluxes coming into the coastal waters may remain at normal levels even when extraordinary amounts of sediments are mobilised due to the rapid scavenging capacity of the newly formed minerals surfaces. This is supported by data presented here as only transient metal releases were observed. Others suggested that dissolved metals display non–conservative mixing in macrotidal environments which can be explained by the presence of additional metal sources associated with sediments, and supports the importance of sediment mobilisation patterns and frequency on TM bioavailability and transport (Martino *et al.*, 2002). Furthermore, these experiments showed that sediment reoxidation led to a shift in TM partitioning (i.e. a greater proportion of TMs was associated with more weakly bound fractions). In the natural environment, before sediments are ultimately scavenged deeper in the sediment column, they will be continuously resuspended (Lee & Cundy, 2001), so the transfer of TMs to weaker binding fractions will have implications in their bioavailability over time.

Under future climate change scenarios more frequent and intense episodes of extreme precipitations over Britain have been predicted (Jones & Reid, 2001; Christensen *et al.*, 2007). Therefore, in terms of budget, the more regular mobilisation of undisrupted subsurface sediment will lead to increasing nutrient and metal inputs to the estuarine water column, and maybe ultimately to coastal waters, which will have important environmental implications. Furthermore, changes in the estuarine dynamics could compromise the conditions needed for estuarine sediments to reach steady state before the next mixing event takes place, which may affect the sediment redox stratification and the development of well-defined geochemical zonations within the sediment profile.

5.5 Conclusions

This study gives an insight into the complex mosaic of processes that result from physical disturbances along the estuarine continuum. The position in the estuarine salinity gradient is the dominant control on sediment geochemistry with a transition from a Mn /Fe-dominated redox chemistry in the inner estuary to a Fe/S-dominated system in the outer estuary. Therefore, understanding the system dynamics and sediment characteristics is key when studying nutrients and metal cycling along a salinity continuum. Sediment resuspension resulted in release of ammonium (where enriched) to surface waters. The nitrate released appears to remain in solution for more than 2-3 days. Reduced pools of $Mn^{2+}_{(aq)}$, $Fe^{2+}_{(s)}$ and, likely, sulphides, in sediments were oxidised during resuspension resulting in Mn and Fe oxyhydroxides precipitation, which produced new sorption sites for the TMs released to solution upon resuspension. Thus, rapid releases of ammonium, Mn and TMs may be reversed in relatively short (few days) timescales, which is important when assessing the overall environmental effects of resuspension episodes on surface waters composition and nutrient and metal cycling. In the Humber estuary, the potential resuspension of outer estuary subsurface sediments would have a greatest effect on the coastal environment (in terms of COD, nutrient and metal release), and it may become a more important process in the future as it is predicted an increase in the frequency of major storms that can mobilise these deeper sediments due to global warming.

5.6 References

[1] Abril, G., Riou, S. A., Etcheber, H., Frankignoulle, M., de Wit, R., & Middelburg, J. J. (2000). Transient, tidal time-scale, nitrogen transformations in an estuarine turbidity maximum-fluid mud system (The Gironde, south-west France). *Estuarine Coastal and Shelf Science*, 50(5), pp.703-715. doi: 10.1006/ecss.1999.0598

[2] Abril, G., Nogueira, M., Etcheber, H., Cabecadas, G., Lemaire, E., & Brogueira, M. J. (2002). Behaviour of organic carbon in nine contrasting European estuaries. *Estuarine Coastal and Shelf Science*, 54(2), pp.241-262. doi: 10.1006/ecss.2001.0844

[3] Allen, H. E., Fu, G. M., & Deng, B. L. (1993). Analysis of acid-volatile sulfide (AVS) and simultaneously extracted metals (SEM) for the estimation of potential toxicity in aquatic sediments. *Environmental Toxicology and Chemistry*, 12(8), pp.1441-1453. doi: 10.1897/1552-8618(1993)12[1441:aoasaa]2.0.co;2

[4] Aller, R. C. (1994). Bioturbation and remineralization of sedimentary organic-matter - effects of redox oscillation. *Chemical Geology*, 114(3-4), pp.331-345. doi: 10.1016/0009-2541(94)90062-0

[5] Alvarez-Salgado, X. A., & Miller, A. E. J. (1998). Dissolved organic carbon in a large macrotidal estuary (the Humber, UK): Behaviour during estuarine mixing. *Marine Pollution Bulletin*, 37(3-7), pp.216-224.

[6] Andrews, J. E., Samways, G., & Shimmield, G. B. (2008). Historical storage budgets of organic carbon, nutrient and contaminant elements in saltmarsh sediments: Biogeochemical context for managed realignment, Humber Estuary, UK. *Science of The Total Environment*, 405(1-3), pp.1-13. doi: 10.1016/j.scitotenv.2008.07.044

[7] Anju, M., & Banerjee, D. K. (2010). Comparison of two sequential extraction procedures for heavy metal partitioning in mine tailings. *Chemosphere*, 78(11), pp.1393-1402. doi: 10.1016/j.chemosphere.2009.12.064

[8] Anschutz, P., Sundby, B., Lefrancois, L., Luther, G. W., & Mucci, A. (2000). Interactions between metal oxides and species of nitrogen and iodine in bioturbated marine sediments. *Geochimica et Cosmochimica Acta*, 64(16), pp.2751-2763. doi: 10.1016/s0016-7037(00)00400-2

[9] Balls, P. W. (1985). Copper, lead and cadmium in coastal waters off the Western North-Sea. *Marine Chemistry*, 15(4), pp.363-378. doi: 10.1016/0304-4203(85)90047-7

[10] Barnes, J., & Owens, N. J. P. (1998). Denitrification and nitrous oxide concentrations in the Humber estuary, UK, and adjacent coastal zones. *Marine Pollution Bulletin*, 37(3-7), pp.247-260.

[11] Berner, R. A. (1980). *Early diagenesis: A theoretical approach*. New York: Princeton University Press.

[12] Boyer, E. W., & Howarth, R. W. (2002). *The Nitrogen Cycle at Regional to Global Scales. Report of the International SCOPE Nitrogen Project*. Dordrecht, Netherlands: Springer.

[13] Bruno, P., Caselli, M., de Gennaro, G., De Tommaso, B., Lastella, G., & Mastrolitti, S. (2003). Determination of nutrients in the presence of high chloride concentrations by column-switching ion chromatography. *Journal of Chromatography A*, 1003(1-2), pp.133-141. doi: 10.1016/s0021-9673(03)00785-4

[14] Burdige, D. J. (1993). The biogeochemistry of manganese and iron reduction in marine-sediments. *Earth-Science Reviews*, 35(3), pp.249-284. doi: 10.1016/0012-8252(93)90040-e

[15] Burke, I. T., Boothman, C., Lloyd, J. R., Mortimer, R. J., Livens, F. R., & Morris, K. (2005). Effects of progressive anoxia on the solubility of technetium in sediments. *Environ Sci Technol*, 39(11), pp.4109-4116. doi: 10.1021/es048124p

[16] Caetano, M., Madureira, M. J., & Vale, C. (2003). Metal remobilisation during resuspension of anoxic contaminated sediment: short-term laboratory study. *Water Air and Soil Pollution*, 143(1-4), pp.23-40. doi: 10.1023/a:1022877120813

[17] Calmano, W., Hong, J., & Forstner, U. (1993). Binding and mobilization of heavy-metals in contaminated sediments affected by pH and redox potential. *Water Science and Technology*, 28(8-9), pp.223-235. doi: 10.15480/882.450

[18] Canfield, D. E., Raiswell, R., Westrich, J. T., Reaves, C. M., & Berner, R. A. (1986). The use of chromium reduction in the analysis of reduced inorganic sulfur in sediments and shales. *Chemical Geology*, 54(1-2), pp.149-155. doi: 10.1016/0009-2541(86)90078-1

[19] Canfield, D. E., Kristensen, E., & Thamdrup, B. (2005). *Aquatic Geomicrobiology*. Advances in Marine Biology. London: Elsevier Academic Press.

[20] Canfield, D. E., & Thamdrup, B. (2009). Towards a consistent classification scheme for geochemical environments, or, why we wish the term 'suboxic' would go away. *Geobiology*, 7(4), pp.385-392. doi: 10.1111/j.1472-4669.2009.00214.x

[21] Canfield, D. E., Glazer, A. N., & Falkowski, P. G. (2010). The Evolution and Future of Earth's Nitrogen Cycle. *Science*, 330(6001), pp.192-196. doi: 10.1126/science.1186120

[22] Cantwell, M. G., Burgess, R. M., & Kester, D. R. (2002). Release and phase partitioning of metals from anoxic estuarine sediments during periods of simulated resuspension. *Environmental Science & Technology*, 36(24), pp.5328-5334. doi: 10.1021/es0115058

[23] Cave, R. R., Andrews, J. E., Jickells, T., & Coombes, E. G. (2005). A review of sediment contamination by trace metals in the Humber catchment and estuary, and the implications for future estuary water quality. *Estuarine, Coastal and Shelf Science*, 62(3), pp.547-557. doi: 10.1016/j.ecss.2004.09.017

[24] Christensen, J. H., Hewitson, B., Busuioc, A., Chen, A., Gao, X., Held, I., Jones, R., Kolli, R. K., Kwon, W.-T., Laprise, R., Magaña Rueda, V., Mearns, L., Menéndez, C. G., Räisänen, J., Rinke, A., Sarr, A., & Whetton, P. (2007). Regional Climate Projections. *In:* Solomon S., Qin D., Manning M., Chen Z., Marquis M., Averyt K.B., Tignor M. &. Miller H.L (Eds.), *Climate Change 2007*: *The Physical Science Basis. Contribution of Working Group I to the Fourth Assessment Report of the Intergovernmental Panel on Climate Change*. Cambridge, United Kingdom and New York, NY, USA: Cambridge University Press, pp.847-940.

[25] Comber, S. D. W., Gunn, A. M., & Whalley, C. (1995). Comparison of the partitioning of trace metals in the Humber and Mersey estuaries. *Marine Pollution Bulletin*, 30(12), pp.851-860. doi: 10.1016/0025-326x(95)00092-2

[26] Couceiro, F., Fones, G. R., Thompson, C. E. L., Statham, P. J., Sivyer, D. B., Parker, R., Kelly-Gerreyn, B. A., & Amos, C. L. (2013). Impact of resuspension of cohesive sediments at the Oyster Grounds (North Sea) on nutrient exchange across the sediment-water interface. *Biogeochemistry*, 113(1-3), pp.37-52. doi: 10.1007/s10533-012-9710-7

[27] Di Toro, D. M., Mahony, J. D., Hansen, D. J., Scott, K. J., Hicks, M. B., Mayr, S. M., & Redmond, M. S. (1990). Toxicity of cadmium in sediments the role of acid volatile sulfide. *Environmental Toxicology and Chemistry*, 9(12), pp.1487-1502. doi: 10.1002/etc.5620091208

[28] Du Laing, G., De Vos, R., Vandecasteele, B., Lesage, E., Tack, F. M. G., & Verloo, M. G. (2008). Effect of salinity on heavy metal mobility and availability in intertidal sediments of the Scheldt estuary. *Estuarine Coastal and Shelf Science*, 77(4), pp.589-602. doi: 10.1016/j.ecss.2007.10.017

[29] Du Laing, G., Rinklebe, J., Vandecasteele, B., Meers, E., & Tack, F. M. G. (2009). Trace metal behaviour in estuarine and riverine floodplain soils and sediments: A review. *Science of The Total Environment*, 407(13), pp.3972-3985. doi: 10.1016/j.scitotenv.2008.07.025

[30] EASAC. (2013). Trends in extreme weather events in Europe: implications for national and European Union adaptation strategies (EASAC policy report 22 ed.): EASAC. Retrieved from http://www.easac.eu/fileadmin/PDF_s/reports_statements/Easac_Report_Extreme_Weather_Events.pdf

[31] Eggleton, J., & Thomas, K. V. (2004). A review of factors affecting the release and bioavailability of contaminants during sediment disturbance events. *Environment International*, 30(7), pp.973-980. doi: 10.1016/j.envint.2004.03.001

[32] Fossing, H., & Jørgensen, B. B. (1989). Measurement of bacterial sulfate reduction in sediments - evaluation of a single-step chromium reduction method. *Biogeochemistry*, 8(3), pp.205-222. doi: 10.1007/BF00002889

[33] Froelich, P. N., Klinkhammer, G. P., Bender, M. L., Luedtke, N. A., Heath, G. R., Cullen, D., Dauphin, P., Hammond, D., Hartman, B., & Maynard, V. (1979). Early oxidation of organic-matter in pelagic sediments of the eastern equatorial atlantic - suboxic diagenesis. *Geochimica et Cosmochimica Acta*, 43(7), pp.1075-1090. doi: 10.1016/0016-7037(79)90095-4

[34] Gerringa, L. J. A., de Baar, H. J. W., Nolting, R. F., & Paucot, H. (2001). The influence of salinity on the solubility of Zn and Cd sulphides in the Scheldt estuary. *Journal of Sea Research*, 46(3-4), pp.201-211. doi: 10.1016/s1385-1101(01)00081-8

[35] Gleyzes, C., Tellier, S., & Astruc, M. (2002). Fractionation studies of trace elements in contaminated soils and sediments: a review of sequential extraction procedures. *Trac-Trends in Analytical Chemistry*, 21(6-7), pp.451-467. doi: 10.1016/s0165-9936(02)00603-9

[36] Gunnars, A., Blomqvist, S., Johansson, P., & Andersson, C. (2002). Formation of Fe(III) oxyhydroxide colloids in freshwater and brackish seawater, with incorporation of phosphate and calcium. *Geochimica et Cosmochimica Acta*, 66(5), pp.745-758. doi: 10.1016/s0016-7037(01)00818-3

[37] Henrichs, S. M. (1992). Early diagenesis of organic matter in marine sediments: progress and perplexity. *Marine Chemistry*, 39(1), pp.119-149. doi: http://dx.doi.org/10.1016/0304-4203(92)90098-U

[38] Hirst, J. M., & Aston, S. R. (1983). Behavior of copper, zinc, iron and manganese during experimental resuspension and reoxidation of polluted anoxic sediments. *Estuarine Coastal and Shelf Science*, 16(5), pp.549-558. doi: 10.1016/0272-7714(83)90085-9

[39] Howarth, R. W., Billen, G., Swaney, D., Townsend, A., Jaworsky, N., Lajtha, K., Downing, J. A., Elmgren, R., Caraco, N., Jordan, T., Berendse, F., Freney, J., Kudeyarov, V., Murdoch, P., & Zhao-Liang, Z. (1996). Regional Nitrogen budgets and riverine N & P fluxes for the drainages to the North Atlanthic Ocean: natural and human influences. *Biogeochemistry*, 35, pp.75-139. doi: 10.1007/BF02179825

[40] Huerta-Diaz, M. A., & Morse, J. W. (1990). A quantitative method for determination of trace metal concentrations in sedimentary pyrite. *Marine Chemistry*, 29(2-3), pp.119-144. doi: 10.1016/0304-4203(90)90009-2

[41] Hulth, S., Aller, R. C., & Gilbert, F. (1999). Coupled anoxic nitrification manganese reduction in marine sediments. *Geochimica et Cosmochimica Acta*, 63(1), pp.49-66. doi: 10.1016/s0016-7037(98)00285-3

[42] Jerez Vegueria, S. F., Godoy, J. M., de Campos, R. C., & Goncalves, R. A. (2013). Trace element determination in seawater by ICP-MS using online, offline and bath procedures of preconcentration and matrix elimination. *Microchemical Journal*, 106, pp.121-128. doi: 10.1016/j.microc.2012.05.032

[43] Jones, P. D., & Reid, P. A. (2001). Assessing future changes in extreme precipitation over Britain using regional climate model integrations. International *Journal of Climatology*, 21(11), pp.1337-1356. doi: 10.1002/joc.677

[44] Joye, S. B., & Hollibaugh, J. T. (1995). Influence of sulfide inhibition of nitrification on nitrogen regeneration in sediments. *Science*, 270(5236), pp.623-625. doi: 10.1126/science.270.5236.623

[45] Kalnejais, L. H., Martin, W. R., & Bothner, M. H. (2010). The release of dissolved nutrients and metals from coastal sediments due to resuspension. *Marine Chemistry*, 121(1-4), pp.224-235. doi: 10.1016/j.marchem.2010.05.002

[46] Lamb, H., & Frydendahl, K. U. (1991). *Historic Storms of the North Sea, British Isles and Northwest Europe*. Cambridge: Cambridge University Press.

[47] Lansdown, K., Heppell, C. M., Dossena, M., Ullah, S., Heathwaite, A. L., Binley, A., Zhang, H., & Trimmer, M. (2014). Fine-scale in situ measurement of riverbed nitrate production and consumption in an armored permeable riverbed. *Environmental Science & Technology*, 48(8), pp.4425-4434. doi: 10.1021/es4056005

[48] Lansdown, K., Heppell, C. M., Trimmer, M., Binley, A., Heathwaite, A. L., Byrne, P., & Zhang, H. (2015). The interplay between transport and reaction rates as controls on nitrate attenuation in permeable, streambed sediments. *Journal of Geophysical Research-Biogeosciences*, 120(6), pp.1093-1109. doi: 10.1002/2014jg002874

[49] Lee, S. V., & Cundy, A. B. (2001). Heavy metal contamination and mixing processes in sediments from the Humber Estuary, Eastern England. *Estuarine, Coastal and Shelf Science*, 53(5), pp.619-636. doi: 10.1006/ecss.2000.0713

[50] Lovley, D. R., & Phillips, E. J. P. (1986). Organic-matter mineralization with reduction of ferric iron in anaerobic sediments. *Applied and Environmental Microbiology*, 51(4), pp.683-689.

[51] Lovley, D. R., & Phillips, E. J. P. (1987). Rapid assay for microbially reducible ferric iron in aquatic sediments. *Applied and Environmental Microbiology*, 53(7), pp.1536-1540.

[52] Luther, G. W., Sundby, B., Lewis, B. L., Brendel, P. J., & Silverberg, N. (1997). Interactions of manganese with the nitrogen cycle: Alternative pathways to dinitrogen. *Geochimica et Cosmochimica Acta*, 61(19), pp.4043-4052. doi: 10.1016/s0016-7037(97)00239-1

[53] Martin, J. M., Nirel, P., & Thomas, A. J. (1987). Sequential extraction techniques - promises and problems. *Marine Chemistry*, 22(2-4), pp.313-341. doi: 10.1016/0304-4203(87)90017-x

[54] Martino, M., Turner, A., Nimmo, A., & Millward, G. E. (2002). Resuspension, reactivity and recycling of trace metals in the Mersey Estuary, UK. *Marine Chemistry*, 77(2-3), pp.171-186. doi: 10.1016/s0304-4203(01)00086-x

[55] Mayer, L. M. (1994). Surface-area control of organic-carbon accumulation in continental-shelf sediments. *Geochimica et Cosmochimica Acta*, 58(4), pp.1271-1284. doi: 10.1016/0016-7037(94)90381-6

[56] Middelburg, J. J., & Herman, P. M. J. (2007). Organic matter processing in tidal estuaries. *Marine Chemistry*, 106(1-2), pp.127-147. doi: 10.1016/j.marchem.2006.02.007

[57] Middleton, R., & Grant, A. (1990). Heavy metals in the Humber estuary : *Scrobicularia* clay as a pre-industrial datum. *Proceedings of the Yorkshire Geological Society*, 48, pp.75-80.

[58] Millward, G., & Liu, Y. (2003). Modelling metal desorption kinetics in estuaries. *Science of The Total Environment*, 314-316, pp.613-623. doi: 10.1016/s0048-9697(03)00077-9

[59] Millward, G. E., & Glegg, G. A. (1997). Fluxes and Retention of Trace Metals in the Humber Estuary. Estuarine, *Coastal and Shelf Science*, 44, pp.97-105. doi: doi:10.1016/S0272-7714(97)80011-X

[60] Morgan, B., Rate, A. W., & Burton, E. D. (2012). Water chemistry and nutrient release during the resuspension of FeS-rich sediments in a eutrophic estuarine system. *Science of The Total Environment*, 432, pp.47-56. doi: 10.1016/j.scitotenv.2012.05.065

[61] Morin, J., & Morse, J. W. (1999). Ammonium release from resuspended sediments in the Laguna Madre estuary. *Marine Chemistry*, 65(1-2), pp.97-110. doi: 10.1016/s0304-4203(99)00013-4

[62] Morris, A. W., Bale, A. J., Howland, R. J. M., Millward, G. E., Ackroyd, R., H., L., & Rantala, R. T. T. (1986). Sediment mobility and its contribution to trace metal cycling and retention in a macrotidal estuary. *Water Science and Technology*, 18, pp.111-119.

[63] Mortimer, R. J. G., Krom, M. D., Watson, P. G., Frickers, P. E., Davey, J. T., & Clifton, R. J. (1998). Sediment-water exchange of nutrients in the intertidal zone of the Humber estuary, UK. *Marine Pollution Bulletin*, 37(3-7), pp.261-279. doi: 10.1016/s0025-326x(99)00053-3

[64] Murray, J. W., Codispoti, L. A., & Friederich, G. E. (1995). Oxidation-reduction environments - the suboxic zone in the black-sea. *Aquatic Chemistry: Interfacial and Interspecies Processes*, 244, pp.157-176. doi: 10.1021/ba-1995-0244.ch007

[65] Nedwell, D. B., Jickells, T. D., Trimmer, M., & Sanders, R. (1999). Nutrients in estuaries. *In:* Nedwell D. B. & Raffaelli D. G. (Eds.), *Advances in Ecological Research, Estuaries*. San Diego: Academic Press, pp.43-92.

[66] NRA. (1995). *Sea Vigil Water Quality Monitoring: the Humber Estuary 1992-1993*. Peterborough: National Rivers Authority Anglian Region. Retrieved from http://www.environmentdata.org/archive/ealit:2851.

[67] NRA. (1996). *Sea Vigil Water Quality Monitoring: The Humber Estuary 1994*. Peterborough: National Rivers Authority Anglian Region. Retrieved from http://www.environmentdata.org/archive/ealit:2868.

[68] Paerl, H. W. (2006). Assessing and managing nutrient-enhanced eutrophication in estuarine and coastal waters: Interactive effects of human and climatic perturbations. *Ecological Engineering*, 26(1), pp.40-54. doi: 10.1016/j.ecoleng.2005.09.006

[69] Percuoco, V. P., Kalnejais, L. H., & Officer, L. V. (2015). Nutrient release from the sediments of the Great Bay Estuary, NH USA. *Estuarine Coastal and Shelf Science*, 161, pp.76-87. doi: 10.1016/j.ecss.2015.04.006

[70] Pethick, J. S. (1990). The Humber Estuary. *In* Ellis S. and Crowther, D.R. (Eds.), Humber Perspectives, A region through the ages. Hull: Hull University, pp. 54-67.

[71] Postma, D., & Jakobsen, R. (1996). Redox zonation: Equilibrium constraints on the Fe(III)/SO_4-reduction interface. *Geochimica et Cosmochimica Acta*, 60(17), pp.3169-3175. doi: 10.1016/0016-7037(96)00156-1

[72] Rauret, G., Rubio, R., & López-Sánchez, J. F. (1989). Optimization of Tessier Procedure for Metal Solid Speciation in River Sediments. *International Journal of Environmental Analytical Chemistry*, 36(2), pp.69-83. doi: 10.1080/03067318908026859

[73] Reed, N. M., Cairns, R. O., Hutton, R. C., & Takaku, Y. (1994). Characterization of polyatomic ion interferences in inductively-coupled plasma-mass spectrometry using a high-resolution mass-spectrometer. *Journal of Analytical Atomic Spectrometry*, 9(8), pp.881-896. doi: 10.1039/ja9940900881

[74] Roberts, K. L., Eate, V. M., Eyre, B. D., Holland, D. P., & Cook, P. L. M. (2012). Hypoxic events stimulate nitrogen recycling in a shallow salt-wedge estuary: The Yarra River estuary, Australia. *Limnology and Oceanography*, 57(5), pp.1427-1442. doi: 10.4319/lo.2012.57.5.1427

[75] Roberts, K. L., Kessler, A. J., Grace, M. R., & Cook, P. M. L. (2014). Increased rates of dissimilatory nitrate reduction to ammonium (DNRA) under oxic conditions in a periodically hypoxic estuary. *Geochimica et Cosmochimica Acta*. 133, pp.313-324. doi: https://doi.org/10.1016/j.gca.2014.02.042

[76] Salomons, W., Derooij, N. M., Kerdijk, H., & Bril, J. (1987). Sediments as a source of contaminants. *Hydrobiologia*, 149, pp.13-30. doi: 10.1007/bf00048643

[77] Sanders, R. J., Jickells, T., Malcolm, S., Brown, J., Kirkwood, D., Reeve, A., Taylor, J., Horrobin, T., & Ashcroft, C. (1997). Nutrient fluxes through the Humber estuary. *Journal of Sea Research*, 37(1-2), pp.3-23. doi: 10.1016/S1385-1101(96)00002-0

[78] Saulnier, I., & Mucci, A. (2000). Trace metal remobilization following the resuspension of estuarine sediments: Saguenay Fjord, Canada. Applied Geochemistry, 15(2), pp.191-210. doi: 10.1016/s0883-2927(99)00034-7

[79] Seitzinger, S. P., & Sanders, R. W. (1997). Contribution of dissolved organic nitrogen from rivers to estuarine eutrophication. *Marine Ecology Progress Series*, 159, pp.1-12. doi: 10.3354/meps159001

[80] Simpson, S. L., Apte, S. C., & Batley, G. E. (1998). Effect of short term resuspension events on trace metal speciation in polluted anoxic sediments. *Environmental Science & Technology*, 32(5), pp.620-625. doi: 10.1021/es970568g

[81] Song, G. D., Liu, S. M., Marchant, H., Kuypers, M. M. M., & Lavik, G. (2013). Anammox, denitrification and dissimilatory nitrate reduction to ammonium in the East China Sea sediment. *Biogeosciences*, 10(11), pp.6851-6864. doi: 10.5194/bg-10-6851-2013

[82] Sørensen, J., & Jørgensen, B. B. (1987). Early diagenesis in sediments from danish coastal waters - microbial activity and Mn-Fe-S geochemistry. *Geochimica et Cosmochimica Acta*, 51(6), pp.1583-1590. doi: 10.1016/0016-7037(87)90339-5

[83] Statham, P. J. (2012). Nutrients in estuaries--an overview and the potential impacts of climate change. *Science of The Total Environment*, 434, pp.213-227. doi: 10.1016/j.scitotenv.2011.09.088

[84] Stumm, W., & Morgan, J. J. (1970). *Aquatic chemistry: an introduction emphasizing chemical equilibria in natural waters*. New York: Wiley-Interscience.

[85] Tessier, A., Campbell, P. G. C., & Bisson, M. (1979). Sequential extraction procedure for the speciation of particulate trace-metals. *Analytical Chemistry*, 51(7), pp.844-851. doi: 10.1021/ac50043a017

[86] Thamdrup, B., Fossing, H., & Jørgensen, B. B. (1994). Manganese, iron, and sulfur cycling in a coastal marine sediment, Aarhus Bay, Denmark. *Geochimica et Cosmochimica Acta*, 58(23), pp.5115-5129. doi: 10.1016/0016-7037(94)90298-4

[87] Thamdrup, B. (2012). New Pathways and Processes in the Global Nitrogen Cycle. *Annual Review of Ecology, Evolution, and Systematics*, 43, pp.407-428. doi: 10.1146/annurev-ecolsys-102710-145048

[88] Triska, F. J., Duff, J. H., & Avanzino, R. J. (1993). The role of water exchange between a stream channel and its hyporheic zone in nitrogen cycling at the terrestrial aquatic interface. *Hydrobiologia*, 251(1-3), pp.167-184. doi: 10.1007/bf00007177

[89] Tyson, R. V. (1995). *Sedimentary organic matter: Organic facies and palynofacies*. London: Chapman & Hall.

[90] Uncles, R. J., Joint, I., & Stephens, J. A. (1998a). Transport and retention of suspended particulate matter and bacteria in the Humber-Ouse Estuary, United Kingdom, and their relationship to hypoxia and anoxia. *Estuaries*, 21(4A), pp.597-612. doi: 10.2307/1353298

[91] Uncles, R. J., Wood, R. G., Stephens, J. A., & Howland, R. J. M. (1998b). Estuarine nutrient fluxes to the Humber coastal zone, UK, during June 1995. *Marine Pollution Bulletin*, 37(3-7), pp.225-233.

[92] Uncles, R. J., Stephens, J. A., & Law, D. J. (2006). Turbidity maximum in the macrotidal, highly turbid Humber Estuary, UK: Flocs, fluid mud, stationary suspensions and tidal bores. *Estuarine, Coastal and Shelf Science*, 67(1-2), pp.30-52. doi: 10.1016/j.ecss.2005.10.013

[93] Viollier, E., Inglett, P. W., Huntrer, K., Roychoudhury, A. N., & Van Cappellen, P. (2000). The ferrozine method revised: Fe(II)/Fe(III) determination in natural waters. *Applied Geochemistry*, 15, pp.785-790. doi: 10.1016/S0883-2927(99)00097-9

Chapter 6

Nitrate-dependent oxidation of undisturbed estuarine sediments and its effects on major and trace elements

Executive Summary

The Humber estuary has received riverine fluxes with high concentrations of nitrate and heavy metals, but due to the loss of intertidal areas, the capacity for sediment transformations of these pollutants has reduced. Nitrogen is conserved along the salinity continuum due to freshwater and seawater mixing plus a balance of denitrification and nitrification processes. However, it is important to understand controls on the rates of and sites for these nitrate removal and addition processes because perturbation of the estuary could disturb the overall conservative behaviour of nitrate. Nitrate-dependent oxidation coupled to the oxidation of different reduced inorganic species is examined in sediment microcosms amended with a high concentration nitrate solution. A combination of nitrate-driven redox processes developed in the non-sterilised microcosms. There was a transition in the dominant terminal-electron accepting processes dependent on the initial geochemical state of the estuarine sediments used. Organic carbon and iron oxidation were the most important electron donating processes coupled to nitrate reduction in the microcosm experiments using inner estuary sediments, followed by a combination of nitrate-dependent iron and sulphur oxidation, towards a sulphur-oxidation dominant environment in the experiments using the outer most estuarine sediments. Additionally, from the analysis of trace metal partitioning, a general shift of trace metals to weaker-binding sites was observed after the sediment incubation as a result of nitrate-dependent oxidation. Therefore benthic sediment anaerobic oxidation processes may have implications for the bioavailability of trace metals that were scavenged in the estuarine sediments. These results confirm that estuarine sediments, and reduced outer estuary sediments in particular, can be an efficient sink for nitrate, although the dominant benthic nitrate removal processes will depend strongly on the local geochemistry.

6.1 Introduction

Estuaries are semi-enclosed coastal environments situated at the river and ocean interface in which seawater is diluted with freshwater derived from land drainage (Perillo, 1995). The fluxes of soluble and particulate material through estuaries are influenced by a range of processes and factors that operate over variable scales of time and space (Nedwell *et al.*, 1999; Statham, 2012). Nutrients (nitrogen, silicon and phosphorus) and particulate material loads naturally enter river systems from land surface runoff and from atmospheric deposition, but manmade sources from industrial wastewater, agricultural fertilizers, and sewage treatment, can greatly increase the fluxes (Nedwell *et al.*, 1999; Statham, 2012). Normally nitrogen is limiting in coastal waters in temperate latitudes, however eutrophic events and the associated environmental impacts on water quality and biological activity may occur due to high nitrate fluxes reaching the sea (Sanders *et al.*, 1997; Howarth *et al.*, 2000; Shao *et al.*, 2010; Statham, 2012). Denitrification is a key process for nitrogen removal in estuarine systems and, consequently, for protection of coastal waters from nutrient pollution (Barnes & Owens, 1998; Howarth & Marino, 2006; Gardner & McCarthy, 2009).

In estuarine sediments the dominant nitrogen species under oxic conditions is nitrate (the result of diffusion from the water column and oxidation of reduced nitrogen species in-situ, Barnes & Owens, 1998), whereas under anoxic conditions the dominant nitrogen species is ammonium (due mainly to microbial breakdown of organic matter and nitrate consumption). The nitrogen cycle in sediments (Fig. 6.1) is a complex set of dissimilatory and assimilatory N transformations into its different oxidation states (Thamdrup, 2012).

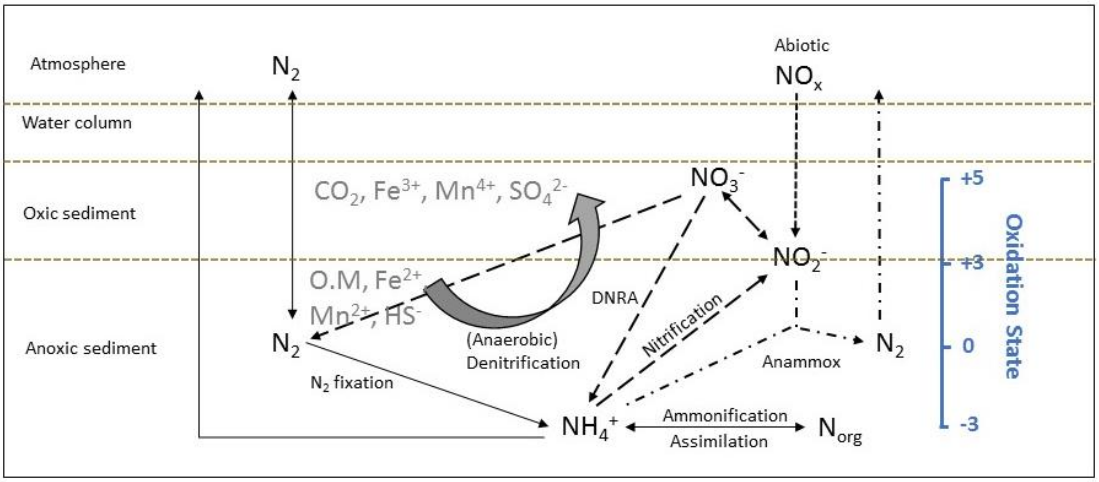

Figure 6.1: Relationship of different N transformation processes in the sedimentary nitrogen cycle (after Godfrey & Falkowski, 2009) including the relative positions of organic matter (OM) oxidation and nitrate dependent metal and sulphur oxidation processes.

There are three possible pathways for microbially mediated nitrate reduction: denitrification; anaerobic ammonium oxidation (anammox); and dissimilatory nitrate reduction to ammonium (DNRA). These processes can be concurrent within the sediments, however it is difficult to determine their relative contribution to total benthic nitrate reduction (Song *et al.*, 2013; Roberts *et al.*, 2014). Denitrification is the respiratory anaerobic sequential reduction of nitrate to eventually dinitrogen gas (N_2) or other gaseous N compounds (NO and N_2O) (equation 6.1; Canfield, 1993). Nitrite is an obligate intermediate in the denitrification and it can sometimes accumulate in the sediments indicating active nitrate reduction (Canfield & Thamdrup, 2009). Denitrification is mainly coupled with the oxidation of organic matter (Canfield *et al.*, 2005; Thamdrup, 2012):

$$5CH_2O + 4NO_3^- \rightarrow 2N_2 + CO_2 + 4HCO_3^- + 3H_2O \qquad \textbf{(Eq. 6.1)}$$

In addition, in anaerobic sediments, nitrate reduction can be also coupled with the oxidation of hydrogen, and reduced iron, manganese, and sulphur species (equations 6.2-6.6) (Straub *et al.*, 1996; Hulth *et al.*, 1999; Kuenen, 1999; Weber *et al.*, 2001; Visscher & Stolz, 2005);

$$10Fe^{2+} + 2NO_3^- + 24H_2O \rightarrow 10Fe(OH)_3 + N_2 + 18H^+ \qquad \textbf{(Eq. 6.2)}$$

$$5\mathrm{FeS} + 8NO_3^- + 8H^+ \rightarrow 5SO_4^{2-} + 4N_2 + 5Fe^{2+} + 4H_2O \quad \textbf{(Eq. 6.3)}$$

$$5Mn^{2+} + 2NO_3^- + 4H_2O \rightarrow 5MnO_2 + N_2 + 8H^+ \quad \textbf{(Eq. 6.4)}$$

$$5S_2O_3^{2-} + 8NO_3^- + H_2O \rightarrow 10SO_4^{2-} + 4N_2 + 2H^+ \quad \textbf{(Eq. 6.5)}$$

$$5HS^- + 8NO_3^- \rightarrow 5SO_4^{2-} + 4N_2 + 3OH^- + H_2O \quad \textbf{(Eq. 6.6)}$$

and such processes can be important for the fate of nitrate in aquatic environments, especially when there is limited supply of organic matter (Weber *et al.*, 2001).

Anammox, a bacterially mediated process where nitrite and ammonium ions are converted into dinitrogen and water (equation 6.7; Jetten *et al.* 1997), has been observed in different aquatic environments (Dalsgaard *et al.*, 2003; Jetten *et al.*, 2003; Mortimer *et al.*, 2004; Trimmer *et al.*, 2005; Trimmer *et al.*, 2013). It has been estimated to account for ~30% of the N_2 production in the marine environment, but its contribution, which normally correlates with water depth (Dalsgaard *et al.*, 2005), varies from <1% to about 80% between different sites (Thamdrup, 2012).

$$NO_2^- + NH_4^+ \rightarrow N_2 + 2H_2O \quad \textbf{(Eq. 6.7)}$$

As the name implies, DNRA is the transformation of nitrate to ammonium by microorganisms during anaerobic respiration (equation 6.8; Brunet & Garcia Gil, 1996). Unlike the other two nitrate reduction pathways, DNRA does not remove nitrogen from the aqueous system as it is reduced to bioavailable ammonium that is retained within the sediments, and can subsequently be released and cycled (An & Gardner, 2002; Rutting *et al.*, 2011; Roberts *et al.*, 2012).

$$CH_2O + NO_3^- \rightarrow NH_4^+ + CO_2 + OH^- \quad \textbf{(Eq. 6.8)}$$

The importance of DNRA in sediment denitrification has been increasingly recognised over the last few decades (Gardner *et al.*, 2006; Dong *et al.*, 2011). It has been found recently that the key factors that seem to regulate DNRA are organic matter loading, nitrate availability, temperature and availability of reductants such as sulphide and reduced iron (Gardner & McCarthy, 2009; Roberts *et al.*, 2014; Robertson *et al.*, 2016). However, despite the efforts to elucidate the environmental and geochemical factors

controlling the partitioning between denitrification and DNRA, what regulates the ratio between these processes is still not fully understood (Gardner *et al.*, 2006; Dong *et al.*, 2011; Roberts *et al.*, 2012; Giblin *et al.*, 2013; Roberts *et al.*, 2014; Robertson *et al.*, 2016).

In aquatic sediments rich in organic matter, aerobic heterotrophic metabolism is restricted to a very thin surface layer, below which the oxidation of organic matter can be completed by microbial dissimilatory reduction of inorganic compounds (Lovley, 1991). In any geochemical setting, the microorganisms that mediate the most energetically favourable biochemical reactions have a competitive advantage, and thus electron acceptors tend to be consumed in sequence (Froelich *et al.*, 1979). This tends to result in the stratification of a sediment profile into geochemical zones associated with dominance of a particular metabolic process; the sequence (determined by the free energy yield per mole of organic carbon oxidised) is usually aerobic metabolism, nitrate, manganese, ferric iron and sulphate reduction, and then methanogenesis (Froelich *et al.*, 1979; Berner, 1980; Jørgensen, 1982; Canfield *et al.*, 1993; Canfield & Thamdrup, 2009). However, in natural systems, this pattern of biochemical zonation is not so clearly delineated because the geochemical/metabolic zones tend to overlap and they can be also disturbed by bioturbation and sediment resuspension (Sørensen & Jørgensen, 1987; Canfield *et al.*, 1993; Postma & Jakobsen, 1996; Canfield & Thamdrup, 2009). During these redox processes, the formation of reactive iron and manganese oxides is also likely to affect the migration of trace metals (TMs) whose behaviour is strongly controlled by sorption reactions to these mineral surfaces (Boyle *et al.*, 1977; Huerta-Diaz & Morse, 1990; Burdige, 1993). Therefore the microbially mediated reactions coupling the redox cycles of N, Fe, Mn and S play a key role in the sedimentary aquatic environments.

Furthermore the interaction between these different redox cycles and their implication on TM cycling in estuarine sediments has been the focus of attention because estuarine sediments often contain high levels of contaminants associated with the anthropogenic activities within the catchment (French, 1993; Cave *et al.*, 2005) that were carried into the estuary associated with suspended particulate matter (SPM) (Horowitz, 1985;

Salomons *et al.*, 1987). The bioavailability of TMs in sediments will depend on the chemical nature of their association with particles (Forstner *et al.*, 1989; Di Toro *et al.*, 1990; Allen *et al.*, 1993; Calmano *et al.*, 1993) that is influenced at the same time by the environmental conditions (redox, salinity, DOC, etc.). The redox-sensitive processes occurring at the oxic-anoxic sediment interface result in changes in metal mobility, mainly due to the coprecipitation or adsorption with the newly formed precipitates or the dissolution of metal-containing precipitates (Di Toro *et al.*, 1990; Caetano *et al.*, 2003). When anaerobic sediments are oxidised, the released metals can be rapidly re-precipitated with insoluble Fe- and Mn-(oxy)hydroxides, and such immobilization has been also observed during anaerobic bio-oxidation (Smith & Jaffe, 1998; Weber *et al.*, 2001; Lack *et al.*, 2002; Hohmann *et al.*, 2010), which may have an important influence on the migration of contaminant metals within subsurface sediments under anaerobic conditions.

The Humber estuary (UK) has been considered an important sink for organic and inorganic contaminants. The rivers flowing into the Humber have received pollution from heavy industry (especially until the first decades of the 20th century), mining, agricultural and urban activities (Goulder *et al.*, 1980, Pethick, 1990; Sanders *et al.*, 1997; Cave *et al.*, 2005). The area surrounding the estuary has been also heavily industrialised; and the estuary is a major locus for gas and oil landing and refining in the North Sea (Cave *et al.*, 2005). Sanders *et al.* (1997) reported nitrate concentrations in the waters of the Humber significantly higher than in most other estuaries around the world. Estuarine sediments are usually rich in organic content due to high sedimentation rates, which increases their potential for denitrification since the oxygen is limited. The importance of denitrification for nitrate removal in the sediment-water interface has been already demonstrated (Barnes & Owens, 1998; Mortimer *et al.*, 1998; Dong *et al.*, 2006). Barnes and Owens (1998) estimated that sediment denitrification removes 25% of the inorganic nitrogen loads entering in the Humber each year, which according to Jickells *et al.* (2000) will represent only a 4% of the total fluvial nitrogen inputs. However, the relative importance of nitrate reduction processes coupled to the oxidation of inorganic substrates remains unknown. Therefore, the aim of this work is to systematically study the anaerobic denitrification via the oxidation of the different

major reduced species (Fe, Mn and S species) in subsurface sediments from four geochemically different settings along the north bank of the Humber estuary amended with a high nitrate solution in a microcosm experiment. The effects of nitrate-driven oxidation on the major element behaviour have been monitored, together with the changes on the trace metal partitioning, in order to improve the understanding of contaminant fate and transport in this post-industrial estuary.

6.2 Material and Methods

6.2.1 Field Sampling

Sediment samples were collected in July 2014 from four sites along the north bank of the Humber estuary during a single tidal cycle. These sites were selected to cover a range of salinity conditions from fresh to high salinity waters: Boothferry (S1) (0.4 psu) and Blacktoft (S2) (3.5 psu) both in the inner estuary; and Paull (S3) (21.6 psu), and Skeffling (S4) (26.1 psu) which are situated towards the outer estuary (see map in Fig. 3.1). Subsurface (5-10 cm) sediments and river water adjacent to each site were collected into polythene containers. River water pH, conductivity and temperature were determined in the field using a Myron Ultrameter PsiII handheld multimeter. The environmental temperature on the day of the sampling was between 19-20°C at all the sites. Samples were transported in a cold box to the laboratory and stored at 4°C until used in the microcosm experiments (two weeks). No air space was left in the polythene containers to avoid air oxidation of redox sensitive elements.

6.2.2 Nitrate-driven oxidation experiments

Microcosm experiments were established with 100 mL of 1:5 sediment-river water ratio suspension in 120 mL glass serum bottles. A litre of sediment-river water suspension was prepared for each of the four sample sites in acid washed polythene bottles using wet sediment, and the final suspension had 20 % of solids by dry weight. For each suspension 100 mL aliquots were transferred in triplicate to 100 mL acid washed serum bottles and sealed with butyl rubber stoppers and aluminium crimps. The triplicate experiments will give the experiment a measure of statistical variability between samples. Low oxygen conditions were maintained during mixing and in the microcosm

bottles by using N_2 gas to displace air in head-spaces. Mixing and homogenising difficulties meant that the final amount of solids in the S3 bottles was ~5%, lower than the 20 % indicated. Three additional replicate microcosms for each sample were autoclaved (3x1 hour cycles at 120°C) as sterile controls. Therefore there were in total 24 microcosms (four biotically active and their respective control experiments all in triplicate). Further replicate microcosm bottles were frozen immediately after preparation and used later for further analysis of the initial microcosm conditions (e.g. porewater characterisation, iron content and TM partitioning).

After a first aliquot was taken aseptically under a stream of N_2 gas, all bottles were amended with 1 mL of a deoxygenated 250 mM nitrate ($NaNO_3$) solution with a sterile syringe. Microcosm bottles were incubated at 10°C in darkness during two months (sampling stopped at a time when no more major changes in the 0.5 N HCl extractable $Fe^{2+}_{(s)}$ levels were observed). Periodically, aliquots of 3 mL of sediment slurry were withdrawn under s stream of N_2 using a sterile syringe and the rubber stopper was carefully wiped with ethanol every time. This volume was split evenly into two micro-centrifuge tubes that were centrifuged (6 min at 16,000 *g*). One of the supernatants was then analysed for Eh and pH using an Orion Dual Star meter with the electrode calibrated at pH 4, 7 and 10. The other supernatant was filtered and stored for nutrient analysis. Nitrate, nitrite and sulphate were determined by ion chromatography (IC) (using a column switching programme, see section 3.3.2.1.2) on a DIONEX CD20 (ED40 Electrochemical detector, %RSD <10%). Ammonium was measured by digital colorimetric analysis on a continuous segmented flow analyser (SEAL AutoAnalyser 3 HR) (%RSD ≤3%). The amount of 0.5 N HCl extractable $Fe^{2+}_{(s)}$ (Lovley & Phillips, 1986a) was determined for the sediment pellets left in the micro-centrifuge tubes by reaction with ferrozine (Viollier *et al.*, 2000).

The same techniques for the analysis of the aqueous phase were used to characterise river water and porewater (recovered by sediment centrifugation (30 min, 6000 *g*)). Dissolved metals (Mn, Fe, Zn, Cu, Cd, As, Pb) were determined in the river waters after sample acidification (1 % v/v HNO_3 trace analytical grade) using ICP-MS (Thermo Scientific ™ ICP-MS). Precautions were taken to avoid potential polyatomic

interferences (see Appendix A for more details) and problems associated with high salinity samples which were diluted (x50 fold). The original sediments used in the microcosm experiment were analysed for: bulk elemental composition by XRF on an Olympus Innovex X-5000 spectrometer; AVS (Canfield *et al.*, 1986); pyrite (Fossing & Jørgensen, 1989); total 0.5 N HCl extractable iron (Lovley & Phillips, 1987); and TOC (after HCl 10% v/v treatment) by combustion with non-dispersive infrared detection on a LECO SC-144DR Sulphur and Carbon Analyser. Solids were also analysed for particle size by laser diffraction on a Malvern Mastersizer 2000E. The analyses of the solid phase were carried out in triplicates, with the exception of the XRF analysis were there were only two replicates.

Sequential extractions were performed on the starting and end point solids using the Tessier *et al.* (1979) procedure as optimised for riverine sediments by Rauret *et al.* (1989). The four extractants used in this procedure were: 1 M $MgCl_2$ at pH 7 (to determine the "exchangeable" fraction), 1 M NaOAc at pH 5 (for the carbonate-bound fraction or 'weak acid extractable'), 0.04 M $NH_2OH{\cdot}HCl$ (in 25% v/v HAc, pH=2) (for the bound to Fe- and Mn-(oxy)hydroxides) and HNO_3 and 30% H_2O_2 at pH 2 followed by NH_4Ac (for metals bound to organic matter and sulphides). The third step of the extraction protocol was modified from the riverine protocol by reducing the extraction temperature (from 96°C to room temperature), and increasing the extraction time (from 6 to 14 hrs). The fifth step of the extraction protocol (for metals associated with the residual fraction) was not performed. The concentrations of the extracted metals were analysed by ICP-MS and all the extractions were carried out in triplicates.

6.3 Results

6.3.1 Sediment and water characterisation

The chemical characteristics of the sediments and water used to make up the sediment slurries for the microcosm experiments are summarised in Table 6.1 (full data set can be found in Chapter 4).

The river water at the inner estuary sites was low in salinity (0.4-3.5 psu), high in nitrate (~250 µM), low in ammonium (<10 µM) and relatively low in sulphate (1-3 mM).

Nitrite was below detection limits. Boothferry (S1) porewater showed some enrichment in ammonium (67 µM), and manganese (82 µM) but depletion of nitrate (37 µM) relative to the river water. Blacktoft (S2) porewater had lower concentrations of ammonium (25 µM) and dissolved manganese (50 µM) than S1, but a similar nitrate concentration (26 µM). Boothferry (S1) sediments contained 2.3% organic carbon (TOC) and 61% of the acid extractable iron was reduced Fe(II), and Blacktoft (S2) sediments contained 1.8% TOC and 53% of the acid extractable iron was reduced Fe(II). No AVS was detected in these sediments.

The river water at the outer estuary sites was brackish (21.6-26.1 psu). The nitrate concentration at Paull (S3) (248 µM) was similar to that in the inner estuary, but it was significantly lower at Skeffling (S4) (24 µM). Ammonium concentrations at S3 and S4 were relatively low, but increased seawards (12 and 23 µM, respectively), and sulphate concentrations were high and again increased seawards (16 and 23 mM, respectively). Nitrite was below detection limits. Sediments porewaters from these sites were low in nitrate (17 and 7 µM at S3 and S4 respectively) in comparison to both the inner estuary porewaters and their respective overlying water. However sulphate (33 and 40 mM respectively) was elevated, and ammonium (934 µM and 126 µM, respectively) and dissolved manganese (41 and 62 µM, respectively) were significantly elevated relative to the overlying water. Paull (S3) sediments contained 2.6% of TOC, and more than 80% of the acid extractable iron was reduced Fe(II), and Skeffling (S4) sediments contained 2.7% TOC and 96% of the acid extractable iron was reduced Fe(II). Both sediments showed Fe-AVS, although the percentage of Fe associated with AVS was low (0.01 and 0.09% in S3 and S4 sediments respectively).

Table 6.1: Geochemical characteristics of the water, sediment porewater and solids from the different sampling locations of the Humber estuary (inner estuary (S1 and S2) and outer estuary (S3 and S4). *Particle size refers to the diameter of the 50% cumulative percentage of finer particles by volume in the sample (D_{50}); nd = not detected. Pb data for brackish-saline (>4 psu) waters are not available (Pb was not measured).

	S1	S2	S3	S4
		River water		
Salinity (psu)	0.4	3.5	21.6	26.1
Conductivity (mS/cm)	0.7383	5.731	30.48	36.42
pH	7.87	7.52	7.90	8.02
NO_3^- (µM)	266	250	248	24
NH_4^+ (µM)	7	7	12	23
SO_4^{2-} (mM)	1	3	16	23
$Fe^{2+}_{(aq)}$ (µM)	0.14	0.09	1.23	1.81
$Mn^{2+}_{(aq)}$ (µM)	1.4	1.0	0.6	22.8
$Zn_{(aq)}$ (µM)	0.15	0.16	8.49	8.03
$Cu_{(aq)}$ (µM)	0.05	0.05	3.70	3.79
$Cd_{(aq)}$ (nM)	0.46	0.84	230	239
$As_{(aq)}$ (µM)	0.06	0.07	0.07	0.07
$Pb_{(aq)}$ (nM)	1.2	4.3	-	-
		Porewater		
Salinity (psu)	0.2	1.8	17.7	32.1
NO^{3-} (µM)	37	26	17	7
NH_4^+ (µM)	67	25	934	126
SO_4^{2-} (mM)	2±0	3±1	33±2	40±2
$Fe_{(aq)}$ (µM)	4.87	0.28	3.55	3.33
$Mn^{2+}_{(aq)}$ (µM)	82	50	41	62
$Zn_{(aq)}$ (µM)	0.09	0.05	8.09	7.83
$Cu_{(aq)}$ (µM)	0.01	0.04	3.62	3.63
$Cd_{(aq)}$ (nM)	0.52	0.81	234	229
$As_{(aq)}$ (µM)	0.19	0.08	0.50	0.25
$Pb_{(aq)}$ (nM)	1.59	1.16	-	-
		Solids		
% Water content in solids	39	28	44	40

Particle size (μm) (D_{50})*	51	49	17	17
Total Fe (%)	3.3±0.7	2.9±0.5	4.1±0.9	4.3±0.9
0.5 N HCl extractable Fe_{TOT} (μmoles/g)	116±10	105±4	206±8	191±28
% 0.5 N HCl extractable $Fe^{2+}{}_{(s)}$ (% Fe^{2+}/Fe_{TOT})	61±5	53±2	84±6	96±3
% Fe-AVS	nd	nd	0.01	0.09
% Fe-Pyrite	0.10	0.10	0.12	0.18
%TOC	2.3±0.7	1.8±0.2	2.6±0.2	2.7±0.0
Mn (μg/g)	785±8	654±1	969±3	732±11
Zn (μg/g)	149±1	129±4	199±13	167±6
Cu (μg/g)	33±3	27±2	31±3	37±11
Cd (μg/g)	<2	<2	<2	<2
As (μg/g)	20±2	18±2	37±4	25±2
Pb (μg/g)	64±1	53±2	90±3	75±1

6.3.2 Major element behaviour during anaerobic nitrate-dependent oxidation

After nitrate amendment, the mean concentration of nitrate in the microcosm bottles was 4.5±1.3 mM. The behaviour of the major elements in the triplicate experiments was monitored for two months. Nitrite was initially below the detection limit in all the replicates. Heat treatment of the controls resulted in ammonium concentrations of 300-400 μM, compared with 30-130 μM in the active experiments, but the ammonium concentration in the controls did not subsequently change significantly over time. Similarly the concentrations of other redox active species did not change during the heat treated controls (see Fig. 6.2 below). In general, there were no important changes in pH between the starting and end point of the experiments; whereas reduction potential (Eh) showed a general decrease with time (Table 6.2).

Table 6.2: Changes in pH and Eh between the initial (before nitrate spike) and final point of the anaerobic nitrate-dependent sediment oxidation experiment. Control samples in brackets. The error represents the standard deviaton (±1σ) of triplicate experiments.

	S1		S2		S3		S4	
	pH	**Eh (mV)**	**pH**	**Eh (mV)**	**pH**	**Eh (mV)**	**pH**	**Eh (mV)**
	7.6±0.0	+73.5±7.8	7.6±0.1	+92.5±4.6	7.4±0.1	+59.2±9.0	7.3±0.2	+66.2±7.5
t_0	(7.1±0.1)	(−31.5±11.5)	(6.9±0.1)	(12.9±10.9)	(6.6±0.1)	(−16.8±2.5)	(6.6±0.1)	(−22.3±8.9)
	7.5±0.3	+56.3±70.1	7.5±0.2	+30.2±52.3	7.0±0.0	+7.5±19.3	6.8±0.1	−55.0±16.9
t_{end}	(7.1±0.0)	(−2.6±8.0)	(7.2±0.1)	(−34.9±10.2)	(6.9±0.0)	(−58.5±10.1)	(7.0±0.1)	(−82.4±9.7)

6.3.2.1 Inner estuary

In the experiments carried out with sediments from the inner estuary, there were no important changes in pH, and the Eh decreased with time, although there was scatter among replicates at the end point sampling (Table 6.2). After the nitrate spike, in S1 experiments, nitrate concentrations gradually decreased from 3.5±0.9 mM to 0.6±0.9 mM in the biotically active samples, whereas nitrate concentrations in the controls remained constant throughout (Fig. 6.3a). By the end of the experiments, 290±151 µmoles of nitrate were consumed. However, in the experiments carried out with S2 sediments, nitrate concentrations modestly decreased from 2.5±0.1 mM to 1.7±0.0 mM in the biotically active samples and remained stable in the controls throughout (Fig. 6.2a). So the overall nitrate loss was very small (82±13 µmoles). Ammonium concentrations in the biotically active experiments were low, although were higher in S1 than in S2 experiments, and decreased in both experiments with time to near detection limit levels (Fig. 6.2b). Following the salinity gradient, sulphate concentrations in S2 microcosms were initially higher than in S1 (3.6 and 1.1 mM respectively), but during the anaerobic incubations no significant change were observed in any of the two biotically active sets of microcosm experiments (Fig. 6.2c). Contemporaneously, the percentage of 0.5 N HCl extractable $Fe^{2+}_{(s)}$ decreased from 70±1 % to 55±3 % in S1 experiments, and from 45±4 % to 36±6 % in S2 experiments (Fig. 6.2d). The net removal of extractable $Fe^{2+}_{(s)}$ was 35±15 µmoles g^{-1} (52% of the total reduced iron inventory in the sediments at t_0) in S1 experiments, whereas in S2

microcosm experiments there was a decrease of 9±15 μmoles g^{-1} during the time of the experiments. Manganese was only measured at the starting and end points of the incubation. Dissolved manganese hardly increased in these tests (1.0±0.5 and 1.1±0.1 μM for S1 and S2 experiments respectively) and 0.5 N HCl extractable $Mn^{2+}_{(s)}$ increased by 6±7 μmoles g^{-1} in S1 experiments but decreased 2±12 μmoles g^{-1} in S2 experiments (note the big scatter in Mn data).

6.3.2.2 Outer estuary

In the microcosms experiments carried out with outer estuary sediments there were not important changes in pH, and the Eh decreased with time in both experiments (Table 6.2). The decrease in the Eh was more pronounced in S4 (Eh returned to negative values within three days after the nitrate spike) than in S3 experiments. After the bottles were spiked with high-concentration nitrate solution, nitrate concentrations gradually decreased from 4.9±0.5 to 2.9±0.8 mM in S3 biotically active samples, while in the controls the concentrations of nitrate did not change (Fig. 6.2e). During the experiments ~40% of the nitrate added (196±131 μmoles of nitrate) was removed, although there was a wide scatter in the S3 replicates at the final sampling points. In the biotically active experiments carried out with S4 sediments, nitrate concentrations sharply decreased during the first week, and went from 4.2±0.8 mM to near detection limits by the end of the experiments (Fig. 6.2e). Therefore, in S4 experiments ~100% of the nitrate added was consumed (420±80 μmoles). Ammonium concentration decreased gradually from 122±14 and 129±0 μM in S3 and S4 experiments respectively to near to detection levels by the end of the experiments (Fig. 6.2f). Sulphate concentrations increased to a different extent in these experiments; there was a net production of 166±90 and 490±60 μmoles of sulphate in S3 and S4 respectively between the amendment and the end of the experiment (Fig. 6.2g). Contemporaneously, the percentage of 0.5 N HCl extractable $Fe^{2+}_{(s)}$ decreased from 81±1% to 28±4 % in S3 experiments, and from 96±0 % to 91±2 % in S4 experiments (Fig. 6.2h). This can be translated in a net removal of 115±29 μmoles g^{-1} of extractable $Fe^{2+}_{(s)}$ in S3 experiments and of only 12±34 μmoles g^{-1} in S4 experiments during the incubations. Although there was considerable scatter in the data, there were not significant changes in concentration of dissolved manganese in either S3 and S4 experiments; and the 0.5 N HCl extractable

$Mn^{2+}_{(s)}$ decreased only in the experiments carried out with S4 sediments (9±5 µmoles g^{-1}) in a similar magnitude than the extractable iron did.

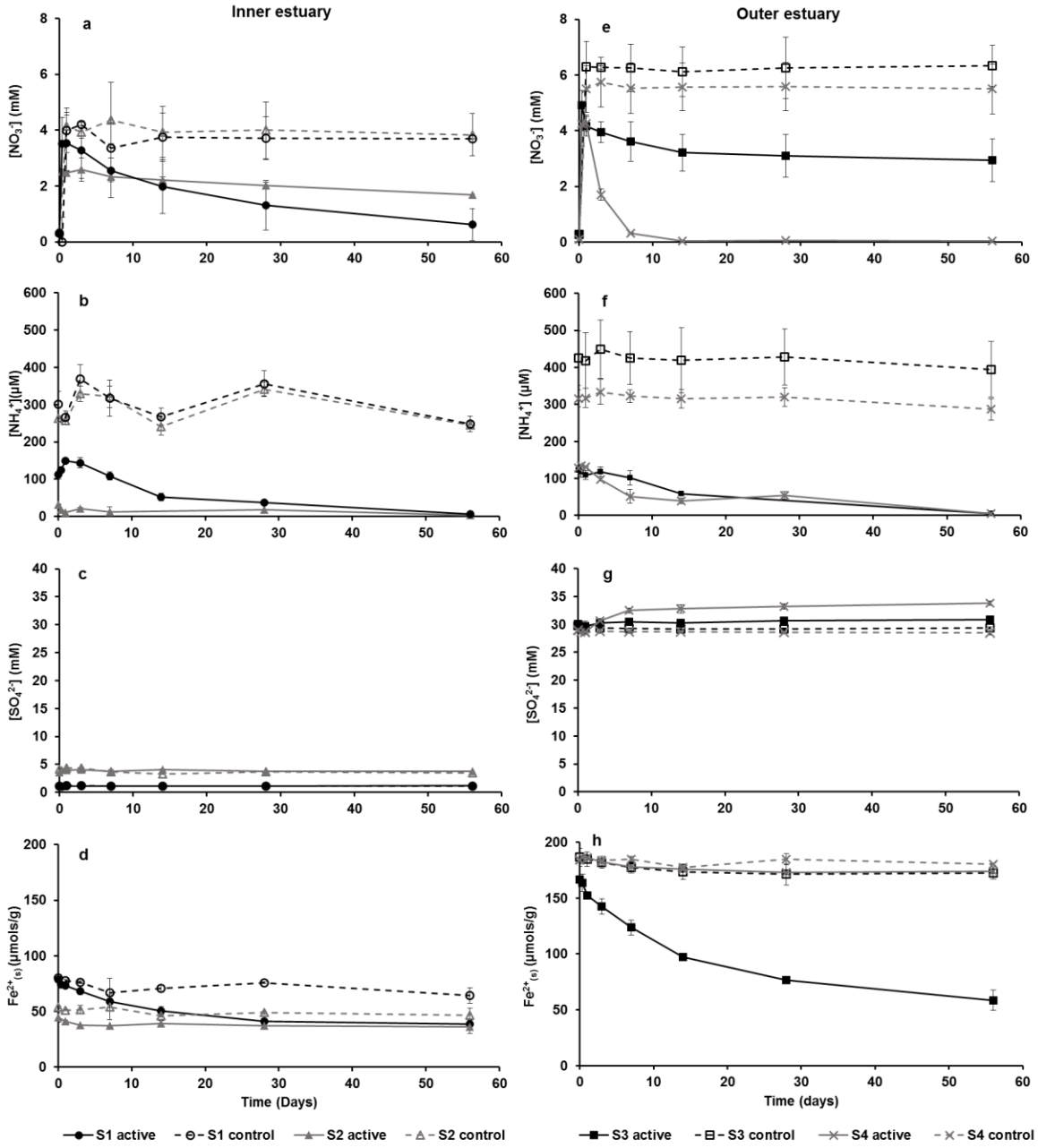

Figure 6.2: Concentration changes in nitrate (a, e); ammonium (b, f); sulphate (c, g); and 0.5 N HCl extractable $Fe^{2+}_{(s)}$ (d, h) during microcosm experiments using sediment from the inner (Boothferry (S1) and Blacktoft (S2) on the left) and outer (Paull (S3) and Skeffling (S4) on the right) Humber estuary. Controls are represented by dashed lines with empty markers, and biotically active experiments by solid lines with filled markers. Error bars show ±1σ of replicates.

6.3.3 Trace metal changes during anaerobic nitrate-dependent oxidation

The concentrations of the dissolved TMs in both the river water and the subsurface sediment porewater showed important differences between the inner and the outer estuary (see Table 6.1). Concentrations of dissolved Zn, Cu, Cd, and As in S1 and S2 water samples were low (all <0.5 μM), whereas, for example Cu and Zn were in the range of ~ 4-8 μM in S3 and S4 river water and porewaters. Fe and Mn aqueous concentrations were slightly greater in porewater than in river water in all the samples. In the solids, the selected TMs (Zn, Cu, Cd, As and Pb) were present in a different range of concentrations (~20-200 μg/g) (Table 6.1), although there was not significant differences in the bulk concentration among sites.

Trace metal partitioning showed in general modest or minor changes between the initial and final solids from the microcosms experiments (Fig. 6.3). Initially, Zn partitioning (Fig. 6.3a) was similar in the four sediments used: Zinc was associated with weak acid-extractable fraction (average 18±7 μg g^{-1}), and, more importantly, with Fe/Mn oxyhydroxides (80±28 μg g^{-1}). After the anaerobic incubation Zn experienced a very modest general shift to weaker bound fraction. Lead was primarily associated with stronger bound fractions (Fig. 6.3b) and, in the end point solids, Pb partitioning showed a general shift towards progressively weaker bound fractions. Copper and As concentrations in all the leachates were relatively low (~10 μg g^{-1}). Initially Cu partitioning showed important differences among the inner and the outer estuarine sediments (Fig. 6.3c); and As partitioning also varied among samples (Fig. 6.3d). In general, Cu (if extracted) and As were associated mainly with strong acid extractable (Fe/Mn oxyhydroxides) fractions. After the anaerobic incubations, only minor changes in Cu and As partitioning were observed, with the exception of S3 sediments, in which Cu showed a significant shift towards weak acid-extractable and strong acid-extractable fractions. The concentrations of Cd in the different leachates were very low (<0.5 μg g^{-1}), and its partitioning varied among samples (Fig. 6.3e). There was a minor shift to weak acid-extractable in sediments from the inner estuary after the nitrate-oxidation experiment. In the initial solids from S3 and S4, Cd was strongly bound, but the end point solids showed a shift towards more ‘easily to extract phases’.

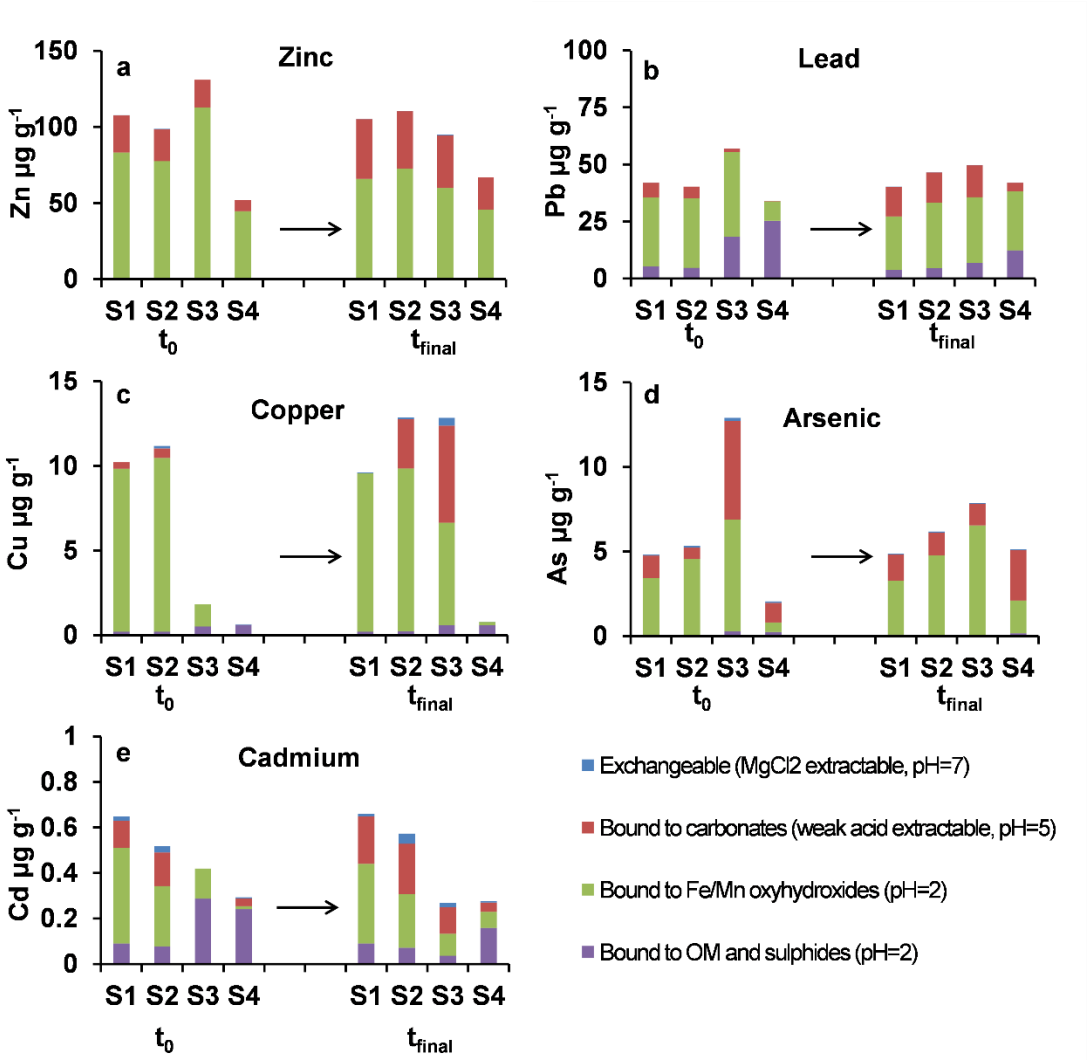

Figure 6.3: Changes in trace metal partitioning between the initial (t_0) and the final (t_{final}) sediments after nitrate-dependent oxidation experiments determined by sequential extractions using Tessier *et al.* (1979) protocol. Zinc partitioning (a); lead partitioning (b); copper partitioning (c); arsenic partitioning (d); and cadmium partitioning (e). Sites are ordered as situated along the salinity gradient and the arrows represent the time of anaerobic oxidation.

6.4 Discussion

6.4.1 Sediment, water and nitrogen dynamics in the Humber estuary

The different estuarine settings along the salinity gradient selected for this study reflected different types of sediment that can be found in the Humber estuary. Humber sediments are not homogeneous and varied from well-mixed oxic sands (like in Blacktoft, S2) to anoxic muds (at the mouth of the estuary) (Barnes & Owens, 1998).

Despite the relatively high concentrations of nitrate found in the river water collected at the different sampling sites (except from S4), the recovered porewaters did not seem to accumulate nitrate in general. Instead, porewaters were generally enriched in ammonium. Mortimer *et al.* (1998) found in the Humber increasing concentrations of ammonium with depth as a product of organic matter degradation, and suggested that sulphate reduction at depth was the primary source of ammonium in the mid-outer estuary. DNRA process could be also a source of ammonium. Under natural conditions, ammonium will be supplied by microbial degradation of organic nitrogen, mixing during sediment resuspension, and/or by direct diffusion through the sediment; and it will be oxidised aerobically in nitrification processes. Nitrification is a key nutrient exchange process occurring in the sediment-water interface and is strongly associated with SPM and bacteria (Barnes & Owens, 1998; Mortimer *et al.*, 1998). The nitrate produced during nitrification, may be denitrified within the sediment or exchanged back to the water column (Barnes and Owens, 1998). Sulphate concentration increased towards the outer estuary and, in the porewaters from the outer estuary sites, sulphate was accumulated with respect to the river water. Aqueous iron concentrations generally were low (0.1-2 µM) in the river waters collected, and slightly higher (~0.3-5 µM) in the recovered porewaters; but there were not significant differences between inner and outer estuary samples. The solubility of iron is very low at the prevailing pH values, and is controlled by iron hydroxides and $FeCO_3$ (Langmuir, 1997). Dissolved iron is expected to be low along the estuarine continuum due to its low solubility, and the flocculation and precipitation processes associated with the increasing salinity (Li *et al*., in press). Instead, it is the particulate iron what accounts for the majority of the total iron fluxes derived from the rivers to the ocean. Poulton & Raiswell (2002) studied the geochemical cycle of iron from continental fluxes to the ocean and concluded that the reactive iron decreases during the transport of particles to the deep ocean and estuaries are important sinks for the riverine reactive iron-rich particles. The results of reactive iron-total iron ratio for the Humber estuary (0.36±0.06) reported in Poulton & Raiswell (2002) were consistent with this global pattern of reactive iron-removal during sediment transport. In the solids from the Humber estuary, the total iron did show an increasing pattern towards the outer estuary but generally the amount of iron was within the range

of estuarine and coastal sediments (Lovley & Phillips, 1986b; Thamdrup *et al*., 1994; Cornwell & Sampou, 1995; Poulton & Raiswell, 2005) and the percentage of the iron pool that was in reduced state was also higher at the outer estuary sites. Although, we did not measure the reactive iron as defined by Canfield (1989) (i.e. "the fraction of the iron that readily reacts with sulphide to form iron sulphide minerals and eventually pyrite"), the measured 0.5 M HCl extractable iron represents part of this reactive iron (i.e. the amorphous and poorly crystalline oxides, Lovley & Phillips, 1986a). So, probably the net total amount of reactive iron would be higher in the outer estuary due to the larger iron pool found in this region of sediment accumulation. Oxide minerals are the most important iron phases in early diagenetic pyrite formation, but lepidocrocite and ferrihydrite are more reactive towards sulphide than goethite and hematite (Canfield, 1989), therefore the role of the later will be less important in estuarine biogeochemical processes.

Iron- and/or sulphate-reducing subsurface sediments were expected in the middle and outer mudflats of the Humber (Mortimer *et al.*, 1998; Burke *et al.*, 2006; Bartlett *et al.*, 2008). The availability of reactive iron in these reducing sediments could be a reason for the rapid free sulphide precipitation (Canfield, 1989). However, the AVS and pyrite measurements (see Table 6.1) only show slight or very minor enrichment in the sediments from the outer estuary sites with respect to those from the inner estuary, which is inconsistent with the amounts of sulphate that were released in S3 and S4 experiments and their initial reducing appearance (dark grey-black colour and characteristic smell). The AVS concentrations measured (<0.02 μmoles AVS g^{-1}) in these Humber sediments were very low relative to other estuarine systems; although low AVS concentrations have been also reported in estuaries and other aquatic environments (Di Toro *et al.*, 1990; Allen *et al.*, 1993; Fang *et al.*, 2005; Monterroso *et al*., 2007). The dynamic nature of the Humber leads to a continuous resuspension and reoxidation of sediments, which will buffer the AVS to a low concentration in this environment, whereas pyrite will accumulate in sediments with time as it is more stable than AVS. This would explain the presence of pyrite in all the samples regardless of the absence of AVS. Furthermore, the availability of dissolved manganese and nitrate will also influence the distribution of free sulphide within the sediments (Thamdrup *et al*.,

1994; Sayama *et al*., 2005). Iron oxides react with free sulphides and, at the same time, the produced Fe^{2+} and H_2S reduce MnO_2 rapidly (Thamdrup *et al*., 1994), which could be another reason for the low AVS detected. Besides, the iron oxides produced in the reaction of MnO_2 with Fe^{2+} will fuel this positive feedback mechanism. Alternatively, it cannot be discarded that the low AVS extracted was an artefact due to the partial oxidation of the sediments during sampling and transport or during the handling in the laboratory prior sediments were freeze-dried for AVS-pyrite extraction. From the two sites at the inner estuary, only sediment from S1 showed iron-reducing characteristics and accumulation of ammonium and manganese; while S2 sediments did not appear to have a well-defined geochemical stratification at the time of sampling. Blacktoft (S2) sediments looked fairly mixed in the field, and, although the porewaters recovered were enriched in manganese with respect to the overlying water, they were not particularly enriched in ammonium nor in dissolved Fe^{2+}. Therefore S2 sediments may not have been poised in reducing conditions at the depth sampled. This is consistent with other studies), in which no suboxic or anoxic characteristics were observed in Blacktoft sediments at the depth sampled (Barnes & Owens, 1998; Mortimer *et al.*, 1998).

According to Uncles *et al.* (1998c), nitrate exhibited steady and conservative mixing between the nitrate-rich waters coming from the rivers at the upper estuary and nitrate-poor waters at the mouth of the Humber. Apart from mixing, the main routes for nitrogen loss in the Humber estuary are expected to be denitrification, principally via microbial breakdown of organic matter, and organic matter burial (Jickells *et al.*, 2000); although the contribution other types of denitrification (i.e. sediment anaerobic denitrification coupled to the oxidation of inorganic reduced substrates) in the overall nitrate removal within the Humber is unknown. In order to identify areas of net nitrate removal and production, nitrate profile along the salinity continuum and its respective mixing line (from near Trent Falls to Spurn Head) have been plotted in Figure 6.4. Combined past records (NRA, 1995, 1996; Uncles *et al.*, 1998c; Burke *et al.*, 2006) have been used as a dataset. The average concentration of nitrate at near east of Trent Falls has been used as the upper end point of the mixing line because it is where the confluence of the two rivers is and the maximum concentrations of nitrate registered in the tidal Trent and Ouse rivers were in the same range than the maximum

concentrations at Trent Falls (Uncles *et al.*, 1999). The other end of the nitrate mixing line is the average concentration at the locations near Spurn Head. Ammonium data points have been also plotted. However, due to the high variability of the ammonium concentrations at near Trent Falls, and the non-conservative behaviour of this species, the ammonium mixing line was not real and therefore has not being plotted. To locate the study sites in Figure 6.4, the salinity variation (calculated from salinity records, see Chapter 7) at each site has been used, and it is represented by the arrows below the plot.

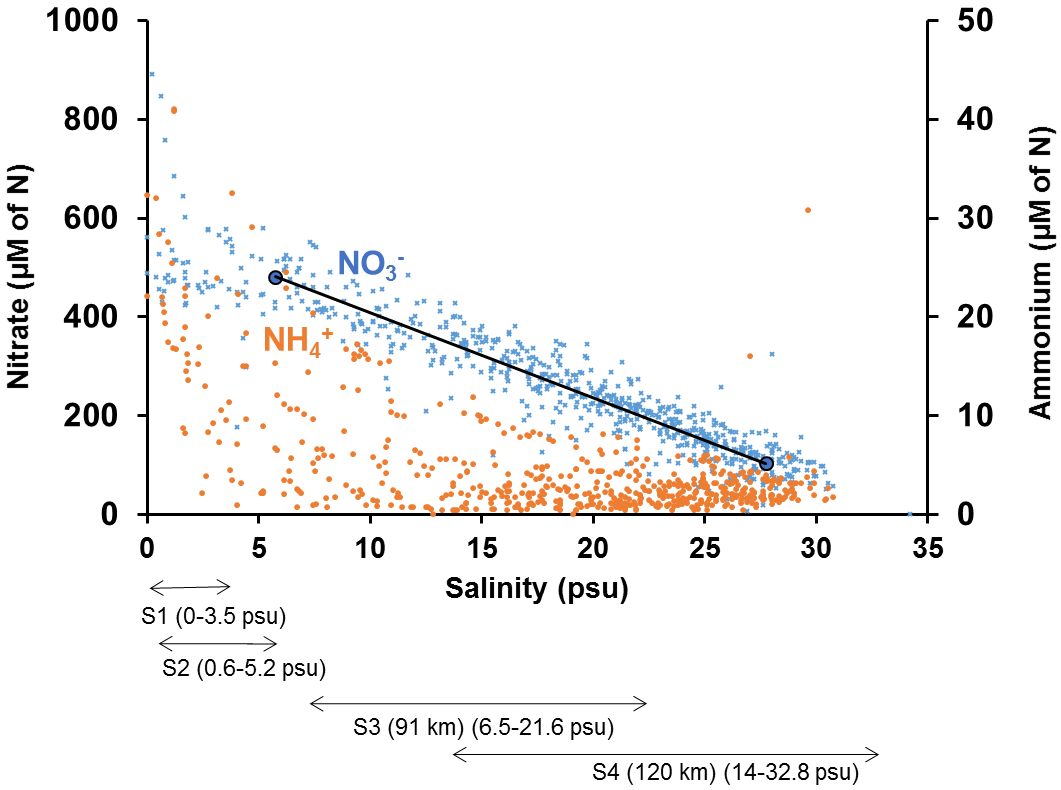

Figure 6.4: Nitrate (blue) and ammonium (orange) concentrations in the river water along the salinity continuum of the Humber Estuary and nitrate mixing line from East of Trent Falls to Spurn Head. Data used are from different surveys (NRA, 1995, 1996) and studies (Uncles *et al.*, 1998c; Burke *et al.*, 2006) in the Humber Estuary. The size of the arrows below the plot shows the salinity variation at the sampling locations of this study (S1-S4) from salinity records of these sites.

Nitrate concentrations generally follow the mixing line, and fluxes into and out of the sediment would be small compared to the river flux (Fig. 6.4). However, between approximately 0-5 psu the high nitrate concentrations seem to decrease sharply which is

perhaps related to the intense nitrification-denitrification processes associated with TMZ at areas of low-salinity waters proximate to the confluence (Plummer *et al.*, 1987; Barnes & Owens, 1998; Uncles *et al.*, 1998b). In the Humber-Trend-Ouse system the TMZ is located in the upper reaches of the tidal rivers at fresh or very low salinity waters (normally between salinities 0-10 psu, average 2.5 psu, Uncles *et al.*, 1998a), although the TMZ location has a strong seasonal component due to the variability of the river flows (Mitchell, 1998; Uncles *et al.*, 1998a). Mortimer *et al.* (1998) found the region of maximum turbidity in the vicinity of Trent Falls (around Blacktoft (S2) and Brough). The nitrate produced in the TMZ region sustains high rates of denitrification (Mortimer *et al.*, 1998). Then, denitrification might decrease down estuary with decreasing nitrate concentrations in the water column (Dong *et al.*, 2006). Towards the mouth of the estuary, nitrate concentrations may be primarily influenced simply by dilution processes due to the dynamics of this area and the combination of estuarine and coastal processes occurring (Arndt *et al.*, 2009). Yet, Barnes & Owens (1998) suggested that nitrate availability cannot entirely explain nitrate removal in the Humber and pointed to multiple controlling factors without a dominating feature neither a constant seasonal pattern. In fact the organic matter availability is key to understand denitrification processes in estuarine sediments. Rivers are the major source of organic carbon to estuaries which is normally low reactive and behaves conservatively decreasing downstream (Abril *et al*., 2002). Organic matter mineralization along a tidal estuary modifies the amounts and characteristics of its transfer from the rivers to the ocean (Middelburg & Herman, 2007; Bauer *et al.*,, 2013). Estuarine sediments have generally high organic content due to high rates of sedimentation, which leads to a diminution of the oxygen status and, therefore, increases the denitrification potential of the sediments (Barnes and Owens, 1998). Organic matter breakdown is thought to be maximum in the TMZ because it is enhanced when metabolizable organic matter and microbial activity increase (Abril *et al*., 2002; Middelburg & Herman, 2007) In the TZM of the Humber, Alvarez-Salgado & Miller (1998) reported a peak in DOC concentration due to anthropogenic discharges, desorption processes and biogeochemical production. The intensive changes in the TZM may induce the repartitioning of organic matter (between DOC and POC) which will have major

implications in its composition and degradability along the gradient (Middelburg & Herman, 2007). However in very turbid estuaries, the extensive mixing, the dilution of possible inputs by the large stock of particles, and simultaneous sources and sinks result in small changes in the bulk concentrations of reactive organic matter (Abril *et al.*, 2002, Middelburg & Herman, 2007). This is because the large POC pool, which shows generally constant low reactivity along the gradient (Abril *et al.*, 2002), buffers the input of high reactive organic rich particles to refractory POC values.

Despite this scheme indicates that nitrate behaves conservatively from near the confluence (i.e. from the TMZ), there may be other nitrogen sink and/or source areas along the estuary. For example, despite the highest denitrification rates are expected in the inner Humber (Barnes & Owens, 1998; Mortimer et al., 1998), the outer estuary could represent also an important sink for nitrate considering its larger area of mudflats (690 km^2 versus the 115 km^2 of the inner estuary, Mortimer *et al*., 1998). There is a lot of uncertainty about the ammonium concentrations in the river water. However there seem to be an upward trend in the data between 15 and 30 psu (Fig. 6.4) suggesting that Humber sediments can act as a source of ammonium in the mid-outer estuary, as concluded by Mortimer *et al*., (1998), which will be rapidly removed from the water column due to chemical oxidation and/or perhaps nitrification processes.

6.4.2 Bacterial nitrate-dependent oxidation processes

To better interpret which processes have dominated during the nitrate-dependent oxidation experiments, electron transfer balances have been calculated (Table 6.3). The major species (N, S, Fe, and Mn) are considered as electron donors or acceptors depending on which part of the redox reaction were involved in. River waters used to prepare the sediment slurries for this experiment were not oxygen free. Therefore, although nitrate was in excess in order to favour nitrate-driven oxidation processes, the remaining DO was surely used together with nitrate as electron acceptor. Hence oxygen has been included in the electron transfer balance and its concentration has been estimated to be between 10-8 ppm according to the temperature of the water and salinity. When considering the complete oxidation pathway from sulphide to sulphate (from -2 to +6 oxidation stage, i.e. transfer of eight electrons per sulphur atom), the

molar balance for electron transfer did not close due to an over-contribution of electron donors. So, as the low values of AVS suggested, sulphate production most probably did not come entirely from the direct oxidation of sulphide. Instead, if an average of four electrons transferred per sulphur atom oxidised to sulphate (i.e. thiosulphate as the intermediate reduced sulphur species) is considered, the electron transfer seems to balance. Thiosulphate is a key intermediate in the sulphur oxidation pathway to sulphate and thus for the regulation of the electron flow in sediments; although its concentrations are normally low because it can be rapidly reduced back to sulphide or undergo disproportionation (Jørgensen, 1990; Jørgensen & Bak, 1991; Jørgensen & Nelson, 2004). Consequently, it has been assumed that rather than a complete oxidation from sulphides to sulphates, a mix of intermediate reduced sulphur species were oxidised during the experiments. Alternative end products of the oxidation of sulphur species are likely to be present in the experiments, although they were not analysed here.

Table 6.3: Calculated electron molar balance for redox processes during anaerobic incubation of non-sulphidic and sulphide-rich sediments in microcosm experiments. The calculations are based on the total electrons produced and consumed in oxidative and reductive processes during two months (56 days) and are expressed in µmoles of electrons in the experiment. The electrons produced in the reduction of oxygen have been calculated assuming a complete consumption of 10 ppm and 8 ppm of oxygen in fresh-brackish (inner estuary) and brackish-saline (outer estuary) waters respectively. Errors have been calculated from ±1σ of triplicate measurements considering error propagation when needed (derived values from multiplications and unit conversion). Manganese data only include the acid extractable $Mn^{2+}_{(s)}$.

		Electrons (µmoles) in the oxidative processes					**Electrons (µmoles) in the reductive processes**				
		$Fe(II) \rightarrow Fe(III) + e^-$	Reduced sulphur → sulphate + $4e^-$	$Mn(II) \rightarrow Mn(IV) + 2e^-$	$NH_4^+ \rightarrow N_2 + 3e^-$	**Total e^- produced**	Oxidised sulphur + $4\ e^- \rightarrow$ intermediate S (thiosulphate)	Nitrate + $5e^- \rightarrow$ nitrogen gas	*Mn(IV) + $2e^- \rightarrow$ Mn(II)	$O_2 + 4e^- \rightarrow 2O^{2-}$	**Total e^- consumed**
Inner estuary	**S1**	885±286	64±33	-	36±2	**984±321**	-	1447±756	275±340	63	**1784±1096**
	S2	153±196	-	68±443	4±1	**226±639**	72±101	409±65	-	63	**544±166**
Outer estuary	**S3**	577±113	663±354	-	34±5	**1273±472**	-	980±656	110 ±360	50	**1140±1016**
	S4	159±692	2725±9	234±130	39±0	**3157±831**	-	2101±391	-	50	**2151±391**

*In these experiments net manganese reduction has been considered since the concentration of acid extractable manganese ($Mn^{2+}_{(s)}$) was higher (with a considerable high error in the measurement) in the final sediments with respect to the original materials.

Nitrate-dependent oxidation processes developed in the microcosms experiments carried out with subsurface sediments from the inner estuary upon nitrate amendment. According to the electron balance, nitrate-dependent oxidation of ferrous iron (acid extractable $Fe^{2+}_{(s)}$) and denitrification were the dominant oxidation processes in S1 and S2 experiments. However, there were differences in the magnitude of such processes due to the different initial redox state of the sediments from S1 and S2. In S2 experiments, the low availability of reduced elements to couple with nitrate reduction should explain the little impact of microbial nitrate-dependent iron oxidation (chemolitoautotrophic denitrification) in these microcosms. Denitrification coupled with the oxidation of organic carbon (equation 6.1) is assumed to be the nitrate-consuming process which compensates the electron donor balances, since the calculations for S1 and S2 experiments showed an imbalance towards the reduction processes. As mentioned above, there is an excess in DOC concentrations in the TMZ of the Humber (Alvarez-Salgado & Miller, 1998) that is associated with higher organic matter breakdown and is progressively removed and controlled by conservative mixing. Although DOC was not monitored in this study, this is consistent with the results observed in S1 and S2 experiments; in which heterotrophic denitrification was an important metabolic process (45 and 58% of the electrons produced in S1 and S2 balances were assumed to be produced in heterotrophic denitrification). Nitrate reduction rate in S1 experiments was 52 µmoles L^{-1} day^{-1} (calculated over 56 days). There was not accumulation of nitrite or ammonium, therefore denitrification to N_2 gas (equation 6.2) (or to N_2O) was most likely the predominant reaction pathway for nitrate (Straub *et al.*, 1996; Benz *et al.*, 1998; Weber *et al.*, 2006). Ammonium was totally consumed in both experiments, but we cannot identify by which process. Additionally, acid extractable $Mn^{2+}_{(s)}$ increased in S1 experiments, whereas it was oxidised in S2; although, considering the big uncertainty of the measurement, no further conclusions about the role of reduced Mn in these systems can be drawn. In general, oxidation of ammonium and sulphur species contributed marginally to the overall electron transfer in the experiments carried out with inner estuary sediments, but no further conclusions about specific processes can be derived.

Towards the outer estuary, processes involving sulphur species will become more important due to the higher concentration of sulphate in seawater, which tallies with

the electron transfer balance calculated for the outer estuary microcosm experiments. Therefore, moving down the estuary, the availability of sulphur species becomes important in the sediment redox processes. It should be pointed that the reported sulphate concentrations in the microcosm bottles were significantly higher than the natural sulphate concentrations in brackish-seawater, which may be due to a combination of porewater contribution, sulphate produced in the oxidation reactions and possibly analytical artefacts. In S3 and S4 microcosm the pool of acid extractable $Fe^{2+}_{(s)}$ (potentially bioavailable) was significantly greater than in the inner estuary sediments; this together with other redox indicators (porewater enrichment in ammonium, manganese, and slightly in reduced iron) confirmed the reducing state of S3 and S4 sediments. Nitrate reduction coupled to the oxidation of inorganic species occurred upon the addition of high nitrate solution to the microcosm. When looking at the electron balance calculations, a transition in the dominant processes from Fe-coupled to S-coupled nitrate-dependent oxidation was observed between these two sites. Despite the scatter, both electron balances closed, so denitrification coupled with the oxidation of organic matter appears to not be as important in these systems as it was in the inner estuary microcosms. The outer estuary sediments had higher organic carbon content than the inner estuary sediments probably due to the high rates of sediment accumulation and, consequently, high organic matter burial in the outer estuarine region. However this organic matter was most likely more refractory than in the inner estuary since metabolizable organic matter is progressively depleted along the gradient (Tyson, 1995). The low reactivity of the organic matter accumulated and the more availability of electron donors in the sediments from the outer estuary may explain the more important role of the nitrate consumption by chemolithotrophic denitrification in these experiments.

In the experiments carried out with Paull (S3) sediments, reduced iron decreased and there was some net sulphate production, so nitrate reduction seemed to be coupled to both, iron and sulphur oxidation processes (equations 6.2, 6.3, 6.5, and 6.6). The rate of nitrate consumption was 35 µmoles L^{-1} day^{-1}, which is in the same order of magnitude that the rate measured at S1; iron oxidation rate was ~2 µmoles $Fe^{2+}_{(s)}$ g^{-1} day^{-1} (~ 3 times larger than S1 experiments, due to the more availability of reduced iron); and sulphate production rate was ~30 µmoles L^{-1} day^{-1}. Site 3 experiments

showed more iron(II) oxidation (Fig. 6.2h) than the inner estuary experiments (Fig. 6.2d); however the fact that S3 microcosms contained less amount of sediments than the other experiments explains why the net amount of electrons produced from iron oxidation in S3 was lower than in S1 (Table 6.3). In short, a combination of Fe(II)- and S-oxidation coupled to nitrate reduction appeared to be the dominant processes in S3 experiments. On the other hand, the behaviour of the major elements in the experiments carried out with sediments from Skeffling (S4) showed important differences with respect to the others. This set of microcosms had the fastest rates of nitrate reduction (75 μmoles L^{-1} day^{-1}) and it was the only set of experiments where nitrate was totally consumed (there was <50 μM of nitrate 14 days after the amendment). In fact, Eh returned to negative values in S4 microcosms within three days after the nitrate spike, which indicates the rapid restoration of the reducing conditions as nitrate was depleted. However nitrate reduction coupled to iron oxidation did not dominate these experiments because the acid extractable $Fe^{2+}_{(s)}$ barely decreased during the incubation time. Instead, chemolithotrophic denitrification was likely coupled to the oxidation of reduced sulphur species. Hence, reactions involving sulphur species (for example equations 6.3, 6.5 and 6.6) were likely the most important in S4 experiments. About 25% of the electrons produced in the oxidation of sulphur occurred after nitrate was almost depleted (after day 7), so perhaps there was an oxygen leak in the bottles during sampling or intermediate oxidised species were acting as electron acceptors. After nitrate was consumed, extractable $Mn^{2+}_{(s)}$ appeared to increase and decrease in S3 and S4 experiments respectively; however the error associated was too big to drawn further conclusions. Ammonium was totally depleted in both experiments likewise in the inner estuary experiments, but no further conclusions about the processes involving ammonium can be derived. Overall, oxidation of reduced sulphur species coupled to nitrate reduction appeared to be the dominant process in S4 experiments. Burke *et al.* (2006) found that sulphate-reducing sediments from the Humber estuary needed higher nitrate concentrations to observe iron oxidation as these sediments contained more reduced species that iron(III)−reducing sediments, therefore it may be that the addition of nitrate in this study was not high enough to burst iron-oxidising bacteria activity but sulphur-oxidising bacteria activity.

Overall, these experiments suggested that there is a general potential for nitrate removal in the subsurface sediment from the Humber Estuary. The absence of nitrate in the sediment porewaters may be an evidence of the nitrate consumption in different denitrification processes. Sediment denitrification will be controlled in the natural system mainly by nitrate availability, organic status of the sediments, macrofaunal density, and temperature (Barnes & Owens, 1998). The removal of nitrate indicates a transitional pattern: from a combination of denitrification coupled to organic matter and iron(II) oxidation in the inner estuary, towards a combination of Fe− and S−oxidation dominated systems in the mid estuary and a S−oxidation dominated environment in the outer most estuary. The dominating processes observed in the experiments are determined by the initial geochemistry of the sediments, or in other words, by the availability of different electron donors in the facultative zone found at the depth sampled. In particular, the availability of reduced iron and sulphur within the sediment profile probably will condition sediments dominated preferably by iron (FeOB) and/or sulphur oxidising bacteria (SOB) along the estuarine continuum.

Previous studies about sediment denitrification in the Humber were based in denitrification rates which took into account nitrate concentrations in the river water and nitrate exchange between sediment and water column. Denitrification accounted for the 25% of the total annual nitrogen inputs to the Humber estuary (Barnes & Owens, 1998), and the mid and outer mudflats were the main sinks of nitrate due to their larger extension despite the higher nitrate removal rates were found in the inner estuary (Mortimer *et al*., 1998). However, the results in the microcosms did not show exactly the same pattern, which may be due to the type of experiments, the particular sampling sites chosen, and/or the type of sediments used (subsurface instead of immediately surface sediment). It is difficult to estimate the fluxes of nitrate between sediment layers in such a disturbed system, so with the available data we cannot quantify how much of the nitrate in the water column will be denitrified in the undisturbed subsurface sediments. Nevertheless, we suggest that denitrification rates likely increase in the subsurface sediments likewise in the surface sediments with increasing nitrate concentrations in the river water. Yet, when assessing nitrate excess in the water and the possible associated eutrophication problems in the coastal environment, it is important to remember that the majority of

the nitrate riverine inputs are not denitrified and the influence of the nitrate concentrations on the denitrification rates is marginal (Barnes & Owens, 1998) and limited (plateau above 500 µM; Jickells, 2000).

Initial ammonium concentrations in the biotically active experiments were higher than the expected concentrations from the mixing of river and porewater. This may be explained by desorption and/or ammonification (microbial oxidation of organic matter) processes occurring in the microcosms at the beginning of the experiment. Ammonium concentrations were increasing seawards but in the microcosm ammonium was consumed in all the experiments, which contrasts with the observations by Mortimer *et al.* (1998) which indicated that the outer estuary was a net source of ammonium to the water column. In the control experiments, the high ammonium concentrations may be a result of the heat-treatment (Salonius *et al.*, 1967; Berns *et al.*, 2008) which could cause the mineralisation of organic matter and also desorption from particle surfaces. Under natural conditions, especially in the outer estuary, where anoxic mudflats are found, the amount of adsorbed ammonium could represent a substantial part of the total ammonium pool in sediments, which could be interpreted as a potential source of bioavailable nitrogen (Rosenfeld, 1979; Laima *et al.*, 1999). Net ammonium production was not observed in the microcosm experiments, so the development of DNRA processes has not been considered. However, we do not know how important DNRA, as an alternative denitrification pathway, is in natural conditions in the Humber estuary. To elucidate which denitrification pathway is favoured in a specific geochemical environment we would need to know not only the availability of nitrate and electron donors, but also the organic carbon loading (Roberts *et al.*, 2014). Lastly, anammox reactions have not been considered since nitrite concentrations have not been detected throughout, although they can also occur in the natural environment.

6.4.3 Trace metals in the Humber estuary and partitioning changes after nitrate-driven oxidation processes

Zinc, Pb, Cu, As and Cd are considered potentially toxic elements in the aquatic environment and have been selected as they were known (with the exception of Cd) to be significantly accumulated in the Humber sediments due to the industrial activity in the catchment (Cave *et al.*, 2005; Andrews *et al.*, 2008). The bulk (total)

concentrations of these metals in the sediments used in this study were above the pre-industrial background, but below the levels registered during the 70s-90s (see Table 6.4). The concentration of each metal in the sediments from the four sites was very similar, and the range of metal concentrations metal was ~20-200 µg/g (see Table 6.1).

Table 6.4: Bulk concentration of trace metals in the Humber estuary over time (after Andrews *et al.*, 2008 and references therein). *Cadmium concentrations have been reported in other studies (NRA, 1993a, b), so the dates of the reported values do not correspond exactly with those of the other metals. The range is expressed as annual mean for individual sites and the average value is the overall mean calculated from 1980 to 1990. (nr = non-reported values).

	Zn (µg/g)	Cu (µg/g)	Cd (µg/g)*	As (µg/g)	Pb (µg/g)
This study	130-200	27-37	<2	18-37	53-90
1980s-1994*	265	51	0.2-1.1 (average 0.5)	50	110
1970s	322	63	nr	61	132
Pre-1969	288	61	nr	50	120
Background	91	19	nr	18	23

In general the concentrations of TMs in solution in the river water and the subsurface sediment porewater showed important differences between the inner and the outer estuary. The concentrations were significantly higher in the outer estuary than in the inner estuary samples (see Table 6.1). The salinity increase could explain these higher concentrations since the mobility of metals such as Cd, Cu or Zn has been noted to be enhanced when salinity increases due to the formation of chlorine complexes (Du Laing *et al.*, 2009). However the interactions between salinity, organic matter (e.g. humic acids) and pH are complex and will affect the extent of metal desorption from sediments in saline waters. Arsenic did not show that trend and values were constant along the salinity gradient.

The oxidation of anoxic sediments is thought to cause shifts in the TM speciation that often mean shifts from higher-energy bound fractions to more reactive or bioavailable phases (Di Toro *et al.*, 1990; Calmano *et al.*, 1993; John & Leventhal, 1995; Saulnier & Mucci, 2000; Zoumis *et al.*, 2001; Caetano *et al.*, 2003). However, the implications of the oxidation of estuarine sediments on metal mobility and partitioning in the absence or near absence of oxygen via nitrate reduction have not

been widely studied to date. Nitrate driven oxidation of the Humber estuary subsurface sediments had different effects on TM partitioning among samples and there was not a common pattern among the different metals analysed. From the sequential extractions performed for this study, the concentrations in the exchangeable phase were generally very low or below detection limit, probably because the adsorption-desorption processes are normally pH-dependent, and therefore desorption of the specifically adsorbed metals may not be complete at neutral pH (Tessier *et al.*, 1979; Du Laing *et al.*, 2009). Trace metals were bound predominantly in acid extractable (weak and strong acid) fractions. Nevertheless, it is known that with this extraction protocol, "weak acid-extractable" fraction may be overestimated because it could not only include metals bound to carbonates, but also specifically sorbed to exchangeable sites of clay, organic matter or oxides surfaces (Gleyzes *et al*., 2002). The modification of the third step, which was performed at ambient temperature and in which the extraction time was increased, may not have been sufficient to complete iron and manganese oxides-associated metals extraction (Gleyzes *et al.*, 2002). Despite Cu, Zn and Cd being expected to occur as CuS, ZnS and CdS in estuarine anoxic sediments due to the availability of sulphate in the water column (Huerta-Diaz *et al.*, 1998), the concentrations found in the leachate for the organic matter-sulphide fraction were very low. This may be explained by weaknesses of the extraction protocol as pointed by Anju & Banerjee (2010) since sulphides may be only partially dissolved and organic matter not completely destroyed. Yet, what can be concluded is that there was a general but modest shift of the TMs towards weaker bound fractions, which suggests that the anaerobic oxidation of estuarine sediments can lead to some changes in metal mobility and bioavailability. Despite the mechanisms of the TM behaviour during nitrate-driven oxidation being beyond the scope of this study, the results suggest that TMs are likely co-precipitating with or adsorbing to carbonates and to the fresh Fe/Mn oxide surfaces produced during sediment oxidation.

6.5 Conclusions

This study presents a systematic study of the biogeochemical effects of the anaerobic denitrification on sediments along the salinity gradient of the Humber estuary. Sediment denitrification is important for the nitrogen budget of the estuary

in the absence or near absence of oxygen since the indigenous microbial populations are capable to use reduced inorganic species (iron, manganese and sulphur) as electron donors besides organic matter. Yet, the majority of the nitrate from riverine inputs is not denitrified and mixing of fresh and seawater is major process in regulating nitrate concentrations. In the experimental conditions, denitrification to nitrogen gas seemed to be the main nitrate removal process; however, the dominant electron donor species coupling nitrate reduction showed a transition from inner estuary towards outer estuary experiments. Denitrification coupled with organic matter and iron oxidation were the most important processes in the microcosm experiments with inner estuary sediments, followed by a combination of iron and sulphur oxidation, towards a sulphur-oxidation dominant environment in the experiments using the outer most estuarine sediments. These results suggest that chemolithoautotrophic denitrification is not only controlled by nitrate availability in the water column, but the geochemical characteristics of the sediments such as the development of suboxic or anoxic conditions, the accumulation of iron and/or manganese, and the presence of reduced sulphur in the sediment column have also implications. Furthermore, during nitrate-driven sediment oxidation, the TMs associated with the sediments experienced changes in their partitioning. We observed a general shift of trace metals from high-energy binding sites towards weaker binding sites. Therefore, upon sediment bio-oxidation, the just-released trace metals may be weakly adsorbed on solid surfaces (such as carbonates), and/or incorporated in the newly formed Fe/Mn oxides, and hence their bioavailability might increase during a certain time window. However, in natural conditions the metals accumulated in the subsurface sediments may be transferred slowly in less reactive mineral phases as sediment is buried, and therefore, their bioavailability will decrease in long time scales.

6.6 References

[1] Abril, G., Nogueira, M., Etcheber, H., Cabecadas, G., Lemaire, E., & Brogueira, M. J. (2002). Behaviour of organic carbon in nine contrasting European estuaries. *Estuarine Coastal and Shelf Science*, 54(2), pp.241-262. doi: 10.1006/ecss.2001.0844

[2] Allen, H. E., Fu, G. M., & Deng, B. L. (1993). Analysis of acid-volatile sulfide (AVS) and simultaneously extracted metals (SEM) for the estimation of potential toxicity in aquatic sediments. *Environmental Toxicology and Chemistry, 12*(8), pp.1441-1453. doi: 10.1897/1552-8618(1993)12[1441:aoasaa]2.0.co;2

[3] Alvarez-Salgado, X. A., & Miller, A. E. J. (1998). Dissolved organic carbon in a large macrotidal estuary (the Humber, UK): Behaviour during estuarine mixing. *Marine Pollution Bulletin*, 37(3-7), pp.216-224.

[4] An, S. M., & Gardner, W. S. (2002). Dissimilatory nitrate reduction to ammonium (DNRA) as a nitrogen link, versus denitrification as a sink in a shallow estuary (Laguna Madre/Baffin Bay, Texas). *Marine Ecology Progress Series, 237*, pp.41-50. doi: 10.3354/meps237041

[5] Andrews, J. E., Samways, G., & Shimmield, G. B. (2008). Historical storage budgets of organic carbon, nutrient and contaminant elements in saltmarsh sediments: Biogeochemical context for managed realignment, Humber Estuary, UK. *Science of The Total Environment, 405*(1-3), pp.1-13. doi: 10.1016/j.scitotenv.2008.07.044

[6] Anju, M., & Banerjee, D. K. (2010). Comparison of two sequential extraction procedures for heavy metal partitioning in mine tailings. *Chemosphere, 78*(11), pp.1393-1402. doi: 10.1016/j.chemosphere.2009.12.064

[7] Arndt, S., Regnier, P., & Vanderborght, J. P. (2009). Seasonally-resolved nutrient export fluxes and filtering capacities in a macrotidal estuary. *Journal of Marine Systems, 78*(1), 42-58. doi: 10.1016/j.jmarsys.2009.02.008

[8] Barnes, J., & Owens, N. J. P. (1998). Denitrification and nitrous oxide concentrations in the Humber estuary, UK, and adjacent coastal zones. *Marine Pollution Bulletin, 37*(3-7), pp.247-260.

[9] Bartlett, R., Mortimer, R. J. G., & Morris, K. (2008). Anoxic nitrification: Evidence from Humber Estuary sediments (UK). *Chemical Geology, 250*(1-4), pp.29-39. doi: 10.1016/j.chemgeo.2008.02.001

[10] Bauer, J. E., Cai, W.-J., Raymond, P. A., Bianchi, T. S., Hopkinson, C. S., & Regnier, P. A. G. (2013). The changing carbon cycle of the coastal ocean. *Nature*, 504(7478), pp.61-70. doi: 10.1038/nature12857

[11] Benz, M., Brune, A., & Schink, B. (1998). Anaerobic and aerobic oxidation of ferrous iron at neutral pH by chemoheterotrophic nitrate-reducing bacteria. *Archives of Microbiology, 169*(2), pp.159-165. doi: 10.1007/s002030050555

[12] Berner, R. A. (1980). *Early diagenesis: A theoretical approach*: Princeton University Press.

[13] Berns, A. E., Philipp, H., Narres, H. D., Burauel, P., Vereecken, H., & Tappe, W. (2008). Effect of gamma-sterilization and autoclaving on soil organic matter structure as studied by solid state NMR, UV and fluorescence spectroscopy. *European Journal of Soil Science, 59*(3), pp.540-550. doi: 10.1111/j.1365-2389.2008.01016.x

[14] Boyle, E. A., Edmond, J. M., & Sholkovitz, E. R. (1977). The mechanism of iron removal in estuaries. *Geochimica et Cosmochimica Acta, 41*, pp.1313-1324. doi: 10.1016/0016-7037(77)90075-8

[15] Brunet, R. C., & Garcia Gil, L. J. (1996). Sulfide-induced dissimilatory nitrate reduction to ammonia in anaerobic freshwater sediments. *FEMS Microbiology Ecology, 21*(2), 131-138. doi: 10.1016/0168-6496(96)00051-7

[16] Burdige, D. J. (1993). The biogeochemistry of manganese and iron reduction in marine-sediments. *Earth-Science Reviews, 35*(3), pp.249-284. doi: 10.1016/0012-8252(93)90040-e

[17] Burke, I. T., Boothman, C., Lloyd, J. R., Livens, F. R., Charnock, J. M., McBeth, J. M., Mortimer, R. J. G., & Morris, K. (2006). Reoxidation Behavior of Technetium, Iron, and Sulfur in Estuarine Sediments. *Environmental Science & Technology, 40*(11), pp. 3529-3535. doi: 10.1021/es052184t

[18] Caetano, M., Madureira, M. J., & Vale, C. (2003). Metal remobilisation during resuspension of anoxic contaminated sediment: short-term laboratory study. *Water Air and Soil Pollution, 143*(1-4), pp.23-40. doi: 10.1023/a:1022877120813

[19] Calmano, W., Hong, J., & Forstner, U. (1993). Binding and mobilization of heavy-metals in contaminated sediments affected by pH and redox potential. *Water Science and Technology, 28*(8-9), pp.223-235. doi: 10.15480/882.450

[20] Canfield, D. E., Raiswell, R., Westrich, J. T., Reaves, C. M., & Berner, R. A. (1986). The use of chromium reduction in the analysis of reduced inorganic sulfur in sediments and shales. *Chemical Geology, 54*(1-2), pp.149-155. doi: 10.1016/0009-2541(86)90078-1

[21] Canfield, D. E. (1989). Reactive iron in marine-sediments. *Geochimica et Cosmochimica Acta*, 53(3), pp.619-632. doi: 10.1016/0016-7037(89)90005-7

[22] Canfield, D. E. (1993). Organic matter oxidation in marine sediments. *In:* Wollast, R., Mackenzie, F.T., Chou, L. (Eds.) *Interactions of C, N, P and S biogeochemical Cycles and Global Change*. Berlin: Springer, pp.333-363

[23] Canfield, D. E., Thamdrup, B., & Hansen, J. W. (1993). The anaerobic degradation of organic-matter in danish coastal sediments - iron reduction, manganese reduction, and sulfate reduction. *Geochimica et Cosmochimica Acta, 57*(16), 3867-3883. doi: 10.1016/0016-7037(93)90340-3

[24] Canfield, D. E., Kristensen, E., & Thamdrup, B. (2005). *Aquatic Geomicrobiology*. Advances in Marine Biology. London: Elsevier Academic Press.

[25] Canfield, D. E., & Thamdrup, B. (2009). Towards a consistent classification scheme for geochemical environments, or, why we wish the term 'suboxic' would go away. *Geobiology, 7*(4), pp.385-392. doi: 10.1111/j.1472-4669.2009.00214.x

[26] Cave, R. R., Andrews, J. E., Jickells, T., & Coombes, E. G. (2005). A review of sediment contamination by trace metals in the Humber catchment and estuary, and the implications for future estuary water quality. *Estuarine, Coastal and Shelf Science, 62*(3), pp.547-557. doi: 10.1016/j.ecss.2004.09.017

[27] Cornwell, J. C., & Sampou, P. A. (1995). Environmental Controls on Iron Sulfide Mineral Formation in a coastal plain estuary. *In* Vairamurthy, M. A. Schoonen, M. A. A. (Eds), *Geochemical Transformations of Sedimentary Sulfur* (Vol. 612, pp. 224-242) Washington D.C.: American Chemical Society, pp.224-242.

[28] Dalsgaard, T., Canfield, D. E., Petersen, J., Thamdrup, B., & Acuna-Gonzalez, J. (2003). N-2 production by the anammox reaction in the anoxic water column of Golfo Dulce, Costa Rica. *Nature, 422*(6932), pp.606-608. doi: 10.1038/nature01526

[29] Dalsgaard, T., Thamdrup, B., & Canfield, D. E. (2005). Anaerobic ammonium oxidation (anammox) in the marine environment. *Research in Microbiology, 156*(4), pp.457-464. doi: 10.1016/j.resmic.2005.01.011

[30] Di Toro, D. M., Mahony, J. D., Hansen, D. J., Scott, K. J., Hicks, M. B., Mayr, S. M., & Redmond, M. S. (1990). Toxicity of cadmium in sediments the role of acid volatile sulfide. *Environmental Toxicology and Chemistry, 9*(12), pp.1487-1502. doi: 10.1002/etc.5620091208

[31] Dong, L. F., Nedwell, D. B., & Stott, A. (2006). Sources of nitrogen used for denitrification and nitrous oxide formation in sediments of the hypernutrified Colne, the nutrified Humber, and the oligotrophic Conwy estuaries, United Kingdom. *Limnology and Oceanography, 51*(1), pp.545-557.

[32] Dong, L. F., Sobey, M. N., Smith, C. J., Rusmana, I., Phillips, W., Stott, A., Osborn, A. M., & Nedwell, D. B. (2011). Dissimilatory reduction of nitrate to ammonium, not denitrification or anammox, dominates benthic nitrate reduction in tropical estuaries. *Limnology and Oceanography, 56*(1), pp.279-291. doi: 10.4319/lo.2011.56.1.0279

[33] Du Laing, G., Rinklebe, J., Vandecasteele, B., Meers, E., & Tack, F. M. G. (2009). Trace metal behaviour in estuarine and riverine floodplain soils and sediments: A review. *Science of The Total Environment, 407*(13), pp.3972-3985. doi: 10.1016/j.scitotenv.2008.07.025

[34] Fang, T., Li, X., & Zhang, G. (2005). Acid volatile sulfide and simultaneously extracted metals in the sediment cores of the Pearl River Estuary, South China. *Ecotoxicology and Environmental Safety, 61*(3), pp.420-431. doi: http://dx.doi.org/10.1016/j.ecoenv.2004.10.004

[35] Forstner, U., Ahlf, W., & Calmano, W. (1989). Studies on the transfer of heavy-metals between sedimentary phases with a multi-chamber device - combined effects of salinity and redox variation. *Marine Chemistry, 28*(1-3), pp.145-158. doi: 10.1016/0304-4203(89)90192-8

[36] Fossing, H., & Jørgensen, B. B. (1989). Measurement of bacterial sulfate reduction in sediments - evaluation of a single-step chromium reduction method. *Biogeochemistry, 8*(3), pp.205-222. doi: 10.1007/BF00002889

[37] French, P. W. (1993). Post-industrial pollutant levels in contemporary Severn Estuary intertidal sediments, compared to pre-industrial levels. *Marine Pollution Bulletin, 26*(1), pp.30-35. doi: http://dx.doi.org/10.1016/0025-326X(93)90594-A

[38] Froelich, P. N., Klinkhammer, G. P., Bender, M. L., Luedtke, N. A., Heath, G. R., Cullen, D., Dauphin, P., Hammond, D., Hartman, B., & Maynard, V. (1979). Early oxidation of organic-matter in pelagic sediments of the eastern equatorial atlantic - suboxic diagenesis. *Geochimica et Cosmochimica Acta, 43*(7), pp.1075-1090. doi: 10.1016/0016-7037(79)90095-4

[39] Gardner, W. S., McCarthy, M. J., An, S., Sobolev, D., Sell, K. S., & Brock, D. (2006). Nitrogen fixation and dissimilatory nitrate reduction to ammonium (DNRA) support nitrogen dynamics in Texas estuaries. *Limnology and Oceanography, 51*(1), pp.558-568.

[40] Gardner, W. S., & McCarthy, M. J. (2009). Nitrogen dynamics at the sediment-water interface in shallow, sub-tropical Florida Bay: why denitrification efficiency may decrease with increased eutrophication. *Biogeochemistry, 95*(2-3), pp.185-198. doi: 10.1007/s10533-009-9329-5

[41] Giblin, A. E., Tobias, C. R., Song, B., Weston, N., Banta, G. T., & Rivera-Monroy, V. H. (2013). The Importance of Dissimilatory Nitrate Reduction to Ammonium (DNRA) in the Nitrogen Cycle of Coastal Ecosystems. *Oceanography, 26*(3), pp.124-131.

[42] Gleyzes, C., Tellier, S., & Astruc, M. (2002). Fractionation studies of trace elements in contaminated soils and sediments: a review of sequential extraction procedures. Trac-Trends in Analytical Chemistry, 21(6-7), 451-467. doi: 10.1016/s0165-9936(02)00603-9

[43] Godfrey, L. V., & Falkowski, P. G. (2009). The cycling and redox state of nitrogen in the Archaean ocean. *Nature Geoscience, 2*(10), pp.725-729. doi: 10.1038/ngeo633

[44] Goulder, R., Blanchard, A. S., Sanderson, P. L., & Wright, B. (1980). Relationships between heterotrophic bacteria and pollution in an industrialized estuary. *Water Res, 14*(6), 591-601. doi: 10.1016/0043-1354(80)90117-7

[45] Hohmann, C., Winkler, E., Morin, G., & Kappler, A. (2010). Anaerobic Fe(II)-oxidizing bacteria show as resistance and immobilize As during Fe(III) mineral precipitation. *Environmental Science & Technology, 44*(1), pp.94-101. doi: 10.1021/es900708s

[46] Horowitz, A. J. (1985). *A primer on trace metal-sediment chemistry*: US Government Printing Office.

[47] Howarth, R. W, Andreson, D., Cloern, J., Elfring, C., Hopkinson, C., Lapointe, B., Malone, T., Marcus, N., McGlathery, K., Sharpley, A., & Walker, D. (2000). *Nutrient Pollution of Coastal Rivers, Bays and Seas*. Issues in Ecology: Ecological Society of America.

[48] Howarth, R. W., & Marino, R. (2006). Nitrogen as the limiting nutrient for eutrophication in coastal marine ecosystems: Evolving views over three decades. *Limnology and Oceanography, 51*(1), pp.364-376. doi: 10.4319/lo.2006.51.1_part_2.0364

[49] Huerta-Diaz, M. A., & Morse, J. W. (1990). A quantitative method for determination of trace metal concentrations in sedimentary pyrite. *Marine Chemistry, 29*(2-3), pp.119-144. doi: 10.1016/0304-4203(90)90009-2

[50] Huerta-Diaz, M. A., Tessier, A., & Carignan, R. (1998). Geochemistry of trace metals associated with reduced sulfur in freshwater sediments. *Applied Geochemistry, 13*(2), pp.213-233. doi: 10.1016/s0883-2927(97)00060-7

[51] Hulth, S., Aller, R. C., & Gilbert, F. (1999). Coupled anoxic nitrification manganese reduction in marine sediments. *Geochimica et Cosmochimica Acta, 63*(1), pp.49-66. doi: 10.1016/s0016-7037(98)00285-3

[52] Jetten, M. S. M., Logemann, S., Muyzer, G., Robertson, L. A., deVries, S., vanLoosdrecht, M. C. M., & Kuenen, J. G. (1997). Novel principles in the microbial conversion of nitrogen compounds. *Antonie Van Leeuwenhoek International Journal of General and Molecular Microbiology, 71*(1-2), pp.75-93. doi: 10.1023/a:1000150219937

[53] Jetten, M. S. M., Sliekers, O., Kuypers, M., Dalsgaard, T., van Niftrik, L., Cirpus, I., van de Pas-Schoonen, K., Lavik, G., Thamdrup, B., Le Paslier, D., Op den Camp, H. J. M., Hulth, S., Nielsen, L. P., Abma, W., Third, K., Engstrom, P., Kuenen, J. G., Jørgensen, B. B., Canfield, D. E., Damste, J. S. S., Revsbech, N. P., Fuerst, J., Weissenbach, J., Wagner, M., Schmidt, I., Schmid, M., & Strous, M. (2003). Anaerobic ammonium oxidation by marine and freshwater planctomycete-like bacteria. *Applied Microbiology and Biotechnology, 63*(2), pp.107-114. doi: 10.1007/s00253-003-1422-4

[54] Jickells, T., Andrews, J., G., S., Sanders, R., Malcolm, S., Sivyer, D., Parker, R., Nedwell, D., Trimmer, M., & Ridgway, J. (2000). Nutrient Fluxes through the Humber Estuary: Past, Present and Future. *Ambio; Royal Swedish Academy of Sciences, 29*(3), pp.130-135.

[55] John, D. A., & Leventhal, J. S. (1995). Bioavailabolity of Metals. *In*: Edward A. du Bray (Ed.), *Preliminary compilation of descriptive geoenvironmental mineral deposit models* (pp.10-18). Denver, Colorado: U.S. Department of the Interior. Retrieved from http://pubs.usgs.gov/of/1995/0831/report.pdf

[56] Jørgensen, B. B. (1982). Mineralization of organic-matter in the sea bed - the role of sulfate reduction. *Nature, 296*(5858), pp.643-645. doi: 10.1038/296643a0

[57] Jørgensen, B. B. (1990). A thiosulfate shunt in the sulfur cycle of marine sediments. *Science, 249*(4965), pp.152-155.

[58] Jørgensen, B. B., & Bak, F. (1991). Pathways and microbiology of thiosulfate transformations and sulfate reduction in a marine sediment (Kattegat, Denmark). *Applied and Environmental Microbiology, 57*(3), pp.847-856.

[59] Jørgensen, B. B., & Nelson, D. C. (2004). Sulfide oxidation in marine sediments: geochemistry meets microbiology. *Geological Society of America Special Papers, 379*, pp.63-81.

[60] Kuenen, J. G. (1999). Oxidation of inorganic compounds by chemilithotrophs. *In:* Lengeler J., Drews G.& Schlegel H.G. (Eds.), *Biology of prokaryotes*. Stuttgart, Germany: Georg Thieme, pp. 234-260.

[61] Lack, J. G., Chaudhuri, S. K., Kelly, S. D., Kemner, K. M., O'Connor, S. M., & Coates, J. D. (2002). Immobilization of radionuclides and heavy metals through anaerobic bio-oxidation of Fe(II). *Applied and Environmental Microbiology, 68*(6), pp.2704-2710. doi: 10.1128/aem.68.6.2704-2710.2002

[62] Laima, M. J. C., Girard, M. F., Vouve, F., Blanchard, G. F., Gouleau, D., Galois, R., & Richard, P. (1999). Distribution of adsorbed ammonium pools in two intertidal sedimentary structures, Marennes-Oleron Bay, France. *Marine Ecology Progress Series*, 182, pp.29-35. doi: 10.3354/meps182029

[63] Langmuir, D. (1997). *Aqueous Environmental Geochemistry*. New Jersey: Prentice Hall.

[64] Li, C., Yang, S., Lian, E., Wang, Q., Fan, D., & Huang, X. (in press). Chemical speciation of iron in sediments from the Changjiang Estuary and East China Sea: Iron cycle and paleoenvironmental implications. *Quaternary International*. doi: http://dx.doi.org/10.1016/j.quaint.2016.07.014

[65] Lovley, D. R., & Phillips, E. J. P. (1986a). Organic-matter mineralization with reduction of ferric iron in anaerobic sediments. *Applied and Environmental Microbiology*, 51(4), pp.683-689.

[66] Lovley, D. R., & Phillips, E. J. P. (1986b). Availability of Ferric Iron for Microbial Reduction in Bottom Sediments of the Freshwater Tidal Potomac River. *Applied and Environmental Microbiology*, 52, pp.751-757.

[67] Lovley, D. R., & Phillips, E. J. P. (1987). Rapid assay for microbially reducible ferric iron in aquatic sediments. *Applied and Environmental Microbiology, 53*(7), pp.1536-1540.

[68] Lovley, D. R. (1991). Dissimilatory Fe(III) and Mn(IV) reduction. *Microbiological Reviews, 55*(2), pp.259-287.

[69] Middelburg, J. J., & Herman, P. M. J. (2007). Organic matter processing in tidal estuaries. *Marine Chemistry*, 106(1-2), pp.127-147. doi: 10.1016/j.marchem.2006.02.007

[70] Mitchell, S. B., West, R.J., Arundale, A.M.W., Guymer, I., Couperthwaite, J.S. . (1998). Dynamic of the Turbidity Maxima in the Upper Humber Estuary System, UK. *Marine Pollution Bulletin, 37*, pp.190-205.

[71] Monterroso, P., Pato, P., Pereira, M. E., Millward, G. E., Vale, C., & Duarte, A. (2007). Metal-contaminated sediments in a semi-closed basin: Implications for recovery. *Estuarine, Coastal and Shelf Science*, 71(1), pp.148-158. doi: http://dx.doi.org/10.1016/j.ecss.2006.07.005

[72] Mortimer, R. J. G., Krom, M. D., Watson, P. G., Frickers, P. E., Davey, J. T., & Clifton, R. J. (1998). Sediment-water exchange of nutrients in the intertidal zone of the Humber Estuary, UK. *Marine Pollution Bulletin, 37*(3-7), pp.261-279. doi: 10.1016/s0025-326x(99)00053-3

[73] Mortimer, R. J. G., Harris, S. J., Krom, M. D., Freitag, T. E., Prosser, J. I., Barnes, J., Anschutz, P., Hayes, P. J., & Davies, I. M. (2004). Anoxic nitrification in marine sediments. *Marine Ecology Progress Series, 276*, 37-51. doi: 10.3354/meps276037

[74] Nedwell, D. B., Jickells, T. D., Trimmer, M., & Sanders, R. (1999). Nutrients in estuaries. *In:* Nedwell D. B. & Raffaelli D. G. (Eds.), *Advances in Ecological Research, Estuaries.* San Diego: Academic Press, pp.43-92.

[75] NRA. (1993a). *The Quality of the Humber Estuary (1980-1990).* Newcastle upon Tyne: National Rivers Authority.

[76] NRA. (1993b). *The water quality of the Humber Estuary 1992: a report from the Humber Estuary Commitee*. (Report of the Humber Estuary Committee of the National Rivers Authority). Bristol: National Rivers Authority. Retrieved from http://ea-lit.freshwaterlife.org/archive/ealit:3122.

[77] NRA. (1995). *Sea Vigil Water Quality Monitoring : the Humber Estuary 1992-1993*. Peterborough: National Rivers Authority Anglian Region. Retrieved from http://www.environmentdata.org/archive/ealit:2851.

[78] NRA. (1996). *Sea Vigil Water Quality Monitoring: The Humber Estuary 1994*. Peterborough: National Rivers Authority Anglian Region. Retrieved from http://www.environmentdata.org/archive/ealit:2868.

[79] Perillo, G. M. E. (1995). Definitions and geomorphic classifications of estuaries. *In:* Perillo G.M.E. (Ed.), *Geomorphology and Sedimentology of Estuaries. Developments in Sedimentology*. New York: Elsevier Science, pp.17-47.

[80] Pethick, J. S. (1990). The Humber Estuary. *In* Ellis S. and Crowther, D.R. (Eds.), *Humber Perspectives, A region through the ages*. Hull: Hull University, pp.54-67.

[81] Plummer, D. H., Owens, N. J. P., & Herbert, R. A. (1987). Bacteria particle interactions in turbid estuarine environments *Continental Shelf Research, 7*(11-12), 1429-1433. doi: 10.1016/0278-4343(87)90050-1

[82] Postma, D., & Jakobsen, R. (1996). Redox zonation: Equilibrium constraints on the Fe(III)/SO_4-reduction interface. *Geochimica et Cosmochimica Acta, 60*(17), pp.3169-3175. doi: 10.1016/0016-7037(96)00156-1

[83] Poulton, S. W., & Raiswell, R. (2005). Chemical and physical characteristics of iron oxides in riverine and glacial meltwater sediments. *Chemical Geology*, 218(3-4), pp.203-221. doi: 10.1016/j.chemgeo.2005.01.007

[84] Rauret, G., Rubio, R., & López-Sánchez, J. F. (1989). Optimization of Tessier Procedure for Metal Solid Speciation in River Sediments. *International Journal of Environmental Analytical Chemistry, 36*(2), pp.69-83. doi: 10.1080/03067318908026859

[85] Roberts, K. L., Eate, V. M., Eyre, B. D., Holland, D. P., & Cook, P. L. M. (2012). Hypoxic events stimulate nitrogen recycling in a shallow salt-wedge estuary: The Yarra River estuary, Australia. *Limnology and Oceanography, 57*(5), pp.1427-1442. doi: 10.4319/lo.2012.57.5.1427

[86] Roberts, K. L., Kessler, A. J., Grace, M. R., & Cook, P. M. L. (2014). Increased rates of dissimilatory nitrate reduction to ammonium (DNRA) under oxic conditions in a periodically hypoxic estuary. *Geochimica et Cosmochimica Acta*. 133, pp.313-324. doi: . doi: https://doi.org/10.1016/j.gca.2014.02.042

[87] Robertson, E. K., Roberts, K. L., Burdorf, L. D. W., Cook, P., & Thamdrup, B. (2016). Dissimilatory nitrate reduction to ammonium coupled to Fe(II) oxidation in sediments of a periodically hypoxic estuary. *Limnology and Oceanography, 61*(1), pp.365-381. doi: 10.1002/lno.10220

[88] Rosenfeld, J. K. (1979). Ammonium adsorption in nearshore anoxic sediments. *Limnology and Oceanography, 24*(2), pp.356-364. doi: 10.4319/lo.1979.24.2.0356

[89] Rutting, T., Boeckx, P., Muller, C., & Klemedtsson, L. (2011). Assessment of the importance of dissimilatory nitrate reduction to ammonium for the terrestrial nitrogen cycle. *Biogeosciences, 8*(7), pp.1779-1791. doi: 10.5194/bg-8-1779-2011

[90] Salomons, W., Derooij, N. M., Kerdijk, H., & Bril, J. (1987). Sediments as a source of contaminants. *Hydrobiologia, 149*, pp.13-30. doi: 10.1007/bf00048643

[91] Salonius, P. O., Robinson, J. B., & Chase, F. E. (1967). A comparison of autoclaved and gamma-irradiated soils as media for microbial colonization experiments. *Plant and Soil, 27*(2), pp.239. doi: 10.1007/bf01373392

[92] Sanders, R. J., Jickells, T., Malcolm, S., Brown, J., Kirkwood, D., Reeve, A., Taylor, J., Horrobin, T., & Ashcroft, C. (1997). Nutrient fluxes through the Humber estuary. *Journal of Sea Research, 37*(1-2), pp.3-23. doi: 10.1016/S1385-1101(96)00002-0

[93] Saulnier, I., & Mucci, A. (2000). Trace metal remobilization following the resuspension of estuarine sediments: Saguenay Fjord, Canada. *Applied Geochemistry, 15*(2), pp.191-210. doi: 10.1016/s0883-2927(99)00034-7

[94] Sayama, M., Risgaard-Petersen, N., Nielsen, L. P., Fossing, H., & Christensen, P. B. (2005). Impact of bacterial NO3- transport on sediment biogeochemistry. *Applied and Environmental Microbiology*, 71(11), pp.7575-7577. doi: 10.1128/aem.71.11.7575-7577.2005

[95] Shao, M. F., Zhang, T., & Fang, H. H. P. (2010). Sulfur-driven autotrophic denitrification: diversity, biochemistry, and engineering applications. *Applied Microbiology and Biotechnology*, *88*(5), pp.1027-1042. doi: 10.1007/s00253-010-2847-1

[96] Smith, S. L., & Jaffe, P. R. (1998). Modeling the transport and reaction of trace metals in water-saturated soils and sediments. *Water Resources Research, 34*(11), pp.3135-3147. doi: 10.1029/98wr02227

[97] Song, G. D., Liu, S. M., Marchant, H., Kuypers, M. M. M., & Lavik, G. (2013). Anammox, denitrification and dissimilatory nitrate reduction to ammonium in the East China Sea sediment. *Biogeosciences*, *10*(11), pp.6851-6864. doi: 10.5194/bg-10-6851-2013

[98] Sørensen, J., & Jørgensen, B. B. (1987). Early diagenesis in sediments from danish coastal waters - microbial activity and Mn-Fe-S geochemistry. *Geochimica Et Cosmochimica Acta, 51*(6), 1583-1590. doi: 10.1016/0016-7037(87)90339-5

[99] Statham, P. J. (2012). Nutrients in estuaries — An overview and the potential impacts of climate change. *Science of The Total Environment, 434*(0), 213-227. doi: http://dx.doi.org/10.1016/j.scitotenv.2011.09.088

[100] Straub, K. L., Benz, M., Schink, B., & Widdel, F. (1996). Anaerobic, Nitrate-Dependent Microbial Oxidation of Ferrous Iron. *Applied and Environmental Microbiology, 62*(4), pp.1458–1460.

[101] Tessier, A., Campbell, P. G. C., & Bisson, M. (1979). Sequential extraction procedure for the speciation of particulate trace-metals. *Analytical Chemistry*, *51*(7), pp.844-851. doi: 10.1021/ac50043a017

[102] Thamdrup, B., Fossing, H., & Jørgensen, B. B. (1994). Manganese, iron, and sulfur cycling in a coastal marine sediment, Aarhus Bay, Denmark. *Geochimica et Cosmochimica Acta*, 58(23), pp.5115-5129. doi: 10.1016/0016-7037(94)90298-4

[103] Thamdrup, B. (2012). New Pathways and Processes in the Global Nitrogen Cycle. *Annual Review of Ecology, Evolution, and Systematics, Vol 43*, *43*, pp.407-428. doi: 10.1146/annurev-ecolsys-102710-145048

[104] Trimmer, M., Nicholls, J. C., Morley, N., Davies, C. A., & Aldridge, J. (2005). Biphasic behavior of anammox regulated by nitrite and nitrate in an estuarine sediment. *Applied and Environmental Microbiology, 71*(4), pp.1923-1930. doi: 10.1128/aem.71.4.1923-1930.2005

[105] Trimmer, M., Engstrom, P., & Thamdrup, B. (2013). Stark Contrast in Denitrification and Anammox across the Deep Norwegian Trench in the Skagerrak. *Applied and Environmental Microbiology, 79*(23), pp.7381-7389. doi: 10.1128/aem.01970-13

[106] Tyson, R. V. (1995). *Sedimentary organic matter: Organic facies and palynofacies*. London: Chapman & Hall.

[107] Uncles, R. J., Easton, A. E., Griffiths, M. L., Harris, C., Howland, R. J. M., King, R. S., Morris, A. W., & Plummer, D. H. (1998a). Seasonality of the turbidity maximum in the Humber-Ouse estuary, UK. *Marine Pollution Bulletin, 37*(3-7), pp.206-215.

[108] Uncles, R. J., Joint, I., & Stephens, J. A. (1998b). Transport and retention of suspended particulate matter and bacteria in the Humber-Ouse Estuary, United Kingdom, and their relationship to hypoxia and anoxia. *Estuaries, 21*(4A), pp.597-612. doi: 10.2307/1353298

[109] Uncles, R. J., Wood, R. G., Stephens, J. A., & Howland, R. J. M. (1998c). Estuarine nutrient fluxes to the Humber coastal zone, UK, during June 1995. *Marine Pollution Bulletin, 37*(3-7), pp.225-233.

[110] Uncles, R. J., Howland, R. J. M., Easton, A. E., Griffiths, M. L., Harris, C., King, R. S., Morris, A. W., Plummer, D. H., & Woodward, E. M. S. (1999). Seasonal variability of dissolved nutrients in the Humber–Ouse Estuary, UK. *Marine Pollution Bulletin, 37*(3–7), pp.234-246. doi: http://doi.org/10.1016/S0025-326X(98)90117-5

[111] Viollier, E., Inglett, P.W., Huntrer, K., Roychoudhury, A. N., and Van Cappellen, P. (2000). The ferrozine method revised: Fe(II)/Fe(III) determination in natural waters. *Applied Geochemistry, 15*, pp.785-790.

[112] Visscher, P. T., & Stolz, J. F. (2005). Microbial mats as bioreactors: populations, processes, and products. *Palaeogeography Palaeoclimatology Palaeoecology, 219*(1-2),pp. 87-100. doi: 10.1016/j.palaeo.2004.10.016

[113] Weber, K. A., Picardal, F. W., & Roden, E. E. (2001). Microbially catalyzed nitrate-dependent oxidation of biogenic solid-phase Fe(II) compounds. *Environmental Science & Technology, 35*(8), pp.1644-1650. doi: 10.1021/es0016598

[114] Weber, K. A., Pollock, J., Cole, K. A., O'Connor, S. M., Achenbach, L. A., & Coates, J. D. (2006). Anaerobic nitrate-dependent iron(II) bio-oxidation by a novel lithoautotrophic betaproteobacterium, strain 2002. *Applied and Environmental Microbiology, 72*(1), pp.686-694. doi: 10.1128/aem.72.1.686-694.2006

[115] Zoumis, T., Schmidt, A., Grigorova, L., & Calmano, W. (2001). Contaminants in sediments: remobilisation and demobilisation. *Science of The Total Environment, 266*(1-3), pp.195-202. doi: 10.1016/s0048-9697(00)00740-3

Chapter 7
Microbial Ecology of the Humber Estuary

Executive summary

Macrotidal estuaries are highly dynamic ecosystems in which freshwater and seawater mix, and sediments are resuspended frequently. In such challenging environments, microbial communities are influenced by high spatiotemporal variability in environmental conditions (e.g. salinity, temperature, water flow, turbidity). This study investigates the microbial community structure of surface and subsurface sediments along the Humber estuary (UK) using a combination of geochemistry and amplicon sequencing of the 16S rRNA gene. The richness of operationally defined taxonomic units (OTUs) shows only a modest decreasing trend from the inner towards the outer estuary sites, whereas the numbers of common and dominant OTUs decrease seawards. Multivariate analyses indicate that water column salinity is likely the major environmental factor influencing the diversity of the bacterial community along the estuarine continuum. Strong redox transitions with depth were only observed in the mid and outer estuary, where shifts in microbial community composition between surface and subsurface sediments were indicated by multivariate analysis tools. Analysis of the regional diversity indicate that the dataset may include two potentially distinct communities, which we suggest are 1) a homogenous community which is regularly mixed and may be transported along the gradient, and is thus subjected to a wide range of salinity conditions; and 2) a separate bacterial community, indigenous to the more reducing subsurface sediments of the mid and outer mudflats of the Humber estuary, where redox transitions in the sediment profile are more abrupt.

7.1 Introduction

Estuaries are transitional environments where substantial physicochemical and biological gradients from freshwater to marine environments develop (Attrill and Rundle, 2002; Crump *et al.*, 2004; Elliott and Whitfield, 2011; Lallias *et al.*, 2015). The continuous mixing of water and sediments leads to high variability in the local physicochemical characteristics (e.g. pH, temperature, salinity, particle size,

turbidity, sulphate concentration, river flow seasonal fluctuations, etc.). This can affect the stability and composition of microbial communities along the estuarine continuum (Crump *et al.*, 1999; O'Sullivan *et al.*, 2013; Liu *et al.*, 2014; Wei *et al.*, 2016). Microbial populations play a key role in the estuarine biogeochemical processes (Federle *et al.*, 1983; Rink *et al.*, 2008). Therefore quantifying the variations in microbial communities along a salinity continuum will improve understanding of their role in these ecosystems (Bier *et al.*, 2015).

Variation in microbial community composition has been extensively studied in estuarine environments (Llobet-Brossa *et al.*, 1998; Crump *et al.*, 1999; Bowman and McCuaig, 2003; Hewson and Fuhrman, 2004; Bernhard *et al.*, 2005; Fortunato *et al.*, 2012; Liu *et al.*, 2014; Wei *et al.*, 2016). Over the past few years, the widespread availability of high-throughput sequencing techniques has led to an increase in data on microbial biodiversity that correlate microbial diversity patterns with environmental parameters (Buttigieg and Ramette, 2014; Liu *et al.*, 2014; Bier *et al.*, 2015). This raises the question of whether or not microbial diversity patterns differ from those for multicellular organisms (Telesh *et al.*, 2011; Wang *et al.*, 2011). The challenge facing microbial ecologists is that these sequencing datasets are very large and increasingly more complex, and therefore difficult to evaluate rigorously (Buttigieg and Ramette, 2014; Oulas *et al.*, 2015; Kang *et al.*, 2016). Therefore, there is no consensus on the factors controlling microbial abundance in estuarine systems, and hence there is currently no widely accepted model on bacterial diversity in estuaries (Elliott and Whitfield, 2011; Telesh *et al.*, 2013).

Salinity is the major environmental factor controlling the patterns of benthic and pelagic diversity in estuaries (Attrill, 2002; Lozupone and Knight, 2007; Elliott and Whitfield, 2011; Herlemann *et al.*, 2011; Telesh *et al.*, 2011; Lallias *et al.*, 2015). The variation in aquatic species diversity in an estuary has been traditionally explained using the Remane diagram (Remane, 1934). This conceptual model (Fig. 7.1), which was based on macrozoobenthos studies in the effectively non-tidal Baltic Sea, shows how the relative numbers of freshwater, brackish and marine species vary along a salinity gradient. It predicts that species diversity reaches a minimum (Artenminimum) in the region of 5-8 psu salinity ('the critical salinity zone'; Khlebovich, 1968) because freshwater and marine components, which potentially contain similar numbers of species, are stressed within the transitional waters. In this

region, organisms tolerant to salinity variation succeed but the less or non-tolerant organisms are likely to be absent (Elliott and Whitfield, 2011). Despite several recent modifications (Schubert *et al.*, 2011; Telesh *et al.*, 2011; Whitfield *et al.*, 2012) and critiques (Barnes, 1989; Bulger *et al.*, 1993; Attrill, 2002; Attrill and Rundle, 2002), the Remane model still retains significant limitations as a description of estuarine systems, especially since it is not applicable to phytoplankton and bacteria (Crump *et al.*, 1999; Hewson and Fuhrman, 2004).

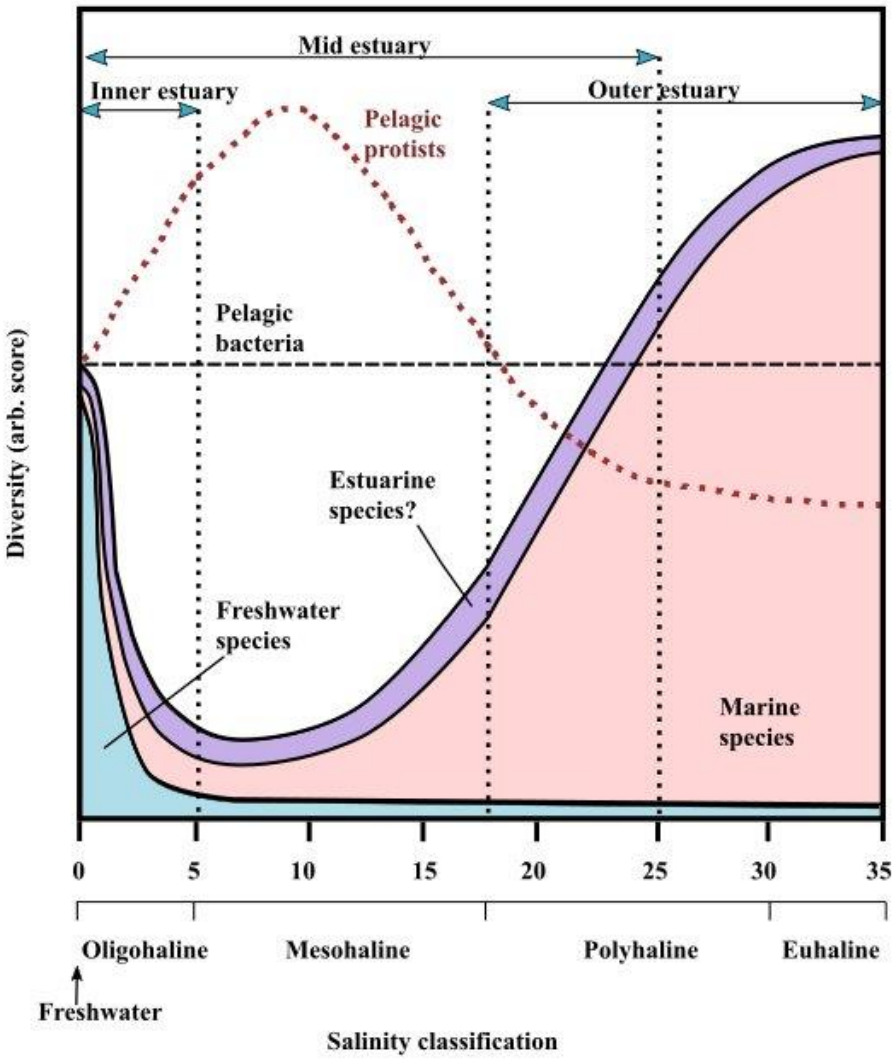

Figure 7.1: Remane's conceptual model for the variation in macrobenthic biodiversity along a salinity gradient (after Whitfield *et al.*, 2012). Observed variations the diversity of pelagic protists (Telesh *et al.*, 2011) and planktonic bacteria (Herlemann *et al.*, 2011) are shown as dashed lines (dark red and black respectively). The dotted lines indicate the empirical boundaries for the salinity zonation defined for the Humber estuary (see discussion).

Telesh *et al.* (2011) conducted a meta-analysis of large data sets from previous studies in the Baltic Sea. They found that phytoplankton show a diversity maximum in a 'critical salinity zone' (5-8 psu salinity; see Fig. 7.1), which is the location of the Arthenminimum (Whitfield *et al.*, 2012). Later, Telesh *et al.* (2013) proposed that salinity changes along the Baltic Sea may create free niches in the brackish waters where there is less competition for resources and less specialists. Therefore, these authors proposed that the potential vacant niches in the brackish water can be occupied by the fast-developing, highly adaptable and fast evolving unicellular organisms (i.e. planktonic organisms that can move with the water column, and thus experience smaller salinity variations than less mobile species). Yet, Herlemann *et al.* (2011) showed that the diversity of pelagic bacteria expressed in terms of operationally defined taxonomic groups (OTUs) displayed a steady distribution in the Baltic Sea with no trend with salinity (Fig. 7.1); although this does not preclude there being niches for specialist bacteria along the salinity gradient.

It is widely accepted that microbial communities are sensitive to environmental change (Lozupone and Knight, 2007; Sun *et al.*, 2012; Jeffries *et al.*, 2016), and thus the large salinity variations that occur in some areas of tidal estuaries might be expected to impact upon community composition, activity and diversity (Bernhard *et al.*, 2005; Feng *et al.*, 2009; Liu *et al.*, 2014; Wang *et al.*, 2015; Wei *et al.*, 2016). Vertical stratification of sediment geochemistry will also influence in the composition and function of microbial communities (Hewson and Fuhrman, 2006; Canfield and Thamdrup, 2009). However, sediments in tidal estuaries are frequently disturbed and thus may not exhibit clear links between geochemical zones and bacterial communities present, particularly as geochemical profiles tend to re-establish more quickly than diversity profiles within the sediments (O'Sullivan *et al.*, 2013). Furthermore, sediment resuspension facilitates the interaction and mixing of microbial assemblages between water and shallow sediments (Crump *et al.*, 1999; Hewson *et al.*, 2007; Feng *et al.*, 2009). Thus sediment dynamics may also be an important environmental factor shaping estuarine microbial diversity.

This study presents the first systematic study of benthic microbial diversity in the Humber estuary (UK) using high-throughput sequencing. Samples were recovered from along the north bank of the estuary at two depths; surface sediments (0-1 cm) that are frequency mobilised on the tidal cycle; and subsurface sediments (5-10 cm)

that are only mobilised by seasonal storms (typically medium/moderate resuspension events occur once or twice a year in the Humber; Mortimer *et al.*, 1998). Bacterial DNA was extracted and characterised using a metabarcoding approach for amplicon sequencing of the V4 hyper-variable region of the 16S rRNA gene on an Illumina MiSeq platform. The distribution of the microbial community along the estuarine continuum and within the sediment profile was determined; and the benthic community structure was correlated with geochemical data using multivariate statistics in order to identify the environmental drivers controlling these microbial diversity patterns.

7.2 Material and Methods

7.2.1 Sampling location

The Humber Estuary (UK) is situated on the east coast of northern England and drains an urbanised catchment with an industrial and mining history (see Fig. 2.6 and 3.1). It is a highly turbid and well-mixed macrotidal estuary, with a tidal range that can reach ~6 m at spring tides (Pethick, 1990). Its catchment area is 24,240 km^2 (20% of the area of England), it has 150 km^2 of mudflats, and nominally it is 60 km in length measured from Trent Falls, the confluence of the main tributaries, the Ouse and the Trent, to the mouth of the estuary at Spurn Head. However the region of freshwater-saltwater mixing stretches inland to Naburn Weir on the Ouse, and Cromwell weir on the Trent. The Humber represents the main UK freshwater input to the North Sea. The estuarine turbidity maximum (3000 mg L^{-1} silt in suspension), moves seasonally with the river flow but it is situated at the inner estuary (Uncles *et al.*, 1998a). Although turbidity has a strong seasonal variability, it often limits pelagic primary production throughout the estuary system (Mortimer *et al.*, 1998; Uncles *et al.*, 2006).

7.2.2 Sample collection

Sediment samples were collected at low tide from the intertidal mudflats along the north bank of the Humber Estuary during the same tidal cycle on 15th July 2014. The four sites were at Boothferry (S1), Blacktoft (S2), Paull (S3), and Skeffling (S4), and they were selected to cover different estuarine environments along the salinity continuum. A sample of surface (s) (0-1 cm) and subsurface (d) (5-10 cm) sediment

were recovered from each location, transported back to the laboratory and subsamples were stored in 2 mL microcentrifuge tubes at −20°C for subsequent DNA extraction. River water pH, conductivity and temperature were determined in the field using a Myron Ultrameter PsiII handheld multimeter. Porewater was recovered from sediments by centrifugation (30 min, 6000 *g*) in the laboratory. All water and porewater samples were filtered (0.2µm Minisart®) and stored accordingly at 4 or −20°C for further analysis. Nutrient concentrations in water were measured by ion chromatography (IC) (nitrate, nitrite, sulphate, and chloride) and colorimetrically (ammonium) on a continuous segmented flow analyser (SEAL AutoAnalyser 3 HR). Dissolved Mn (for other trace elements, see Table 4.4) were determined after acidification with 1 % v/v AnalaR HNO_3 (VWR) using ICP-MS (Thermo Scientific ™ ICP-MS). Solids were analysed for: particle size by laser diffraction on a Malvern Mastersizer 2000E; extractable iron (Lovley and Phillips, 1987; Viollier *et al.*, 2000); AVS (Canfield *et al.*, 1986); pyrite (Fossing and Jørgensen, 1989); and TOC (after HCl 10% v/v treatment) by combustion with non-dispersive infrared detection on a LECO SC-144DR Sulphur and Carbon Analyser.

7.2.3 DNA extraction and sequencing of the V4 hyper−variable region of the 16S rRNA gene

Bacterial DNA was extracted from environmental samples (~0.5 g of wet sediment) using a FastDNA spin kit for soils (MP Biomedicals, USA). DNA fragments larger than 3 kb were isolated on a 1% agarose "1x" Tris-borate-EDTA (TBE) gel stained with ethidium bromide for viewing under UV light (10x TBE solution supplied by Invitrogen Ltd., UK). The DNA was extracted from the gel using a QIAquick gel extraction kit (QIAGEN Ltd, UK); final elution was by 1/10th strength elution buffer (unless explicitly stated, the manufacturer's protocols supplied with all kits employed were followed precisely). DNA concentration was quantified fluorometrically using a Qubit dsDNA HS Assay (Thermo Fisher Scientific Inc., USA).

DNA samples (1ng/µL in 20 µL aqueous solution) were sent for sequencing at the Centre for Genomic Research, University of Liverpool, where Illumina TruSeq adapters and indices were attached to DNA fragments in a two-step PCR amplification that targets hyper-variable V4 region of the 16S rRNA gene (Caporaso

et al., 2011). Pooled amplicons were paired-end sequenced on the Illumina MiSeq platform (2x250 bp) generating ~12M clusters of data. Illumina adapter sequences were removed, and the trimmed reads were processed using the UPARSE pipeline (Edgar, 2013) within the USEARCH software package (version 8.1.1861) (Edgar, 2010) on a Linux platform. First of all, overlapping paired-end reads were assembled using the *fastq_mergepairs* command. Then the reads from single environmental samples were quality-filtered, relabelled, and de-replicated before they were randomly sub-sampled (500,000 paired-end reads with an average length of 296 bp) to produce a manageable sample size for combined analysis (~4M reads). After further de-replication of the combined pool of reads, clustering, chimera filtering and singletons removal were performed simultaneously within the pipeline by using the *cluster_otus* command. Operationally taxonomic units (OTUs) were defined based on a minimum sequence identity of 97% between the putative OTU members. The *utax* command was applied to assign to them a taxonomic group using a confidence value of 0.7 to give a reasonable trade-off between sensitivity and error rate in the taxonomy prediction. The entire dataset (~6M paired-end reads) was then allocated to the OTUs using the *usearch_global* command and the results were reported in an OTU-table, with the OTU-abundance data and the taxonomy annotation for each OTU. Sequence reads were uploaded to the National Center for Biotechnology Information (NCBI), Sequence Read Archive (SRA) (https://www.ncbi.nlm.nih.gov/sra/?term=SRP105158).

7.2.4 Community composition and statistical analysis

Traditional estimates of bacterial diversity can be distorted by rare taxa because these can be a small proportion of the bacteria population, but a large proportion of species present, so Hill numbers, D_q, will be used in this study to evaluate diversity (Hill, 1973; Jost, 2006). Hill numbers define biodiversity as the reciprocal mean of proportional abundance, and compensate for the disproportionate impact of rare taxa by weighting taxa based on abundance (see Appendix E; Hill, 1973; Jost, 2006, 2007; Kang *et al.*, 2016). The degree of weighting D_q is controlled by the index q (increasing q places progressively more weight on the high-abundance species within a population). The unweighted Hill number, D_0, is exactly equivalent to the species richness. D_1 is a measure of the number of common species and is equivalent to the exponential of Shannon entropy; and D_2 is a measure of the

number of dominant species and is equivalent to the inverse of Simpson concentration (Hill, 1973; Jost, 2006, 2007).

A heat map of OTU abundance was generated in Rstudio v 0.99.486 (RStudio Team, 2015) (see figure in Appendix E.4). The OTU diversity in each individual sample (alpha-diversity, D_q^{α}) was evaluated with different weightings on the high-abundance species (D_0^{α}, D_1^{α}, D_2^{α}). The regional OTU diversity (gamma-diversity, D_1^{γ}) was calculated using the combined dataset (more information in Appendix E). The beta-diversity, D_1^{β} (which reflects the proportion of regional diversity contained in a single average community), was calculated from the gamma diversity and the statistically weighed alpha-diversity ($*D_1^{\alpha}$; Jost 2007) using Whittaker multiplicative law ($*D_1^{\alpha} \times D_1^{\beta} = D_1^{\gamma}$) (Whittaker, 1972). Additionally, beta-diversity was analysed using compositional dissimilarities between two different samples (Bray-Curtis dissimilarity) in PAST software (https://folk.uio.no/ohammer/past/).

Non-metric Multi-Dimensional Scaling (NMDS) was used to graphically represent the similarity between bacterial assemblages in an optimised low-dimensional space by using Bray-Curtis dissimilarity matrix. NMDS was carried out in the package 'vegan' (Oksanen *et al.*, 2013) in RStudio (v 0.99.486) (RStudioTeam, 2015). The microbial community data were input as a matrix of the relative abundance of each OTU in each of the eight samples. CCA was also performed using the package 'vegan' (input data were the OTU relative abundances and the environmental variables). BIOENV ('biota-environment') analysis (Clarke and Ainsworth, 1993) was carried out (see Appendix E) to further investigate the relationship between the microbial populations, and the environmental variables using Spearman's rank correlation method and Bray Curtis dissimilarities. This test determines which combinations of environmental variables best explain patterns in the community composition. The environmental data used in these two tests included: salinity, major ion concentrations in the porewater, organic matter content, particle size and a range of redox indicators such as percentage of acid extractable $Fe^{2+}_{(s)}$, ammonium and dissolved Mn concentrations in porewater. The sample S3d was excluded in the CCA and BIOENV analyses.

7.3 Results

7.3.1 Environmental characteristics

The environmental variables measured in river water and sediment samples from the study sites along the salinity continuum of the Humber are summarized in Table 7.1. The surface water temperature of the Humber on the day of sampling was around 20°C. The locations chosen showed a salinity variation between the river end and the sea end of the estuary. Nitrate concentrations in the water column decreased along the estuary, and nitrate did not seem to accumulate in the porewater. Ammonium concentrations in the water column increased slightly along the continuum and were observed to accumulate in porewater, especially in the sites where more reducing sediments were found. Sulphate concentrations were correlated with salinity. The amount of iron in solids did not vary with sediment depth but increased along the estuary. The proportion of the acid extractable Fe that was Fe(II) was constant in the surface sediment, however in the subsurface sediments it increased along the estuary. Sediments of the mid and outer estuary (S3 and S4) mudflats were also finer and contained slightly more organic matter. The salinity of the porewater was slightly lower than the water column salinity in all sites with the exception of S4.

Table 7.1: Characterisation of the water column, sediment porewater and sediments at the study sites (S1-S4). Suffixes s and d refer to surface and subsurface sediments respectively.

River water				
	S1	**S2**	**S3**	**S4**
Salinity (psu)	0.4	3.5	21.6	26.1
pH	7.87	7.52	7.90	8.02
Conductivity (mS/cm)	0.7383	5.731	30.48	36.42
NO_3^- (µM)	266	250	248	24
NO_2^- (µM)	1.6	1.6	0.4	0.7
NH_4^+ (µM)	7	7	12	23
SO_4^{2-} (mM)	1	3	16	22
Cl^- (mM)	2	38	306	443

Sediment porewater								
	S1s	**S1d**	**S2s**	**S2d**	**S3s**	**S3d**	**S4s**	**S4d**
Porewater salinity	0.3	0.2	3.1	1.8	17.0	17.7	28.0	32.1
NO_3^- (µM)	36	37	17	26	66	17	78	7
NO_2^- (µM)	0.2	0.4	0.1	0.3	0.9	<DL	1.0	<DL
NH_4^+ (µM)	12	67	12	25	73	934	166	126
SO_4^{2-} (mM)	2	2	6	3	33	33	32	40
Cl^- (mM)	4	3	49	28	265	276	347	501
Fe (aq) (µM)	0.4	4.9	0.1	0.3	1.6	3.6	0.9	3.3
Mn^{2+} (aq) (µM)	3.4	82.3	5.1	49	60	0	15	62

Sediment								
	S1s	**S1d**	**S2s**	**S2d**	**S3s**	**S3d**	**S4s**	**S4d**
(%) Acid extractable $Fe^{2+}_{(s)}$	52	61	53	53	39	84	57	96
Total Fe (wt %)	2.1	2.7	2.7	2.4	3.5	4.0	4.3	3.9
%TOC	1.3	2.3	2.5	1.8	2.1	2.6	2.2	2.7
%TS	0.16	0.18	0.18	0.14	0.22	0.35	0.31	0.52
*Grain size (µm) (D_{50})	57	51	52	49	14	17	14	17

7.3.2 Structure and diversity of the bacterial community along the salinity gradient

The Illumina MiSeq run yielded >500,000 paired-end reads per sample after quality control. This dataset was randomly sampled to give exactly 500,000 reads per sample. The combined pool of 4 million reads was used to identify the characteristic OTUs in the regional dataset. A total of 3,596,003 reads in the combined pool passed the chimera check, and these were clustered into OTUs (>97% sequence identity) in the UPARSE

pipeline, and assigned to taxonomic groups. Then the entire dataset of 6,179,119 reads were allocated to these OTUs. OTUs classified as archaea (4% of non-chimeric reads), and the OTUs which were not classified to the level of bacterial phylum with a confidence >0.7 (14% of non-chimeric reads) were excluded for further analysis. This resulted in 7656 OTUs that were classified to the level of bacterial phylum with a confidence level >0.7, which were used to characterise the local and regional microbial diversity of the Humber estuary sediments.

There were 33 phyla that individually represented more than 0.1% of the population of any sample (Fig 7.2), the most abundant of which were *Proteobacteria* (51% of the reads), *Acidobacteria* (11%), *Bacteroidetes* (10%) and *Chloroflexi* (9%). OTUs classified in a phylum, which individually represented less than 0.1% (on average of the total reads) of the microbial community of a specific site were grouped as "Other phyla" in Figure 7.2. At this taxonomic level, the community structure of all the samples had a similar composition, with the exception of the sample of subsurface sediment from Paull (S3d). In this sample *Proteobacteria* were dominant, accounting for 92% of the OTUs present versus the 45% (on average) that *Proteobacteria* represented in the other sites. Overall the largest class within the phylum *Proteobacteria* was *Gammaproteobacteria*, which comprised 18% of total reads in the inner estuary to 25% of the total reads in the outer estuary, although sample S3d was dominated by *Epsilonproteobacteria* (94% of the *Proteobacteria* in S3d). *Acidobacteria* were slightly more prevalent at S1 and S2 (15% of total reads in the inner estuary) than at S3 and S4 (8% of total reads in the mid and outer estuary, excluding sample S3d). Within the *Acidobacteria,* bacteria from the class *Acidobacteria* subdivision 6 were most numerous in the inner estuary (~6% of total reads), but were 1% of total reads in the mid-outer estuary. *Bacteroidetes* were the third most abundant phylum in the estuary, representing ~9% of reads in the inner estuary, but 16% of reads in the mid-outer estuary. Within the *Bacteroidetes,* bacteria form the class *Flavobacteriia* are the most abundant in both the inner and the outer estuary (~3% and 12% of total reads). *Chloroflexi* was the fourth most abundant phylum, and it exhibited very little systematic change along the estuary. The most abundant classes within the *Chloroflexi* were *Caldilinea* and *Anaerolineae* (~3% and 2% of total reads from the whole estuary).

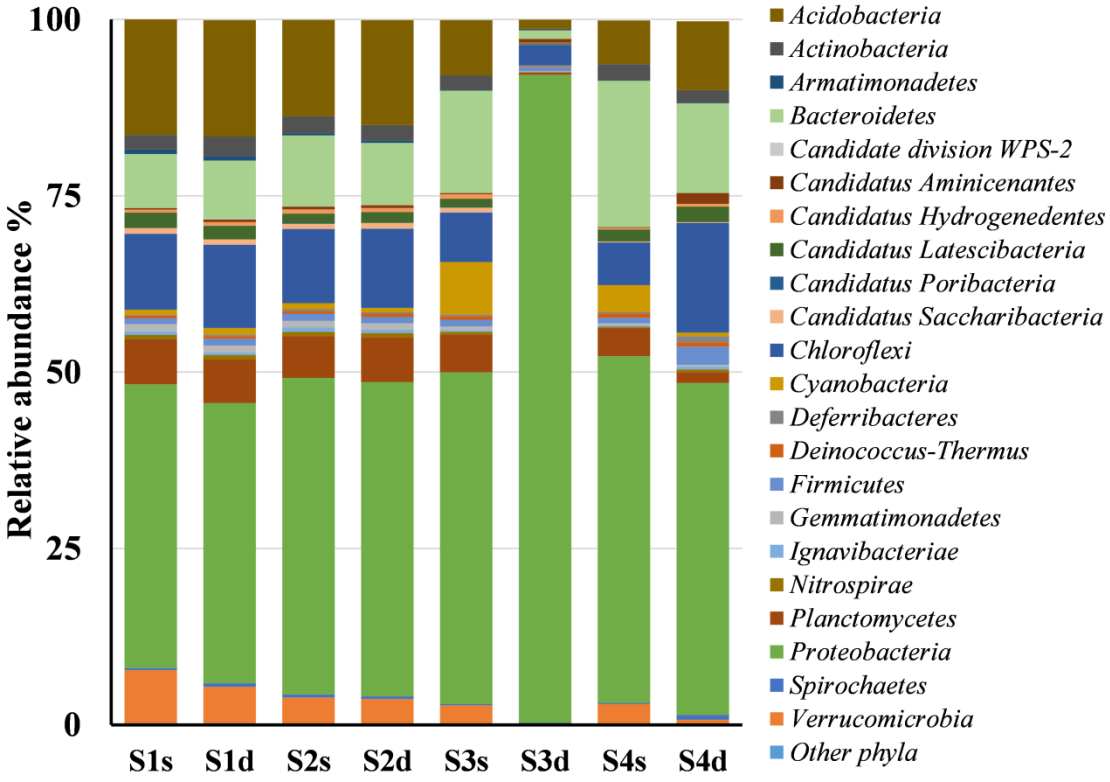

Figure 7.2: Taxonomic distribution of the bacterial community at phylum level. The phyla with relative abundance below 0.1% are grouped as "Other phyla".

The OTU richness, D_0^{α}, in each sample is plotted in Fig. 7.3a (richness takes no account OTU relative abundance). The average richness at the different sites and sediment depths was ~5000 OTUs; although sites towards the outer estuary showed slightly lower richness. Diversity measurements that indicate the number of common OTUs (D_1^{α}) and dominant OTUs (D_2^{α}) showed a different pattern (Fig. 7.3b and 7.3c). Both D_1^{α} and D_2^{α} revealed a general decreasing trend for OTU diversity along the salinity gradient. Between the innermost and outermost estuary samples (S1 and S4) there was a drop in both D_1^{α} and D_2^{α} for the surface and the subsurface sediments by 60-70%. For comparative purposes, the OTUs in each sample were ranked by number of reads, and D_1^{α} was used to identify the common OTUs thus defined. Common OTUs accounted for >80% of total sequence reads in all samples, and dominant OTUs account for ~60% of total reads (excluding Sd3). Therefore the decrease in the number of common and dominant OTUs along the estuary represents a shift towards fewer but more abundant

OTUs towards the sea. The statistically weighted alpha-diversity (${}^{*}D_1^{\alpha}$) was 438; the regional diversity (D_1^{γ}) was 934; which following Whittaker's multiplicative law, ($D_1^{\beta}=D_1^{\gamma}/{}^{*}D_1^{\alpha}$), gives a beta component (D_1^{β}) of 2.

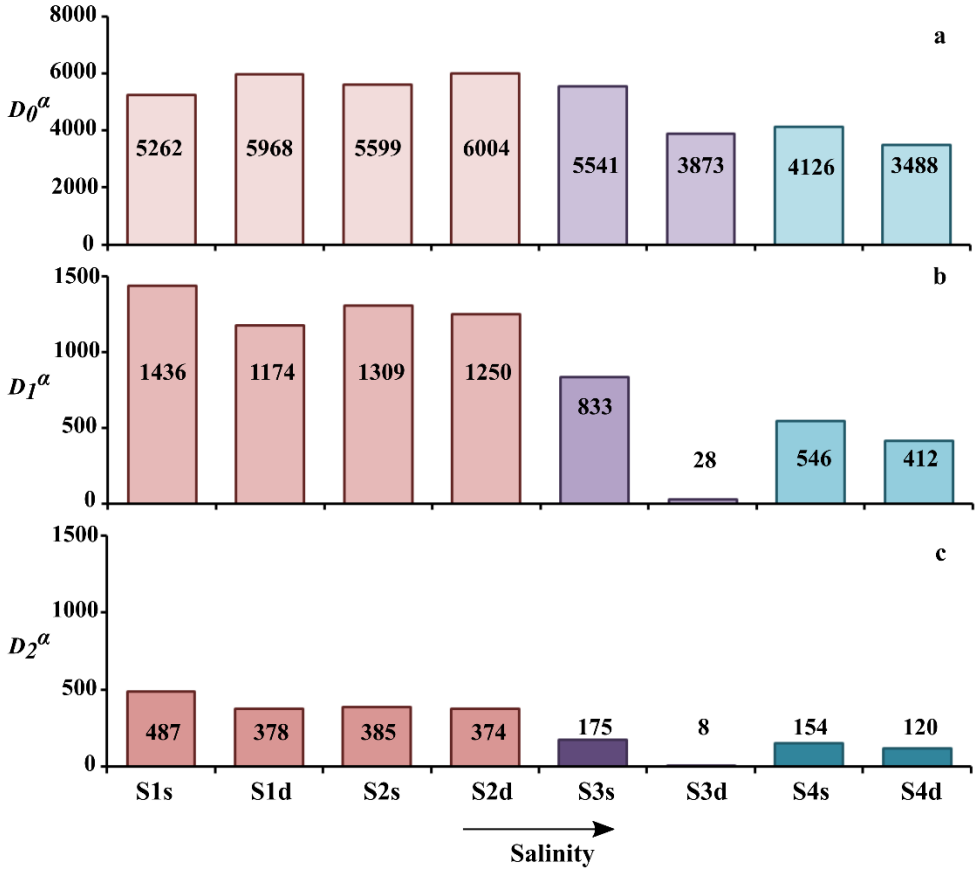

Figure 7.3: Alpha-diversity D_q^{α} measurements: (a) D_0^{α} or OTUs richness; (b) D_1^{α} exponential of Shannon entropy; and (c) D_2^{α} or inverse of Simpson concentration for each location (see more information in Appendix E).

In the two-dimensional NMDS representation of species frequencies in the eight samples (Fig. 7.4), the inner estuary sites (S1 and S2) in a relatively close group ("inner estuary cluster", dashed ellipse in Fig. 7.4) without a clear depth trend and only small separation between the two sites (average Bray-Curtis dissimilarity within this group was 24%). The S3 and S4 bacterial populations fall progressively further from the inner estuary cluster without clear cluster amongst them, and with a significant distance between the surface (S3s and S4s) and subsurface (S3d and S4d) samples. For example the bacterial populations of S3d is approximately equidistant from that of the surface sample from the

same location (S3s) and the inner estuary cluster (the Bray-Curtis dissimilarity is ~90% in both cases). NMDS is a robust indirect gradient analysis approach which produces an optimised ordination based on a distance or dissimilarity matrix, and does not take absolute distances into account. However the NMDS analysis suggests that, within the context of the Humber estuary, the bacterial populations of all the inner estuary samples are similar, but that progression towards the outer estuary causes a shift in the bacterial community.

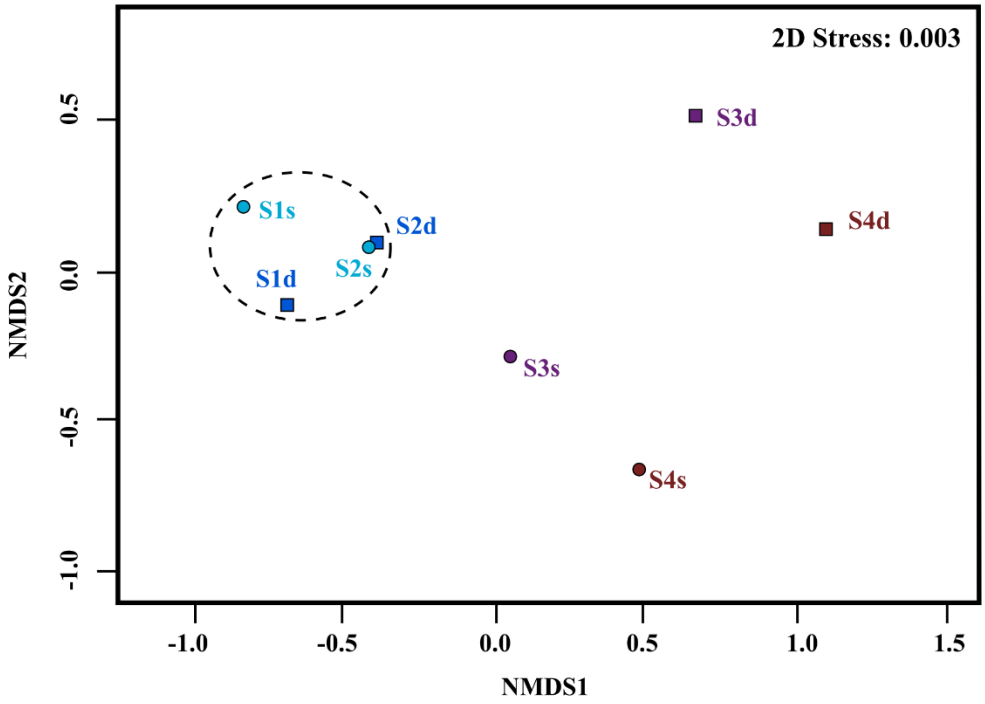

Figure 7.4: Two-dimensional non-metric multidimensional scaling (NMDS) ordination for differences in the bacterial community distribution based on Bray-Curtis distances of the community (OTUs) by site/sample matrix. The stress value associated with these two dimensional representation is <0.05 which suggest a good fit of the data.

In the CCA analysis salinity and the presence of FeS-rich sediments seem to split the inner estuary (S1 and S2) from the mid- and outer estuary S3 and S4 samples (Fig 7.5). The BIOENV analysis showed that salinity and sulphate concentration in porewater were the subset of environmental variables that best correlated (0.96) with the community composition of the different sites along the Humber estuary (Mantel statistic for the

correlation of the matrices, r=0.88, p<0.05) (see Appendix E). The sample S3d was excluded in the CCA and BIOENV tests because the significant differences in the microbial community composition were disproportionately influencing the ordination plots masking patterns in the remaining dataset.

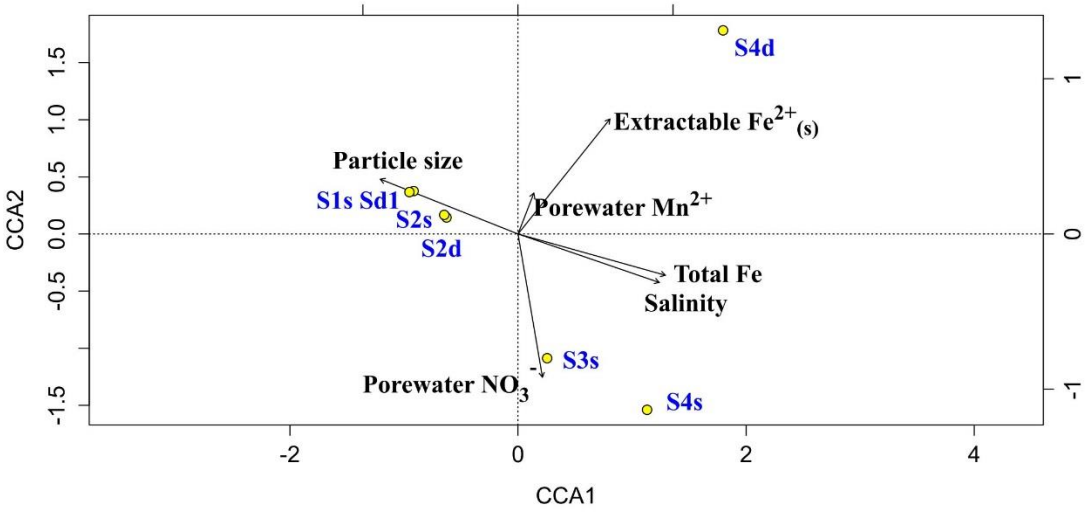

Figure 7.5: Environmental vectors in the CCA for the Humber estuary bacterial community (relative abundance data). Sample S3d was omitted from this analysis to show patterns in the remaining dataset. Arrows indicate the direction of the environmental gradients. Yellow dots represent the ordination of the samples/sites.

7.4 Discussion

The Humber estuary is a shallow well-mixed estuary. This type of estuary is characterised by water mixing that is strongly driven by tidal forcing. Surface and subsurface sediments in the Humber are both subjected to reoxidation processes due to resuspension, albeit at different frequencies. Additionally, the spatial heterogeneity of nutrient concentrations and the patterns of movement of the turbidity maxima within the Humber are influenced by seasonal variations of river flow (Sanders *et al.*, 1997; Mitchell, 1998; Uncles *et al.*, 1998a). Concentrations of nitrate decrease in the water column towards the outer estuary, while sulphate becomes a more important species as seawater has more influence on the water column composition. The sediments recovered from the mudflats of the mid and outer estuarine show some iron enrichment compared to

the sites from the inner estuary (Table 7.1 and Table 4.3). Field observations of sample colour at the outer estuary sites (reddish-brown at the surface but dark grey-black in the subsurface), the amounts of Fe and NH_4^+ in the pore fluid, and the proportion of acid extractable Fe that is Fe(II), taken together evidence an abrupt redoxcline at these sites (others report that the subsurface sediments of the outer estuary mudflats can be sulfidic; Mortimer *et al.*, 1998; Andrews *et al.*, 2000). Such an abrupt redox change with depth was not seen at the inner estuary sites, where the subsurface sediments appear to be poised between nitrate and iron reducing conditions. These underlying environmental gradients likely shape the spatial distribution of the bacterial communities in estuaries (Crump *et al.*, 2004; Fortunato *et al.*, 2012; O'Sullivan *et al.*, 2013; Liu *et al.*, 2014; Jeffries *et al.*, 2016).

Salinity has been shown to be a critical factor in shaping bacterial diversity patterns in estuarine systems (Bernhard *et al.*, 2005; Lozupone and Knight, 2007; Herlemann *et al.*, 2011; Liu *et al.*, 2014; Lallias *et al.*, 2015). Therefore Humber water column salinity records from 14 locations over a period of ~25 years have been collated (Fig. 7.6) to provide a proxy for the salinity range experienced by surficial sediments. Deeper sediment pore water salinity will vary more slowly than river water salinity and probably remains close to the long term average of river water salinity at that location (pore water salinity values, calculated from chlorine concentrations, are also plotted on Fig.7.6). As a result, three salinity zones have been empirically identified. Firstly, the inner estuary extends from 0 to 60 km below Naburn weir (the tidal limit of the Ouse system) where the water column salinity is always ≤5 psu (blue area in Fig.7.6, see also annotation in Fig. 7.1). Depending on the river flow and state of the tide, the inner estuary water would be described as freshwater (0 psu) or oligohaline (≤5 psu). Secondly, the middle estuary extends from 60 to 100 km downstream of Naburn weir, and in this zone the water column salinity ranges between 0 to ~25 psu (purple area in Fig 7.6, see annotation in Fig. 7.1). This range in the mid estuary includes oligohaline, mesohaline and polyhaline waters. Finally the outer estuary extends from 100 km below Naburn weir to open coastal waters. Here the water column typically varies from ~18 psu salinity to seawater (35 psu) (pink area in Fig 7.6, see annotation in Fig 7.1), which includes polyhaline to euhaline

waters. Based on this subdivision of the Humber estuary, sites S1 and S2 are in the inner estuary, site S3 is in the mid estuary, and site S4 is in the outer estuary.

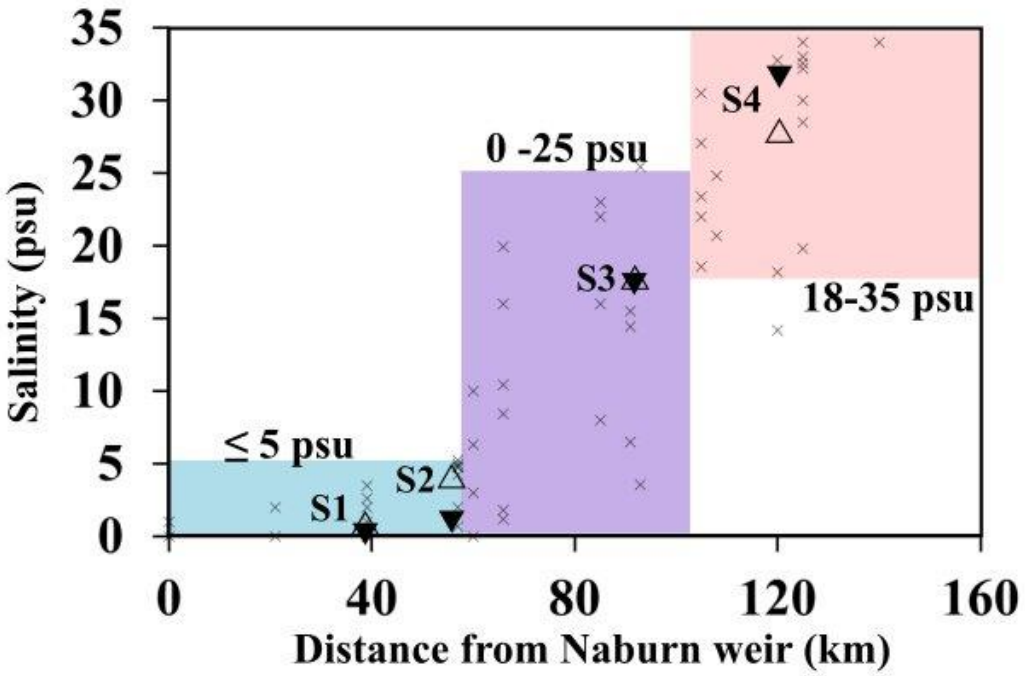

Figure 7.6: Salinity records of different sites along the Humber estuary (x markers) (Freestone, 1987; Prastka & Malcolm, 1994; NRA, 1995, 1996; Sanders *et al.*, 1997; Barnes & Owens, 1998; Mitchell, 1998; Uncles *et al.*, 1998b; Mortimer *et al.*, 1999; Williams & Millward, 1999; ABP Research 2000; Millward *et al.*, 2002; Burke *et al.*, 2005; Uncles *et al.*, 2006; Fujii & Raffaelli, 2008; Garcia-Alonso *et al.*, 2011). The triangle markers indicate the porewater salinity measurements made for this study (S1-S4) (empty and coloured markers for surface and subsurface porewater salinity respectively). The blue area: 0-60km from Naburn weir, salinity ≤5 psu; the purple area: 60-100 km from Naburn weir, salinity range from 0-25 psu; and the pink area: 100-160 km from Naburn weir, salinity range from 18-35 psu.

Macroscopic species richness usually has a minimum in areas of estuarine systems that undergo high salinity variation (Whitfield *et al.*, 2012). Whereas Telesh *et al.* (2011) found that phytoplankton richness reached a maximum in this 'critical salinity zone'. This study found that bacterial OTU richness, D_0^{α}, was relatively uniform along the Humber estuary (Fig. 7.3a), which conforms to previous reports of uniform richness along a salinity gradient (Herlemann *et al.*, 2011). However the hyperdiverse nature of microorganisms in many ecosystems means that richness can give a distorted view of

microbial diversity because it gives equal weight to common and rare taxa. Also it is rarely possible to evaluate richness accurately, as it is extremely difficult adequately sample rare taxa even with high-throughput sequencing technologies (Kang *et al.*, 2016). Hill numbers of higher order (q = 1 or 2) are a better mathematical approach to microbial diversity that give consistent measures of the prominence of common or dominant species in a community that are not sensitive to the depth of sequencing (Kang *et al.*, 2016).

In the Humber ${}^{1}D^{\alpha}$ and ${}^{2}D^{\alpha}$ (Fig 7.3b and 7.3c) revealed that the number of common and dominant OTUs in the outer estuary samples were only about 40% and 35% the average in the inner estuary. This indicates a change towards a community structure with a smaller number of more abundant OTUs along the estuarine salinity gradient. Generally Site 3, which is situated in the area of highest salinity variation (purple area in Fig. 7.6), fitted this trend. The surface sample (S3s) had ${}^{1}D^{\alpha}$ and ${}^{2}D^{\alpha}$ values that were intermediate between the inner and outer estuary values, which is not surprising given the regular resuspension and mixing processes of surface sediments by tidal forces. The subsurface sample (S3d) had lower ${}^{1}D^{\alpha}$ and ${}^{2}D^{\alpha}$ values than any other sample analysed. This may be associated with salinity stress, but it is likely that some other environmental pressure had produced a specialist niche that favours just a few bacterial species at this location (bacterial DNA was extracted from <0.5 g of sediment, and thus very local geochemical effects can affect the bacterial community within individual samples).

The NMDS and CCA analyses clustered the inner estuary samples together. Whilst distance on both these plots is comparative, and the relationship between distance and dissimilarity is not linear on the NMDS plot, when taken with the beta diversity across all the samples (${}^{1}D^{\beta} \sim 2$), it suggests that the communities of the inner estuary sediments (in terms of common species) are similar. The colour pattern in the heat map (see Appendix E) also showed these samples as being similar in their composition. Furthermore, the NMDS and CCA analyses also separated the subsurface mid and outer estuary samples from their surface counterparts. Field observations and geochemical measurements indicated that these samples were more reducing than the other samples. Estuarine surface sediments are mobilized on tidal timescales, whereas subsurface sediments will

be disrupted less frequently. These differences on remobilization timescales will depend on the location and the magnitude of the resuspension event, but any such remobilization will impact on sediment redox state. For this reason, stronger redox stratification would be expected in the less-frequently disturbed subsurface sediments of the outer estuary, which may provide the geochemical conditions for more specialist communities to develop.

Taxonomically, all samples with the exception of S3d showed a similar composition. *Proteobacteria* was the most represented phylum in all the bacterial communities, followed by *Acidobacteria*, *Bacteroidetes* and *Chloroflexi*. This distribution of phyla is consistent with other studies in coastal and estuarine sediments (Wang *et al.*, 2012; Halliday *et al.*, 2014; Liu *et al.*, 2014; Jeffries *et al.*, 2016; Wei *et al.*, 2016). *Gammaproteobacteria* were the most represented class within the *Proteobacteria* in most of the samples (as was observed in these previous studies), but the bacterial community of sample S3d was dominated *Epsilonproteobacteria*. *Epsilonproteobacteria* have been found in other estuarine and coastal sediments, and pelagic redoxclines (Labrenz *et al.*, 2005; Campbell *et al.*, 2006; Grote *et al.*, 2008; Bruckner *et al.*, 2013; Jeffries *et al.*, 2016), and are occasionally abundant (Wang *et al.*, 2012). Many *Epsilonproteobacteria* within the order of *Campylobacterales* (the most important class of *Epsilonproteobacteria* in sample S3d) are microaerophilic chemolitotrophs that can couple the oxidation of sulphur compounds or hydrogen to the reduction of oxygen or nitrate (Labrenz *et al.*, 2005; Campbell *et al.*, 2006; Grote *et al.*, 2008; Bruckner *et al.*, 2013). It has even been suggested that *Epsilonproteobacteria* could be one of the dominant microorganisms involved in the coupling of C, N and S cycles (Campbell *et al.*, 2006). Thus the dominance of *Epsilonproteobacteria* in sample S3d may be related to the S-reducing conditions found in subsurface sediments of the outer Humber estuary.

The regional microbial diversity of the Humber estuary (D_1^{γ} = 934) indicates that many of the OTUs that are common in individual samples are common within regional dataset. Further, the beta-diversity calculated for common species (D_1^{β} ~ 2) indicates that the regional diversity can be explained by there being two distinct compositional groups dispersed amongst the various local communities. The first of these compositional units

may be a community that is subjected to remobilisation and is regularly mixed and transported along the estuary, but is stressed by the varying salinity conditions (in frequently disturbed estuarine sediments there is less of a direct link between the geochemistry and the bacterial assemblages present; O'Sullivan *et al.*, 2013). The second compositional unit may develop in the more strongly reducing and less frequently disturbed subsurface sediments of the mid and outer estuary mudflats.

7.5 Conclusions

Overall, this study has provide the first insight to the microbial diversity of the Humber estuary. The large amount of data produced by using high throughput sequencing technologies resulted in a deep coverage of the individual samples. A taxonomic approach to the community data did not show clear differences between sampling sites. Similarly OTU richness, D_0^{α}, was relatively uniform in the estuary. However Hill numbers of higher order (D_1^{α} and D_2^{α}) decreased towards the sea, which indicates a change towards communities where a smaller number of OTUs represent a larger proportion of the population. Discovery of this trend illustrates the importance of using a rigorous and consistent mathematically approach to characterise bacterial diversity, particularly when working with amplicon sequencing data. Beyond salinity variation, there was some evidence that redox transitions with depth may apply further selective pressure on the microbial populations of the mid and outer mudflats. To conclude, salinity seems to be the main environmental driver for diversity in the Humber estuary, but other spatiotemporal fluctuations in the physicochemical conditions (redox gradients and sediment remobilisation and mixing) will have also an impact on the bacterial community composition.

7.6 References

[1] ABP Research & Consultancy, L. (2000). Humber geomorphological studies - Stage 2: 3-D Modelling of Flows, Salinity and Sediment Transport in the Humber Estuary. Southampton.

[2] Andrews, J. E., Samways, G., Dennis, P. F., & Maher, B. A. (2000). Origin, abundance and storage of organic carbon and sulphur in the Holocene Humber Estuary: emphasizing human impact on storage changes. *Geological Society, London, Special Publications, 166*(1), pp.145-170. doi: 10.1144/gsl.sp.2000.166.01.09

[3] Attrill, M. J. (2002). A testable linear model for diversity trends in estuaries. *Journal of Animal Ecology, 71*(2), pp.262-269. doi: 10.1046/j.1365-2656.2002.00593.x

[4] Attrill, M. J., & Rundle, S. D. (2002). Ecotone or ecocline: Ecological boundaries in estuaries. *Estuarine Coastal and Shelf Science, 55*(6), pp.929-936. doi: 10.1006/ecss.2002.1036

[5] Barnes, J., & Owens, N. J. P. (1998). Denitrification and nitrous oxide concentrations in the Humber estuary, UK, and adjacent coastal zones. *Marine Pollution Bulletin, 37*(3-7), pp.247-260.

[6] Barnes, R. S. K. (1989). What, if anything, is a brackish water fauna?. *Transactions of the Royal Society of Edinburgh: Earth Sciences, 80*(3), pp.235-240. doi: 10.1017/S0263593300028674

[7] Bernhard, A. E., Colbert, D., McManus, J., & Field, K. G. (2005). Microbial community dynamics based on 16S rRNA gene profiles in a Pacific Northwest estuary and its tributaries. *FEMS Microbiology Ecology, 52*(1), pp.115-128. doi: 10.1016/j.femsec.2004.10.016

[8] Bier, R. L., Bernhardt, E. S., Boot, C. M., Graham, E. B., Hall, E. K., Lennon, J. T., Nemergut, D. R., Osborne, B. B., Ruiz-Gonzalez, C., Schimel, J. P., Waldrop, M. P., & Wallenstein, M. D. (2015). Linking microbial community structure and microbial processes: an empirical and conceptual overview. *FEMS Microbiology Ecology, 91*(10). doi: 10.1093/femsec/fiv113

[9] Bowman, J. P., & McCuaig, R. D. (2003). Biodiversity, community structural shifts, and biogeography of prokaryotes within Antarctic continental shelf sediment. *Applied and Environmental Microbiology, 69*(5), pp.2463-2483. doi: 10.1128/aem.69.5.2463-2483.2003

[10] Bruckner, C. G., Mammitzsch, K., Jost, G., Wendt, J., Labrenz, M., & Juergens, K. (2013). Chemolithoautotrophic denitrification of epsilonproteobacteria in marine pelagic redox gradients. *Environmental Microbiology, 15*(5), pp.1505-1513. doi: 10.1111/j.1462-2920.2012.02880.x

[11] Bulger, A. J., Hayden, B. P., Monaco, M. E., Nelson, D. M., & McCormickray, M. G. (1993). Biologically-based estuarine salinity zones derived from a multivariate-analysis. *Estuaries, 16*(2), pp.311-322. doi: 10.2307/1352504

[12] Burke, I. T., Boothman, C., Lloyd, J. R., Mortimer, R. J., Livens, F. R., & Morris, K. (2005). Effects of progressive anoxia on the solubility of technetium in sediments. *Environ Sci Technol, 39*(11), pp.4109-4116. doi: 10.1021/es048124p

[13] Buttigieg, P. L., & Ramette, A. (2014). A guide to statistical analysis in microbial ecology: a community-focused, living review of multivariate data analyses. *FEMS Microbiology Ecology, 90*(3), pp.543-550. doi: 10.1111/1574-6941.12437

[14] Campbell, B. J., Engel, A. S., Porter, M. L., & Takai, K. (2006). The versatile epsilon-proteobacteria: key players in sulphidic habitats. *Nature Reviews Microbiology, 4*(6), pp.458-468. doi: 10.1038/nrmicro1414

[15] Canfield, D. E., Raiswell, R., Westrich, J. T., Reaves, C. M., & Berner, R. A. (1986). The use of chromium reduction in the analysis of reduced inorganic sulfur in sediments and shales. *Chemical Geology, 54*(1-2), pp.149-155. doi: 10.1016/0009-2541(86)90078-1

[16] Canfield, D. E., & Thamdrup, B. (2009). Towards a consistent classification scheme for geochemical environments, or, why we wish the term 'suboxic' would go away. *Geobiology, 7*(4), pp.385-392. doi: 10.1111/j.1472-4669.2009.00214.x

[17] Caporaso, J. G., Lauber, C. L., Walters, W. A., Berg-Lyons, D., Lozupone, C. A., Turnbaugh, P. J., Fierer, N., & Knight, R. (2011). Global patterns of 16S rRNA diversity at a depth of millions of sequences per sample. *Proceedings of the National Academy of Sciences, 108* (Supplement 1), pp.4516-4522. doi: 10.1073/pnas.1000080107

[18] Clarke, K. R., & Ainsworth, M. (1993). A method of linking multivariate community structure to environmental variables. *Marine Ecology Progress Series, 92*(3), pp.205-219. doi: 10.3354/meps092205

[19] Crump, B. C., Armbrust, E. V., & Baross, J. A. (1999). Phylogenetic analysis of particle-attached and free-living bacterial communities in the Columbia river, its estuary, and the adjacent coastal ocean. *Applied and Environmental Microbiology, 65*(7), pp.3192-3204.

[20] Crump, B. C., Hopkinson, C. S., Sogin, M. L., & Hobbie, J. E. (2004). Microbial biogeography along an estuarine salinity gradient: Combined influences of bacterial growth and residence time. *Applied and Environmental Microbiology, 70*(3), pp.1494-1505. doi: 10.1128/aem.70.3.1494-1505.2004

[21] Edgar, R. C. (2010). Search and clustering orders of magnitude faster than BLAST. *Bioinformatics, 26*(19), pp.2460-2461. doi: 10.1093/bioinformatics/btq461

[22] Edgar, R. C. (2013). UPARSE: highly accurate OTU sequences from microbial amplicon reads. *Nature Methods, 10*(10), pp.996-1000. doi: 10.1038/nmeth.2604

[23] Elliott, M., & Whitfield, A. K. (2011). Challenging paradigms in estuarine ecology and management. *Estuarine Coastal and Shelf Science, 94*(4), pp.306-314. doi: 10.1016/j.ecss.2011.06.016

[24] Federle, T. W., Hullar, M. A., Livingston, R. J., Meeter, D. A., & White, D. C. (1983). Spatial-distribution of biochemical parameters indicating biomass and community composition of microbial assemblies in estuarine mud flat sediments. *Applied and Environmental Microbiology, 45*(1), pp.58-63.

[25] Feng, B.-W., Li, X.-R., Wang, J.-H., Hu, Z.-Y., Meng, H., Xiang, L.-Y., & Quan, Z.-X. (2009). Bacterial diversity of water and sediment in the Changjiang estuary and coastal area of the East China Sea. *FEMS Microbiology Ecology, 70*(2), pp.236-248. doi: 10.1111/j.1574-6941.2009.00772.x

[26] Fortunato, C. S., Herfort, L., Zuber, P., Baptista, A. M., & Crump, B. C. (2012). Spatial variability overwhelms seasonal patterns in bacterioplankton communities across a river to ocean gradient. *Isme Journal, 6*(3), pp.554-563. doi: 10.1038/ismej.2011.135

[27] Fossing, H., & Jørgensen, B. B. (1989). Measurement of bacterial sulfate reduction in sediments - evaluation of a single-step chromium reduction method. *Biogeochemistry, 8*(3), pp.205-222. doi: 10.1007/BF00002889

[28] Freestone, D., Jones, N., North, J.,Pethick, J., Symes, D., and Ward, R. (1987). The Humber Estuary, Environmental Background: Institute of Estuarine and Coastal Studies.

[29] Fujii, T., & Raffaelli, D. (2008). Sea-level rise, expected environmental changes, and responses of intertidal benthic macrofauna in the Humber estuary, UK. *Marine Ecology Progress Series, 371*, pp.23-35. doi: 10.3354/meps07652

[30] Garcia-Alonso, J., Greenway, G. M., Munshi, A., Gomez, J. C., Mazik, K., Knight, A. W., Hardege, J. D., & Elliott, M. (2011). Biological responses to contaminants in the Humber Estuary: Disentangling complex relationships. *Marine Environmental Research, 71*(4), pp.295-303. doi: 10.1016/j.marenvres.2011.02.004

[31] Grote, J., Jost, G., Labrenz, M., Herndl, G. J., & Juergens, K. (2008). Epsilonproteobacteria Represent the Major Portion of Chemoautotrophic Bacteria in Sulfidic Waters of Pelagic Redoxclines of the Baltic and Black Seas. *Applied and Environmental Microbiology, 74*(24), pp.7546-7551. doi: 10.1128/aem.01186-08

[32] Halliday, E., McLellan, S. L., Amaral-Zettler, L. A., Sogin, M. L., & Gast, R. J. (2014). Comparison of Bacterial Communities in Sands and Water at Beaches with Bacterial Water Quality Violations. *Plos One, 9*(3). doi: 10.1371/journal.pone.0090815

[33] Herlemann, D. P. R., Labrenz, M., Jurgens, K., Bertilsson, S., Waniek, J. J., & Andersson, A. F. (2011). Transitions in bacterial communities along the 2000 km salinity gradient of the Baltic Sea. *Isme Journal, 5*(10), pp.1571-1579. doi: 10.1038/ismej.2011.41

[34] Hewson, I., & Fuhrman, J. A. (2004). Richness and diversity of bacterioplankton species along an estuarine gradient in Moreton Bay, Australia. *Applied and Environmental Microbiology, 70*(6), pp.3425-3433. doi: 10.1128/aem.70.6.3425-3433.2004

[35] Hewson, I., & Fuhrman, J. A. (2006). Spatial and vertical biogeography of coral reef sediment bacterial and diazotroph communities. *Marine Ecology Progress Series, 306*, pp.79-86. doi: 10.3354/meps306079

[36] Hewson, I., Jacobson-Meyers, M. E., & Fuhrman, J. A. (2007). Diversity and biogeography of bacterial assemblages in surface sediments across the San Pedro Basin, Southern California Borderlands. *Environmental Microbiology, 9*(4), pp.923-933. doi: 10.1111/j.1462-2920.2006.01214.x

[37] Hill, M. O. (1973). Diversity and evenness: a unifying notation and its consequences. *Ecology, 54*(2), pp.427-432. doi: 10.2307/1934352

[38] Jeffries, T. C., Fontes, M. L. S., Harrison, D. P., Van-Dongen-Vogels, V., Eyre, B. D., Ralph, P. J., & Seymour, J. R. (2016). Bacterioplankton Dynamics within a Large Anthropogenically Impacted Urban Estuary. *Frontiers in Microbiology, 6*. doi: 10.3389/fmicb.2015.01438

[39] Jost, L. (2006). Entropy and diversity. *Oikos, 113*(2), pp.363-375. doi: 10.1111/j.2006.0030-1299.14714.x

[40] Jost, L. (2007). Partitioning diversity into independent alpha and beta components. *Ecology, 88*(10), pp.2427-2439. doi: 10.1890/06-1736.1

[41] Kang, S., Rodrigues, J. L. M., Ng, J. P., & Gentry, T. J. (2016). Hill number as a bacterial diversity measure framework with high-throughput sequence data. *Scientific Reports, 6*. doi: 10.1038/srep38263

[42] Khlebovich, V. V. (1968). Some peculiar features of the hydrochemical regime and the fauna of mesohaline waters. *Marine Biology, 2*(1), pp.47-49. doi: 0.1007/BF00351637

[43] Labrenz, M., Jost, G., Pohl, C., Beckmann, S., Martens-Habbena, W., & Jurgens, K. (2005). Impact of different in vitro electron donor/acceptor conditions on potential chemolithoautotrophic communities from marine pelagic redoxclines. *Applied and Environmental Microbiology, 71*(11), pp.6664-6672. doi: 10.1128/aem.71.11.6664-6672.2005

[44] Lallias, D., Hiddink, J. G., Fonseca, V. G., Gaspar, J. M., Sung, W., Neill, S. P., Barnes, N., Ferrero, T., Hall, N., Lambshead, P. J. D., Packer, M., Thomas, W. K., & Creer, S. (2015). Environmental metabarcoding reveals heterogeneous drivers of microbial eukaryote diversity in contrasting estuarine ecosystems. *Isme Journal, 9*(5), pp.1208-1221. doi: 10.1038/ismej.2014.213

[45] Liu, J., Yang, H., Zhao, M., & Zhang, X.-H. (2014). Spatial distribution patterns of benthic microbial communities along the Pearl Estuary, China. *Systematic and Applied Microbiology, 37*(8), pp.578-589. doi: 10.1016/j.syapm.2014.10.005

[46] Llobet-Brossa, E., Rossello-Mora, R., & Amann, R. (1998). Microbial community composition of Wadden Sea sediments as revealed by fluorescence in situ hybridization. *Applied and Environmental Microbiology, 64*(7), pp.2691-2696.

[47] Lovley, D. R., & Phillips, E. J. P. (1987). Rapid assay for microbially reducible ferric iron in aquatic sediments. *Applied and Environmental Microbiology, 53*(7), pp.1536-1540.

[48] Lozupone, C. A., & Knight, R. (2007). Global patterns in bacterial diversity. *Proceedings of the National Academy of Sciences of the United States of America, 104*(27), pp.11436-11440. doi: 10.1073/pnas.0611525104

[49] Millward, G. E., Sands, T. K., Nimmo, M., Turner, A., & Tappin, A. D. (2002). Nickel in the Humber plume: Influences of particle dynamics and reactivity. *Estuarine Coastal and Shelf Science, 54*(5), pp.821-832. doi: 10.1006/ecss.2001.0859

[50] Mitchell, S. B., West, R.J., Arundale, A.M.W., Guymer, I., Couperthwaite, J.S. . (1998). Dynamic of the Turbidity Maxima in the Upper Humber Estuary System, UK. *Marine Pollution Bulletin, 37,* pp.190-205.

[51] Mortimer, R. J. G., Krom, M. D., Watson, P. G., Frickers, P. E., Davey, J. T., & Clifton, R. J. (1998). Sediment-water exchange of nutrients in the intertidal zone of the Humber Estuary, UK. *Marine Pollution Bulletin, 37*(3-7), pp.261-279. doi: 10.1016/s0025-326x(99)00053-3

[52] Mortimer, R. J. G., Davey, J. T., Krom, M. D., Watson, P. G., Frickers, P. E., & Clifton, R. J. (1999). The effect of macrofauna on porewater profiles and nutrient fluxes in the intertidal zone of the Humber Estuary. *Estuarine Coastal and Shelf Science, 48*(6), pp.683-699. doi: 10.1006/ecss.1999.0479

[53] NRA. (1995). *Sea Vigil Water Quality Monitoring : the Humber Estuary 1992-1993*. Peterborough: National Rivers Authority Anglian Region. Retrieved from http://www.environmentdata.org/archive/ealit:2851.

[54] NRA. (1996). *Sea Vigil Water Quality Monitoring: The Humber Estuary 1994*. Peterborough: National Rivers Authority Anglian Region. Retrieved from http://www.environmentdata.org/archive/ealit:2868.

[55] O'Sullivan, L. A., Sass, A. M., Webster, G., Fry, J. C., Parkes, R. J., & Weightman, A. J. (2013). Contrasting relationships between biogeochemistry and prokaryotic diversity depth profiles along an estuarine sediment gradient. *FEMS Microbiology Ecology, 85*(1), pp.143-157. doi: 10.1111/1574-6941.12106

[56] Oksanen, J., Blanchet, F. G., Kindt, R., Legendre, P., Minchin, P. R., O'Hara, R. B., Simpson, G. L., Solymos, P., Stevens, M. H. H., & Wagner, H. (2013). vegan: Community Ecology Package. R package version 2.0-10. Retrieved 22-08-2016, from http://CRAN.R-project.org/package=vegan

[57] Oulas, A., Pavloudi, C., Polymenakou, P., Pavlopoulos, G. A., Papanikolaou, N., Kotoulas, G., Arvanitidis, C., & Iliopoulos, I. (2015). Metagenomics: Tools and Insights for Analyzing Next-Generation Sequencing Data Derived from Biodiversity Studies. *Bioinformatics and Biology Insights, 9*, pp.75-88. doi: 10.4137/bbi.s12462

[58] Pethick, J. S. (1990). The Humber Estuary. *In* Ellis S. and Crowther, D.R. (Eds.), *Humber Perspectives, A region through the ages*. Hull: Hull University, pp.54-67.

[59] Prastka, K. E., & Malcolm, S. J. (1994). Particulate phosphorus in the Humber estuary. *JOurnal of Aquatic Ecology, 28*(3), pp.397:403. doi: 10.1007/BF02334209

[60] Remane, A. (1934). Die Brackwasserfauna. *Zoologischen Anzeiger (Supplement), 7*, pp.34-74.

[61] Rink, B., Martens, T., Fischer, D., Lemke, A., Grossart, H. P., Simon, M., & Brinkhoff, T. (2008). Short-term dynamics of bacterial communities in a tidally affected coastal ecosystem. *FEMS Microbiology Ecology, 66*(2), pp.306-319. doi: 10.1111/j.1574-6941.2008.00573.x

[62] Sanders, R. J., Jickells, T., Malcolm, S., Brown, J., Kirkwood, D., Reeve, A., Taylor, J., Horrobin, T., & Ashcroft, C. (1997). Nutrient fluxes through the Humber estuary. *Journal of Sea Research, 37*(1-2), pp.3-23. doi: 10.1016/S1385-1101(96)00002-0

[63] Schubert, H., Feuerpfeil, P., Marquardt, R., Telesh, I., & Skarlato, S. (2011). Macroalgal diversity along the Baltic Sea salinity gradient challenges Remane's species-minimum concept. *Marine Pollution Bulletin, 62*(9), pp.1948-1956. doi: 10.1016/j.marpolbul.2011.06.033

[64] Sun, M. Y., Dafforn, K. A., Brown, M. V., & Johnston, E. L. (2012). Bacterial communities are sensitive indicators of contaminant stress. *Marine Pollution Bulletin, 64*(5), pp.1029-1038. doi: 10.1016/j.marpolbul.2012.01.035

[65] Team, R. (2015). RStudio: Integrated Development Environment for R (Version.0.99.486). Boston, MA: RStudio, Inc. Retrieved from http://www.rstudio.com/

[66] Telesh, I. V., Schubert, H., & Skarlato, S. O. (2011). Revisiting Remane's concept: evidence for high plankton diversity and a protistan species maximum in the horohalinicum of the Baltic Sea. *Marine Ecology Progress Series, 421*, pp.1-11. doi: 10.3354/meps08928

[67] Telesh, I. V., Schubert, H., & Skarlato, S. (2013). Life in the salinity gradient: Discovering mechanisms behind a new biodiversity pattern. *Estuarine Coastal and Shelf Science, 135*, pp.317-327. doi: 10.1016/j.ecss.2013.10.013

[68] Uncles, R. J., Easton, A. E., Griffiths, M. L., Harris, C., Howland, R. J. M., King, R. S., Morris, A. W., & Plummer, D. H. (1998a). Seasonality of the turbidity maximum in the Humber-Ouse estuary, UK. *Marine Pollution Bulletin, 37*(3-7), pp.206-215.

[69] Uncles, R. J., Joint, I., & Stephens, J. A. (1998b). Transport and retention of suspended particulate matter and bacteria in the Humber-Ouse Estuary, United Kingdom, and their relationship to hypoxia and anoxia. *Estuaries, 21*(4A), pp.597-612. doi: 10.2307/1353298

[70] Uncles, R. J., Stephens, J. A., & Law, D. J. (2006). Turbidity maximum in the macrotidal, highly turbid Humber Estuary, UK: Flocs, fluid mud, stationary suspensions and tidal bores. *Estuarine, Coastal and Shelf Science, 67*(1-2), pp.30-52. doi: 10.1016/j.ecss.2005.10.013

[71] Viollier, E., Inglett, P. W., Huntrer, K., Roychoudhury, A. N., & Van Cappellen, P. (2000). The ferrozine method revised: Fe(II)/Fe(III) determination in natural waters. *Applied Geochemistry, 15*, pp.785-790. doi: 10.1016/S0883-2927(99)00097-9

[72] Wang, J. J., Yang, D. M., Zhang, Y., Shen, J., van der Gast, C., Hahn, M. W., & Wu, Q. L. (2011). Do Patterns of Bacterial Diversity along Salinity Gradients Differ from Those Observed for Macroorganisms? *Plos One, 6*(11). doi: 10.1371/journal.pone.0027597

[73] Wang, K., Ye, X., Chen, H., Zhao, Q., Hu, C., He, J., Qian, Y., Xiong, J., Zhu, J., & Zhang, D. (2015). Bacterial biogeography in the coastal waters of northern Zhejiang, East China Sea is highly controlled by spatially structured environmental gradients. *Environmental Microbiology, 17*(10), pp.3898-3913. doi: 10.1111/1462-2920.12884

[74] Wang, Y., Sheng, H.-F., He, Y., Wu, J.-Y., Jiang, Y.-X., Tam, N. F.-Y., & Zhou, H.-W. (2012). Comparison of the Levels of Bacterial Diversity in Freshwater, Intertidal Wetland, and Marine Sediments by Using Millions of Illumina Tags. *Applied and Environmental Microbiology, 78*(23), pp.8264-8271. doi: 10.1128/aem.01821-12

[75] Wei, G., Li, M., Li, F., Li, H., & Gao, Z. (2016). Distinct distribution patterns of prokaryotes between sediment and water in the Yellow River estuary. *Applied Microbiology and Biotechnology, 100*(22), pp.9683-9697. doi: 10.1007/s00253-016-7802-3

[76] Whitfield, A. K., Elliott, M., Basset, A., Blaber, S. J. M., & West, R. J. (2012). Paradigms in estuarine ecology - A review of the Remane diagram with a suggested revised model for estuaries. *Estuarine Coastal and Shelf Science, 97*, pp.78-90. doi: 10.1016/j.ecss.2011.11.026

[77] Whittaker, R. H. (1972). Evolution and measurement of species diversity. *Taxon, 21*(2-3), pp.213-251. doi: 10.2307/1218190

[78] Williams, M. R., & Millward, G. E. (1999). Dynamics of particulate trace metals in the tidal reaches of the Ouse and Trent, UK. *Marine Pollution Bulletin, 37*(3-7), pp.306-315. doi: 10.1016/s0025-326x(99)00054-5

Chapter 8
Conclusions and Future Work

8.1 Conclusions

The overall aim of this PhD study was to improve understanding of the biogeochemical processes occurring in estuarine sediments and their living microbial community along the salinity gradient of the Humber Estuary.

Three different redox scenarios were simulated in order to elucidate the principal pathways of N, Fe, Mn and S and the interlinks between their cycles. The effects of sediment (re)oxidation on trace metal behaviour and speciation were also a focus of investigation.

In Chapter 5, experiments simulated the aerobic resuspension of estuarine sediments from two different sediment pools mobilized at different frequency in natural conditions. When sediments are resuspended, any nitrate released (from porewater or as a product of nitrification) will result in an increase of nitrate concentrations in the oxic water column. However, this addition may be insignificant in the short term considering the high nitrate levels of the water and the consumption through denitrification processes. In general, nitrate showed no immediate changes upon resuspension, although in the timeframe of a big storm net increases were observed. If we contrast these findings with the salinity-nitrate distribution plot (Fig 6.4), we can confirm that nitrate behaves conservatively along the salinity gradient since coupled nitrification-denitrification will maintain the concentrations of the river water relatively level and it will be the dilution of the freshwater flows in the mixing processes what largely regulates the nitrate concentrations in the river water. Nevertheless, the third type of sediment oxidation (anaerobic oxidation) analysed in microcosms experiments (Chapter 6) confirmed that if nitrate is available (note that nitrate was in excess over any DO left in the river water), biotic denitrification occurred via a combination of heterotrophic and chemolithotrophic microbial activity. These processes will contribute to the nitrogen removal in the

Humber, especially in the outer estuary due to the greater availability of electron donors and the large extension of the mudflat area (95% of the total intertidal sediment area of the Humber, ~115 km^2 between Spurn Head and Trent Falls, are intertidal sand and mudflats). This is the main area for sediment deposition and, hence, for retention of nutrient and nitrogen removal (by denitrification and organic matter burial). Therefore the management of the intertidal areas is very important due to their highly valuable ecosystem function and their role in terms of coastal protection. This systematic study along the gradient has confirmed how important the local geochemistry in the N cycling is, and additionally a clear transition in the dominating processes from the inner to the outer estuary has been detected in aerobic and anaerobic oxidation experiments.

The initial geochemical state of the sediments and their position along the salinity gradient influence the geochemical progression during resuspension. From the results of presented in Chapter 5, it can be concluded that there is a transition between Mn/Fe-dominating systems in the inner estuary towards Fe/S dominating systems in the outer estuary mudflats. Furthermore, an immediate release of trace metals to solution during resuspension, even if there is an extreme event, will be rapidly reversed likely due to the co-precipitation and/or sorption of the dissolved species to the newly formed iron and manganese oxides, and sorption to SPM surfaces, colloids, etc. Therefore it can be said that estuarine sediments act as an ultimate sink for trace metals. However, the role of the sediments in terms of nutrients may vary with the intensity of the resuspension (i.e. the sediment depth mobilised), which may be important in a climate change scenario since more severe storms are predicted for the UK in future. The potential release of more reduced species will add reductive potential, or in other words COD, to the water column during an extreme resuspension event, but this is likely to be attenuated by the DO in the water column which is maintained due to the constant oxygenation of the river water in this highly dynamic estuary.

From the results presented in Chapter 6, it can be concluded that microbially mediated nitrate-depended oxidation processes are likely to occur in regions of the sediments where oxygen is absent or nearly absent. Anaerobic denitrification did not develop in the microcosms of one of the study sites (S2). The geochemical state of the subsurface

sediments in S2 (neither in situ nor after the laboratory analyses) did not suggest that those sediments were poised at suboxic/anoxic conditions, which may explain the lack of denitrifying activity. The calculation of electron balances for these experiments was useful to recognise which were the dominant processes but it was not enough to deduce which were exactly the reaction pathways. The results suggested that a combination of many different biological reactions account for the nitrate consumption and there is a transition with salinity towards S-dominated systems. A similar trend was observed in the air-oxidation experiment.

To finish the conclusions about sediment oxidation effects on geochemistry, there was an effect on the trace metal partitioning in the three oxidation scenarios (surface and subsurface sediments in aerobic conditions and subsurface sediment anaerobic oxidation) studied. In general terms, trace metals experienced a shift towards more 'easily to extract' fractions as a consequence of sediment (re)oxidation. So, even if the sediments act as an ultimate sink for trace elements, their oxidation may have effects on the fate, bioavailability and mobility of trace metals. This may have further implications in the system, for example if remobilisation patterns change and anoxic sediments are mobilised more often.

So overall, this work has demonstrated the complex interlinks between the major elements and trace metal cycles and the importance of the coupling between physical and geochemical processes.

In Chapter 7, the analysis of bacterial DNA by using amplicon sequences of the 16S rRNA gene showed that there is a trend in bacterial diversity along the estuarine salinity gradient. The sequence depth allowed by the current high-throughput sequencing technology provided large amount of data to characterise bacterial communities. However, for that very reason, the use of conventional diversity indices is not as informative as it used to be for the microbial ecologist community. Challenges for describing bacterial diversity nowadays are associated with some intrinsic properties of the bacteria (species concept debate, hyperdiversity and increasing capture of rare taxa, and variability on the copies of the 16S rRNA gene) and technological difficulties. Hence Hill numbers were applied as a measure of diversity, which is what is currently claimed

to be the new approach to microbial diversity. Only by using such metrics, the taxa (OTUs in this case) are weighted based on their abundance, which controls the variability associated with rare taxa and overcomes the misleading interpretation of large datasets. By analysing alpha diversity with Hill numbers, it can be concluded that salinity is the main environmental factor controlling microbial diversity. However, there was further evidence of strong redox transitions with depth being a secondary selective pressure for the bacterial communities in the outer estuary Humber mudflats. The results suggested that: i) there is a widespread surface sediment community subjected to frequent mobilization, and, therefore bacterial communities are being mixed, homogenised and transported together with the SPM along the estuary; while ii) there is a potential community of more specialists developing at the more reducing and less disturbed sediment layers. Again, it is demonstrated how important sediment resuspension is, this time for the biology and hence for the ecological functioning of the system.

8.2 Future work

The sediment resuspension approach and the microcosm approach are useful to simulate a wide variety of geochemical scenarios to give an overall picture of the key processes operating in an estuarine system, but more detailed follow up studies using particularly target techniques could help to elucidate individual reaction pathways.

For example, in the study of the aerobic resuspension, improvements could be made by controlling key environmental parameters in such scenarios (e.g. dissolved oxygen or sediment-solution ratio) to obtain a more solid understanding of the processes developing. It will also be very instructive to study the mechanisms of metal precipitation during resuspension and if there are differences by depth in the newly formed precipitated/aggregates. Field studies, measuring *in situ* nutrient fluxes and sampling the suspended solids could be used in combination to laboratory studies to constrain the multiprocesses occurring during a tidal cycle. High resolution studies of the TMZ combining geochemistry and microbiology in a properly defined sedimentological context have not been made to date. This will be a future area of research regarding the intense transformations of nutrients and other reactive elements in these “natural

bioreactors" and the potential alterations that the TMZ will experience as a consequence of the more frequent intensive rainfall events associated with global warming.

The use of ^{15}N labelled nitrogen substrates will be also useful in the analysis of the nitrate reduction pathways, and ammonium removal from solution. For example microsensors or diffusive equilibrium in thin layer (DET) gels could be used to analyse microprofiles of nitrate reduction in intact cores. This can be combined also with further microcosm studies using different treatments. For example addition of inhibitors, and different amendments or a combination of them (e.g. nitrate at different concentrations, electron acceptors such as ammonium, Fe(II), etc.).

Rapid release-uptake trends have been recognised during sediment reoxidation experiments. To improve the understanding of the trace metal cycling (behaviour, mobility and precipitation dynamics), further experiments could be performed with selective trace metals and/or minerals. For example the use of imaging technology (SEM), and also X-ray absorption spectroscopy (XAS) could be used to investigate the atomic level structure and to characterise the chemical form of the trace elements associated with different sediment particles. This could be used to study the nature of the sorption and co-precipitation onto and with biogenic and non-biogenic minerals formed during sediment oxidation under anaerobic conditions.

The microbiology part of this thesis is a very preliminary study of the benthic microbial diversity along the Humber. Small number of sites were used to begin with, and due to the large amount of genetic data obtained, those few sites were deeply characterise. Furthermore, interesting patterns in microbial diversity have been observed. To further test those diversity trends, a larger sampling survey could be carried out in the Humber. Considering the decreasing cost/effort of the sequencing facilities at the moment, an extension of this work would include more sampling sites along the salinity range, and more replicates. Decreasing sequencing depth (number of reads per sample) will allow more samples per run and this is sensible since the use of Hill numbers has demonstrated that the reliability of these diversity measurements will not be affected by decreasing to a certain level the sequencing depth. Furthermore using coring as a sampling method in order to more accurately delineate sediment depths could also provide additional

information. For the study of specific microbial assemblages, qPCR studies could be carried out in order to detect differences in the communities by depth associated to the available redox species.

Appendix A
Methods

This appendix includes further information about the ICP-MS analysis (protocol, errors and limits of detection)

A.1 Instrument information

The analyses were performed using a Thermo Scientific iCAPQc Inductively Coupled Plasma Mass Spectrometer (ICP-MS).

Aluminium was analysed in standard mode and all other elements in Kinetic Energy Discrimination (KED) mode using helium as a collision gas to remove polyatomic interferences.

Table A.1: Summary of the elements and modes used.

Element	Mass (m/z)	Instrument Mode
Al	27	Std
V	51	KED
Cr	52	KED
Mn	55	KED
Fe	56	KED
Co	59	KED
Cu	63	KED
Zn	64	KED
As	75	KED
Cd	112	KED

A.2 Sample and standard preparation

NASS-6 Seawater Certified Reference Material (CRM) was used as reference material (http://www.nrc-cnrc.gc.ca/eng/solutions/advisory/crm/certificates/nass_6.html).

For the brackish-seawater analysis, samples were diluted 50 fold in 1 % v/v HNO_3 before analysis (0.2 ml sample + 9.8 ml diluent) to reduce matrix effects during the analysis.

Standard additions type calibration was used for the analysis using 1:50 diluted NASS-6 Seawater Certified Reference Material (CRM) as the standard matrix.

Calibrations were performed in the range of 1-100 µg L^{-1}.

Blanks of 3 % w/v NaCl solution were prepared.

As internal standardisation, Rhodium at a concentration of 1 ppb was added to all standards and samples for use as an internal standard.

For the freshwaters, everything was run as above except they were analysed with no dilution.

A.3 Analytical figures of merit

Limits of detection were calculated from repeated measurements of 5 individual blank solutions using the equation below.

$$LOD = 3\sigma_{5\ Blanks}$$

Accuracy of the method was estimated by spiking a sample with a known amount of analyte and measuring the analyte recovery. Sample and Sample + Spike were analysed 5 times.

$$\%\ Recovery = 100 \times \frac{M_{Spike} - M_{Sample}}{C_{spike}}$$

Where M_{spike} = Measured concentration of spiked sample.

M_{Sample} =Measured concentration of sample.

C_{Spike} = Actual concentration of spike.

Precision of the method was assessed from the repeated measurement of one sample 6 times and reported as the 95% confidence interval of these results.

$$\bar{x} \pm \frac{t_{n-1}s}{\sqrt{n}}$$

Where n = number of measurements

n-1 = degrees of freedom (5)

t = t value (2.78 for 4 degrees of freedom)

s = calculated standard deviation of 5 measurements

x = calculated mean of 5 measurements

Certified Reference Material

The Certified Reference Material (CRM) used was NASS-6 Certified reference material. This is a seawater reference material.

A.4 Quality Control, LOD and error details for ICP-MS analyses

See table below for details about the Quality Control (Table A.2) and the LOD and errors of the different ICP-MS analyses (Tables A.3).

The quality control data (Table A.2) show that, with the exception of the aluminium, the concentrations detected from samples containing 1:50 fold dilution of the seawater certified material (zero standard) spiked with a 5 ppb metal concentration solution, were in fact around 5 ppb. From this control test the recovery was >95%, the LOD was 0.027 ppb and the uncertainty 3.72 %.

For the method validation, the protocol followed was:

1) Two blanks are run to start to start with.

2) The calibration is carried out with standards (from 0-10 ppb) made up with 1:50 seawater reference material.

3) Subsequently, blanks (x6) are run.

4) Then, 1:50 seawater spiked with 0.5ppb (metal concentrations) solution is run (x3 times) followed by a 1:50 seawater spiked with 5ppb (metal concentrations) solution (x3 times).

5) Afterwards, two different samples diluted 1:50 (with no spike) (x5 times) are run; followed by the same samples (x5 times) diluted 1:50 but spiked with 10 ppb standard solution.

6) Next, 1:50 seawater spiked with 0.5ppb (metal concentrations) solution (x3 times) and 1:50 seawater spiked with 5ppb (metal concentrations) solution (x3) are run again.

6) To finish, more blanks are run (x6 times).

Table A.2: Summary of the Quality Control.

	27Al (STD) [ppb]	51V (KED) [ppb]	52Cr (KED) [ppb]	55Mn (KED) [ppb]	56Fe (KED) [ppb]	59Co (KED) [ppb]	63Cu (KED) [ppb]	64Zn (KED) [ppb]	75As (KED) [ppb]	112Cd (STD) [ppb]	60Ni (KED) [ppb]
Zero Std	4,539	0,07	0,049	0,04	0,563	0,003	0,136	0,418	0,061	0,008	0,18
Blank	4,662	0,005	0,03	0,04	1,031	0,003	0,202	0,416	0,009	0,005	0,589
1:50 NASS6 + 5 ppb	10,032	4,63	4,892	4,988	5,029	4,957	5,043	5,694	4,887	5,191	5,086
1:50 NASS6 + 5 ppb	11,569	5,106	5,055	4,971	5,485	4,993	5,063	5,115	5,052	4,914	4,801
1:50 NASS6 + 5 ppb	10,278	4,425	4,469	4,395	4,929	4,526	4,674	4,965	4,793	5,14	5,371
1:50 NASS6 + 5 ppb	10,501	4,632	4,648	4,579	5,135	4,63	4,807	5,103	4,965	5,063	4,898
1:50 NASS6 + 5 ppb	10,797	4,696	4,798	4,758	5,293	4,74	4,889	5,164	4,995	5,085	4,896
1:50 NASS6 + 5 ppb	11,512	5,007	5,003	5,04	5,551	4,941	4,981	5,216	5,179	5,005	4,959
1:50 NASS6 + 5 ppb	11,374	5,183	5,147	5,253	5,707	4,974	5,1	5,796	5,132	4,888	5,088
1:50 NASS6 + 5 ppb	11,909	5,164	5,124	5,328	5,814	4,952	5,021	5,219	5,032	4,758	5,199
Mean	10,997	4,855	4,892	4,914	5,368	4,839	4,947	5,284	5,004	5,006	5,037
Adjusted Mean (Mean- Zero Std)	6,458	4,785	4,843	4,874	4,805	4,836	4,811	4,866	4,943	4,998	4,857
Stdev	0,687	0,293	0,241	0,320	0,323	0,181	0,146	0,297	0,125	0,144	0,187
% Recovery	129,2	95,7	96,9	97,5	96,1	96,7	96,2	97,3	98,9	100,0	97,1

Table A.3: Additional information of LOD and uncertainty (% error at 95% confidence interval) for the different analyses carried out.

Analysis and details		Al	V	Cr	Mn	Fe	Co	Ni	Cu	Zn	As	Cd	Pb
Step 1 from Sequential Extractions. 1 M $MgCl_2$ (1% v/v HNO3)	LOD / ppb	23.5	0.363	1.34	2.00	26.50	0.069	0.610	1.10	2.73	0.298	0.137	0.238
	% uncertainty	4.14	2.81	1.93	5.15	4.2	0.92	1.15	1.37	1.40	4.19	0.89	2.32
	LOD / ppb	23.5	0.36	1.34	2.00	26.5	0.07	0.61	1.10	2.73	0.30	0.14	0.24
	% uncertainty	4.14	2.81	1.93	5.15	4.2	0.92	1.15	1.37	1.40	4.19	0.89	2.32
Step 2 from Sequential Extractions. 1 M NaOAc (1% v/v HNO3)	LOD / ppb	36.4	0.26	0.60	3.65	60.5	0.18	1.58	6.99	2.46	0.58	0.19	0.38
	% uncertainty	4.50	3.64	2.87	5.24	4.20	3.43	4.48	8.33	5.70	4.41	2.21	3.18
	LOD / ppb	36	0.26	0.60	3.65	60.5	0.18	1.6	7.0	2.5	0.58	0.19	0.38
	% uncertainty	4.50	3.64	2.87	5.24	4.20	3.43	4.48	8.33	5.70	4.41	2.21	3.18
Step 3 from Sequential Extractions. 0.04 M $NH_2OH{\cdot}HCl$ in 25% v/v HOAc (1% v/v HNO3).	LOD / ppb	55.07	0.20	0.91	1.19	0.13 ppm	0.17	2.72	2.45	4.83	0.54	0.15	0.23
	% uncertainty	3.74	2.67	2.71	2.48	5.44	3.30	3.76	4.05	3.69	3.11	2.91	2.94
	LOD / ppb	55	0.20	0.91	1.2	0.13 ppm	0.17	2.7	2.5	4.8	0.54	0.15	0.23
	% uncertainty	3.74	2.67	2.71	2.48	5.44	3.30	3.76	4.05	3.69	3.11	2.91	2.94
Step 4 from Sequential Extractions. HNO_3 + 30% H_2O_2 + 3.2 M NH_4OAc (1% v/v HNO3)	LOD / ppb	122	0.53	0.96	3.44	0.06 ppm	0.25	1.86	2.32	1.73	1.08	0.22	0.25
	% uncertainty	5.55	3.14	2.88	3.43	3.27	2.53	2.95	2.66	2.74	1.09	1.15	1.31
	LOD / ppb	122	0.53	0.96	3.44	0.06 ppm	0.25	1.9	2.3	1.7	1.1	0.22	0.25
	% uncertainty	5.55	3.14	2.88	3.43	3.27	2.53	2.95	2.66	2.74	1.09	1.15	1.31
"Salt water" samples (S3 and S4) from filtered river water and resuspension experiment (x50 fold)	LOD / ppb after DF50	7.91	0.14	0.09	0.87	2.16	0.35	0.027	1.35	6.04	0.24	0.03	-
	% uncertainty	0.45	0.48	0.26	0.48	0.80	0.58	3.72	0.68	1.28	1.39	1.00	-
"Fresh water" samples (S1 and S2) from filtered river water and resuspension experiment	LOD µg/L	0.974	0.003	0.016	0.1	0.651	0.001	0.096	0.249	0.701	0.005	0.014	0.059
	% uncertainty	2.0	1.5	1.0	3.1	1.7	2.7	8.9	1.2	5.9	5.1	3.0	8.4
0.5 N HCl Mn extraction from solids	LOD µg/L				0.04								
	% uncertainty				3.13								

The following table (Table A.4) shows the summary of the low detection limits (before and after the dilution factor has been applied) and the uncertainties.

Table A.4: Summary of LOD and uncertainties.

	Al	V	Cr	Mn	Fe	Co	Cu	Zn	As	Cd
LOD / ppb	0,158	0,003	0,002	0,017	0,043	0,007	0,027	0,121	0,005	0,001
LOD / ppb after DF50	7,91	0,14	0,09	0,87	2,16	0,35	1,35	6,04	0,24	0,03
% Uncertainty	0,45	0,48	0,26	0,48	0,80	0,58	0,68	1,28	1,39	1,00

Appendix B
Sediment characterisation

This appendix includes the XRD patterns and the results for the grain size characterisation of the eight sediments used throughout the experiments.

B.1 XRD results

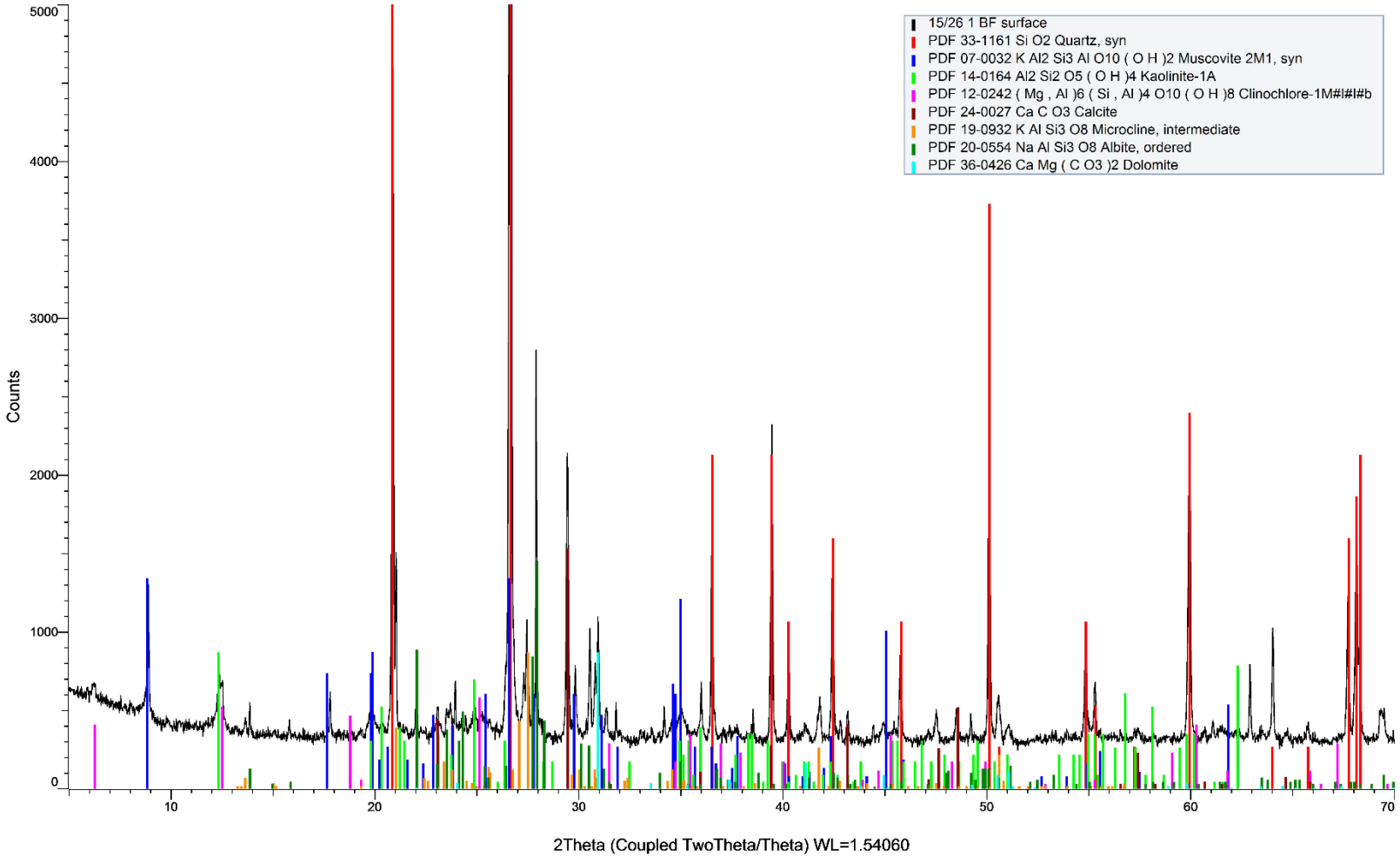

Figure B.1: XRD pattern of Boothferry (S1) surface sediment.

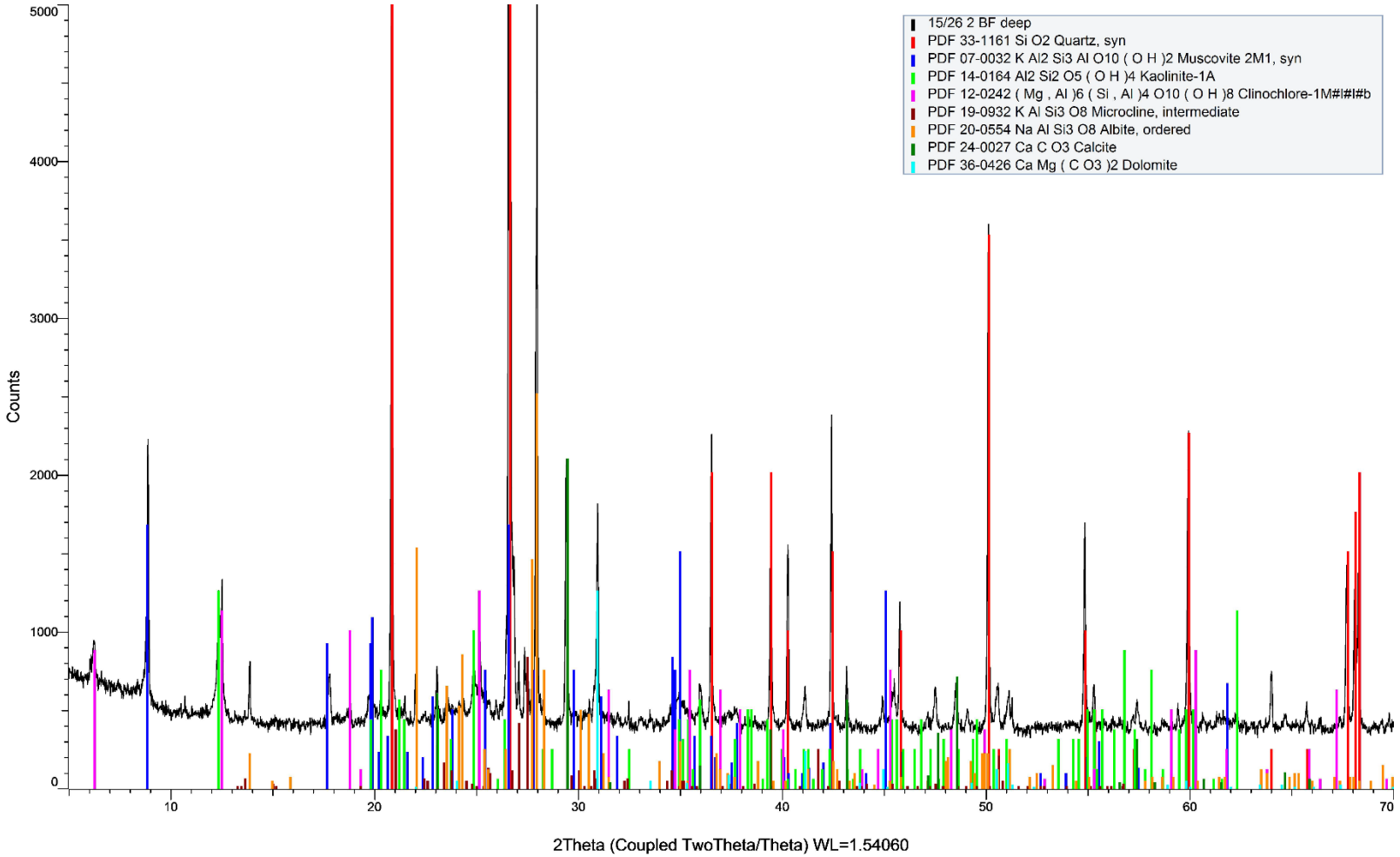

Figure B.2: XRD pattern of Boothferry (S1) subsurface sediment.

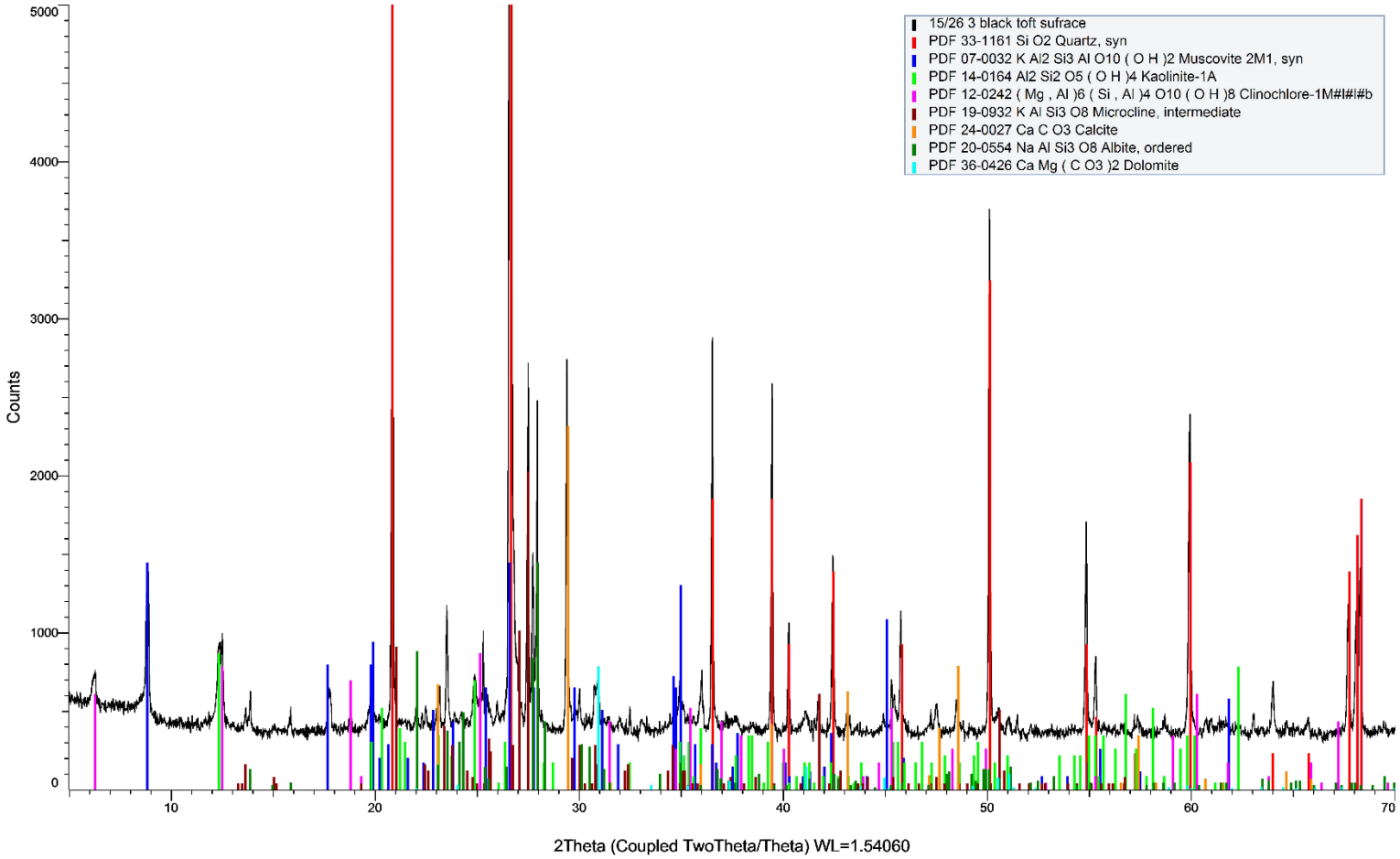

Figure B.3: XRD pattern of Blacktoft (S2) surface sediment.

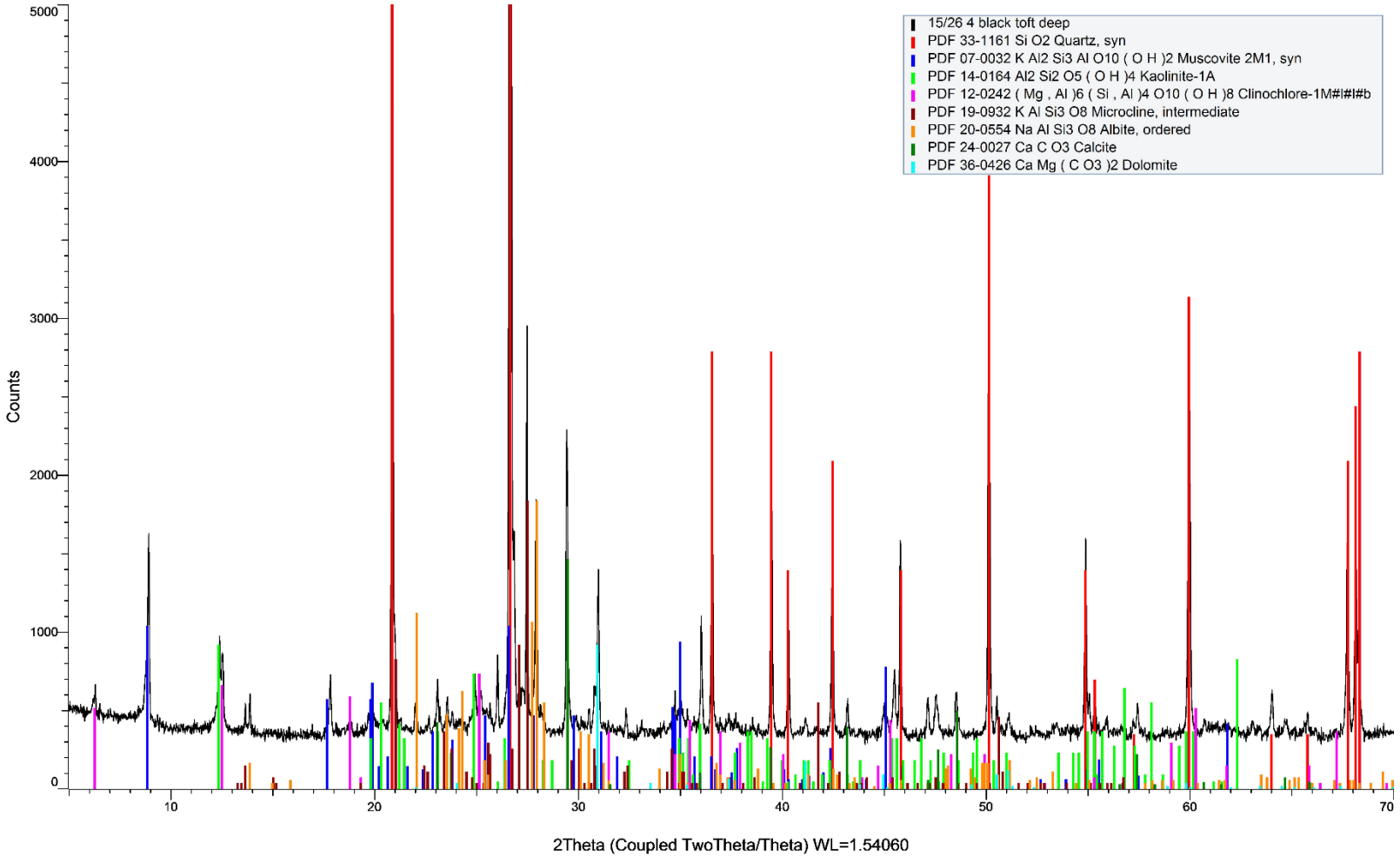

Figure B.4: XRD pattern of Blacktoft (S2) subsurface sediment.

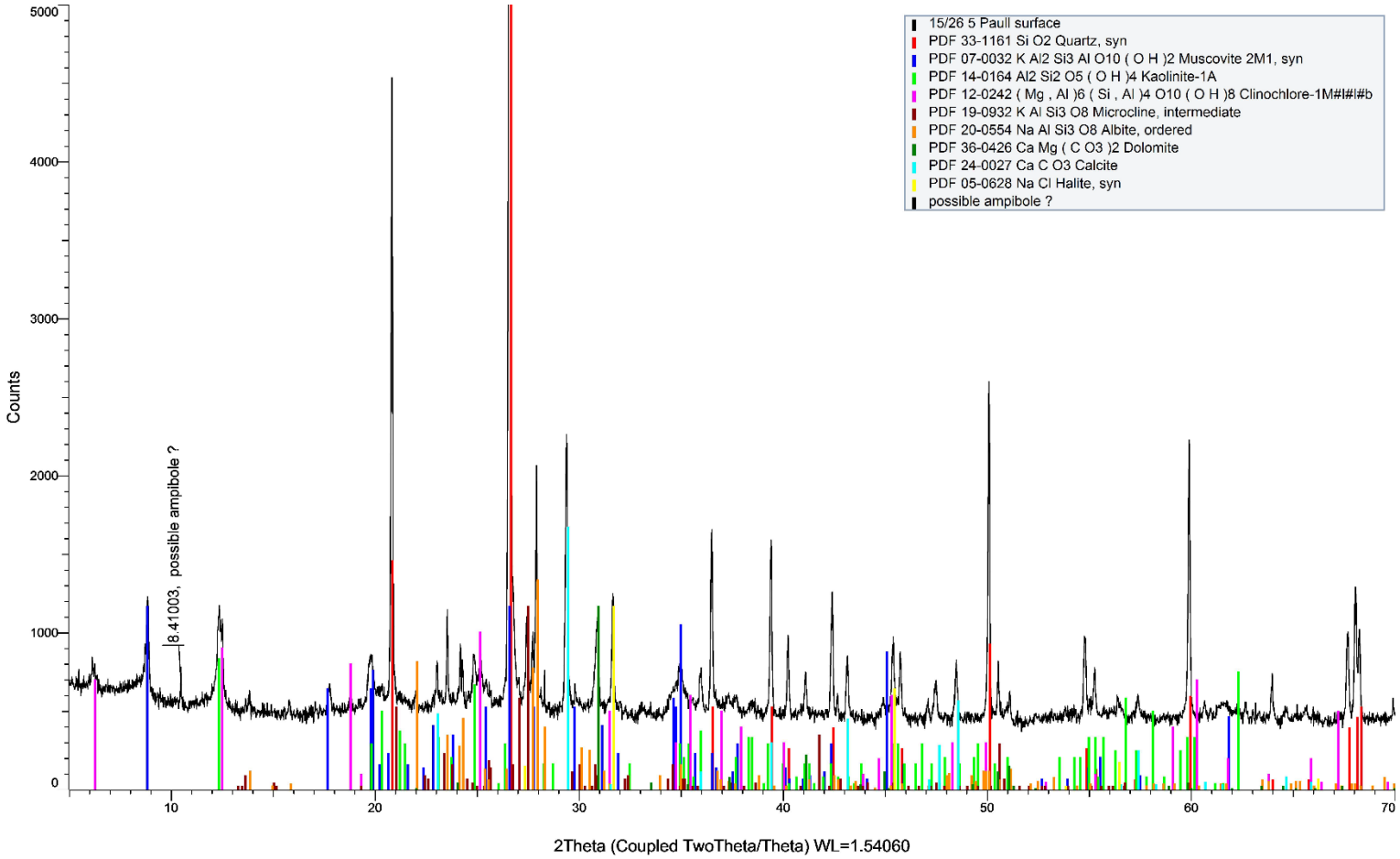

Figure B.5: XRD pattern of Paull (S3) surface sediment.

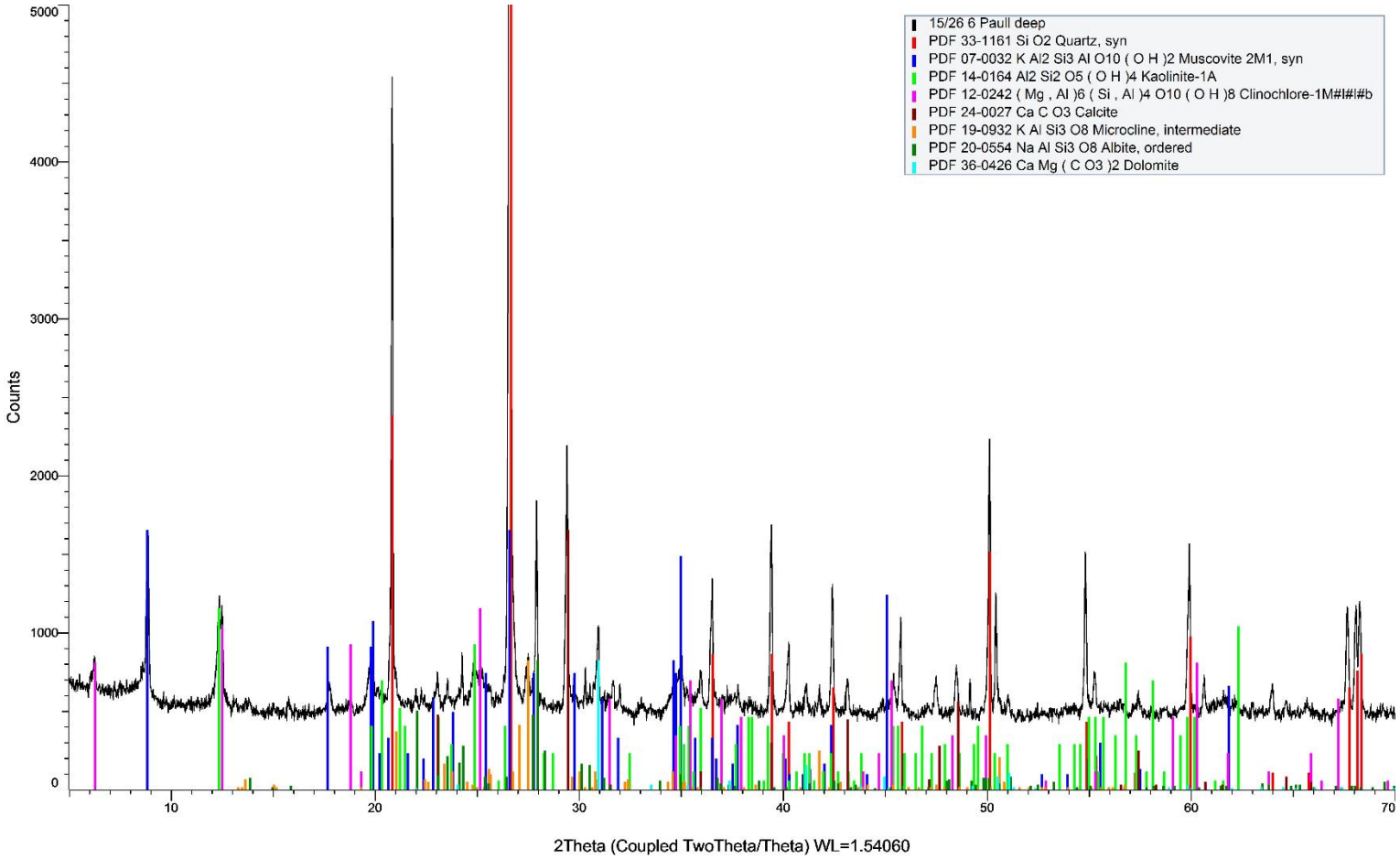

Figure B.6: XRD pattern of Paull (S3) subsurface sediment.

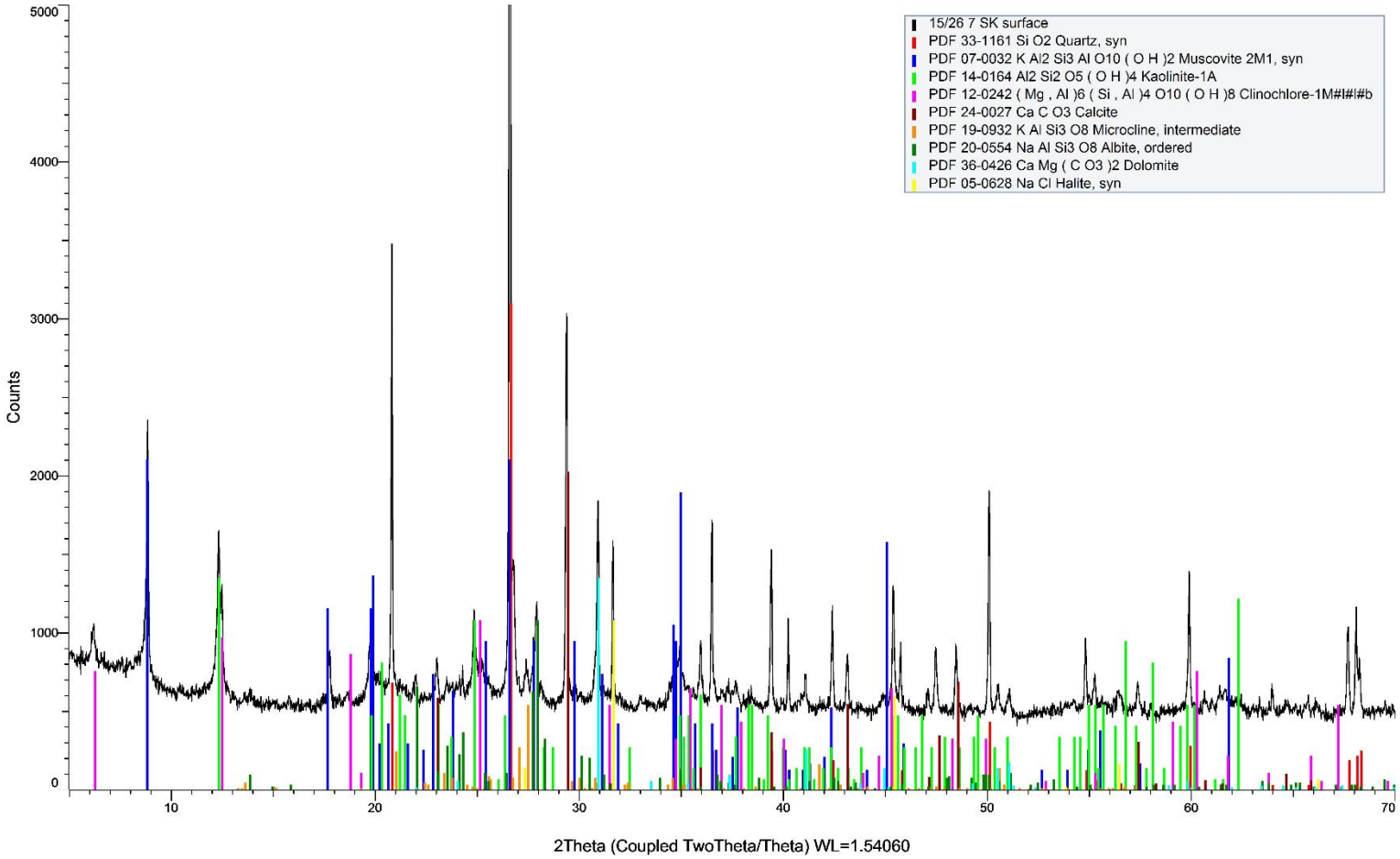

Figure B.7: XRD pattern of Skeffling (S4) surface sediment.

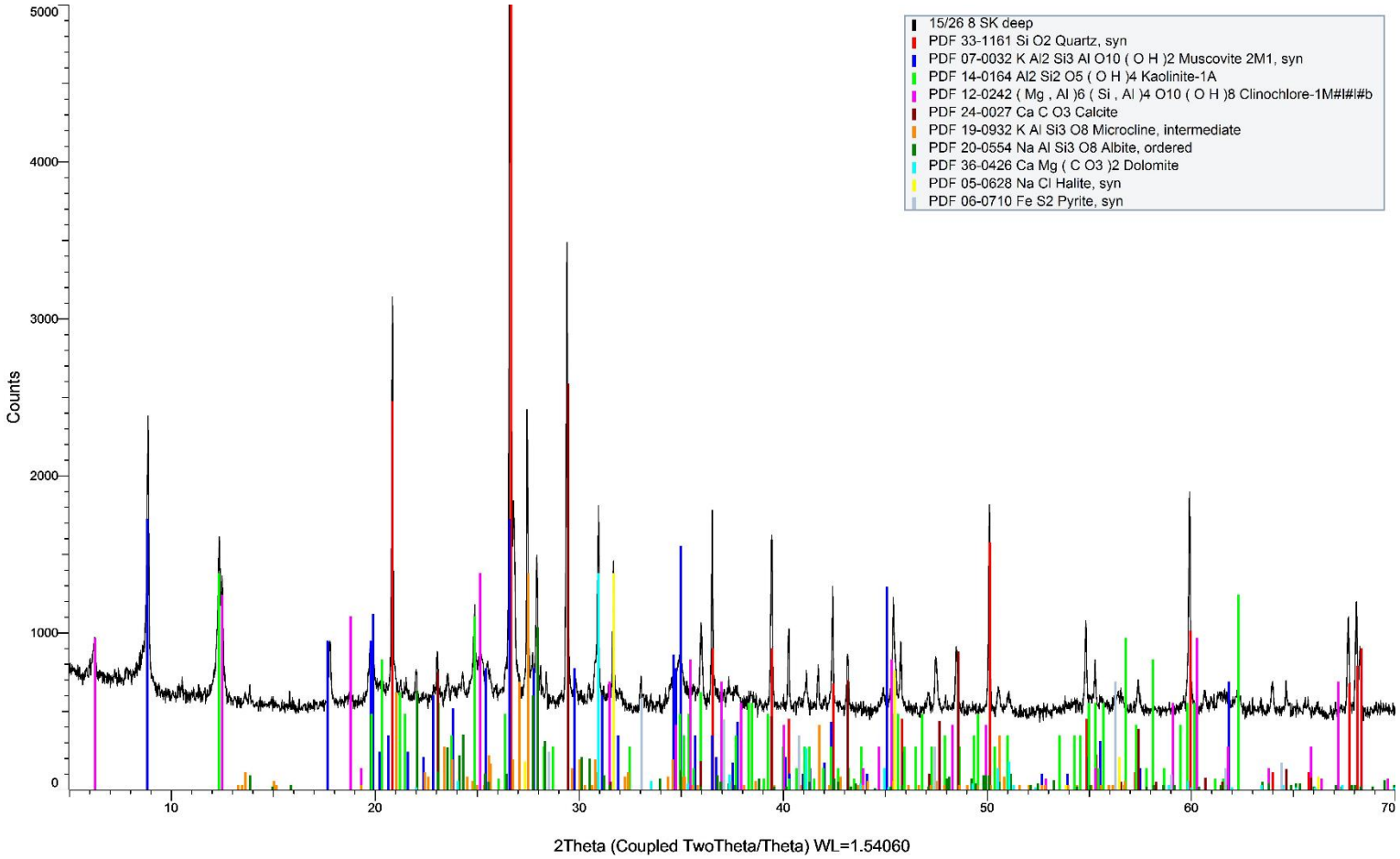

Figure B.8: XRD pattern of Skeffling (S4) subsurface sediment.

B.2 Grain size characterisation

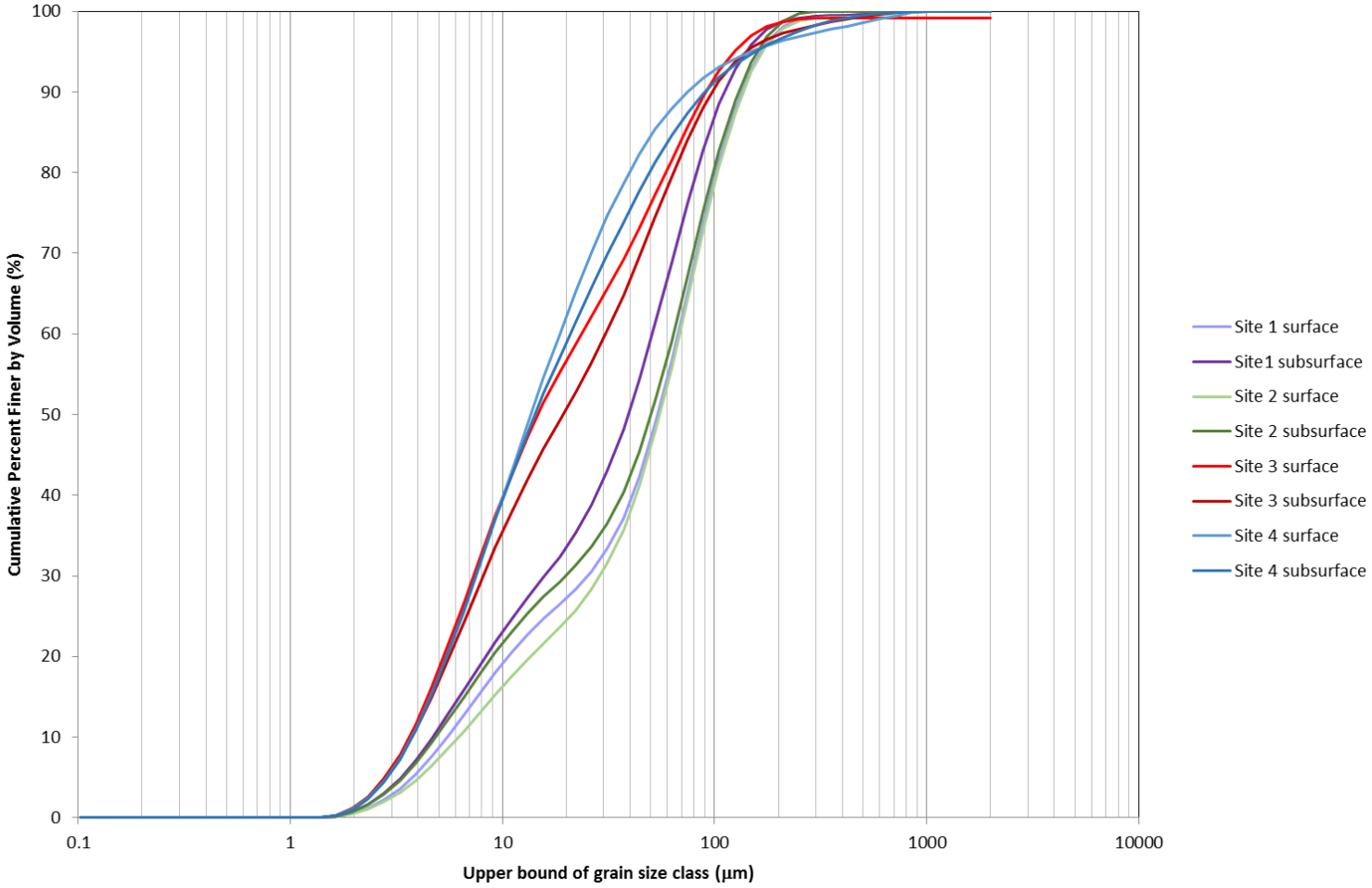

Figure B.9: Distribution curve for finer material (in cumulative percentage of finer material).

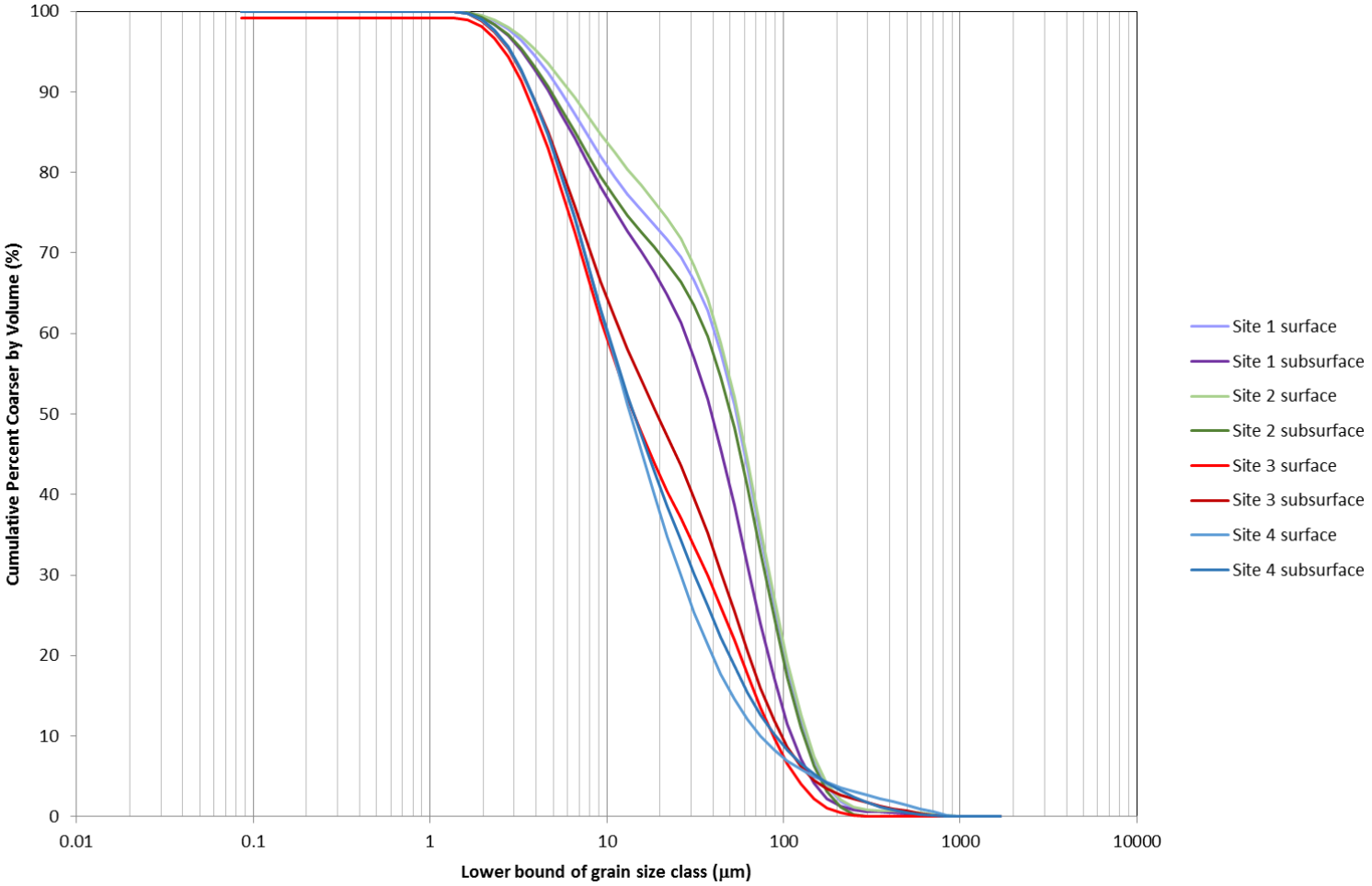

Figure B.10: Distribution curve for coarser material (in cumulative percentage of coarser material).

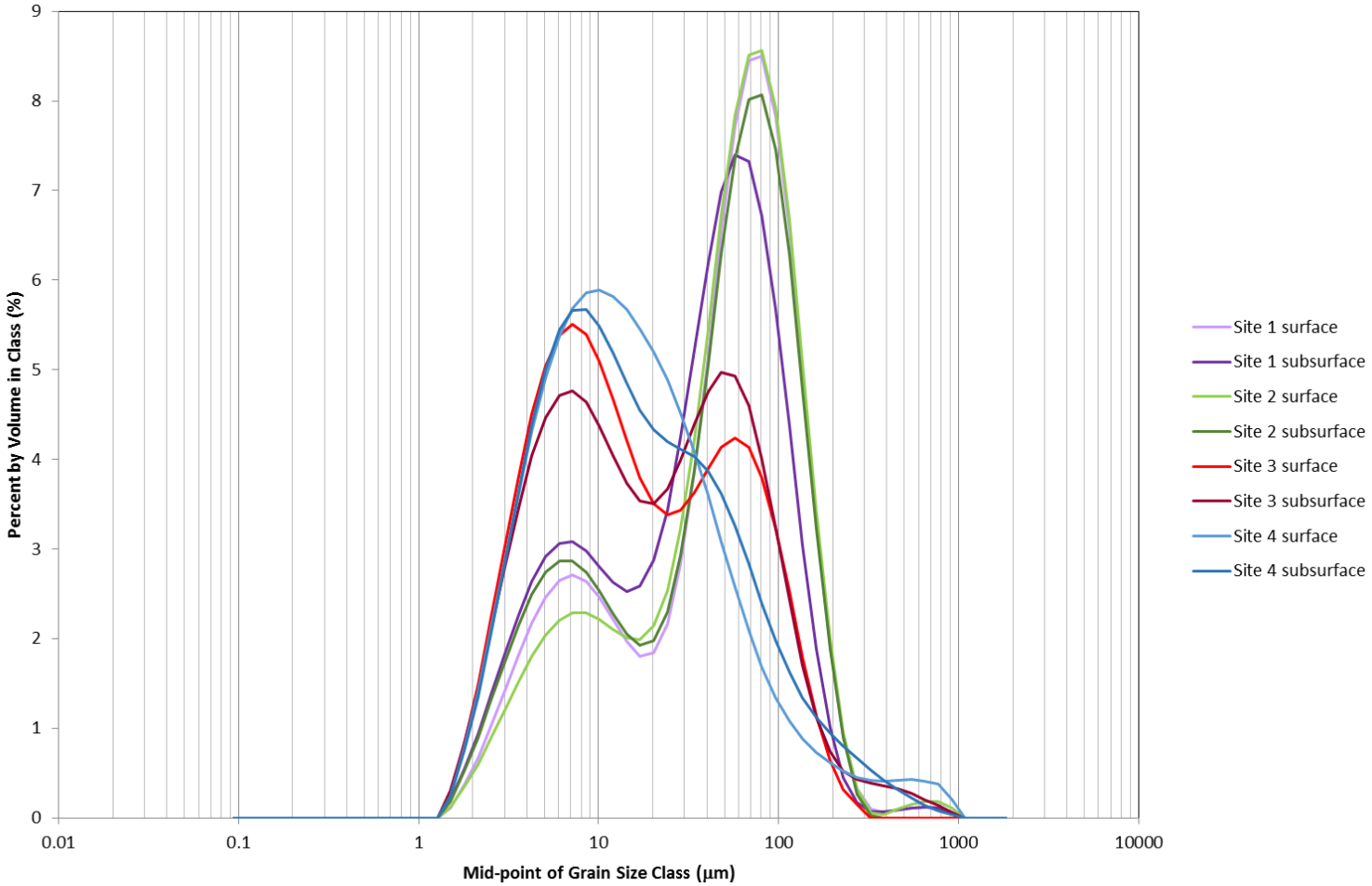

Figure B.11: **Distribution curve for grain-size classes.**

Appendix C
Supplementary information for Chapter 5

"Reoxidation of estuarine sediments during simulated resuspension events: Effects on nutrient and trace metal mobilisation"

Andrea Vidal-Durà, Ian T. Burke, Robert J.G. Mortimer and Douglas I. Stewart

(in preparation for submission to *Estuarine and Coastal Shelf Science*)

C.1 Changes in pH and Eh during sediment resuspension

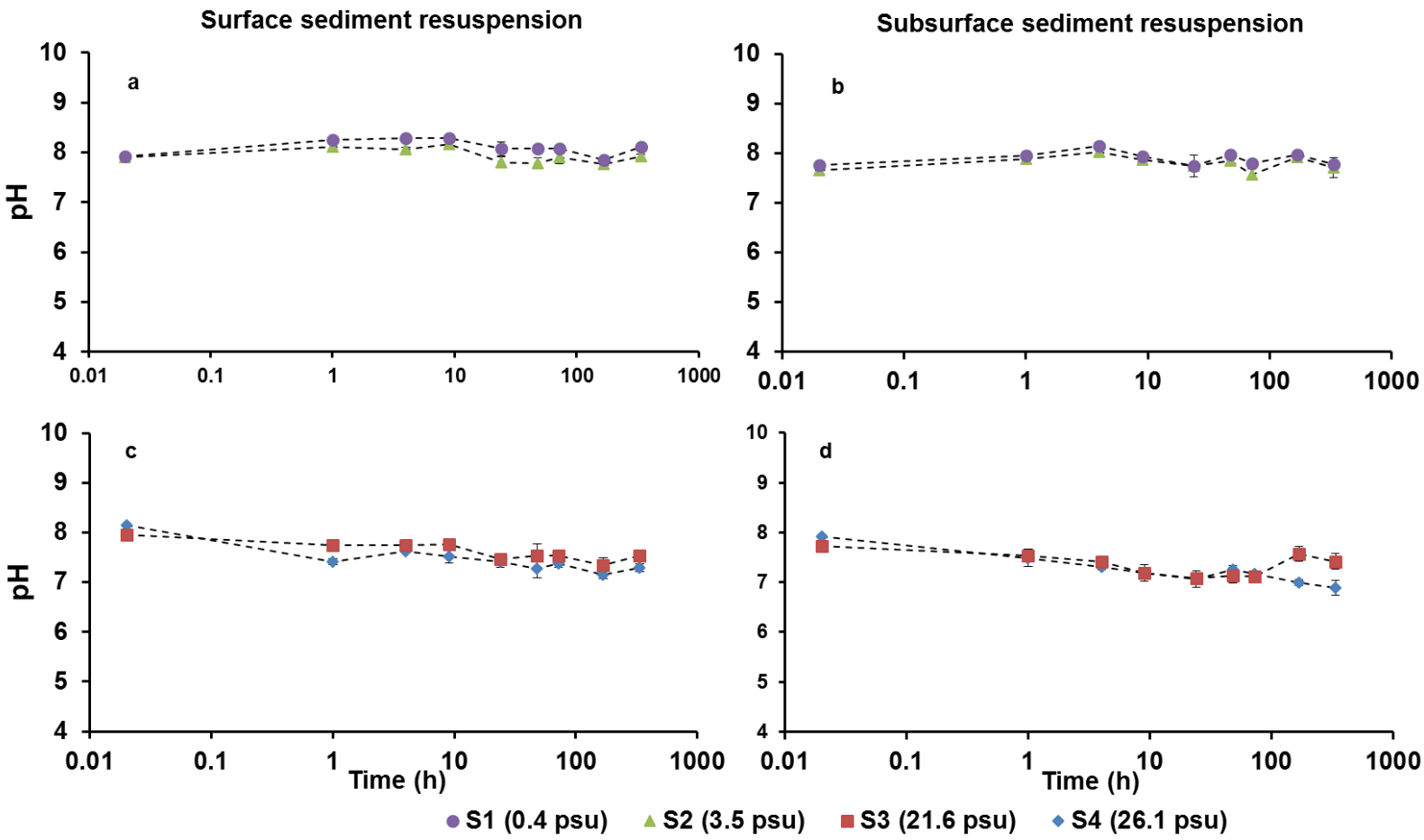

Figure C.1: pH changes during the resuspension experiments using surface (a) and subsurface (b) sediments from the inner estuary sites; and surface (c) and subsurface (d) sediments from the outer estuary sites.

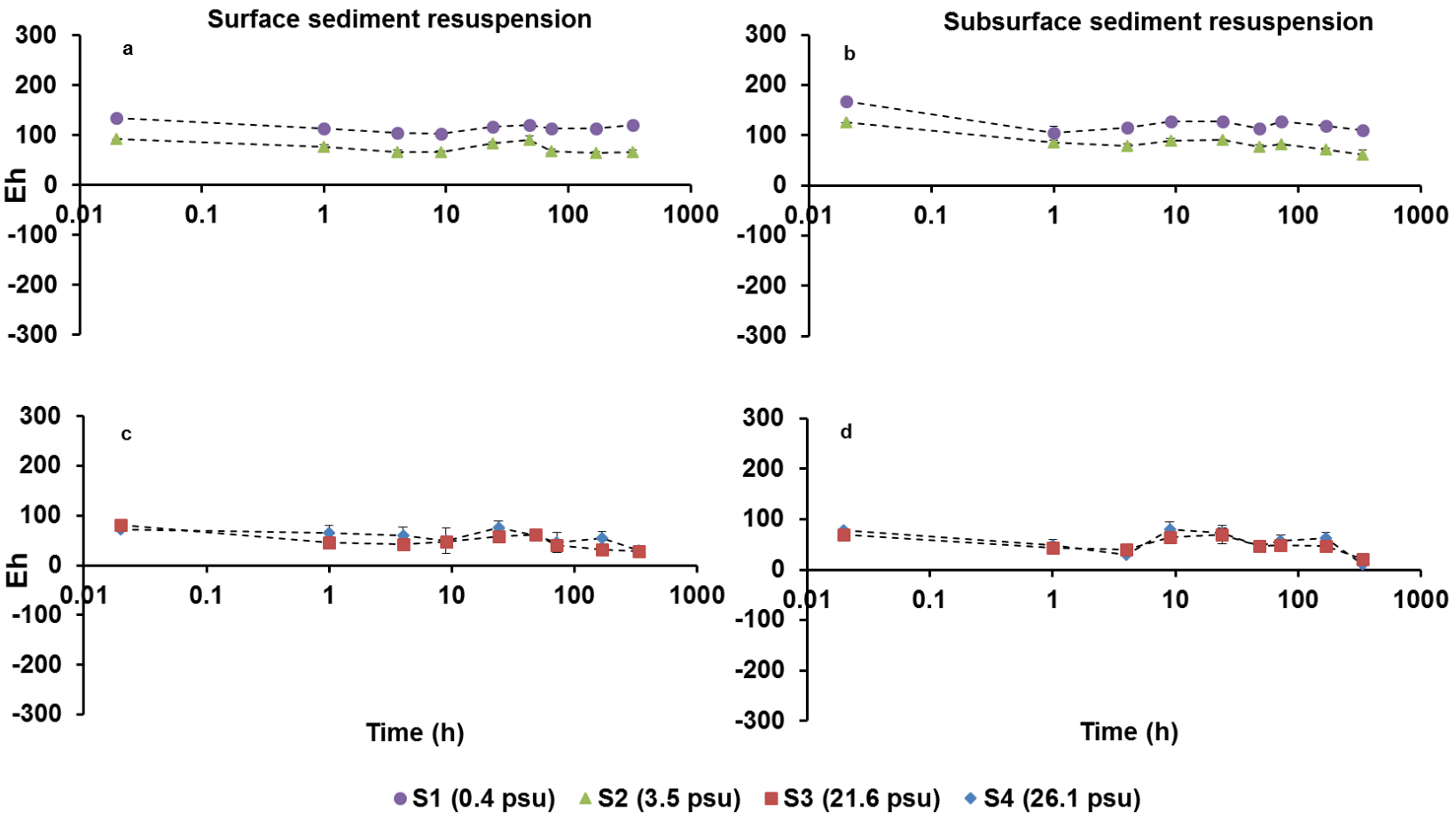

Figure C.2: Eh changes during the resuspension experiments using surface (a) and subsurface (b) sediments from the inner estuary sites; and surface (c) and subsurface (d) sediments from the outer estuary sites.

C.2 Trace metals behaviour in the aqueous phase during sediment resuspension

Table C.1: Trace metal in the aqueous phase during S1 (Boothferry) sediment resuspension.

S1 Boothferry	Sediment type	Al	Fe	Mn	As	Cd	Cr	Co	Cu	V	Zn	Ni
Total in sample (mg)	**surface**	537±166	484±133	11.45±0.15	0.40±0.07	<DL	1.20±0.06	<DL.	0.53±0.06	1.06±0.01	2.27±0.05	<DL
	subsurface	757±33	644±145	15.29±0.37	0.38±0.04	<DL	1.59±0.04	<DL	0.64±0.06	1.37±0.05	2.90±0.06	<DL
Initial in aqueous phase (mg/Kg)	**surface**	0.06±0.00	0.07±0.00	0.67±0.01	0.04±0.00	0.00±0.00	0.00±0.00	0.04±0.00	0.03±0.00	0.06±0.00	0.07±0.00	0.03±0.00
	subsurface	0.05±0.00	0.22±0.01	3.37±0.15	0.04±0.00	0.00±0.00	0.00±0.00	0.04±0.00	0.02±0.00	0.05±0.00	0.06±0.00	0.03±0.00
Maximum release (mg/Kg)	**surface**	0.26±0.02	0.15±0.01	2,13±0.10	0.06±0.01	0.01±0.00	0.01±0.01	0.08±0.12	0.12±0.01	0.07±0.00	0.15±0.09	0.04±0.00
	subsurface	0.24±0.01	0.47±0.55	7.89±0.17	0.06±0.01	<DL	0.01±0.00	0.14±0.00	0.12±0.01	0.09±0.00	0.08±0.08	0.04±0.01
Final in aqueous phase (mg/Kg)	**surface**	0.13±0.01	0.10±0.02	0.34±0.23	0.06±0.01	<DL	0.00±0.00	0.00±0.00	0.12±0.00	0.06±0.01	<DL	0.04±0.00
	subsurface	0.14±0.02	0.37±0.16	1.45±1.21	0.10±0.01	<DL	0.00±0.00	0.00±0.00	0.12±0.01	0.06±0.00	0.04±0.00	0.04±0.01

Table C.2: Trace metal in the aqueous phase during S2 (Blacktoft) sediment resuspension.

S2 Blacktoft	Sediment type	Al	Fe	Mn	As	Cd	Cr	Co	Cu	V	Zn	Ni
Total in sample (mg)	**surface**	721±55	587±127	13.11±0.89	0.35±0.06	<DL	1.46±0.26	<DL	0.61±0.06	1.19±0.07	2.67±0.18	<DL
	subsurface	871±40	646±117	14.60±0.32	0.40±0.04	<DL	1.71±0.30	<DL	0.59±0.05	1.37±0.08	2.93±0.10	<DL
Initial in aqueous phase (mg/Kg)	**surface**	0.06±0.00	0.04±0.00	0.55±0.04	0.04±0.00	0.00±0.00	0.00±0.00	0.04±0.00	0.02±0.00	0.06±0.00	0.07±0.00	0.03±0.00
	subsurface	0.05±0.00	0.04±0.00	1.98±0.08	0.03±0.00	0.00±0.00	0.00±0.00	0.03±0.00	0.02±0.00	0.05±0.00	0.06±0.00	0.03±0.00
Maximum release (mg/Kg)	**surface**	0.29±0.13	0.10±0.04	0.98±0.13	0.06±0.02	0.00±0.00	0.01±0.01	0.01±0.00	0.10±0.02	0.08±0.00	0.15±0.06	0.04±0,00
	subsurface	0.20±0.04	0.05±0.01	4.50±0.27	0.05±0.00	0.00±0.00	0.01±0.00	0.01±0.00	0.10±0.00	0.06±0.00	0.06±0.01	0.03±0.00
Final in aqueous phase (mg/Kg)	**surface**	0.11±0.02	0.06±0.01	0.23±0.22	0.06±0.02	<DL	0.00±0.00	0.00±0.00	0.10±0.02	0.06±0.01	<DL	0.03±0.00
	subsurface	0.11±0.00	0.05±0.01	0.03±0.02	0.05±0.00	<DL	0.01±0.00	0.00±0.00	0.10±0.00	0.05±0.00	<DL	0.03±0.00

Table C.3: Trace metal in the aqueous phase during S3 (Paull) sediment resuspension.

S3 Paull	Sediment type	Al	Fe	Mn	As	Cd	Cr	Co	Cu	V	Zn	Ni
Total in sample (mg)	**surface**	735±52	536±107	12.10±0.38	0.26±0.03	<DL	1.53±0.05	<DL	0.58±0.03	1.14±0.03	2.34±0.08	<DL
	subsurface	859±69	699±149	16.65±0.65	0.63±0.07	<DL	2.03±0.09	<DL	0.56±0.05	1.68±0.07	3.64±0.28	<DL
Initial in aqueous phase (mg/Kg)	**surface**	12.33±0.40	0.68±0.02	4.27±0.13	0.06±0.00	0.25±0.01	0.02±0.00	0.06±0.00	2.28±0.07	0.04±0.00	5.30±0.16	0.00±0.00
	subsurface	9.95±0.39	0.64±0.02	0.87±0.03	0.10±0.00	0.20±0.01	0.02±0.00	0.09±0.00	1.82±0.07	0.04±0.00	4.29±0.17	0.00±0.00
Maximum release (mg/Kg)	**surface**	60.55±2.20	6.73±3.81	17.13±0.52	0.15±0.08	3.33±0.49	0.16±0.07	0.16±0.07	6.21±0.19	0.11±0.06	14.18±0.47	0.01±0.00
	subsurface	43.04±2.44	4.04±1.62	6.01±3.20	0.20±0.03	2.27±0.30	0.12±0.06	0.11±0.01	4.33±0.20	0.07±0.01	9.86±0.44	0.01±0.00
Final in aqueous phase (mg/Kg)	**surface**	10.74±0.51	1.55±0.10	0.44±0.21	0.11±0.01	0.25±0.01	0.07±0.01	<DL	0.81±0.04	0.07±0.01	2.03±0.13	0.00±0.00
	subsurface	9.82±0.67	1.72±0.48	6.01±3.20	0.07±0.01	0.22±0.02	0.06±0.00	0.02±0.01	0.75±0.08	0.04±0.00	2.04±0.36	0.00±0.00

Table C.4: Trace metal in the aqueous phase during S4 (Skeffling) sediment resuspension.

S4 Skeffling	Sediment type	Al	Fe	Mn	As	Cd	Cr	Co	Cu	V	Zn	Ni
Total in sample (mg)	**surface**	839±75	670±153	11.48±0.73	0.45±0.03	<DL	1.73±0.11	<DL	0.51±0.04	1.38±0.09	2.66±0.16	<DL
	subsurface	1027±95	801±171	13.84±0.66	0.46±0.04	<DL	2.11±0.12	<DL	0.71±0.20	1.85±0.18	3.27±0.18	<DL
Initial in aqueous phase (mg/Kg)	**surface**	12.01±0.74	0.87±0.05	10.04±0.62	0.04±0.00	0.25±0.02	0.02±0.00	0.04±0.00	2.19±0.13	0.03±0.00	4.88±0.30	0.00±0.00
	subsurface	9.40±0.43	0.77±0.04	10.28±0.47	0.04±0.00	0.19±0.01	0.02±0.00	0.04±0.00	1.69±0.08	0.03±0.00	3.71±0.17	0.00±0.00
Maximum release (mg/Kg)	**surface**	64.76±6.16	5.57±2.59	33.56±3.09	0.14±0.02	3.16±0.25	0.17±0.05	0.17±0.02	13.28±1.42	0.07±0.00	32.94±4.05	0.02±0.01
	subsurface	41.59±4.32	2.91±0.93	11.37±0.85	0.10±0.01	2.22±0.14	0.10±0.03	0.10±0.01	7.73±3.49	0.04±0.00	19.28±9.27	0.01±0.00
Final in aqueous phase (mg/Kg)	**surface**	10.56±0.67	2.69±1.38	2.76±4.30	0.14±0.02	0.25±0.02	0.11±0.02	0.03±0.01	0.87±0.12	0.07±0.00	2.21±0.31	0.00±0.00
	subsurface	8.45±0.47	1,43±0.38	0.04±0.00	0.04±0.00	0.20±0.01	0.08±0.03	<DL	0.70±0.15	0.03±0.00	1.60±0.15	0.00±0.00

C.3 Changes in metal partitioning during sediment resuspension

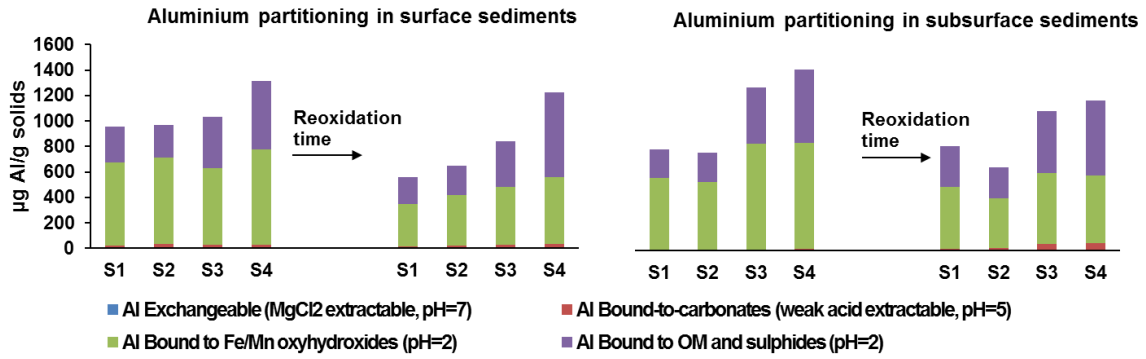

Figure C.3: Aluminium partitioning after estuarine sediment reoxidation determined by sequential extractions using Tessier *et al.* (1979) protocol. The concentration is expressed has been normalised to µg $Al_{(aq)}$ in the extractant solution by the mass of solids (dry weight) used in the extraction. Surface sediments are on the left and subsurface sediments on the right. Sites are ordered according to the salinity gradient and the arrows represent 2-weeks of reoxidation experiment.

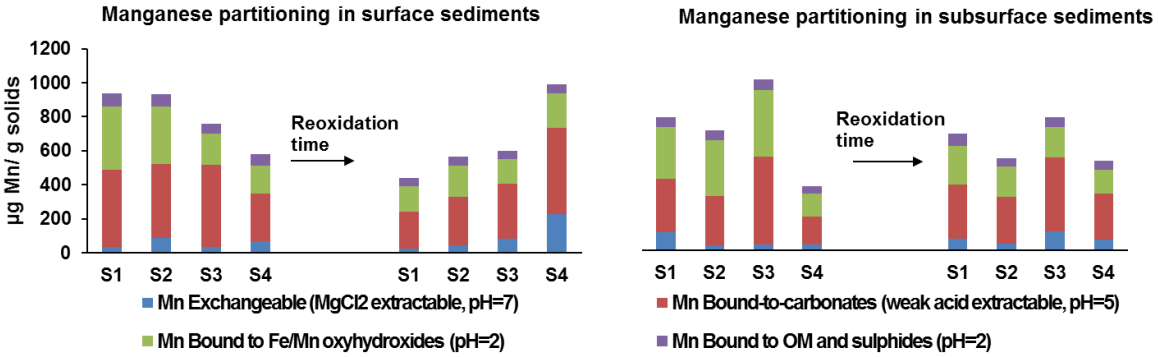

Figure C.4: Manganese partitioning after estuarine sediment reoxidation determined by sequential extractions using Tessier *et al.* (1979) protocol. The concentration is expressed has been normalised to µg $Mn_{(aq)}$ in the extractant solution by the mass of solids (dry weight) used in the extraction. Surface sediments are on the left and subsurface sediments on the right. Sites are ordered according to the salinity gradient and the arrows represent 2-weeks of reoxidation experiment.

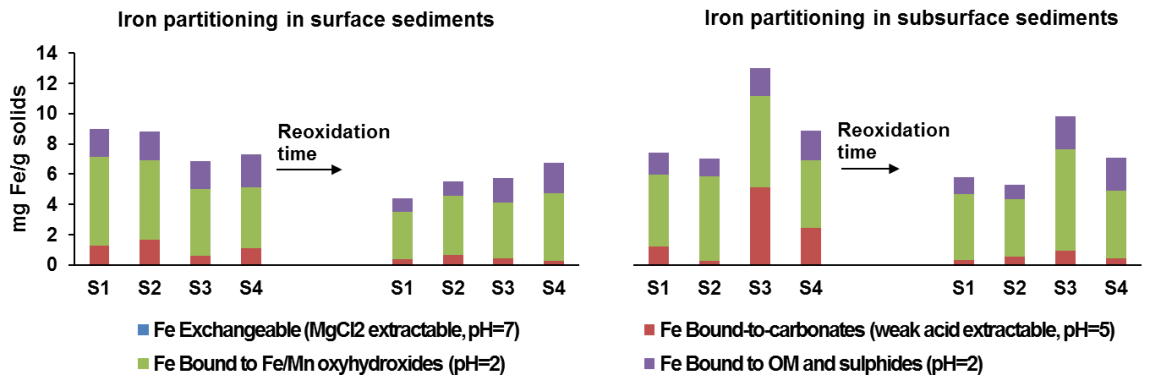

Figure C.5: Iron partitioning after estuarine sediment reoxidation determined by sequential extractions using Tessier *et al.* (1979) protocol. The concentration is expressed has been normalised to mg $Fe_{(aq)}$ in the extractant solution by the mass of solids (dry weight) used in the extraction. Surface sediments are on the left and subsurface sediments on the right. Sites are ordered according to the salinity gradient and the arrows represent 2-weeks of reoxidation experiment.

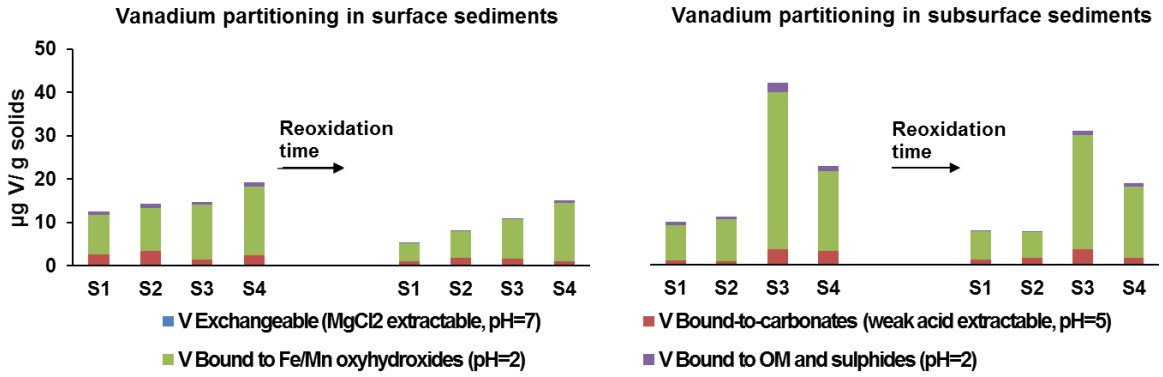

Figure C.6: Vanadium partitioning after estuarine sediment reoxidation determined by sequential extractions using Tessier *et al.* (1979) protocol. The concentration is expressed has been normalised to µg $V_{(aq)}$ in the extractant solution by the mass of solids (dry weight) used in the extraction. Surface sediments are on the left and subsurface sediments on the right. Sites are ordered according to the salinity gradient and the arrows represent 2-weeks of reoxidation experiment.

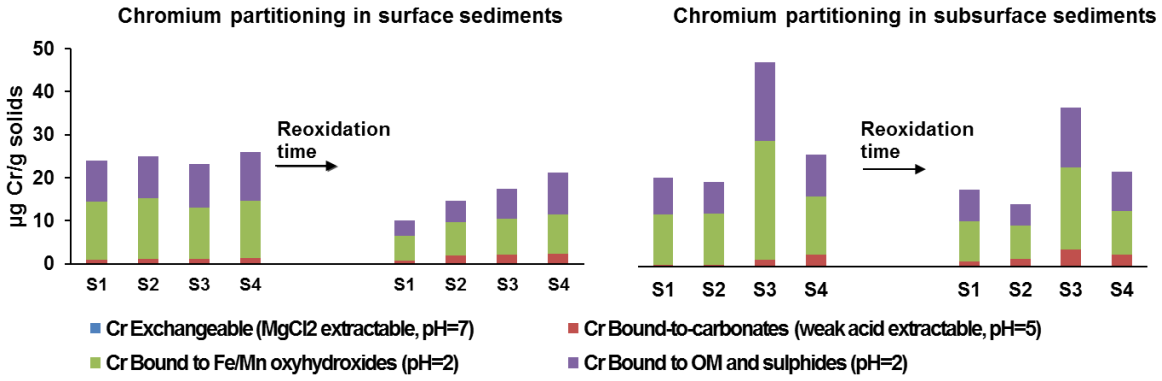

Figure C.7: Chromium partitioning after estuarine sediment reoxidation determined by sequential extractions using Tessier *et al.* (1979) protocol. The concentration is expressed has been normalised to µg $Cr_{(aq)}$ in the extractant solution by the mass of solids (dry weight) used in the extraction. Surface sediments are on the left and subsurface sediments on the right. Sites are ordered according to the salinity gradient and the arrows represent 2-weeks of reoxidation experiment.

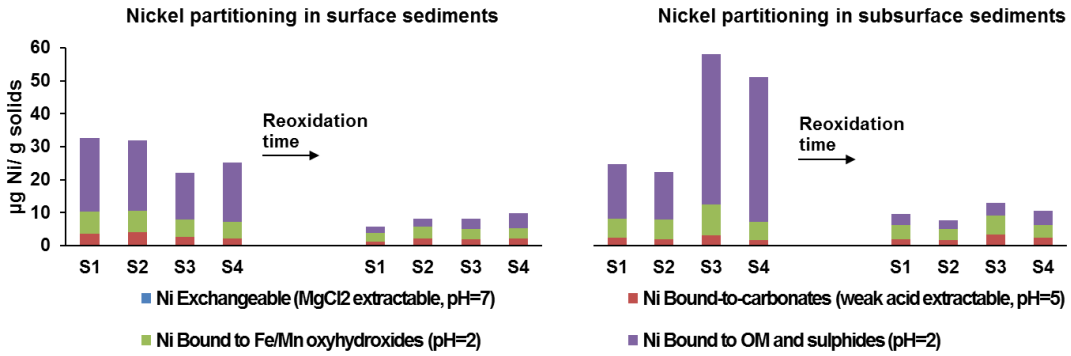

Figure C.8: Nickel partitioning after estuarine sediment reoxidation determined by sequential extractions using Tessier *et al.* (1979) protocol. The concentration is expressed has been normalised to µg $Ni_{(aq)}$ in the extractant solution by the mass of solids (dry weight) used in the extraction. Surface sediments are on the left and subsurface sediments on the right. Sites are ordered according to the salinity gradient and the arrows represent 2-weeks of reoxidation experiment.

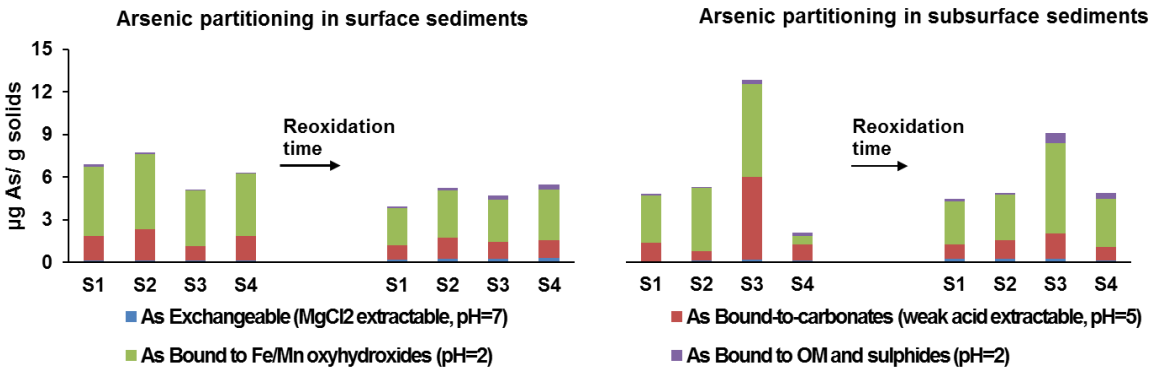

Figure C.9: Arsenic partitioning after estuarine sediment reoxidation determined by sequential extractions using Tessier *et al.* (1979) protocol. The concentration is expressed has been normalised to µg As(aq) in the extractant solution by the mass of solids (dry weight) used in the extraction. Surface sediments are on the left and subsurface sediments on the right. Sites are ordered according to the salinity gradient and the arrows represent 2-weeks of reoxidation experiment.

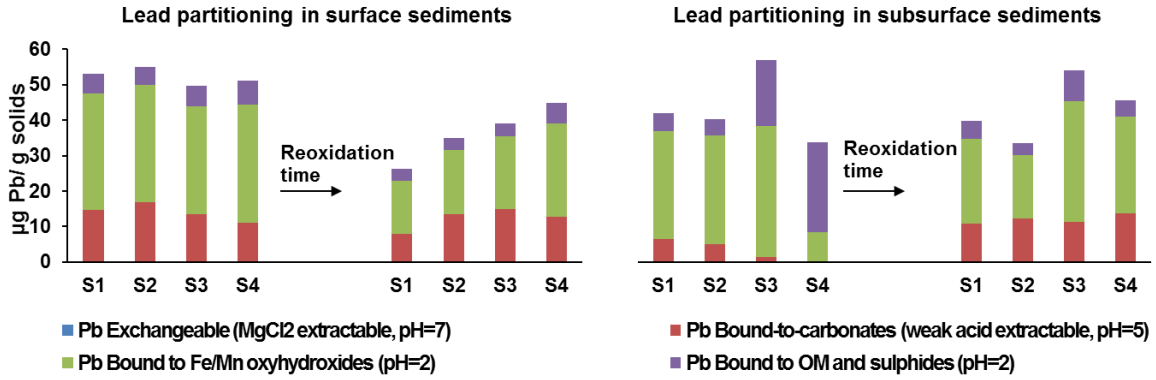

Figure C.10: Lead partitioning after estuarine sediment reoxidation determined by sequential extractions using Tessier *et al.* (1979) protocol. The concentration is expressed has been normalised to µg $Pb_{(aq)}$ in the extractant solution by the mass of solids (dry weight) used in the extraction. Surface sediments are on the left and subsurface sediments on the right. Sites are ordered according to the salinity gradient and the arrows represent 2-weeks of reoxidation experiment.

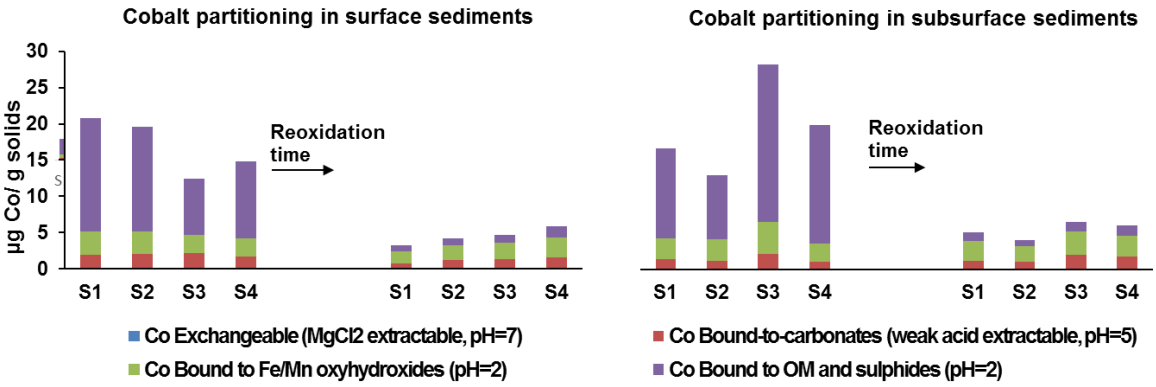

Figure C.11: Cobalt partitioning after estuarine sediment reoxidation determined by sequential extractions using Tessier *et al.* (1979) protocol. The concentration is expressed has been normalised to µg $Co_{(aq)}$ in the extractant solution by the mass of solids (dry weight) used in the extraction. Surface sediments are on the left and subsurface sediments on the right. Sites are ordered according to the salinity gradient and the arrows represent 2-weeks of reoxidation experiment.

Appendix D

Supplementary Information for Chapter 6

"Nitrate-dependent oxidation of undisturbed estuarine sediments and its effects on major and trace elements"

D.1 Trace metal partitioning changes during anaerobic nitrate-dependent oxidation

D.1.1 Chromium partitioning

Chromium speciation did not differ significantly between sediments and over the time of the anaerobic incubations, although S3 showed initially more extractable (~2 times) Cr in the less reactive phases (Fe- and Mn-(oxy)hydroxides and organic and/or sulphide minerals) than the other samples. Cr was associated with these less reactive phases and there was a minor increase in the Cr associated to carbonates in the final sediments.

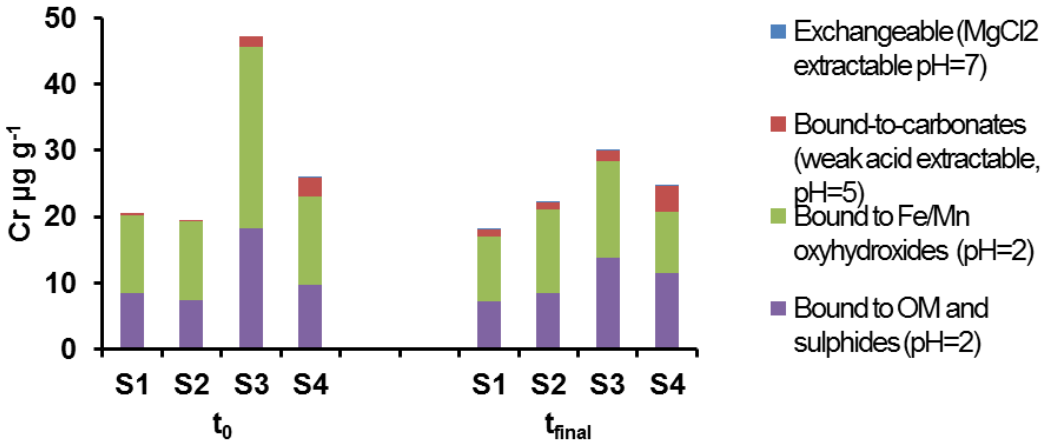

Figure D.1: Changes in Cr partitioning after anaerobic incubation experiments (the time difference between the initial (t_0) and the final point (t_{final}) is 2 months).

D.1.2 Vanadium partitioning

The majority of the extractable Vanadium was associated with the Fe/Mn oxyhydroxides fraction and the changes over the anaerobic incubations were not

significant. Overall, more V was extracted from S3 and S4 sediments. The mismatch between the extractable V in S3 initial and final sediments may be due heterogeneity in the sediment samples or some errors during the procedure.

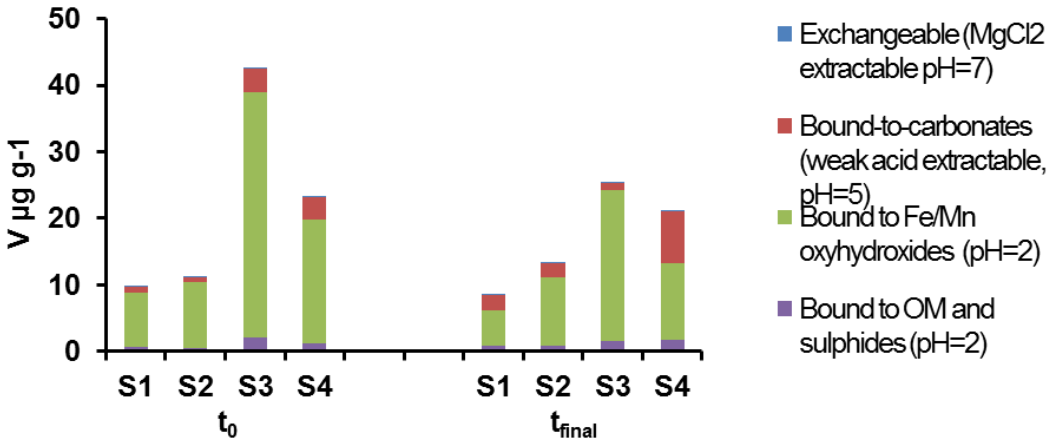

Figure D.2: Changes in V partitioning after anaerobic incubation experiments (the time difference between the initial (t_0) and the final point (t_{final}) is 2 months).

D.1.3 Nickel partitioning

The Nickel was associated mainly with the less reactive pool, organic matter and sulphide minerals, and in a less important proportion to the metal oxides pool. No changes in the Ni partitioning were observed after the anaerobic incubations.

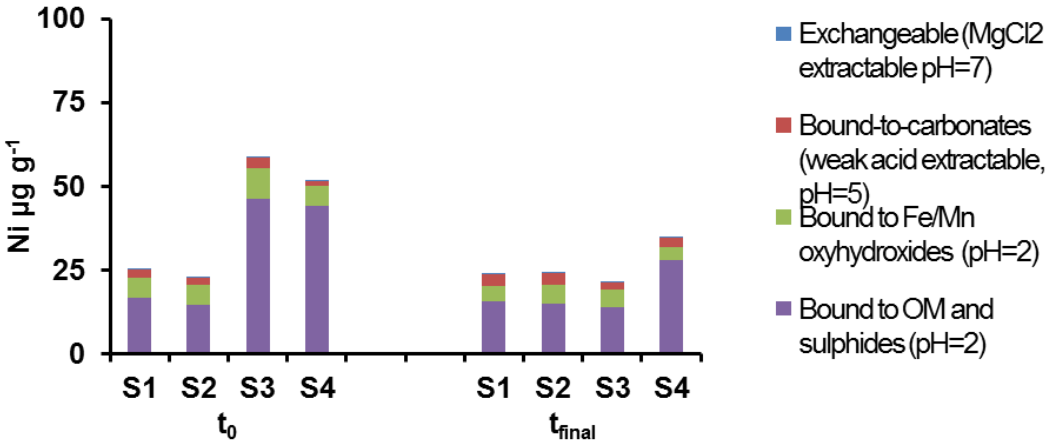

Figure D.3: Changes in Ni partitioning after anaerobic incubation experiments (the time difference between the initial (t_0) and the final point (t_{final}) is 2 months).

D.1.4 Cobalt partitioning

Cobalt was chiefly associated with the less reactive pool in all the sediments, with a small proportion was associated with the Fe/Mn oxides and the carbonates fractions. Co experienced no shifts towards other mineral phases during the anaerobic incubations, although there is a mismatching between the final and initial extractions carried out with S3 sediments.

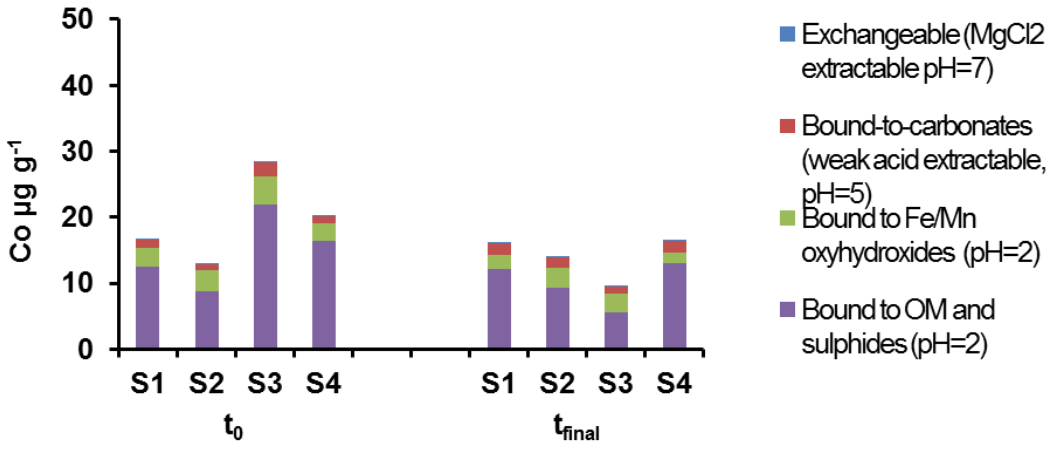

Figure D.4: Changes in Co partitioning after anaerobic incubation experiments (the time difference between the initial (t_0) and the final point (t_{final}) is 2 months).

D.1.5 Iron, Manganese and Aluminium partitioning

Iron partitioning was considerable similar among sediments, with the exception of S3 sediments that showed originally an important fraction of iron associated with carbonates. The iron associated with sulphides and organic matter remained relatively stable over the anaerobic incubations. Iron in S4 sediments experienced a shift towards the weak-acid extractable phase during the anaerobic incubation time, however in S3 sediments the contrary occurred and the proportion of iron associated to carbonates decreased.

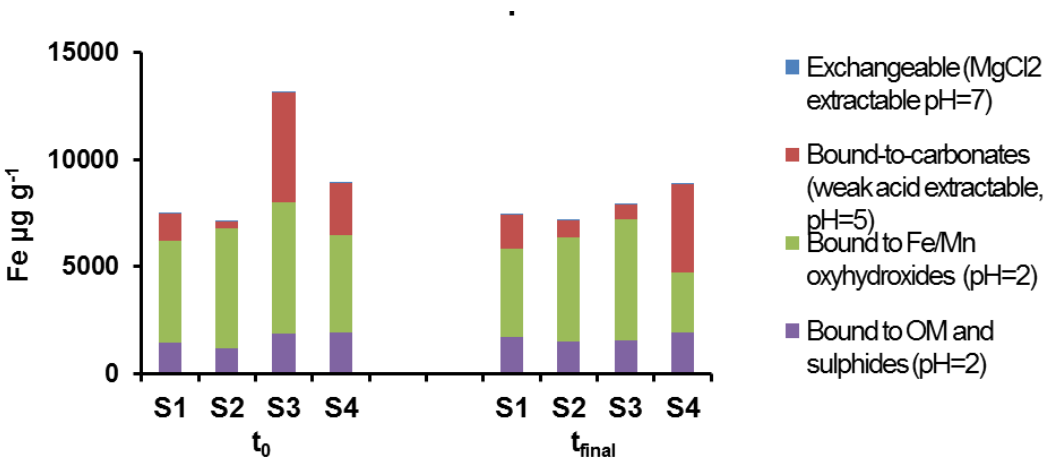

Figure D.5: Changes in Fe partitioning after anaerobic incubation experiments (the time difference between the initial (t_0) and the final point (t_{final}) is 2 months).

Aluminium is not a heavy metal but is an important element in the earth surface. The majority of the aluminium will be associated with the residual material (Tessier 1979) as the $MgCl_2$ (pH 7) treatment does not affect silicates, sulphides or organic matter, and the weak and strong acid (third step) treatments affect minimally those minerals. The combination of H_2O_2, HNO_3 and NH_4OAc in the fourth treatment of the Tessier's protocol, attacks very slightly the major silicate phases, so the aluminium extracted is still very low compared to the bulk concentration (~40,000-55,000 ppm). However, the results of the aluminium partitioning showed some aluminium associated to mainly the less reactive fractions in the four sediments, without significant changes between the initial and the final sediments.

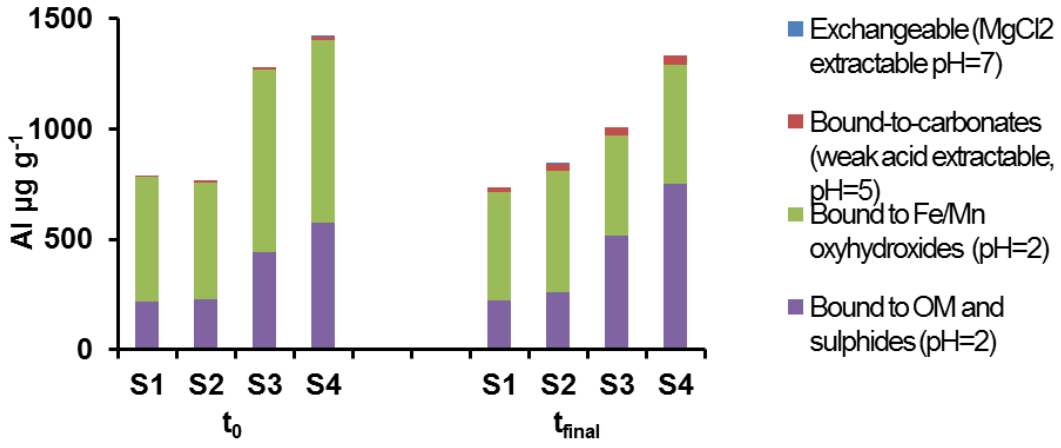

Figure D.6: Changes in Al partitioning after anaerobic incubation experiments (the time difference between the initial (t_0) and the final point (t_{final}) is 2 months).

Manganese partitioning showed that the Mn was more importantly associated to carbonates, and it was also dissolved from Mn oxides. Mn associated with carbonates seemed to increase slightly after the incubation time (except in the solids recovered from S3 experiments), whereas the proportion recovered from the oxides fraction decreased in the final materials. Very low manganese was recovered from the exchangeable fraction, and from the organic and sulphide fraction at both tests.

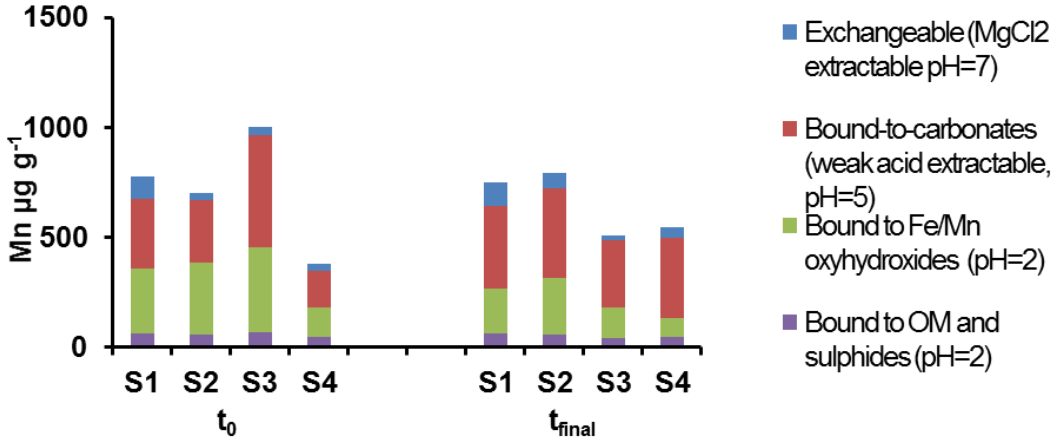

Figure D.7: Changes in Mn partitioning after anaerobic incubation experiments (the time difference between the initial (t_0) and the final point (t_{final}) is 2 months).

Major elements such as Fe, Al and Mn have been also measured from the sequential extraction solution. Manganese and Fe- oxides should not be significantly solubilized at

pH 7 so concentrations in the first leachate were expected to be low. Manganese concentrations in the exchangeable phase suggest that this metal is found in reduced form adsorbed to the sediment particles. However, Fe and Mn concentrations from the weak-acid extraction were probably from the dissolution of divalent salts (ferrous and manganous carbonates) (Tessier *et al.*, 1979). In fact, the Mn boun-to-carbonate was generally higher in the samples than that extracted from the Mn-oxides. Manganese oxides are more easily leached than Fe oxides so that can be an explanation for the higher concentrations of Mn in the carbonate-bound phase. The low concentrations of Mn extracted form the organic matter and sulphides fraction may indicate that the Mn extraction was almost complete after the first strong acid treatment. Iron partitioning did not show changes in the sediments from S1 and S2, while S4 sediments show a modest shift from the less to more reactive fractions. Less Fe was extracted from the final S3 solids (there was a significant decrease in the initial Fe associated to the carbonate-bound phase that did not have a correspondent increase in other phase in the final sediment extractions), which can be likely due to an error during the extraction protocol.Aluminium was extracted at pH=2 which indicates that the silicate components of the sediments are attacked at this stage of the extraction. Aluminium partitioning did not change significantly after the microcosms incubations, but some Al was found in the carbonate-bound fraction in the final solids.

Appendix E
Supplementary information for Chapter 7

"Diversity patterns of benthic bacterial communities along the salinity continuum of the Humber estuary (UK)"

Andrea Vidal-Durà, Ian T. Burke, Robert J.G. Mortimer and Douglas I. Stewart

(in review with *Frontiers in Aquatic Microbiology*)

E.1 Supplementary diversity data

In this study we used "Hill numbers" (Hill, 1973) to analyse bacterial diversity since they are thought to be a unified measure for diversity that take into account the abundance of each species (OTUs in this case). Hill numbers define biodiversity as the reciprocal mean of proportional abundance, and compensate for the disproportionate impact rare taxa by weighting taxa based on abundance (Hill, 1973; Jost, 2006, 2007). So they are more suitable for working with the large datasets produced by amplicon sequencing technologies (Kang *et al.*, 2016). The basic expression for the "Hill numbers" is represented in equation E.1.

$$D_q = \left(\sum_{i=1}^{S} p_i^q\right)^{\frac{1}{1-q}} \qquad \text{(Eq E.1)}$$

Where S is total number of species (OTUs in this study) and p_i is the proportion of individuals belonging to the i^{th} species in the dataset. The parameter q, is the "order of the diversity measure" and determines how the abundance is weighted. By increasing the index q the diversity measurement places progressively more weight on the high-abundance (more common) OTUs within a population. The unweighted Hill number, D_0, is exactly equivalent to the species richness. D_1 is a measure of the number of common species and is equivalent to the exponential of Shannon entropy; and D_2 is a measure of the number of dominant species and is equivalent to the inverse of Simpson concentration (Hill, 1973; Jost 2006, 2007). The conversion of traditional diversity

indices to D_q of different order is presented in Table E.1. Complete information about the diversity results in this study are gathered in Table E.2.

Table E.1: Conversion of traditional diversity indices to "Hill numbers" (D_q) for q=0 q=1 and q=2 (D_0, D_1, and D_2) (modified from Jost, 2007). D means diversity index; S represents the total number of species in the community; and pi are species proportions.

Order of the diversity measurement (q)	**Traditional Diversity Index (D)**	**To convert diversity indices (D) to measurement of diversity (D_q)**	**Diversity in terms of p_i (D_q)**
0	Species Richness $D \equiv \sum_{i=1}^{S} p_i^0$	D	$D_0 = \sum_{i=1}^{S} p_i^0$=S
1	Shannon entropy $D \equiv -\sum_{i=1}^{S} p_i \ln p_i$	exp (D)	$D_1 = \exp\left(-\sum_{i=1}^{S} p_i \ln p_i\right)$
2	Simpson concentration $D \equiv \sum_{i=1}^{S} p_i^2$	1/D	$D_2 = {}^{1}/_{\sum_{i=1}^{S} p_1^2}$

Hills numbers are measures of number of species, which are also called "number of equivalents" and are symbolised by D_q (equation E.1). The sum in equation 1 is symbolised in Jost (2007) by ${}^{q}\lambda$, and it is the key of these calculations:

$$\lambda^q = \sum_{i=1}^{S} p_i^q \qquad \text{(Eq. E.2)}$$

So equation E.1 will look like:

$$D_q = \left(\sum_{i=1}^{S} p_i^q\right)^{1/(1-q)} = \left(\lambda^q\right)^{1/(1-q)} \qquad \text{(Eq. E.3)}$$

To analyse regional diversity (gamma diversity D_q^{γ}), we need to calculate its different components (alpha and beta diversities, D_q^{α} and D_q^{β}). The alpha (single community), beta (between the different communities considered), and gamma (regional) components of a diversity index, can be individually converted to diversity

measurements (D_q^{α}, D_q^{β} and D_q^{γ}). Following Whittaker's multiplicative law (Whittaker, 1972) alpha, beta and gamma diversities are related like so:

$$D_q^{\gamma} = D_q^{\alpha} \times D_q^{\beta} \qquad \text{(Eq. E.4)}$$

For the alpha component of any diversity index (D^{α}):

$$D^{\alpha} \equiv D\left({}_{q}^{\alpha}\lambda\right) = D\left[\frac{w_1^q \sum_{i+1}^{S} p_{i1}^q + w_2^q \sum_{i=1}^{S} p_{i2}^q + \cdots}{w_1^q + w_2^q + \cdots}\right] \qquad \text{(Eq. E.5)}$$

w_j is the statistical weight of community j (number of individuals (valid reads) in the community *j* (sample *j*) divided by the total number of reads in the region). Therefore, the diversity measurement, or Jost index of order q (D_q^{α}) equivalent to that diversity index (D^{α}):

$$D_q^{\alpha} \equiv D\left({}_{q}^{\alpha}\lambda\right) = \left[\frac{w_1^q \sum_{i+1}^{S} p_{i1}^q + w_2^q \sum_{i=1}^{S} p_{i2}^q + \cdots}{w_1^q + w_2^q + \cdots}\right]^{1/(1-q)} \qquad \text{(Eq. E.6)}$$

That expression is undefined at q=1, but the limit exists as q approaches 1 ($\lim_{q\to 1}$) being the exponential of alpha Shannon entropy:

$$D_1^{\alpha} \equiv exp\left[-w_1 \sum_{i=1}^{S}(p_{i1} \ln p_{i1}) + -w_2 \sum_{i=1}^{S}(p_{i2} \ln p_{i2}) + \cdots\right] \qquad \text{(Eq. E.7)}$$

If we solve this equation for our data set (considering unequal community weights):

${}^{*}D_1^{\alpha}$=438[1]

Regional diversity measurement of order 1 (D_1^{γ}) of all the pooled samples equals:

$$D_1^{\gamma} \equiv exp\left[\sum_{i=1}^{S} -(w_1 p_{i1} + w_2 p_{i2} + \cdots) \times \ln(w_1 p_{i1} + w_2 p_{i2} + \cdots)\right] \qquad \text{(Eq. E.8)}$$

[1] Note that the alpha diversity measurement when different communities are considered is not the average of the alpha diversity of each individual site since it considers the weights of the different communities, for more details see Jost, L. (2007). Partitioning diversity into independent alpha and beta components. Ecology 88, 2427-2439. doi: 10.1890/06-1736.1

D_1^{γ}=934

Then we can calculate the beta diversity (D_1^{β}) which is the measurement of the relative change in species composition between locations or communities by using equation E.4:

$$D_1^{\beta} = D_1^{\gamma} / D_1^{\alpha}$$

D_1^{β} = 934/438 = 2.13

D_1^{β} has been described as the number of distinct communities or samples in the region (Jost 2007). This measurement can be converted into MacArthur's (1965) homogeneity measure (equation E.9). This ratio answers the question of "*what proportion of total diversity is found within the averaged community or sample?"* (Jost 2007). According to this homogeneity measure, 47% of the total diversity is found in the average community.

$$M = 1 \Big/ D_1^{\beta} = \exp(D^{\alpha}) \Big/ \exp(D^{\beta}) \text{ (Eq. E.9)}$$

$M = 1/D_1^{\beta}$ = 1/2.13 = 0.47

Table E.2: Bacterial Diversity Measurements. The total number of reads include sequences classified as archaea and bacteria (including poorly classified reads (<0.7 confidence)). Number of reads per sample are the sum of all the reads allowed (after quality control, and only classified as bacterial with a confidence value >0.7 at phylum level). D_0^{α} is equivalent to OTUs richness, i.e. the number of OTUs present in each sample. D_1^{α} and D_2^{α} equivalents to the exponential of Shannon Entropy and the inverse of the Simpson concentration respectively (Hill, 1973; Jost, 2006, 2007; Kang *et al.*, 2016). $*D_1^{\alpha}$ is a special case of alpha diversity which represents an averaged D_1^{α} when different communities are considered, however is not the arithmetic average of the individual alpha diversity (D_1^{α}) of each sample because community weights are considered in it is calculation (equation E.6) (Jost, 2007).

	S1		**S2**		**S3**		**S4**	
	S1s	**S1d**	**S2s**	**S2d**	**S3s**	**S3d**	**S4s**	**S4d**
Total number of paired-end reads	712402	976928	638252	821137	577701	1208696	721187	522816
Number of reads classified as bacteria	556621	802492	492132	641797	454121	1113761	633444	370056
Species richness	5262	5968	5599	6004	5541	3873	4126	3488
Average Richness	4983							
Shannon Entropy	7.1	7.3	7.1	7.2	3.3	6.7	6.0	6.3
Hill numbers of order 1 (D_1^{α})	1436	1174	1309	1250	833	28	546	412
Hill numbers of order 2 (D_2^{α})	487	378	385	374	175	10	154	120
Alpha (single-community, $^{*}D_1^{\alpha}$), gamma (regional, D_1^{γ}), and beta (between communities, D_1^{β}) diversities of order 1	$^{*}D_1^{\alpha} = 438$ $D_1^{\gamma} = 934$ $D_1^{\beta} = 2.13$							

E.2 Taxa Accumulation Curves (TAC)

Taxa accumulation curves (TAC) (Figure E.1) have been calculated for the full raw dataset, without replacement (reads are picked at random and a given read can only be picked once and results are averaged over multiple trials; here 8 iterations). TACs cannot be easily calculated at the moment from the dataset after removal of artefacts due to the way the sequence analysis pipeline operates. The full dataset used contained the pool unfiltered reads from the eight samples used in this study, and therefore it included reads from before quality checks were applied in the sequence analysis pipeline. Some of the reads that were clustered into the OTUs generated were later removed from the diversity analysis, such as OTUs identified as archaea and OTUs which were not classified to the level of bacterial phylum with a confidence >0.7.

TAC for the regional OTUs richness shows that D_0^{γ} varies by less than 0.1 once >60% of the dataset is subsampled. However, this does not mean that more "rare" taxa would not be found when the sequencing density were higher.

TAC for common and dominant OTUs show that both D_1^{γ} and D_2^{γ} vary by less than 0.1% once 20% of the dataset is subsampled. Further, because these metrics characterise the number of common and dominant OTUs it is inconceivable that the values calculated would be any different in deeper sequencing had been undertaken.

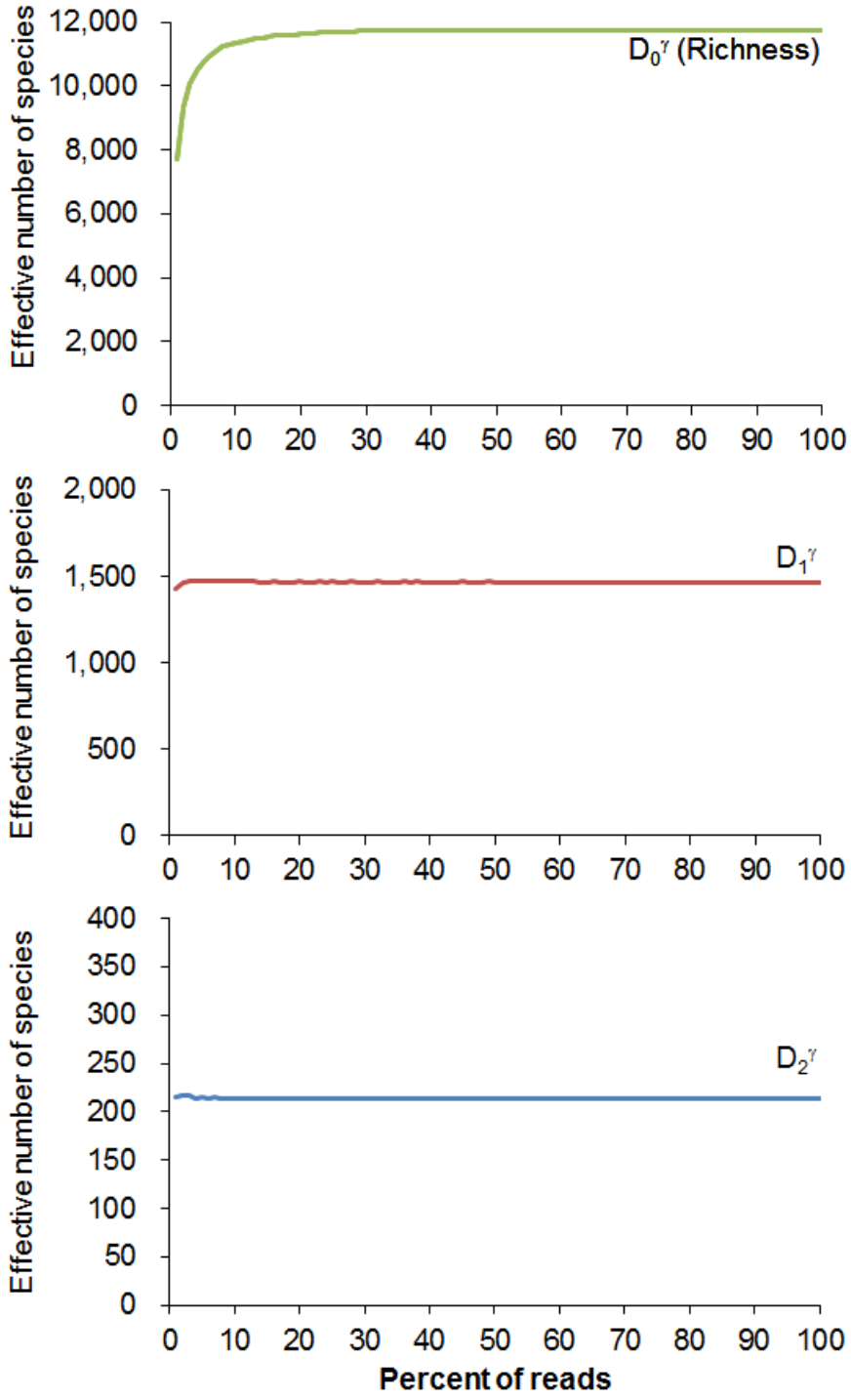

Figure E.1: Taxa accumulation curves for the unfiltered regional dataset subsampled without replacement (average of 8 replications) indicating that D_1^{α} and D_2^{α} converge very rapidly, and D_0^{α} converges when >60% of the dataset is subsampled. The unfiltered dataset contains OTUs later removed from the diversity analysis, such as OTUs identified as archaea and OTUs which were not classified to the level of bacterial phylum with a confidence > 0.7. In the diversity analysis, taxa represented unique OTUs at 97% similarity cutoff.

E.3 Bray Curtis Dissimilarity Matrix

To obtain the matrix in RStudio we need the package "vegan" (Oksanen *et al.*, 2013). First we import the data of the bacterial community (relative abundance data):

```
>community_data <-read.csv("relativeabundancetable.csv",row.names = 1, check.names = FALSE)
```

Then we can obtain the matrix by applying the following command:

```
>vegdist("community_data",method="bray", binary=FALSE, diag=FALSE, upper=FALSE, na.rm=FALSE)
```

Table E.3: Bray-Curtis dissimilarity matrix

	S1s	**S1d**	**S2s**	**S2d**	**S3s**	**S3d**	**S4s**	**S4d**
S1s	0							
S1d	0.239	0						
S2s	0.265	0.284	0					
S2d	0.240	0.246	0.130	0				
S3s	0.553	0.553	0.442	0.447	0			
S3d	0.911	0.913	0.902	0.901	0.900	0		
S4s	0.705	0.706	0.635	0.638	0.424	0.913	0	
S4d	0.762	0.773	0.705	0.705	0.636	0.874	0.550	0

E.4 Heat map

To obtain the heat map in RStudio we need the packages required: "gplots" and "RColorBrewer":

First we import the data of the bacterial community (relative abundance data)

```
>community_data <-read.csv("relativeabundancetable.csv",row.names = 1, check.names = FALSE)
```

```
> matrix_community <-community_data(x[,2:ncol(x)])
```

The colours are defined by the colorRampPalette command (example of 5 colours). The intervals are defined as well.

```
>my_palette<- colorRampPalette(c("antiquewhite3", "skyblue1",
"yellowgreen", "salmon", "red3")

> col_breaks = c(seq(0,0.001,length=100),
seq(0.001,0.01,length=100), seq(0.01,0.1, length=100), seq(0.1,1,
length=100), seq(1,100, length=100))
```

Finally we use the heatmap2 function to create the heat map and we define separately the legend:

```
> heatmap.2(matrix_community, Rowv= FALSE, main= "Heatmap",
dendogram="none", col=my_palette, breaks=col_breaks, trace="none",
density.info = "none", key= TRUE, symkey = FALSE, scale = "none",
rowsep = 1:nrow(matrix_communinity), sepcolor = "white", sepwidth =
c(0.05, 0.05))

>legend("left", fill = my_palette(5), legend = c("0 to 0.001",
"0.001 to 0.01", "0.01 to 0.1", "0.1 to 1", ">1"))
```

The heat map is another graphical representation of the similarities and dissimilarities of the bacterial community composition along the salinity gradient. The green and red bands (from 0.01 to >1) are the important ones to look at. We can interpret the grey bands as absence or extremely low abundances. Samples from the inner estuary (S1s, S1d, S2s, and S2d) share the bands with the greatest abundances (right part of the heat map). S3s also shares a similar pattern although the green areas are a modestly more spread than at the inner samples. The S3d shows again the most unalike community composition. It was also the less diverse of the whole set of samples when D_1^{α} and D_2^{α} were applied. In fact, in further multivariate analyses (CCA and BIOENV) S3d has been considered as an outsider and it has been excluded from the tests performed. The S4s and S4d samples in the Heat map vary slightly from the rest of the samples (see some green bars that are not seen in other samples), which may indicate the differences in the bacterial community composition in the outer most estuary.

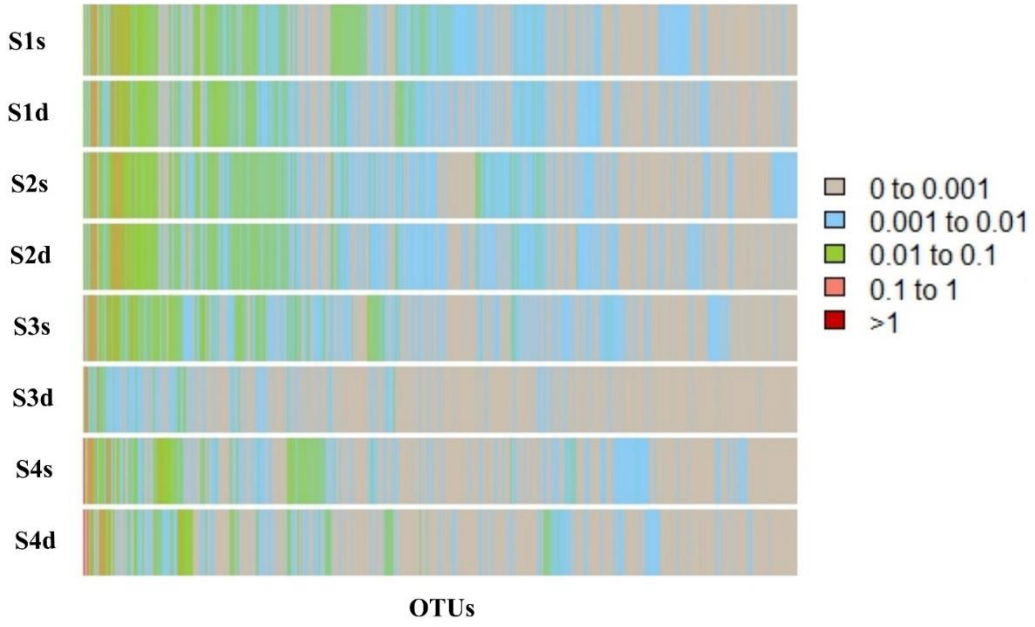

Figure E.2: Heat map displaying relative abundance (%) of the bacterial community (7656 OTUs) for the eight estuarine sediment samples.

E.5 Canonical Correspondence Analysis (CCA) and BIOENV test

E.5.1 CCA

CCA has been also performed in R Studio by the function `cca`. The input data were the OTU table (relative abundance) and environmental variables (salinity, porewater nitrate, porewater sulphate, porewater ammonium, porewater manganese, porewater iron, TOC, % acid extractable $Fe^{2+}_{(s)}$, total iron, particle size, Fe as pyrite and FeS_2).

The sample S3d was not considered in the CCA (neither in the BIOENV, see below) because the important differences in the bacterial community composition in this sample were strongly distorting the results.

```
> CCA <-cca(formula=community_matrix_noS3d ~ Salinity + PW_Nitrate
+ Fe2_solids + FeTOT + PW_Mn2 + D50 + PW_Ammonium + PW_Sulphate +
TOC + Fe_Pyrite + PW_Fe2 + FeS2,
data=environmental_variables_noS3d, subset= TRUE)
> CCA
Call: CCA(formula = community_matrix_noS3d ~ Salinity + PW_Nitrate
+ Fe2_solids + FeTOT + PW_Mn2 + D50 + PW_Ammonium + PW_Sulphate +
TOC + Fe_Pyrite + PW_Fe2 + FeS2, data =
environmental_variables_noS3d, subset = TRUE)
```

```
              Inertia Proportion Rank
Total           1.042      1.000
Constrained     1.042      1.000    6
Unconstrained   0.000      0.000    0
Inertia is mean squared contingency coefficient
Some constraints were aliased because they were collinear
(redundant)
4 species (variables) deleted due to missingness

Eigenvalues for constrained axes:
   CCA1    CCA2    CCA3    CCA4    CCA5    CCA6
0.47735 0.28451 0.13232 0.06868 0.06253 0.01650
```

Then we plot the result of the cca by:

```
> plot(CCA, type ="n"))
> text(CCA, dis="cn")
> points(cca2.5, pch=21, col="black", bg="yellow", cex=1.2)
```

(see Figure 7.6)

The constrained (or canonical) correspondence analysis (CCA) has been used as a method of constrained ordination to explore the relationship between microbial communities (OTU's abundance) and the environmental variables available. The total variability of the dataset was captured in the constrained axes. The first axis (CCA1) accounted for the 48% of the constrained (or total in this case) variance, and the second axis (CCA2) did for the 28%. The arrows indicate the direction of environmental variable gradient represented. Sites from the inner estuary have coarser particles and their relative position to the other environmental variables suggests these sites have low iron content (total and reduced acid extractable iron) and low nitrate concentrations in porewater. Likewise it was observed in the NMDS ordination plot, sites from the inner estuary (S1 and S2) appeared grouped regardless the sediment depth. S3 (only surface) and S4 appeared to be well separated (S4s and S4d also by depth) according to their relative position along the estuarine continuum. Salinity and total Fe (both in the approximate direction of the CCA1 axis) appeared to be the underlying variables most responsible of the differentiation of the microbial communities from the middle and outer estuary (S3 and S4). Moreover, S4d, besides being positively correlated with salinity and total iron content, shows high acid extractable $Fe^{2+}_{(s)}$ and low nitrate concentrations in the

porewater which indicate reducing conditions found at certain depth in the intertidal mudflats.

E.5.2 BIOENV test

We use the function **BIOENV** in RStudio. The environmental parameters used were the following: Salinity; concentration in porewater of nitrate, ammonium, sulphate, $Fe^{2+}_{(aq)}$ and $Mn^{2+}_{(aq)}$; 0.5 N HCl extractable $Fe^{2+}_{(s)}$; total iron in sediments; Fe-pyrite; Fe-FeS_2; Total Organic Carbon (TOC); and granulometry (D_{50}).

The sample S3d was not considered for the BIOENV analysis.

The function `bioenv` was applied as follows:

```
> bioenv_solution <-bioenv(community_data_noS3d,
environmental_variables_noS3d, fix.dist.method="bray",
var.dist.method="euclidean",scale.fix=FALSE, scale.var=TRUE,
var.max=ncd(var.mat))
4095 possible subsets (this may take time...)
> bioenv_solution
Call:
bioenv(comm = community_matrix_noS3d, env = env_variables_noS3d,
fix.dist.method = "bray", var.dist.method = "euclidean",
scale.fix = FALSE, scale.var = TRUE, var.max = ncd(var.mat))
Subset of environmental variables with best correlation to
community data.
Correlations:      spearman
Dissimilarities:   bray
Best model has 2 parameters (max. 12 allowed):
Salinity PW_Sulphate
with correlation  0.9593509
```

This was the output solution of the BIOENV, in which we can see that the salinity together with sulphate concentrations in porewater were the environmental parameters with the best correlation (0.96) with the bacterial community data.

```
> summary(bioenv_solution)
```

	size	correlation
Salinity	1	0.9136
Salinity PW_Sulphate	**2**	**0.9594**
Salinity PW_Sulphate Fe_Pyrite	3	0.9481
Salinity PW_Sulphate Fe2_solids FeTOT	4	0.9416
Salinity PW_Nitrate PW_Sulphate FeTOT Fe_Pyrite	5	0.9455

Salinity Fe2_solids PW_Fe2 FeTOT FeS2 D50	6	0.9455
Salinity PW_Nitrate PW_Sulphate Fe2_solids PW_Fe2 FeTOT D50	7	0.9506
Salinity PW_Nitrate PW_Sulphate Fe2_solids PW_Fe2 FeTOT FeS2 D50	8	0.9455
Salinity PW_Sulphate PW_Ammonium Fe2_solids PW_Fe2 FeTOT Fe_Pyrite FeS2 D50	9	0.9351
Salinity PW_Nitrate PW_Sulphate PW_Ammonium Fe2_solids PW_Fe2 FeTOT Fe_Pyrite FeS2 D50	10	0.9247
Salinity PW_Nitrate PW_Sulphate PW_Ammonium Fe2_solids PW_Fe2 PW_Mn2 FeTOT Fe_Pyrite FeS2 D50	11	0.9182
Salinity PW_Nitrate PW_Sulphate PW_Ammonium Fe2_solids PW_Fe2 PW_Mn2 FeTOT Fe_Pyrite FeS2 TOC D50	12	0.8844

In order to test the significance of bioenv results, we have used function mantel.The result for the Mantel statistic was r=0.88 which indicates strong positive correlation between the two distance matrices.

```
> veg.dist <- vegdist(community_matrix_noS3d, method = "bray",
binary = FALSE, diag = FALSE, upper = FALSE, na.rm = FALSE)
> env.dist<-vegdist(scale(env_variables_noS3d), "euclid")
> mantel(veg.dist, env.dist)

Mantel statistic based on Pearson's product-moment correlation

Call:
mantel(xdis = veg.dist, ydis = env.dist)

Mantel statistic r: 0.8829
      Significance: 0.001 CC

Upper quantiles of permutations (null model):
  90%   95% 97.5%   99%
0.396 0.490 0.595 0.711

Based on 999 permutations
mantel(xdis = veg.dist, ydis = env.dist)
```

E.6 References

[1] Hill, M.O. (1973). Diversity and evenness: a unifying notation and its consequences. *Ecology*, 54, pp.427-432. doi: 10.2307/1934352

[2] Jost, L. (2006). Entropy and diversity. *Oikos*, 113, pp.363-375. doi: 10.1111/j.2006.0030-1299.14714.x

[3] Jost, L. (2007). Partitioning diversity into independent alpha and beta components. *Ecology*, 88, pp.2427-2439. doi: 10.1890/06-1736.1

[4] Kang, S., Rodrigues, J.L.M., Ng, J.P., and Gentry, T.J. (2016). Hill number as a bacterial diversity measure framework with high-throughput sequence data. *Scientific Reports*, 6. doi: 10.1038/srep38263

[5] MacArthur, R.H. (1965). Patterns of species diversity. *Biological reviews*, 40, pp.510-533.

[6] Oksanen, J., Blanchet, F.G., Kindt, R., Legendre, P., Minchin, P.R., O'Hara, R.B., Simpson, G.L., Solymos, P., Stevens, M.H.H., and Wagner, H. (2013). vegan: Community Ecology Package. R package version 2.0-10 [Online]. Available: http://CRAN.R-project.org/package=vegan [Accessed 22-08-2016].

[7] Team, R. (2015). "RStudio: Integrated Development Environment for R". .0.99.486 ed. (Boston, MA: RStudio, Inc). Retrieved from http://www.rstudio.com/

[8] Whittaker, R.H. (1972). Evolution and measurement of species diversity. *Taxon*, 21, pp.213-251. doi: 10.2307/1218190